MINERALOGICAL AND GEOCHEMICAL PROFILING OF

ARSENIC-CONTAMINATED ALLUVIAL AQUIFERS IN

THE GANGES-BRAHMAPUTRA FLOODPLAIN

MANIKGANJ, BANGLADESH

Except where reference is made to the work of others, the work described in this thesis is my own or was done in collaboration with my advisory committee. This thesis does not include proprietary or classified information.

_____

Mohammad Shamsudduha

Certificate of Approval:

_____	_____
James A. Saunders Professor Geology and Geography	Ashraf Uddin, Chair Associate Professor Geology and Geography
_____	_____
Ming-Kuo Lee Professor Geology and Geography	Willis E. Hames Professor Geology and Geography

_____

Joe F. Pittman
Interim Dean
Graduate School

MINERALOGICAL AND GEOCHEMICAL PROFILING OF ARSENIC-CONTAMINATED ALLUVIAL AQUIFERS IN THE GANGES-BRAHMAPUTRA FLOODPLAIN MANIKGANJ, BANGLADESH

Mohammad Shamsudduha

A Thesis

Submitted to

the Graduate Faculty of

Auburn University

in Partial Fulfillment of the

Requirements for the

Degree of

Master of Science

Auburn, Alabama
August 4, 2007

MINERALOGICAL AND GEOCHEMICAL PROFILING OF

ARSENIC-CONTAMINATED ALLUVIAL AQUIFERS IN

THE GANGES-BRAHMAPUTRA FLOODPLAIN

MANIKGANJ, BANGLADESH

Mohammad Shamsudduha

Mohammad Shamsudduha

August 4, 2007

Date of Graduation

VITA

Mohammad Shamsudduha, son of Mr. Md. Mahtab Uddin and Mrs. Rabeya Khatun, was born in 1976 in Kishoreganj, Bangladesh. He passed his Secondary School Certificate Examination in 1991 from Kishoreganj Govt. Boys' High School and Higher Secondary Certificate Examination in 1993 from Gurudayal Govt. College with distinctions. He received his Bachelor of Science and Master of Science degrees in Geology in 1998 and 2001 respectively from Dhaka University, Bangladesh. He received his second Master of Science degree in Hydrogeology and Groundwater Management from University of Technology Sydney, Australia in 2004. He entered the graduate school at Auburn University in fall 2005.

THESIS ABSTRACT

MINERALOGICAL AND GEOCHEMICAL PROFILING OF

ARSENIC-CONTAMINATED ALLUVIAL AQUIFERS IN

THE GANGES-BRAHMAPUTRA FLOODPLAIN

MANIKGANJ, BANGLADESH

Mohammad Shamsudduha

Master of Science, August 4, 2007
(M.Sc., University of Technology Sydney, Australia, 2004)
(M.Sc., Dhaka University, Bangladesh, 2000)
(B.Sc., Dhaka University, Bangladesh, 1998)

203 Typed pages

Directed by Ashraf Uddin

The present study investigated three major components – groundwater, sediment and minerals of arsenic-affected Quaternary alluvial aquifers in Manikganj town, which is located in one of the As-hotspots in central Bangladesh. Approximately 60% of surveyed tubewells (n=88) within an area of 40 km^2 in and around Manikganj town contain arsenic concentrations exceeding 10 µg/L. Measured arsenic concentrations are as high as 191 µg/L with a mean value of 33 µg/L. Groundwater both in shallow (< 100 m) and deeper (> 100 m) aquifers is mainly Ca-HCO_3 type with a mean redox potential of -88 mV and a mean pH value of 6.75. Multivariate statistical analyses revealed that As in groundwater is closely associated with Fe, Mn, Si and pH. Groundwater As is negatively

correlated with SO_4. Results suggest that the As-contaminated groundwaters are under Fe- and/or Mn-reducing conditions.

Several fining-upward sequences form the aquifers in Manikganj. Shallow aquifers are composed mainly of gray sands with silts and gravels toward the bottom. Deeper aquifers are yellow to yellowish-brown, medium to fine sands with occasional gravels. High arsenic concentrations (as high as 8.8 mg/kg) are found in fine-grained sediments, mostly clay and silty clay that were probably deposited as overbank and natural levee deposits mainly by meandering river channels. Alluvial sediments, which were probably deposited during the Holocene sea-level lowstand, form the deeper aquifers that are As-free (< 50 μg/L). Sediments both in shallow and deep aquifers are composed of quartz, feldspars (mainly K-feldspar), lithic fragments and abundant (3-10 wt%) heavy minerals including magnetite, ilmenite, biotite, amphibole, pyroxene, garnet, kyanite, sillimanite, apatite, sphene, epidote and zircon. Authigenic Fe-oxyhydroxides (goethite), and siderite concretions are found in drill-core sediments. Goethite grains, which contain significant amounts of arsenic (as high as 341 mg/kg), are abundant in shallow sediments. Results suggest that microbially mediated reductive dissolution of Fe-oxyhydroxides is the principal mechanism for releasing arsenic into groundwater. Detrital magnetite, apatite, biotite and amphibole, which are also abundant in shallow sediments, are additionally considered as potential As-carriers for groundwater in the alluvial shallow aquifers in Bangladesh.

ACKNOWLEDGMENTS

It is a great pleasure to thank the people who made this thesis possible. This work would not have been a successful study of geoscience without the enthusiastic support of my thesis advisor, Dr. Ashraf Uddin. I thank my advisor for bringing me to Auburn University for a Master's degree in Geology. Dr. Uddin has been the best advisor and teacher I could have wished for. He has been actively involved in my research and brought the best out of me in my work. I show my immense gratitude and respect to Dr. Uddin for his constant support and inspiration that has brought me many awards throughout the period I have been at Auburn University.

I would also like to express my gratitude to Drs. James Saunders, Ming-Kuo Lee and Willis Hames for their guidance and support. My knowledge in aqueous geochemistry has significantly improved because of Dr. Saunders. I thank Dr. Lee for being very supportive in every aspect of my research. Dr. Hames helped me immensely in the development of my knowledge in metamorphic petrology. I would like to thank Dr. Luke Marzen for training me in the GIS and remote sensing techniques, which were very helpful in preparing illustrations for my thesis and posters that I presented in several professional meetings. I also would like to thank the other faculty members in the department of Geology and Geography for being very inspirational to me.

This research was possible for financial support from the U.S. National Science Foundation (EAR-0352936 and EAR-0445250), Geological Society of America (Grant

no. 8396-06) and Auburn University. I thank the Department of Geology and Geography of Auburn University for providing me support through graduate teaching and research assistantships. I would like to thank Dr. Kazi Matin Ahmed of Dhaka University for his support and help during the field investigation in Manikganj, Bangladesh. Help from Mr. Tareq during the field investigation and data collection is greatly acknowledged. I also acknowledge the help from Mr. Chris Fleisher at University of Georgia for electron microprobe analysis. I thank Jamey Turner and Sadia Arafin for prior work in Manikganj. I am grateful to departmental staff at Auburn University for their friendly support. Thanks are also due to my fellow graduate students and friends at Auburn University for their friendship and pleasure they have provided, especially during the football games at Auburn.

Most importantly, I wish to thank and express my devotion to my parents, Mr. Mohammad Mahtab Uddin and Mrs. Rabeya Khatun and my beloved sisters for their support and inspiration. Lastly, but most lovingly, I would like to thank my precious wife, Samsun Nahar Shonima for her enormous sacrifice by letting me come to the United States leaving her home behind for the last two longest years in our lives. I greatly recognize her support and inspiration in every step of my research and graduate study.

Finally, I dedicate this thesis to my beloved parents and dearest wife.

Style manual or journal used

Applied Geochemistry

Computer software used

Adobe Acrobat 6 Professional

Adobe Illustrator 8.0

Adobe Photoshop 5.5

ArcGIS 9.1

Golden Software Grapher 3.0

Golden Software Surfer 8.0

Microsoft Excel 2003

Microsoft Word 2003

MINITAB 13

RockWare 2004

TABLE OF CONTENTS

LIST OF FIGURES

LIST OF TABLES

CHAPTER 1

INTRODUCTION

1. Introduction

1.1. Groundwater arsenic in Bangladesh

Naturally occurring high concentration of dissolved arsenic (As) in groundwater of alluvial aquifers in Bangladesh (Fig. 1.1) has been causing serious health problems in millions of people for almost last three decades. Given the extensive occurrences of high arsenic concentrations in groundwaters and exposure of a large population, the groundwater arsenic-contamination in Bangladesh has been recognized as the most cataclysmic environmental problem in the world (BGS and DPHE, 2001). In Bangladesh, groundwater is the principal source of drinking and irrigation water supplies. Millions of tubewells were installed in the Ganges-Brahmaputra-Meghna (GBM) delta complex in almost last four decades that provided pathogen-free water for domestic and irrigation purposes in Bangladesh (Smith et al., 2000; BGS and DPHE, 2001). The major switch from polluted surface water to groundwater in early 1970's helped people avoid waterborne diseases, but detection of elevated dissolved arsenic in groundwater has frightened the people of Bangladesh (Nickson et al., 2000; BGS and DPHE, 2001). In 1993, the Department of Public Health Engineering (DPHE) of Bangladesh first reported the existence of arsenic poisoning in the groundwater of Bangladesh in an area bordering

Fig.1.1 Map of major administrative divisions, major river channels, and road networks in Bangladesh. India surrounds Bangladesh in most parts, and only a small portion of the country in the southeast is bordered with Myanmar (Burma). Bay of Bengal is located to the south.

the West Bengal, India, but it was not until 1995 that the extensive occurrence of high arsenic was widely known (Dhar et al., 1997; WARPO, 2000; BGS and DPHE, 2001). The National Hydrochemical Survey of Bangladesh (NHS), which was carried out by DPHE and British Geological Survey (BGS), and Mott MacDonald Ltd. in 1998 and 1999 analyzed 4,140 tubewells (including special study areas) for arsenic and other elements (Fig. 1.2). The survey found that nearly 35 million people were drinking groundwater containing As with a concentration of more than 50 µg/L (Bangladesh standard), and about 57 million people exposed to a concentration exceeding 10 µg/L (World Health Organization standard), mostly extracted from alluvial aquifers located within 10-50 m of the ground surface (BGS and DPHE, 2001).

The occurrence, origin, and mobility of arsenic in groundwater in Bangladesh and many other parts of the world in similar environments are reported (Ravenscroft et al., 2001). The mode of occurrence and mobility of arsenic in sedimentary aquifers are mainly influenced by local geology, geomorphology, hydrogeology, and geochemistry of sediments and water, as well as anthropogenic activities, such as mining and land use (Bhattacharya et al., 1997; BGS and DPHE, 2001; Smedley and Kinniburgh, 2002). In Bangladesh, the occurrence of arsenic and its mobilization is associated with geochemically reducing subsurface environment. Several recent studies agreed that biogenic reductive dissolution of Fe-oxyhydroxides is the primary release mechanism that puts arsenic into groundwater in Bangladesh alluvial aquifers (Bhattacharya et al., 1997; Nickson et al., 1998; Zheng et al., 2004). A study in the central Bangladesh by Harvey et al. (2002) suggested that arsenic mobilization may also be associated with recent inflow of carbon due to large-scale irrigation pumping, which needs further

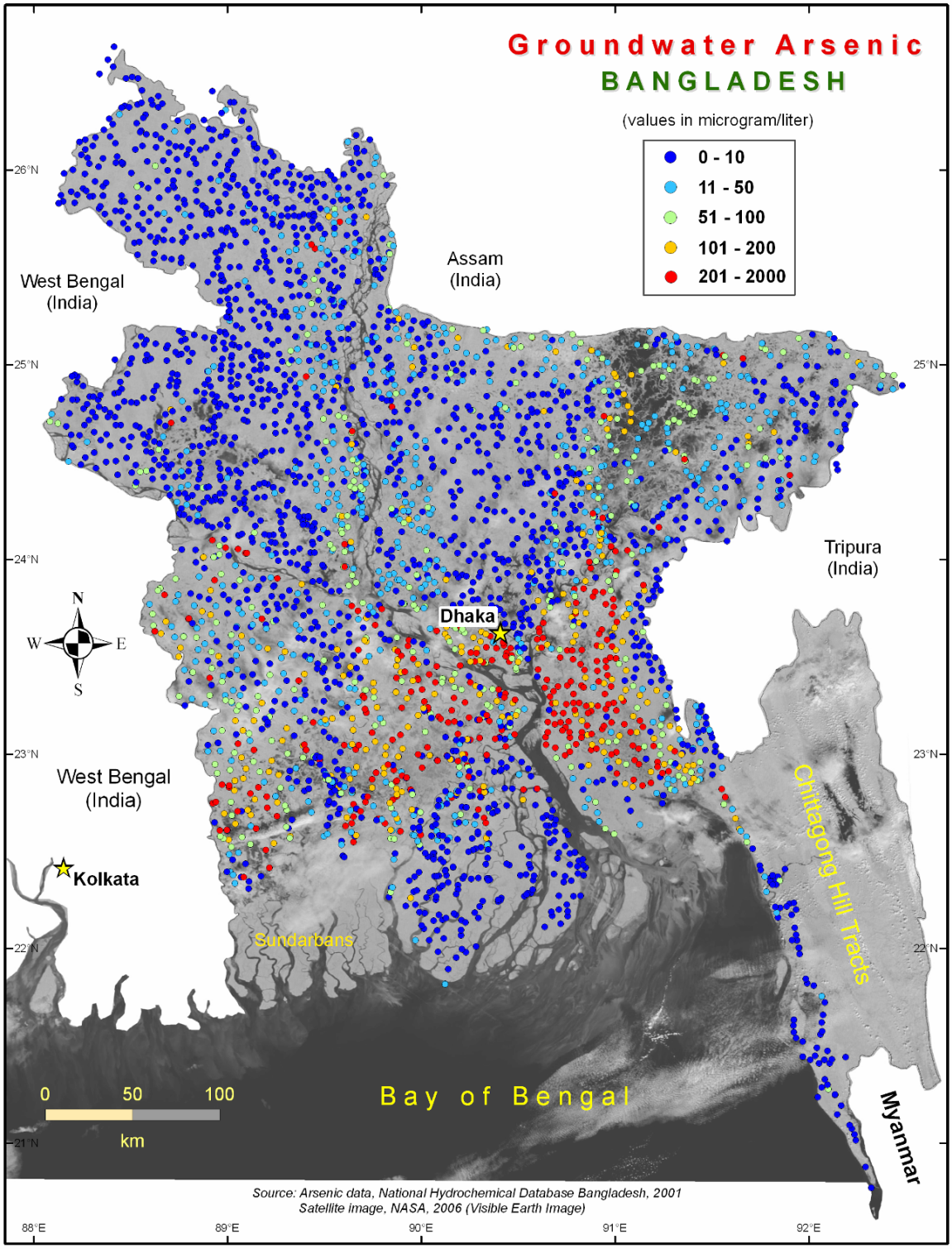

Fig. 1.2 Map of groundwater arsenic concentration in tubewells in Bangladesh. Tubewell arsenic concentration data collected from the National Hydrochemical Survey (NHS) of Bangladesh (BGS and DPHE, 2001).

investigation. Saunders et al. (2005) attempted to link the elevated arsenic occurrences in groundwater with the retreat of continental glaciation at the end of Pleistocene, which led to the rise of sea level during the Early to Middle Holocene, and deposition of alluvium and extensive marsh and peat and finer sediments in Bengal lowlands (Ravenscroft et al., 2001). During the Pleistocene time the mechanical weathering of rocks in source areas (e.g., Himalayas, Indian Shield, and Indo-Burman mountains) was enhanced due to mountain building activities and glaciation. The aquifer sands in the Bengal Basin were largely derived from physical weathering and erosion at a time of extended glaciation in the Himalayas, but the intensity of chemical weathering was limited by the low temperatures during erosion (McArthur et al., 2004).

In Bangladesh, high groundwater arsenic occurrences and distributions are confined within the Holocene sediments, particularly in lower Meghna estuaries at shallow depths, in Sylhet trough at relatively deeper depths, and the lower GBM delta excluding the present-day tidally influenced delta plains (Fig. 1.2). The spatial distribution of arsenic shows a very good correlation with surface elevations in Bangladesh and possibly in West Bengal located within the Bengal Basin (Shamsudduha et al., 2006). Higher arsenic concentrations are mainly confined within low surface elevation with very low slope and most likely lower hydraulic gradient in the country. Results show that the mean arsenic concentration in groundwaters is more than 50 μg/L in the wells shallower than 60 m in depth and where the surface elevation is below 10 m.

The relationships between groundwater arsenic and aquifer mineralogy, geochemistry and sediments characteristics are not well studied. Few studies in Bangladesh and West Bengal, India, found that fine-grained sediments (e.g., clay), and

peat in the Holocene deposits contain high arsenic concentrations (e.g., BGS and DPHE, 2001; Pal et al., 2002; Tareq et al., 2003; Sengupta et al., 2004). Within the coarse-grained sediment layers, the sand coated by iron-oxyhydroxides, residual magnetite, ilmenite, illite, iron hydroxides-coated grains, biotite, and siderite concretions contain most of the arsenic (Pal et al., 2002; Ahmed et al., 2004). Dissolved arsenic shows a moderate to strong statistical and spatial correlation with iron and phosphorous in groundwaters located underneath the Holocene geologic-geomorphic units of Bangladesh (Shamsudduha et al., 2006). Few studies that were performed on heavy mineral assemblages in the arsenic-contaminated aquifers suggested that the arsenic-bearing sediments are primarily derived from the Himalayas and the shield areas. However, the presence of high arsenic in sediments is not associated directly with primary arsenic-bearing minerals, rather mostly appears to be secondary in origin (Ghosh and De, 1995).

1.2. Global arsenic scenario

A number of large aquifers in various parts of the world have been identified with problems from arsenic occurring at concentrations above 50 μg/L or so (Fig. 1.3). Arsenic contamination of natural origin in groundwater has also been reported in many other parts of the world, including Argentina, Australia, China, Chile, Pakistan, Taiwan, Thailand, Mexico, Vietnam, and many parts of the United States (Smedley and Kinniburgh, 2002; Nickson et al., 2005; Liu et al., 2006). However, the human health-effects of groundwater arsenic in the Bengal Basin are the most widespread. Recent reconnaissance surveys of groundwater quality in other areas, such as parts of Nepal, Myanmar and Cambodia have also revealed concentrations of arsenic in groundwaters

exceeding 50 µg/L. Arsenic associated with geothermal waters has also been reported in several areas, including hot springs from parts of Argentina, Japan, New Zealand, Chile, Iceland, France, Dominica and parts of the USA (Smedley and Kinniburgh, 2002). Mining related arsenic problems in water have been identified in many parts of the world, including Ghana, Greece, Thailand and the USA (Fig. 1.3).

Groundwaters in the Quaternary alluvial aquifers around the world are mostly contaminated with elevated arsenic. Several aquifers around the world contain unacceptably high concentrations of dissolved arsenic. These include aquifers in parts of Argentina, Chile, Mexico, southwest United States, Hungary, Romania, Bangladesh, India, China (including Taiwan), Myanmar, Nepal, and Vietnam (Fig. 1.3). These areas have similarities in geology and hydrogeology. The majority of the high-arsenic groundwater provinces are in young unconsolidated sediments mostly of Holocene (<12,000 years) age (Ravenscroft et al., 2005). These aquifers are usually large inland closed basins in arid or semiarid settings (e.g., Argentina, Mexico, and southwest United States) or large alluvial and deltaic plains (e.g., Bengal delta, Yellow River plain, Irrawaddy delta, Red River delta) (Smedley and Kinniburgh, 2002).

Groundwater arsenic-contamination in South and Southeast Asia, particularly in the Bengal Basin, Red River delta, Indus delta, and in alluvial plains in Nepal has affected millions of people for last few decades (Fig. 1.4). The scale of groundwater arsenic occurrences and the numbers of affected people in this region have led to significant attention of the scientific community around the world.

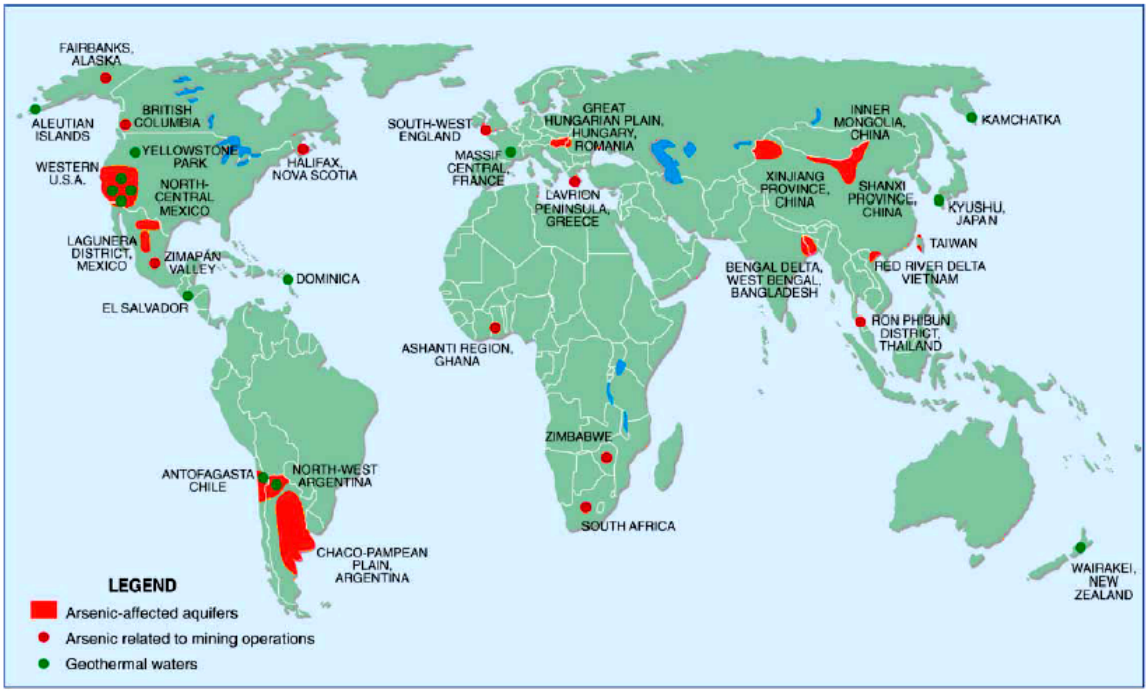

Fig. 1.3 Global groundwater arsenic distribution map shows the major arsenic-affected groundwater aquifers around the world (modified after Smedley and Kinniburgh, 2002).

1.3. Sources of arsenic in nature

Arsenic occurs naturally in all minerals and rocks, mainly in sedimentary and igneous rocks. However, the concentration of arsenic varies within different types of rocks in nature (Table 1.1). Both natural and anthropogenic activities can bring in arsenic in the environment. Erosion and weathering of crustal rocks lead to the breakdown of translocation of arsenic from the primarily sulfide minerals (Bhattacharya et al., 2002).

Arsenic occurs as a major constituent in more than 200 minerals, including elemental arsenic, arsenides, sulfides, oxides, arsenates, and arsenites (Smedley and Kinniburgh, 2002). The most abundant arsenic ore mineral is arsenopyrite (FeAsS), commonly associated with igneous rocks. Other arsenic bearing ore minerals are chalcopyrite, galena, and marcasite, where concentrations of arsenic can be very variable (Table 1.2). Pyrite is also formed in low-temperature sedimentary environments under reducing conditions. It is present in sediments of many rivers, lakes, oceans, and in many aquifers around the world. High concentrations of arsenic are also found in many oxide minerals and hydrous metal oxides, either as part of the mineral structure or adsorbed to surfaces. Concentrations of arsenic in iron-oxides minerals are also high (Table 1.2).

Adsorption of arsenate to hydrous iron-oxides is known to be particularly strong. Adsorption to hydrous aluminum and manganese oxides may also be important if these oxides are present in sediments in great quantity (Brannon and Patrick 1987; Smedley and Kinniburgh, 2002). Groundwater arsenic contamination in the Bengal Basin and other similar geologic setup are believed to be associated with high concentrations of iron-oxides and iron-oxyhydroxides (Nickson et al., 1998; Smedley and Kinniburgh, 2002; Sengupta et al., 2004).

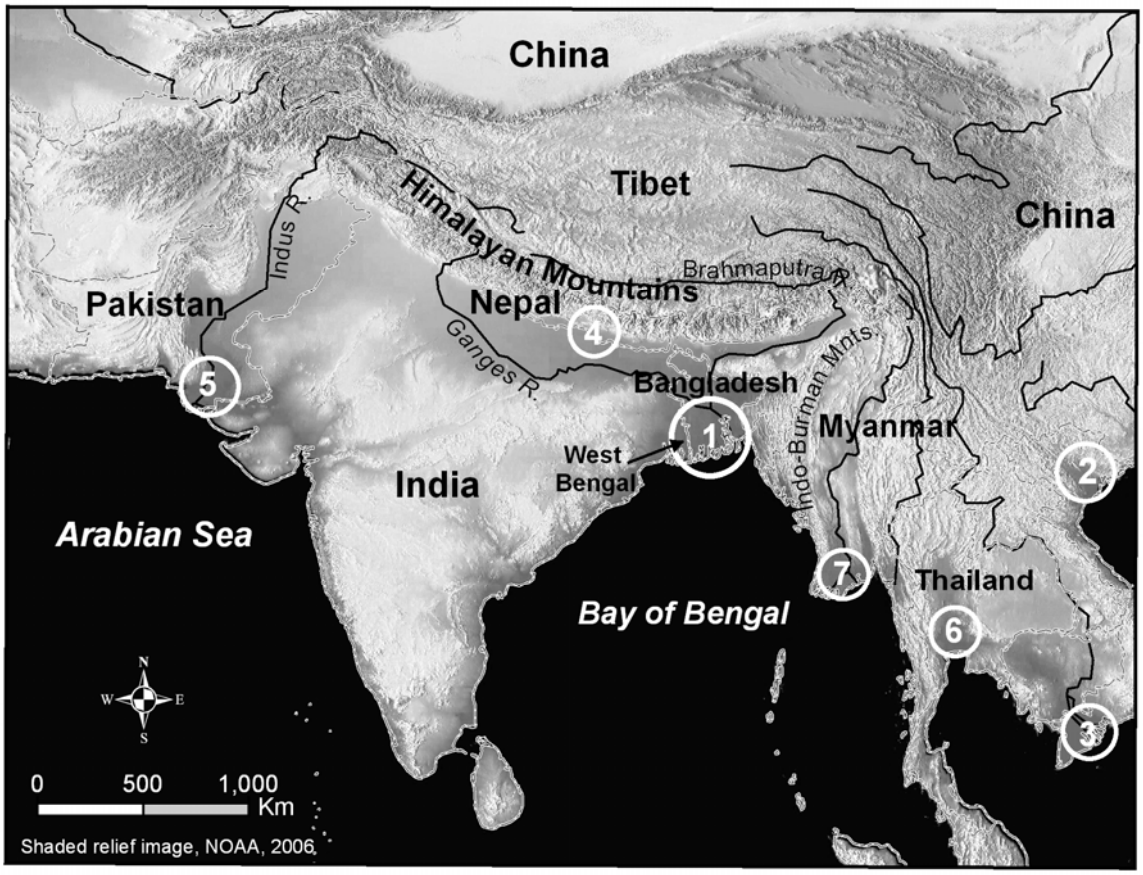

Fig. 1.4 Map of groundwater arsenic contamination in the major deltaic and floodplains in South Asian countries. Locations shown within white circles are: (1) Ganges-Brahmaputra-Meghna delta, Bangladesh and West Bengal; (2) Red river delta, Hanoi, Vietnam; (3) Mekong delta, Vietnam and Cambodia; (4) Terai alluvial plain, Nepal; (5) Indus delta, Pakistan; (6) Central Thailand; and (7) Irrawaddy river delta, Myanmar.

Table 1.1 Typical arsenic concentrations in rock-forming minerals (Source: Smedley and Kinniburgh, 2002 and references therein).

.

Name of mineral	Arsenic concentration range (mg/kg)
Sulfide minerals:	
Pyrite	100–77,000
Pyrrhotite	5–100
Marcasite	20–126,000
Galena	5–10,000
Sphalerite	5–17,000
Chalcopyrite	10–5,000
Oxide minerals:	
Hematite	up to 160
Fe oxide (undifferentiated)	up to 2,000
Fe(III) oxyhydroxide	up to 76,000
Magnetite	2.7–41
Ilmenite	< 1.0
Silicate minerals:	
Quartz	0.4–1.3
Feldspar	< 0.1–2.1
Biotite	1.4
Amphibole	1.1–2.3
Olivine	0.08–0.17
Pyroxene	0.05–0.8
Carbonate minerals:	
Calcite	1–8
Dolomite	< 3.0
Siderite	< 3.0
Sulfate minerals:	
Gypsum/anhydrite	< 1–6
Barite	< 1–12
Jarosite	34–1,000
Other minerals:	
Apatite	< 1–1,000
Halite	< 3–30
Fluorite	< 2.0

Table 1.2 Typical arsenic concentration ranges in rocks, sediments, and soils (Source: Smedley and Kinniburgh, 2002 and references therein).

Classification	Rock/sediment type	Arsenic range (mg/kg)
Igneous rocks	Ultrabasic rocks	0.03–16
	Basic rocks	1.5–110
	Intermediate	0.09–13
	Acidic rocks	0.2–15
Metamorphic rocks	Quartzite	2.2–7.6
	Hornfels	0.7–11
	Phyllite/slate	0.5–140
	Schist/gneiss	< 0.1–19
	Amphibolite/greenstone	0.4–45
Sedimentary rocks	Shale/mudstone	3–490
	Sandstone	0.6–120
	Limestone	0.1–20
	Phosphorite	0.4–190
	Iron formations and iron-rich sediment	1–2,900
	Evaporite deposits	0.1–10
	Coal	0.3–35,000
	Bituminous shale	100–900
Unconsolidated sediments and soils	Sediments	0.5–50
	Soils	0.1–55
	Soils and near sulfide deposits	2–8,000

1.4. Objectives of present study

The objectives of the present study are designed to address three broad questions. Each of these questions is described in detail under the following headings:

(1) Are there any significant differences in mineralogy and sediment geochemistry from high arsenic-rich areas at relatively shallower depth (<100 m) to low arsenic area at deeper depth (>100 m) in the vertical sequences of core samples from the study area? If so, then what mechanism (s) is/are influencing the vertical distribution of arsenic in groundwater?

Studies on groundwater chemistry in connection with arsenic contamination have mostly been focused in Bangladesh for a number of years, but primarily since 1993. A few studies aimed at mineralogy and sediment geochemistry to find out the relationship with groundwater arsenic (e.g., Ghosh and De, 1995; Ahmed et al., 2004; Horneman et al., 2004; Sikder et al., 2005) both in Bangladesh and West Bengal, India, but were mainly limited to shallow depths (0-50 m). No systematic study has provided any detail mineralogical profiling (i.e., detrital and authigenic phases) of alluvial aquifers in Bangladesh. This study focuses on detail mineralogical studies on sediment core samples as deep as 152 m depth collected from the central part (Manikganj Town) of Bangladesh located within the Ganges-Brahmaputra floodplain, where aquifers are contaminated with moderate to high concentration of groundwater arsenic. The main purpose of this study was to identify mineralogical assemblages within aquifer sediments both in arsenic-contaminated shallow aquifers (< 100 m) and arsenic-free deep aquifers (> 100 m). Systematic variations in arsenic concentrations in different sediment layers of the above mentioned core samples have been analyzed in this study.

(2) What are the mineral phases (detrital and authigenic) associated with high concentration of arsenic in sediments and how do they control the mobility of arsenic and other elements in groundwater?

The occurrence of arsenic in sediments and minerals and the processes that cause the release and mobilization of arsenic into groundwater have yet not been clearly understood. Though few studies (e.g., Sikder et al., 2005) carried out mineralogical analyses on arsenic-bearing sediments in Bangladesh, but no attempts have been made to study heavy minerals and authigenic mineral phases from aquifer sediments. Reductive dissolution of Fe (III)-oxyhydroxides present as coating on sand grains as well as altered mica (biotite) is expected to play a major role in arsenic mobilization in groundwater (Ahmed et al., 2004). Residual magnetite and ilmenite are also considered as one of the sources of groundwater arsenic (Pal et al., 2002). A recent study (Turner, 2006) has found that siderite in aquifer sediments in Manikganj may control Fe concentration and thus could affect arsenic mobilization in groundwater. The present study focused on several heavy minerals in sediments, such as magnetite, ilmenite, biotite, chlorite, apatite, and authigenic minerals like siderite, rhodochrosite, and pyrite to evaluate the principal source and sink of arsenic in water. Provenance information has been obtained through petrofacies studies that have indicated type of source rocks eroding from orogenic belts, craton and plateaus, and recycled orogenic exposures (Uddin and Lundberg, 1998b).

(3) How are groundwater geochemistry and arsenic occurrences correlated with sediment geochemistry, mineralogy and depositional environments?

Groundwater in Holocene alluvial aquifers at shallower depth (0-50 m) in Bangladesh is often contaminated by arsenic. Aquifers in the Pleistocene uplands and

Tertiary hills are low in arsenic concentrations (Ahmed et al., 2004). Pleistocene deposits, composed of yellowish-brown to orange oxidized sands are generally devoid of organic matters and arsenic. Elevated arsenic, which is often associated with high dissolved iron and manganese, occurs within the highly reducing Holocene aquifers containing abundant organic matter. Arsenic release is likely controlled by anaerobic iron- and manganese-reducing bacteria (McArthur et al., 2001; Islam et al., 2004; Saunders et al., 2005). This study has incorporated the groundwater chemistry with sediment geochemistry and characteristics to investigate the changes of subsurface geochemical environments within a vertical profile.

1.5. Location of the study area

The study area is located approximately 70 km northwest of Dhaka city, the capital of Bangladesh (Fig. 1.5). Geographically, the study area is confined within 23.80° to 23.90° N latitudes, and 89.95° to 90.05° E longitudes, and mostly occurs within Ganges-Brahmaputra floodplain deposits. Dhaleshwari and Kaligonga rivers are the major distributaries of the Brahmaputra river within the study area (Fig. 1.6). Flooding is common in the floodplains of Kaligonga and Dhaleshwari rivers and within some topographic depressions during the monsoon season. Annual temperatures of Manikganj district range from 36°C to 12.7°C. The total annual rainfall in Manikganj area is approximately 2,376 mm.

Fig. 1.5 Map showing major administrative divisions of Manikganj District with major river channels and road networks. The study area is located in Manikganj Thana itself bounded by Kaligonga and Dhaleswari rivers (Source: Banglapedia, 2003).

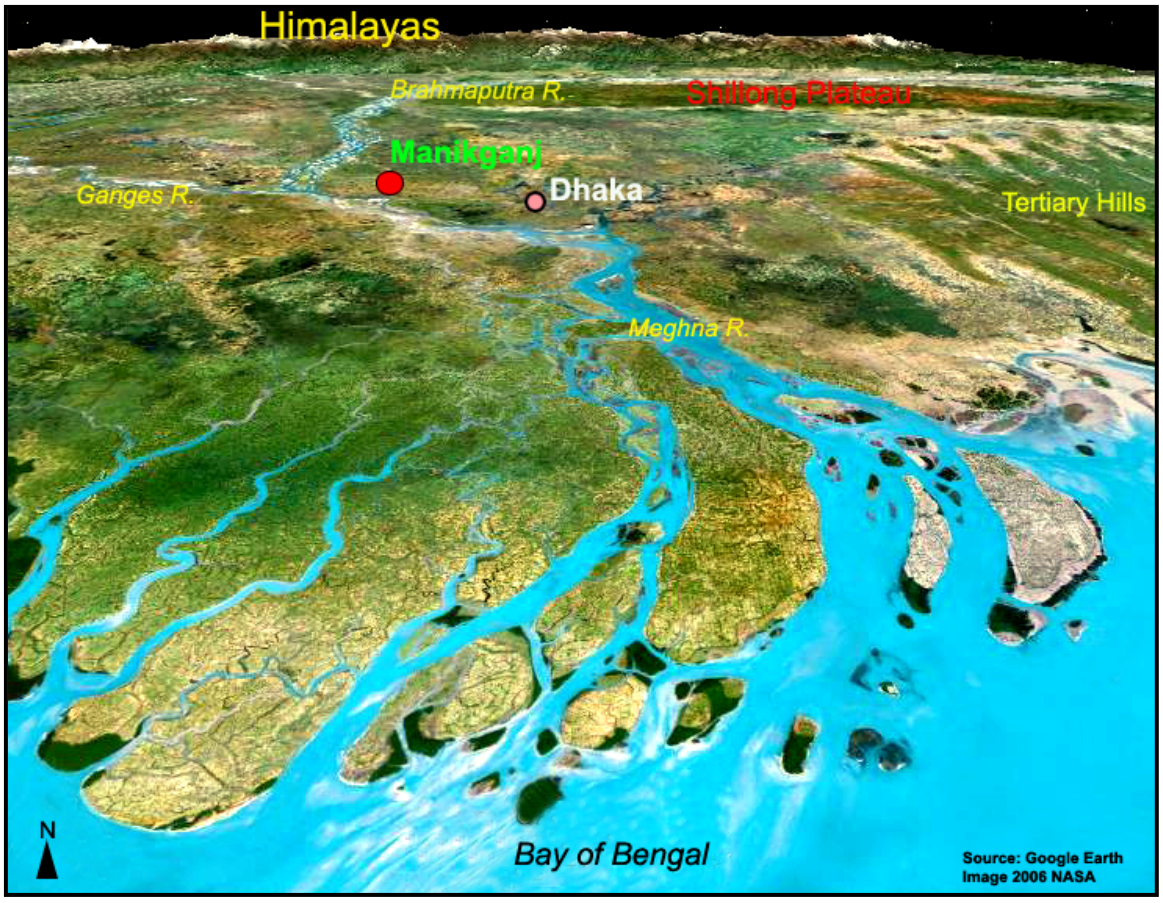

Fig. 1.6 False-colored satellite image shows the major physiographic features of the Bengal Basin. Himalayas are located in the far north. Two major rivers – the Ganges and Brahmaputra along with Meghna form the major deltaic systems in the basin. Manikganj is located within the Ganges-Brahmaputra floodplains (Source of image: Google Earth).

1.6. Thesis outline

This thesis contains three major components – groundwater, sediments and mineralogy of the Quaternary deposits in Manikganj area. A total of eight chapters form this thesis paper. The first chapter gives the general background of groundwater arsenic occurrences in Bangladesh as well as other countries around the world. Objectives of this study are also described in this chapter. Chapter two describes the geology and geomorphology of the Bengal Basin and the study area. Chapter three outlines all the methods used in this thesis. Stratigraphy and hydrogeology of the study area are described in chapter four. This chapter also describes the influence of climatic conditions on the regional and local geology and hydrogeology. Groundwater chemistry, distribution of arsenic and other geochemical parameters are shown in chapter five. Chapter six describes the lithology, sediment geochemistry and petrography of the Quaternary deposits in the study area. Mineralogy and connection with groundwater arsenic occurrences in aquifers are also explained in this chapter. Chapter seven discusses the results and explains the occurrences of elevated groundwater arsenic in shallow alluvial aquifers in Manikganj and other locations in Bangladesh. Finally, chapter eight concludes the thesis with a summary of the major findings. Description of core samples from both MG and MN sites are presented in the Appendix of this thesis.

CHAPTER 2

GEOLOGY AND GEOMORPHOLOGY

2. Geology and Geomorphology

2.1. Regional geology of the Bengal Basin

The Bengal Basin, located in South Asia has been the major depocenter of sedimentary flux from the Himalayas and Indo-Burman ranges drained by the Ganges-Brahmaputra-Meghna, the largest river system in the world (Fig. 2.1). The basin is bounded by the Himalayas to the distant north, the Shillong Plateau, a Precambrian massif to the immediate north, the Indo-Burman ranges to the east, the Indian craton to the west, and the Bay of Bengal to the south (Uddin and Lundberg, 1998a). The basin includes one of the largest delta complexes (GBM delta) in the world, covering a vast portion of the basin filled with about $5x10^5$ km^3 of sediments (Johnson, 1994). Thick sedimentary deposits of the basin fill have been uplifted significantly along the north and eastern margins of the Sylhet trough in the northeast and along the Chittagong foldbelts of eastern Bangladesh (Uddin and Lundberg, 1998b).

The alluvial plains of the GBM delta slope from north to south on a regional scale, but are interrupted locally by ridges and tectonically developed depressions, such as, Sylhet trough and Atrai depression. The Bengal Basin (Fig. 2.1) comprises lowland

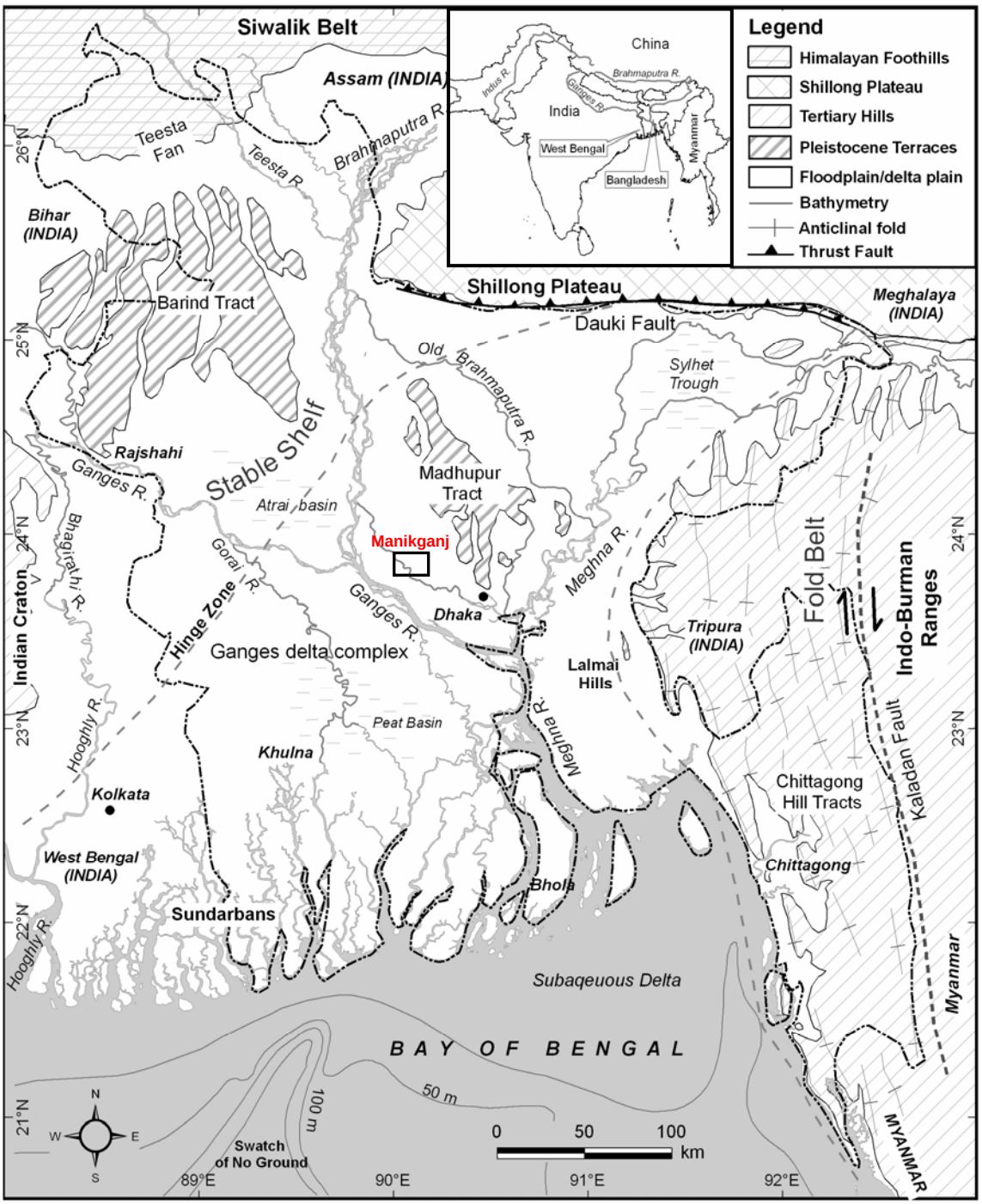

Fig. 2.1 Simplified geological map of the Bengal Basin. Ganges, Brahmaputra and Meghna rivers formed one of the largest deltaic systems, occupied by Bangladesh and West Bengal, India. Manikganj study area is shown as a rectangle, located to the southwest of Madhupur Tract (after Goodbred and Kuehl, 2000; Uddin et al., 2007).

floodplain and delta plain, and is surrounded by the Tertiary hills of various origins (Goodbred and Kuehl, 2000; Ravenscroft et al., 2005). Within the eastern Bengal Basin, the Madhupur Tract and Barind Tract are uplifted alluvial deposits of Pleistocene age interrupt the regional surface gradient of the central basin (Morgan and McIntire, 1959). Neotectonically uplifted Lalmai Hills located to the southeast of Madhupur Tract are composed of highly oxidized clay and sand of Pleistocene age. Underneath the Pleistocene tracts, there is yellowish-brown colored sandy aquifer, formed within the Pliocene-Pleistocene Dupi Tila sand (Uddin and Lundberg, 1998a).

The basin borders the Indian craton (Fig. 2.1) to the west and once formed part of Gondwana sediments, which are still preserved in faulted troughs or grabens below the Cretaceous-Tertiary cover (Stüben et al., 2003). The Rajmahal Trap, a flood basalt unit, separates the Gondwana sequence from the younger Cretaceous-Tertiary sediments. Although the initial convergence of the Indian and Eurasian Plates began in the early Eocene time (40-41 m.y. ago), uplift of the eastern Himalayas resulted in the Early Miocene (Uddin and Lundberg, 1998b). As a result of this convergence, the Ganges delta and the proto-Brahmaputra delta sediments were juxtaposed and gradually merged.

Surface elevation of the Bengal Basin is mostly less than 25 m above mean sea level, except for the Himalayan foothills in the northwest, Pleistocene tracts, and Chittagong hills in the eastern Bangladesh where surface elevations range from 25 m to about 1,000 m. In the eastern GBM delta, the surface elevation is less than 15 m, with a minimum of less than 1 m in the south. However, surface elevation of the GBM delta is slightly higher in the western part of the basin.

Elevation is also low (< 1-5 m) in the northeast Sylhet trough. Landforms in the Brahmaputra floodplains are mainly characterized by natural levees, and crevasse splays, alluvial sands, and channel fill deposits. Large marshes and peat lands characterize the Sylhet trough, which is flooded during the monsoon season by runoff from the adjoining hills. The easternmost part of the GBM delta, which is known as the Tippera surface (Morgan and McIntire, 1959), is slightly higher than adjacent floodplains, might have been tilted due to the neotectonic activities associated with east-west compression in the eastern Bengal Basin. Numerous tidal creeks and mangrove forests (Sundarbans) characterize the southern delta plain.

2.2. Geology of Manikganj area

Surface geology of Manikganj area is fairly simple. The whole district area is covered with the alluvial silt and clay, alluvial silt, and marsh peat and clay units (Fig. 2.2). Tectonically, Manikganj district is located in the southern periphery of the Madhupur Tract (a Pleistocene inlier), which is surrounded by the Brahmaputra (Jamuna) river to the west and Ganges (Padma) river to the south. These two major rivers are flowing along two major inherited neotectonic faults.

The stratigraphy of the study area is mainly covered by the Quaternary alluvial deposits, composed mostly of sand, silt, and clay (Fig. 2.3). Two major fining upward sedimentary sequences were identified in a comprehensive study by Geohazard Research Group and Hydrogeology Group of University College London in 2002, which will be abbreviated as GRG and HG (2002) for the rest of this thesis.

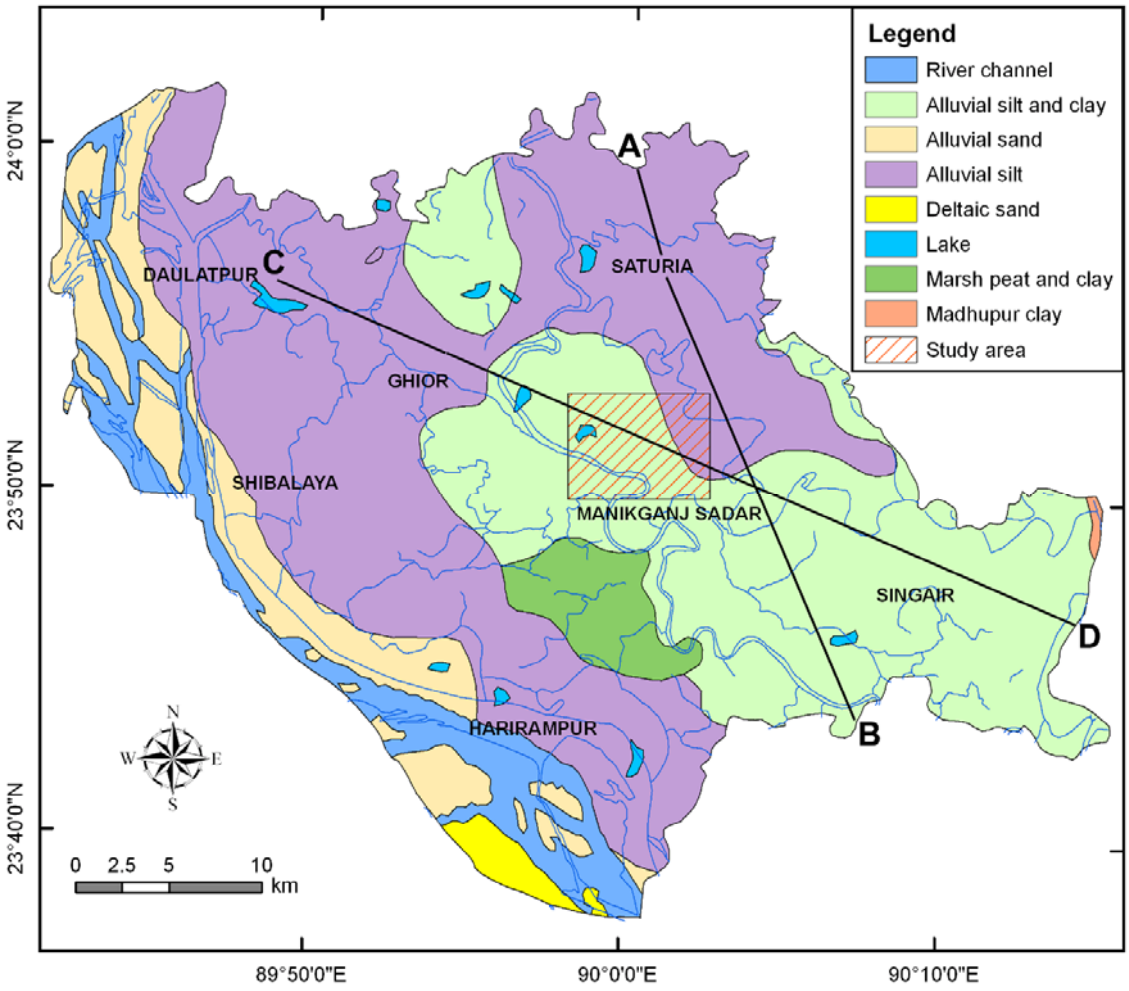

Fig. 2.2 Simplified surface geological map of Manikganj district. Alluvial silt and clay and Alluvial silt are the major two geological units in the study area, shown as a rectangle in the central part of the map. Lines A-B (north-south) and C-D (northwest-southeast) are the subsurface geological profiles shown on Fig. 2.3.

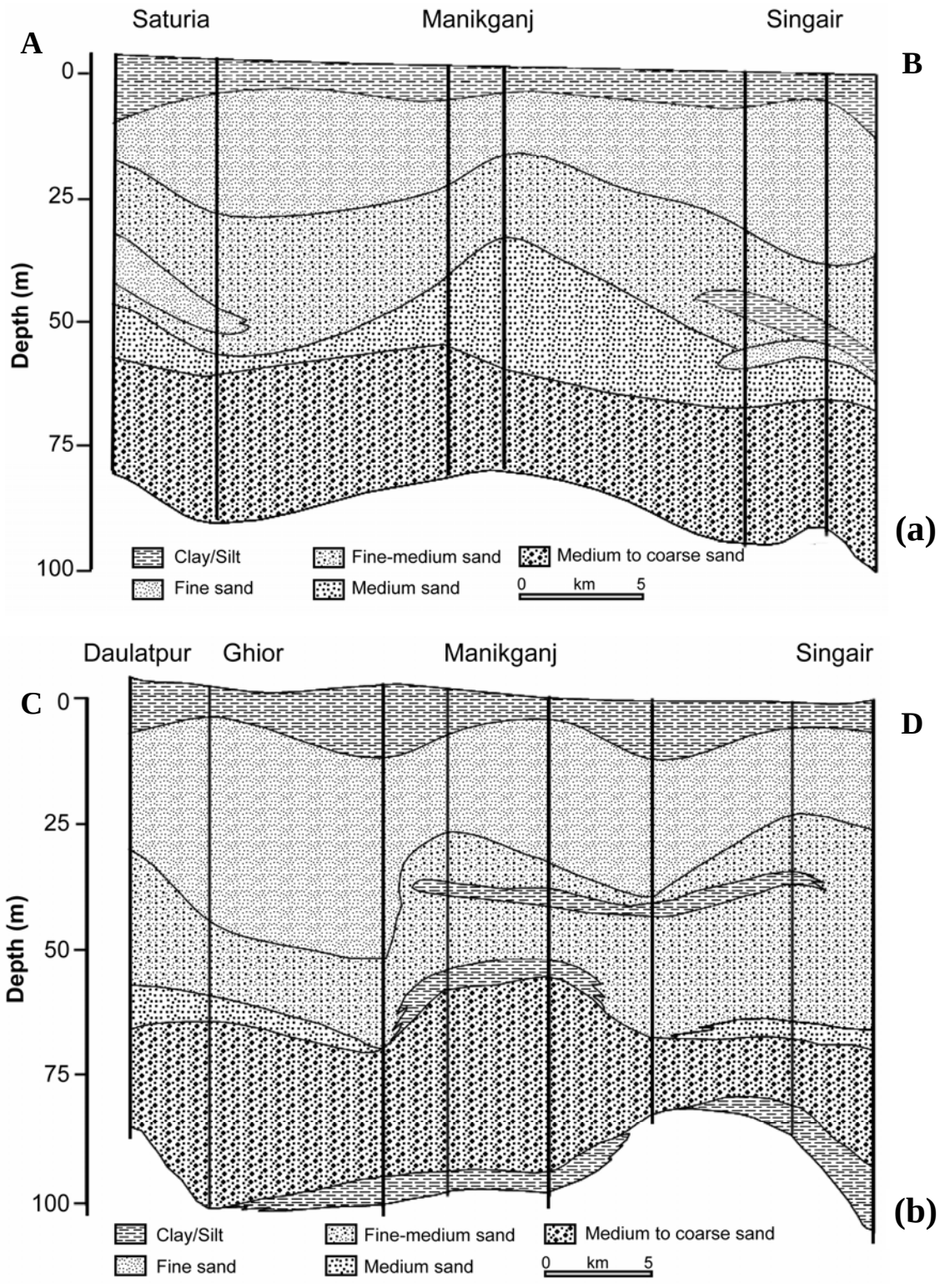

Fig. 2.3 Two geological cross-sections across Manikganj district. See locations of cross-sections on Fig. 2.2. (a) N-S (A-B) profile and (b) NW-SE (C-D) profile show fairly similar subsurface geology within the upper 100 m (modified from GRG and HG, 2002).

Based on several borehole lithologs, the subsurface geology of the study area has been divided into three major units: (i) the lower unit of yellowish-brown to yellowish-gray fine to medium sand with occasional coarse sand having a thickness ranging from 100-110 m; (ii) the middle unit of mostly gray-colored medium to fine sand with a thickness of about 80 m; and (iii) the uppermost unit of gray to light yellowish-gray colored fine sand, silt and clay with a thickness varying from 10-15 m.

The subsurface geology of Manikganj district is shown in two regional stratigraphic cross-sections, which run from north to south (Fig. 2.3a) and from northwest to southeast (Fig. 2.3b). Both cross-sections show the upper 100 m of stratigraphic succession in Manikganj. This illustrates the upper fining upward sedimentary sequence of Middle-Upper Holocene age (GRG and HG, 2002).

2.3. Geomorphology of Manikganj

Manikganj lies in the Brahmaputra-Ganges floodplain, located between the Madhupur Tract in the east and Ganges delta in the south (Fig. 2.1). The landscape of the study area is typically fluvial, characterized mainly by active channels, abandoned channels, natural levees, backswamps, and floodplains. Distribution of the geomorphic features throughout the study area suggests that the landforms were developed mostly over during the late Quaternary period (GRG and HG, 2002).

Two active meandering channels are located within the study location of which the Kaligonga flows to the southeast from the western side and the Dhaleshwari flows to the south from the eastern part (Fig. 2.4). The Kaligonga is the principal river, which is wider than the Dhaleshwari. However, the Dhaleshwari was the principal river channel of this

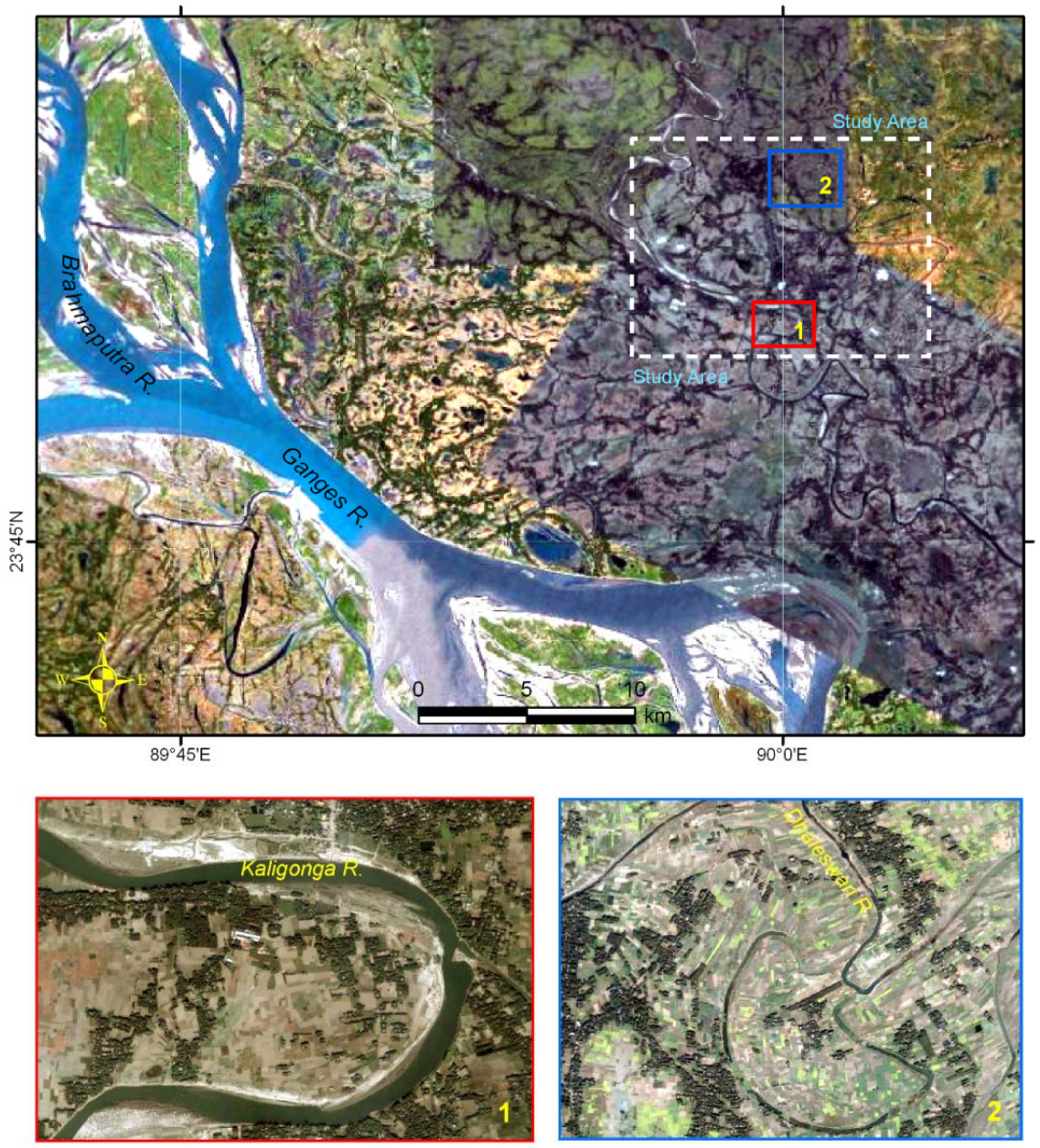

Fig. 2.4 False-colored satellite image shows the major two rivers and the location of Manikganj study area within white dotted line. Two areas were selected to zoom in and show the geomorphology of the study area. Kaligonga (Window-1) and Dhaleswari (Window-2) rivers are the major fluvial systems within the study area.

region in the historical past based on information from local elderly people. Numerous abandoned channels can also be identified in the satellite image. Most of the abandoned channels are associated with Dhaleshwari river flowing in the eastern side of the area, which indicates the persistent channel shifting in the past (GRG and HG, 2002). Numerous abandoned channels, flowing in the middle part of the area, were abandoned as the hydrodynamic conditions of the present-day major rivers changed with time.

Broad and well-developed natural levee deposits, which are mainly associated with the abandoned channels, suggest that this region was fluvially very active in the past (GRG and HG, 2002). However, the distributions of sand bodies are rather sparse that are generally associated with the seasonally active riverbeds and adjoining floodplains. In addition, some sand bodies are also present in the floodplain adjacent to the recently abandoned channels (Fig. 2.4).

Floodplains are distributed uniformly all over this study area. However, the floodplains of the western side are associated with some backswamps. These swampy lands are rejuvenated during the monsoon when the adjacent rivers are overflowed due to seasonal floods (GRG and HG, 2002). Moreover, numerous isolated smaller water bodies are located on the floodplains, mostly in the middle portion of the study area, where several abandoned channels and natural levees form a complex landscape.

Surface elevation of Manikganj district varies from 12 m to 2 m as shown in a digital elevation model (Fig. 2.5). Elevation is higher in the northern parts of the district and gradually decreases to the south. The major rivers are also flowing to the southeast, which indicates the general slope of this region. The difference in surface elevation within the study area is minimal, but the gradient is toward the southeast.

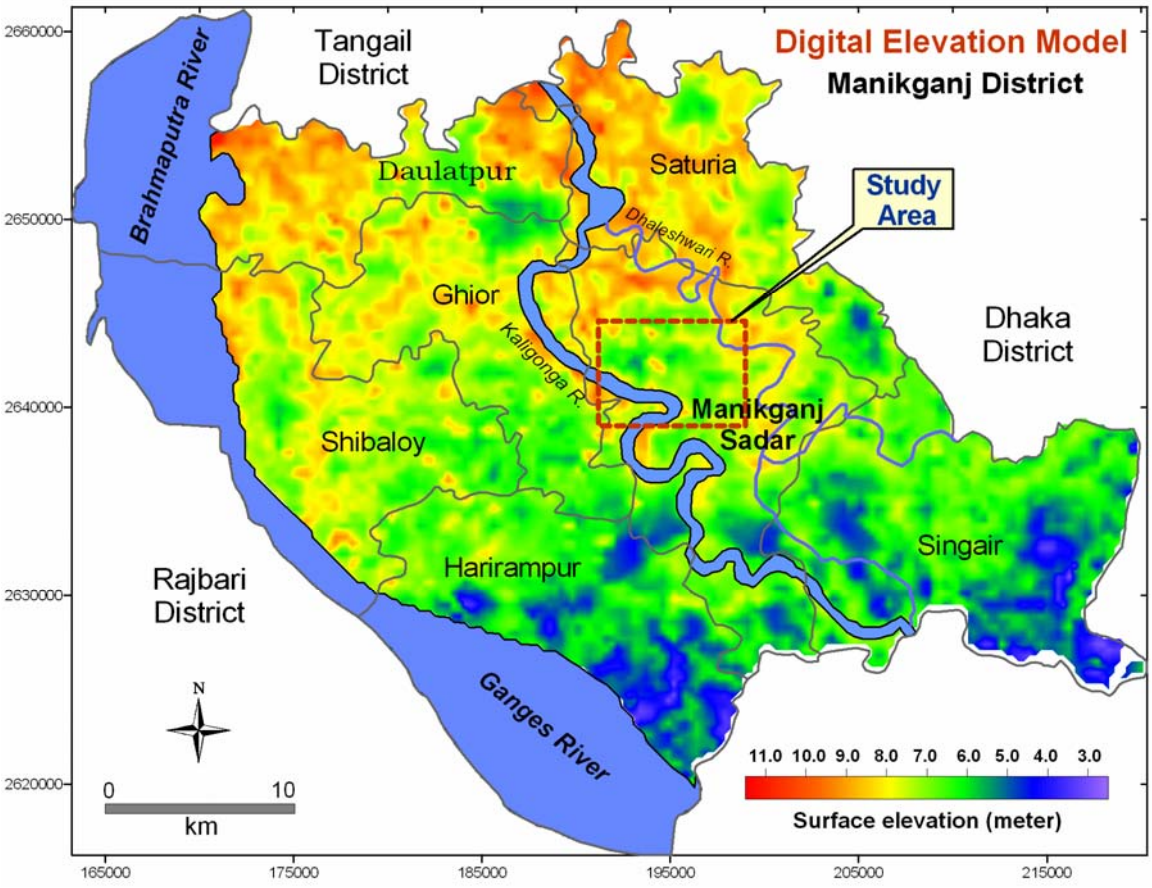

Fig. 2.5 Digital elevation model of Manikganj district. The general slope of this district is toward the southeast. Elevation varies from 12 m to as low as 2 m above mean sea level. Study area is located within a rectangle on the map.

CHAPTER 3

METHODOLOGY

3. Methodology

3.1. Field investigation

A field investigation was carried out between December 25, 2005 and January 8, 2006 in the study area located in the Manikganj Town. During the field investigation groundwater samples were collected from tubewells around the study location. A set of sediment core samples were also collected during the same period of field investigation. A detail description of field investigation and sampling procedure for groundwater and sediments is given below:

3.1.1. Groundwater sampling

Groundwater sampling was conducted at 23 tubewells (Fig. 3.1) in the study area. It is noteworthy to mention that present study also compiles geochemical results from other studies (e.g., BSG and DPHE, 2001; McCarthy, 2001; Arafin, 2003; Turner, 2006) conducted in the study location in order to create a large groundwater geochemical database. This database consists of a total of 88 groundwater samples with their geochemical results. The present study did not sample in the previously sampled tubewells in order to avoid duplication of data. However, only two tubewells were re-

sampled this time where a time series geochemical analysis has been conducted for bioremediation pilot project within the study area. This fieldwork was conducted by a team of five people: Dr. Ashraf Uddin, Dr. James Saunders, Dr. Mark Liles and the author himself from Auburn University, and Md. Tareq Chowdury from Dhaka University.

At each sampling site, the geographic location was recorded by a hand-held Global Positioning System (GPS), and information on well depth was acquired through personal communication with tubewell owner on spot. Before sampling, each tubewell was purged for an average of 10 minutes in order to expel the water sitting in the well casing and sample the representative water from the aquifer itself where the well in screened. At each well, raw water was pumped into a plastic beaker in which the field parameters such as temperature, oxidation-reduction potential (ORP), pH, dissolved oxygen (DO) and specific conductance were measured using hand-held instruments. Both pH and ORP were measured using Hanna portable meters. Dissolved oxygen was measured with YSI portable meter. H_2S measurements were taken in the field using HACH colorimetric methods. Raw water samples were collected into two distilled water washed 60 ml plastic bottles for analyses of $\delta^{13}C$ of DIC and DOC, alkalinity, and anions. One sample from each well was filtered through a 0.45 μm filter into a 60 ml clear plastic bottle and was acidified with concentrated nitric acid (HNO_3) for cation and trace metal analyses. All samples were securely sealed and stored in a cooler until they were analyzed in several laboratories.

3.1.2. Core-drilling and lithosampling

Sediment core samples from a drilled well within the study area (Fig. 3.1) were collected by a split-spoon sampler with a rotary drill rig (Fig. 3.2) operated by the Bangladesh Water Development Board (BWDB) from December 2005 to January 2006. The length of the core sample was 152 m and a total of 100 core samples were collected with a continuous core recovery from the top 30 m, and discontinuously (sampling interval of 3 m from 30 m to 90 m, and 6 m from 100 m to152 m) collected to the bottom of the borehole. The core samples were collected in plastic PVC tubes with a maximum length of 60 cm, but the average length is about 30 cm. The ends of tubes containing sediment were wax-sealed on site immediately after recovery from the drill-hole. Each tube was kept into a clear plastic bag and sealed on spot to avoid any direct contact with atmosphere. The sealed core samples were stored temporarily at the drill site at ambient temperature for few days before shipping to Auburn University. Another set of sediment core samples (47 samples) that were collected in January 2001 from another site in Manikganj Town by GRG and HG (2002) has been incorporated in this study. For convenience, the recent (Dec. 2005 – Jan. 2006) drill-core site is called “Core MN” and previous (Jan. 2001) site is “Core MG” throughout this thesis report.

3.2. Laboratory analyses

3.2.1. Groundwater quality analysis

Groundwater samples were analyzed in chemical laboratories. McCarthy (2001) and Arafin (2003) analyzed water chemistry of 51 samples in Geochemistry Laboratories of University College London, and Dhaka University following standard techniques.

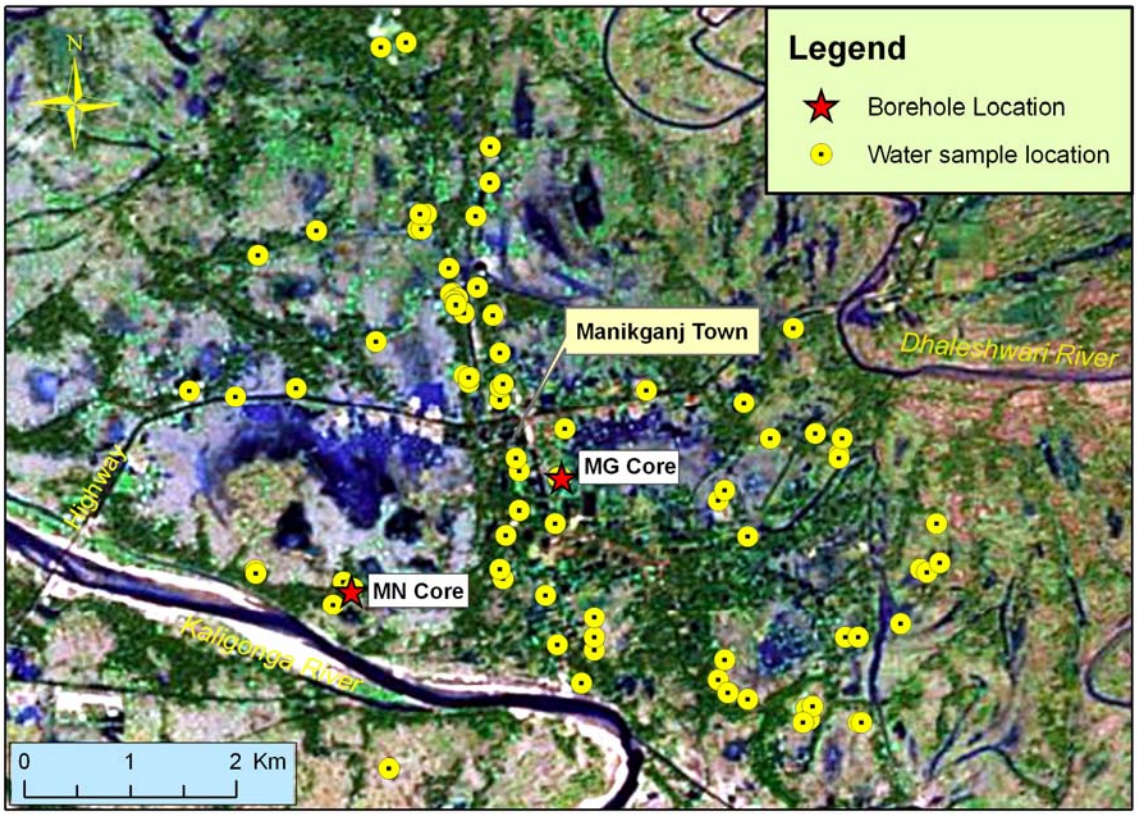

Fig. 3.1 Map showing the groundwater sampling locations within the study area on a satellite image. Groundwater was sampled from 88 tubewells of various depths. Two sediment core sampling locations are shown as two red stars. Core MG was collected in 2001 and MN was collected in Dec. 2005 to Jan. 2006.

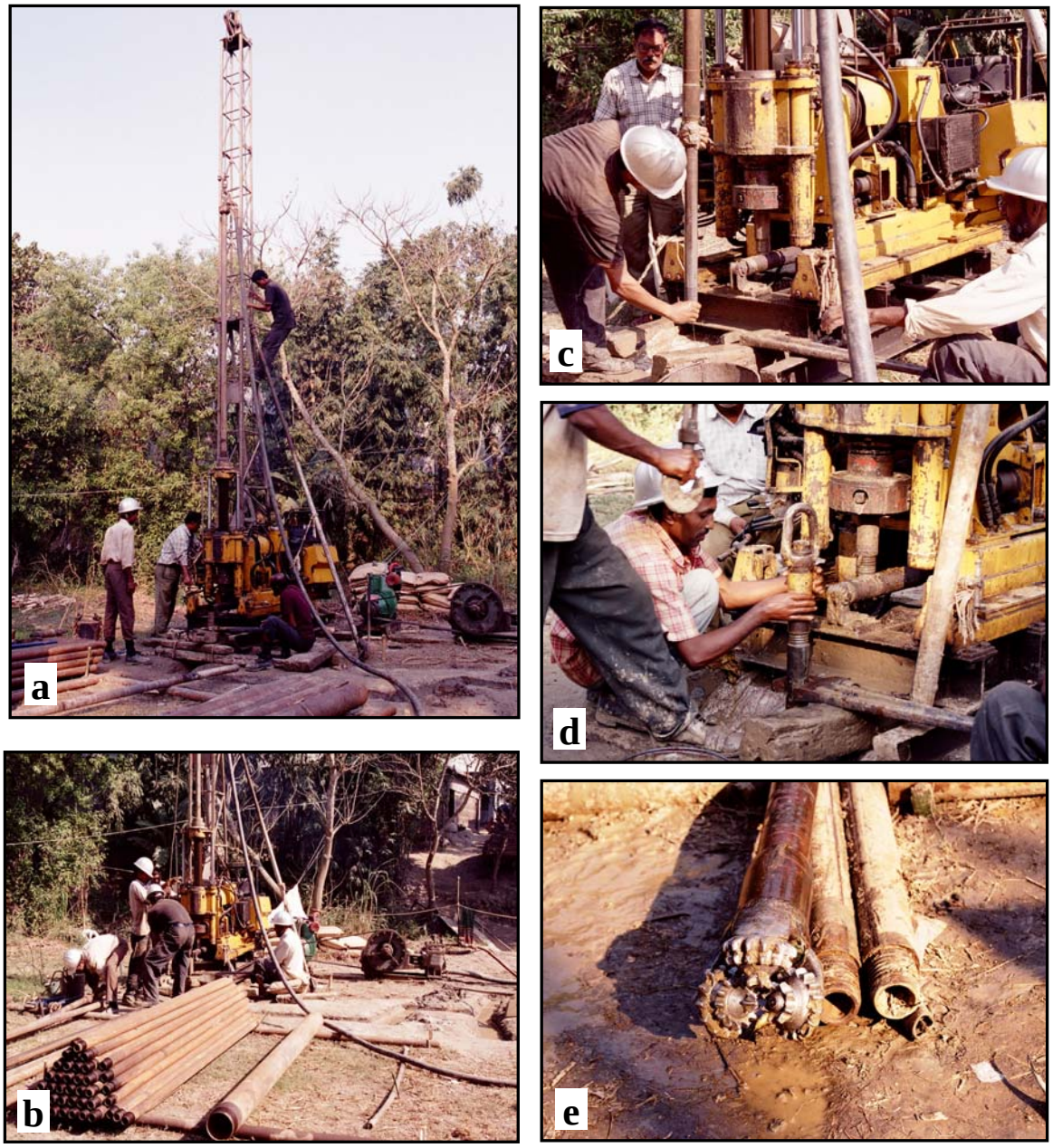

Fig. 3.2 Sediment core sampling process. (a) rotary drilling rig, (b) drilling rod and the team, (c) sediment sampler withdrawal, (d) withdrawal of drilling rod after drilling through a specific target depth, and (e) drilling bit used for sediment cutting.

Turner (2006) collected 15 samples including 4 sampled previously by Arafin (2003) and analyzed in the Activation Laboratories Ltd. Twenty three samples in this study were analyzed also in the Activation Laboratories Ltd., which conducted analyses of cations and trace metals using inductively coupled plasma mass spectrometry (ICP-MS) method. The sample laboratory measured the anion concentrations using ion chromatography (IC). Twenty three groundwater samples were analyzed for different isotopes. Carbon ($^{13}C/^{12}C$), Oxygen ($^{18}O/^{16}O$), and Hydrogen ($^{2}H/^{1}H$) isotope ratios were analyzed by the National High Magnetics Field Laboratory at Florida State University, Tallahassee, Florida.

3.2.2. Sediment lithology description

Sediment samples were studied after removing from wax-sealed PVC tubes in laboratory at ambient temperature and pressure condition. A power-operated cutting device was used to cut PVC tube to expose sediment samples to analyze. Textural description of each core samples was performed following a standard sediment description guideline. Any sedimentary structure that was preserved within the core was also noted. A total of 83 core samples was described and recorded in a database for future reference. A detail description of sediment core samples can be found in the Appendix of this report.

3.2.3. Whole rock geochemistry

A total of 32 samples were selected from both the MN and MG sediment cores based on the information on groundwater arsenic concentrations at different depths in the

study area. Frequency of sediment sampling for geochemical analysis was primarily based on the occurrences of higher arsenic concentration in groundwaters. Mostly finer sediments were targeted for whole rock geochemical analysis since studies shown that arsenic concentration is high in fine-grained sediments. Lithological descriptions of the selected sediment samples can be found in the Appendix. Samples were dried in an oven at about 50°C for approximately 24 hours. Approximately 20 gm of dried sediment for each sample was crushed with a mortar and pestle in the laboratory. Only 0.5 gm of powdered sediment of each sample was sent to the ACME Laboratories Ltd. for analysis. In the lab, a split of 0.5 gm for each sample was leached in hot (95°C) Aqua Regia (HNO_3 + HCL of 1:3). The chemical composition of the sediment core samples were analyzed by Inductively Coupled Plasma-Mass Spectrometry (ICP-MS) method. Results from the whole rock analysis can be found in chapter six of this thesis.

3.2.4. Sequential extraction analysis

Sequential extractions were mostly developed to fractionate heavy metals occurring in trace amounts in contaminated soils or sediments at different phases. In sequential extraction, contaminated sediment (e.g., arsenic) is reacted with a number of chemical solutions of increasing strengths to extract selective geochemical fractions (Pickering, 1981). Sequential extraction techniques are now widely used in heavy metal contamination to determine the mineral phases that are suspected for certain heavy metal contamination, especially in groundwater. Sequential extractions of arsenic, iron and other elements from the core samples have been performed following standard extraction methods.

Three extractants were used to react with selected sediment samples, which contain relatively high arsenic concentrations as predetermined by whole rock analysis. Ten sediment samples were selected from both cores MN and MG for sequential extractions. Magnesium chloride ($MgCl_2$) and Hydroxylamine Hydrochloride ($NH_2OH.HCl$) were used for sequential leaching experiment. $MgCl_2$ targets only the ionically-bound exchangeable or loosely adsorbed arsenic in sediments (Keon et al., 2001). $NH_2OH.HCl$ of two different chemical strengths were used that generally targets amorphous and/or crystalline Fe-oxyhydroxides or reducible Fe-oxyhydroxides (Tessier et al., 1979; Chao and Zhou, 1983; Amacher and Kotuby-Amacher, 1994).

Each sample was dried and powdered with a mortar and pestle. Only 0.5 gm of sediment for each sample was reacted sequentially with three different extractants of increasing chemical strength. Firstly, 40 ml of 1M $MgCl_2$ was used to react with each sample. The solution was shaken vigorously for approximately 15 min for several times over a period of 24 hours. Once the sediments got settled down at the bottom of the reaction bottle (HDPE-High Density Polyethylene), the solution was filtered with a 0.2 μm using a plastic disposable syringe for each sample. The residue of sample was dried in an oven and again put into a separate reaction bottle with the second extraction, 0.1M solution of $NH_2OH.HCl$, and followed the sample procedure as mentioned earlier. Finally, the residue after second leaching phase was put into 40 ml of third extraction, 0.25M solution of $NH_2OH.HCl$, which is the strongest of all three extractants. All 30 samples were stored in a fridge before they were analyzed in the Activation Laboratories Ltd. using ICP-MS method.

3.2.5. Mineralogical analyses

Petrographic analysis

Petrographic analysis was performed with a petrographic microscope (Nikon model no. E600 POL) attached with an automatic point-counter and a photomicrographic setup. Sixteen thin-sections were prepared from core sands at different depth intervals. Thin-sections were stained for both potassium and plagioclage feldspars.

Modal analyses were conducted following the Gazzi-Dickinson method, whereby sand-sized minerals included in lithic fragments are counted as the mineral phase rather than the host lithic fragment in order to normalize for grain-size variation (Dickinson, 1970; Ingersoll et al., 1984). A minimum of 250 points were counted per sample. However, up to 300 framework points were counted for the samples that had greater compositional diversity. Modal sandstone compositions have been plotted on standard ternary diagrams (QtFL, QmFLt, QmPK, LsLvLm, etc.) and used to assess temporal changes in provenance (Dickinson, 1970; Uddin and Lundberg, 1998b).

Heavy mineral separation

Heavy mineral species have affinities to certain grain-size fractions because of the effect of hydraulic sorting. To remove the sorting effect, coherent samples were disintegrated first to liberate individual grains. Concentration of heavy minerals was performed by means of high-density liquids. There is a considerable difference in density between the framework grains and heavy accessory minerals. For this study, a gravity settling method was used with tetrabromoethane ($Br_2CHCHBr_2$, density 2.89-2.96 gm/cc). Dry and weighed samples were added to the heavy liquid in a separating funnel.

The mixture was stirred periodically to ensure that the grains were thoroughly wetted. Heavy minerals then gradually accumulated in the bottom of the funnel above the pinch clip. When sinking of the heavy minerals stopped (after 20-24 hours), the stopcock was opened slowly, and heavy fractions were allowed to pour into filter paper in the lower funnel. The stopcock was then closed immediately to leave a layer of clear liquid below the lighter fraction. The light fraction was then drained into a new funnel. Both fractions were washed thoroughly with acetone and put into an oven for drying.

Sixteen polished thin-sections of heavy minerals of variable magnetic susceptibility were made in a petrographic laboratory. On each thin-section, four different heavy mineral fractions of decreasing magnetic susceptibility were used in each spot. Magnetic separation technique as described in the following section.

Magnetic separation

Magnetic minerals were separated by a hand-magnet and Frantz magnetometer at Auburn University. The heavy mineral fraction was separated by magnetic separation to produce four fractions of different magnetic susceptibility. These four fractions are: Group-A: Highly Magnetic (HM); Group-B: Moderately Magnetic (MM); Group-C: Weakly Magnetic (WM); and Group-D: Poorly Magnetic (PM). Highly magnetic fraction was separated by a powerful hand magnet first. The other three fractions were separated by Frantz magnetometer with different magnetic intensities using a standard procedure described in Hess (1966).

Five categories of heavy minerals of different mass magnetic susceptibility were identified in Hess (1966). In this study, a total of four categories were considered.

Strongly magnetic minerals are classified as Group-A, which includes magnetite, pyrrhotite, etc. The 0.4-ampere magnetic group (Group-B, moderately magnetic) at slide slope of 20º separates ilmenite, garnet, olivine, chromite, and chloritoid. The 0.8-ampere group at 20º slide slope isolates hornblende, hypersthene, augite, actinolite, staurolite, epidote, biotite, chlorite, and tourmaline (dark). The 1.2-ampere group at slide slope of 20º separates diopside, tremolite, enstatite, spinel, staurolite (light), muscovite, zoisite, clinozoisite, and tourmaline (light). These two magnetic fractions were combined together and classified as Group-C (weakly magnetic) since this group does not include a lot of minerals. The rest of the heavy minerals were classified as Group-D (poorly magnetic). This group includes slightly magnetic minerals, such as sphene, leucoxene, apatite, andalusite, monazite, and xenotime, and other non-magnetic minerals like zircon, rutile, pyrite, corundum, fluorite, kyanite, sillimanite and beryl (Hess, 1966).

Scanning Electron Microscopy and Energy Dispersive Spectroscopy

Scanning Electron Microscopy (SEM) and Energy Dispersive Spectroscopy (EDS) techniques were used to identify both detrital and authigenic minerals in aquifer sediments. Polished thin-sections of minerals from only the core MG and several concretions from both the cores MG and MN core samples were used for SEM and EDS analyses. Sediment grains exhibiting secondary mineral overgrowths, extracted from the MG-core, were imaged using a field-emission SEM. EDS is a procedure performed in conjunction with an SEM for identifying the elemental composition of sample.

SEM facility at the Materials Engineering Division of Auburn University was used to image some secondary mineral concretions (e.g., siderite, goethite) found in sediments

at different depths. High resolution scanning electron images were shot for several grains/concretions. EDS with a standard (Princeton Gamma-Tech, Inc.) and automatic spectrum report was used to identity each mineral grain or concretion. Electron beams with 20 kV and a beam current of 2 nA were used for identifying elements present in each mineral grain or concretion.

Electron microprobe analysis

The electron microprobe provides a complete micro-scale quantitative chemical analysis of inorganic solids such as minerals. The method is nondestructive and utilizes the characteristic x-rays stimulated by an electron beam incident on a flat surface of the sample. X-rays are emitted by the sample in response to a finely focused electron beam incident on the sample at a right angle. Some of the beam electrons are scattered backward. The backscattered electrons, as well as the characteristic x-rays of the elements, carry information about chemical composition. These electrons are called backscattered electrons because they come back out of the sample. Because they are moving so fast, they travel in straight lines. In order to form an image with BSE (backscattered electrons), a detector is placed in their path. When they hit the detector a signal is produced which is used to form the TV image. Because of energy differences between backscattered, characteristic X-rays, and secondary electrons, different detector setups are required for the detection of the three types of electron signal.

There are two principal objectives that the electron microprobe serves: (1) it provides a complete quantitative chemical analysis of microscopic volumes of solid materials through x-ray emission spectral analysis; and (2) it provides high-resolution

scanning electron and scanning x-ray images. There are two types of scanning electron images: backscattered electron (BSE) images, which show compositional contrast; and secondary electron (SE) images, which show enhanced surface and topographic features. Scanning-cathodoluminescence images form by light emission in response to the interaction between the scanning electron beam and the sample. In this study, mostly backscatter imaging technique was used for imaging minerals.

Samples were analyzed with the University of Georgia JEOL 8600 electron microprobe using a 15 KeV accelerating voltage and 15 nA beam current. Mineral grains were qualitatively identified using a Noran Microtrace energy dispersive spectrometer (EDS) equipped with a SiLi detector and controlled by a PGT Avalon 4000 multichannel analyzer running eXcalibur software. Attempts were made to do some quantitative analyses that were performed with wavelength dispersive spectrometers (WDS) automated with Geller Microanalytical Laboratory's dQANT software, using natural and synthetic mineral standards. However, no data from the WDS analysis was shown in this thesis. Analyses were calculated using Armstrong's (1988) Phi-Rho-Z matrix correction model. Backscattered electron (BEI) was acquired using Geller Microanalytical Laboratory's dPICT imaging software.

CHAPTER 4

STRATIGRAPHY AND HYDROGEOLOGY

4. Stratigraphy and Hydrogeology

4.1. Stratigraphy of study area

The study area consists of floodplain alluvial detritus deposited mostly during the Holocene through recent time. Drilling wells helped reveal subsurface stratigraphic information of the area. The subsurface geology of the Manikganj study area was established through core sample analysis, sedimentology and petrographic studies. Two bore holes, approximately 182 m and 152 m deep, were drilled within the study area in 2001 and 2006 respectively (Fig. 4.1). The stratigraphy of Manikganj area is described below:

4.1.1. Stratigraphy and sedimentology

Several fining-upward sedimentary sequences formed the subsurface geology of the study area. Information from two drill-holes reveals the stratigraphy and sedimentary history of Manikganj and adjoining areas. Alluvial sediments ranging in size from clay to gravel formed the sedimentary sequences. Color of the sediments varies from dark-gray (highly reduced) to orange-brown (oxidized) as noticed in many other fluvial-deltaic sedimentary sequences in Bangladesh (e.g., BGS and DPHE, 2001).

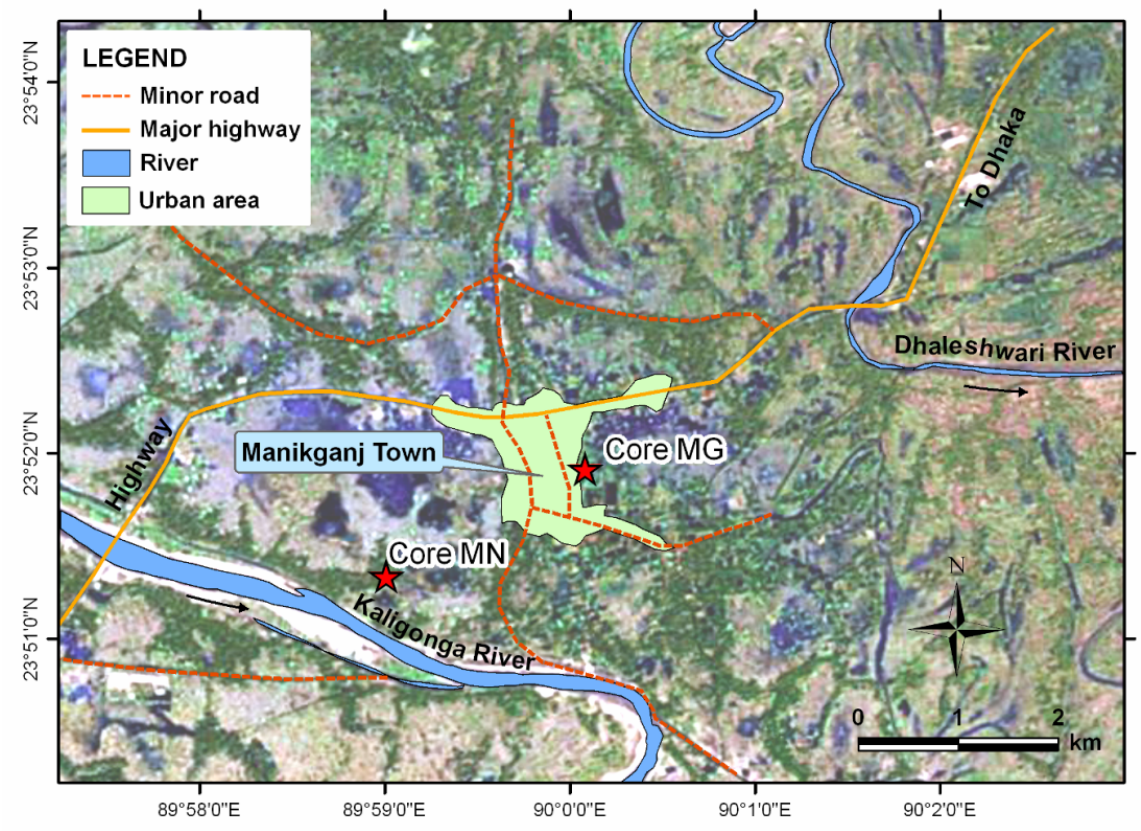

Fig. 4.1 Map showing the locations of sediment core drill sites in Manikganj study area. Wells MG and MN were drilled in 2001 and 2006 respectively.

Three distinct fining-upward sedimentary sequences have been observed in two core samples (Fig. 4.2). The uppermost fining-upward sequence is approximately 33 m thick in both drilling sites within the Manikganj Town. The stratigraphy of this uppermost sequence at the MG core site is slightly different than the MN core, which is located in the natural levees of the Kaligonga river. Presence of several clay and silty-clay layers interbedded with sand in the MG core suggests a typical floodplain alluvial deposit by a meandering river. Thin layers rich in dark-colored heavy minerals are observed in sandy units. Some sand and silt layers contain organic matter (e.g., plant debris). Gray micaceous silts and clays within the sequence were probably deposited within the meandering channels. Basal medium sand with occasional coarse sands with some plant debris and mica were deposited within the active meandering channels in the study area. Lithological characteristics and depositional patterns suggest a highstand sediment cycle, which is also seen in other locations of the country (BGS and DPHE, 2001).

The middle fining-upward sequence is very distinct in both well sites. The thickness of this sequence is approximately 55-60 m starting with coarse sand with gravels in MN core, but gravels in clay layer in MG core site (Fig. 4.2, 4.3). The top of this fining-upward sequence is mostly fine sand. However, in MN site, there is a silty-sand layer at 45 m deposited on top of fine sand suggesting a change in depositional energy for a short time. The bottom of this middle fining-upward sequence is characterized by gravel-rich sediments, although the gravel-rich layer is significantly thick (30-35 m) in the MN site, which is located next to the Kaligonga river (Fig. 4.1). Compared to MN location, the gravel-rich layer in the MG drill site is thin (~ 6 m) and embedded within dark-gray clay.

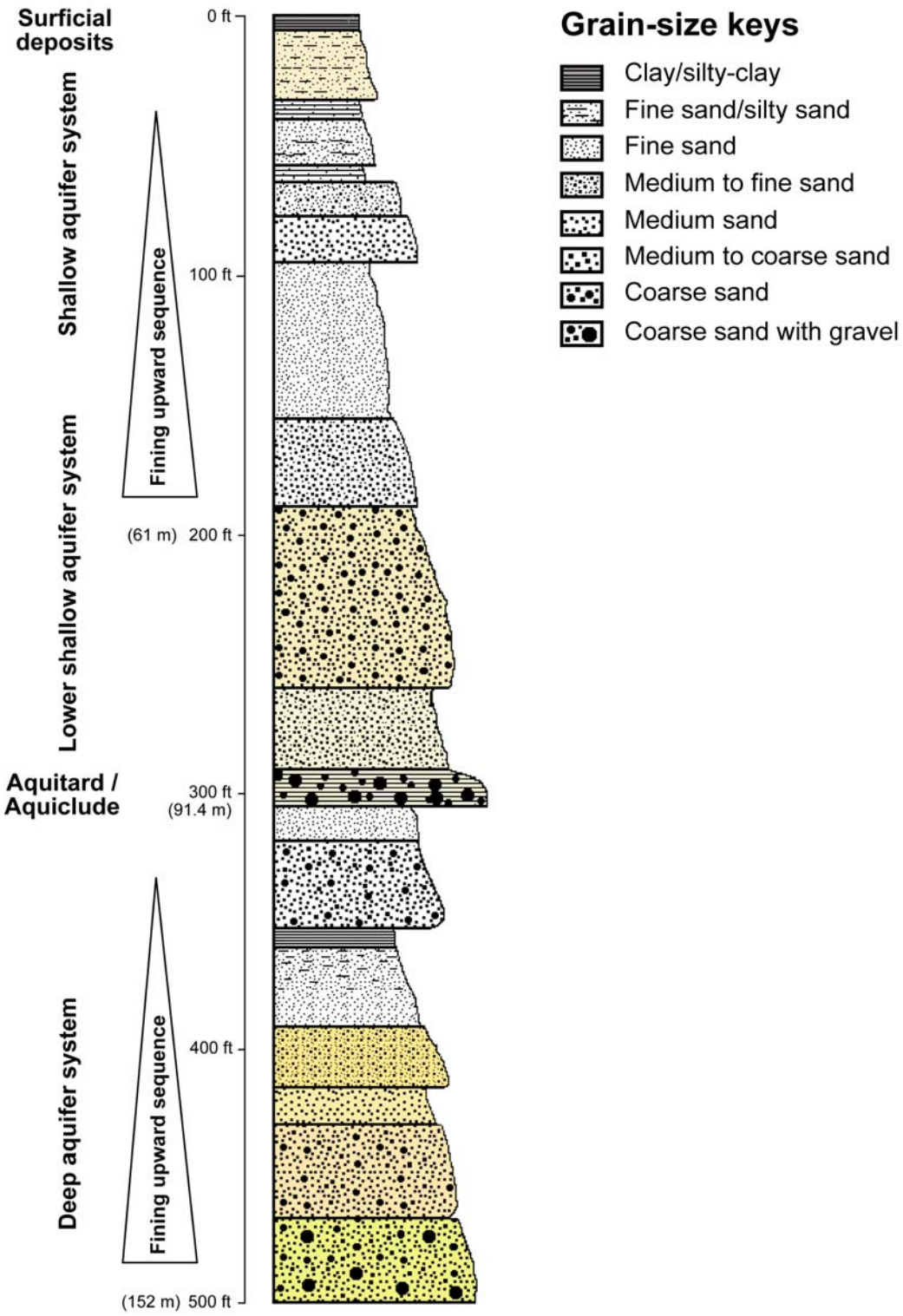

Fig. 4.2 Stratigraphic column of Manikganj study area revealed from MG drill core.

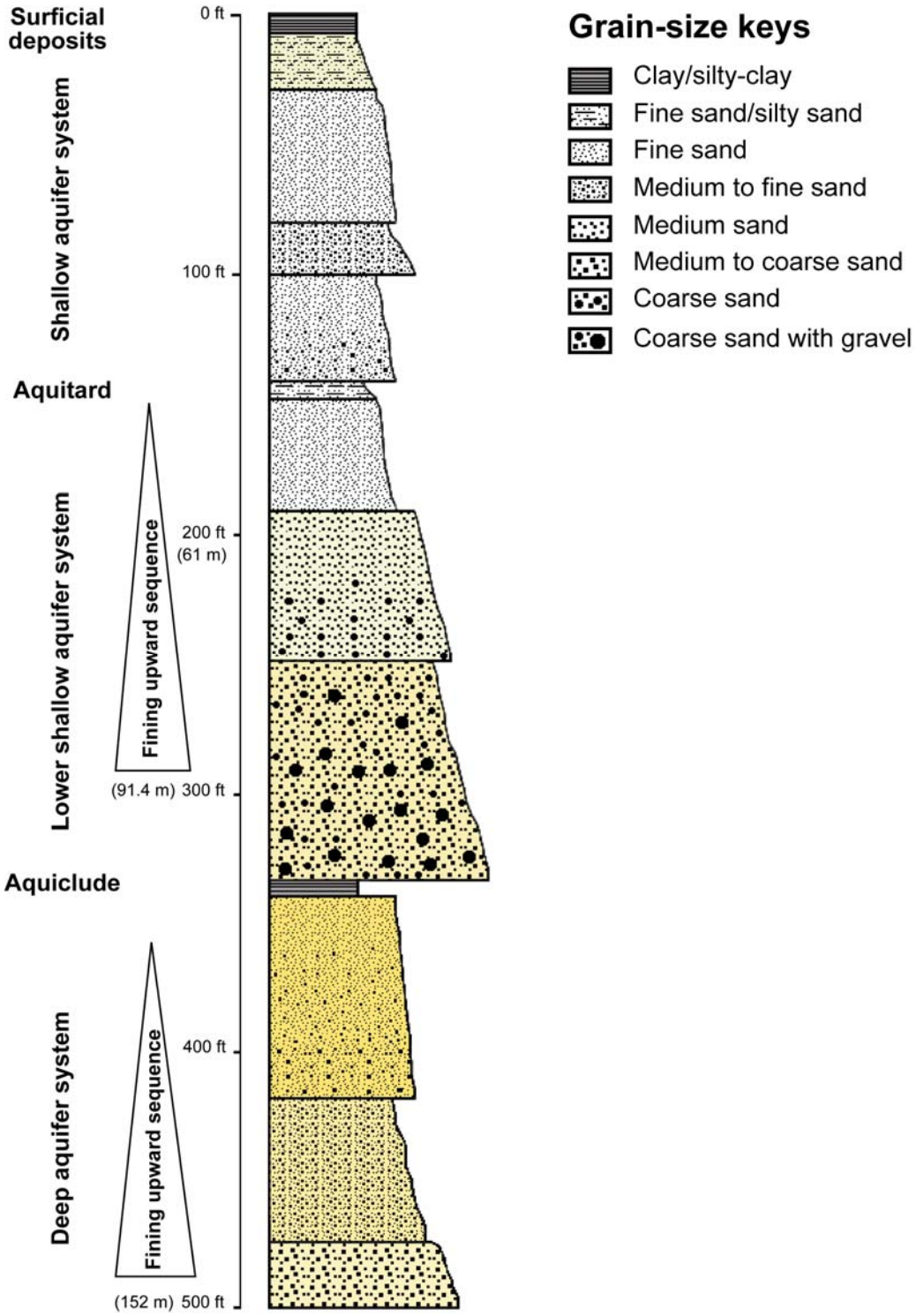

Fig. 4.3 Stratigraphic column of Manikganj study area revealed from MN drill core.

The gravels in both locations are mostly sub-rounded to rounded fragments of chert, quartzite and granite. This middle fining-upward sequence (45-90 m) can be interpreted as transgressive and lowstand sedimentary deposits found in other areas of the country. Based on lithological characteristics of this middle stratigraphic unit the sedimentary deposits can be correlated with the deposits beneath the Brahmaputra (Jamuna) floodplain described as Dhamrai Formation (Table 4.1; Davies, 1989).

The bottom fining-upward sequence (100-152 m) is also distinct in both core sites in Manikganj study area. This sedimentary sequence is different from the top and middle units both in physical properties and composition. The average color of sediments in this unit ranges from yellowish-brown to orange brown as opposed to gray to dark-gray color in the younger sediments. The bottom of this sequence is composed of coarse to medium sands. These sediments are lithologically similar to the Dupi Tila Formation of Pliocene-Pleistocene age, which serves as the best aquifer in Bangladesh (BGS and DPHE, 2001). There is a transitional deposit in the MG core site composed of light-gray colored medium sand overlain by fine sand that can be considered as a separate smaller fining-upward unit, which is not found at the MN site.

4.1.2. Depositional environments

Sediments in Manikganj area were mainly deposited in fluvial environments by meandering and braided rivers. The lowermost sedimentary unit of the study area is the Dupi Tila Formation that spreads all over the country probably excepting the southern two-third of the Ganges deltaic area where the recent alluvium is very thick (Khan, 1991). The lithology, texture and sedimentary patterns suggest that the Dupi Tila

sediments were deposited in predominantly single channel, mud-rich meandering river systems (Gani and Alam, 2004). The fining-upward sequences of the Dupi Tila Sandstone, with alternating channel and floodplain deposits, have been interpreted as meandering river deposits (Johnson and Nur Alam, 1991). Younger Pleistocene deposits have been identified only locally as relatively thin subaerial deposits unconformably overlying the Dupi Tila Formation (Uddin and Lundberg, 1999). The middle stratigraphic unit, which contains very think gravel-rich medium sand deposits were deposited by big meandering or braided river system (Table 4.1). The depositional energy was very high that carried larger gravel-size sediments and probably deposited in the river beds as well as adjoining floodplains. This coarse sedimentary facies of the lower Dhamrai Formation were deposited within the lowstand sea level condition in incised river valley at higher gradients (BGS and DPHE, 2001). The upper Dhamrai Formation with coarse to medium sand of maximum 7 Ka BP age were deposited mainly by smaller braided and meandering rivers during the rapid rise in base-level conditions. Incised channels were filled with fining-upward fluvial sedimentary sequences at moderate energy conditions. Micaceous very fine sands with silt and clay were deposited between active river channels and anastomosing distributaries during the rapid sea-level rising phase in the Bengal Basin (BGS and DPHE, 2001).

Table 4.1 Simplified stratigraphic succession of the Quaternary deposits in Manikganj study area (modified after Davies, 1989).

Age	Stratigraphic unit	Subdivision in Manikganj area	Lithology and facies description	Thickness (meter)
Recent	Alluvium		Fine sand, silt, silty-clay and clay with micas and plat fragments	5-10
Holocene	Dhamrai Formation	Upper fining-upward sequence	Light-gray to dark-gray, fine to medium sand with silt and occasional clay. Some sand layers are rich in mica and dark-colored heavy minerals. Highstand fluviatile deposits	20-30
		Middle fining-upward sequence	Fine to medium sand, with coarse sand and gravel toward the bottom of the sequence. Color of the sediments varies from gray to light yellowish-gray. Less organic matter in sediments. Lowstand System Tract to Transgressive Tract alluvial deposits	65-75
Pliocene-Pleistocene	Dupi Tila Formation	Lower fining-upward sequence	Yellowish-brown to orange brown colored fine to medium sand with occasional gravel. Sediments are highly oxidized and iron-coatings are common on sand grains. Pre-Lowstand fluvial deposits	> 50

4.1.3. Quaternary sea level and climatic changes

Late Pleistocene and Holocene sedimentation in the delta plain of the Bengal Basin, and occurrence of groundwater arsenic have been strongly influenced by glaciation and global changes in sea level during the Quaternary period (Bhatacharya and Banerjee, 1979; Umitsu, 1993; Islam and Tooley, 1999; Goodbred and Kuehl, 2000; Saunders et al., 2005). A clearly overlapping condition exists between location of arsenic-enriched zones within the Bengal Basin and distributions of organic-rich sediments, occurrences of marsh and peats, and Holocene sea level fluctuations (Acharyya et al., 2000; Ravenscroft et al., 2001).

The basal sand and gravel beds deposited in the Bengal Basin toward the end of the Pleistocene during a relatively colder and drier climatic conditions in a low sea level stand (Banerjee and Sen, 1987). Dry climatic conditions with reduced vegetation triggered widespread and extended weathering and erosion in the Himalayas, Shillong Plateau, Rajmahal Hills, and Indo-Burman ranges causing oxidation and recrystalization of iron oxyhydroxides (Ravenscroft et al., 2005) in the upper catchment area. Over several thousands of years, relatively steep hydraulic gradients and deeper water table in the Bengal Basin extensively flushed the pre-existing sediments (e.g., Dupi Tila sands), which are free of arsenic contamination. The deeper aquifer (> 100 m) in the Manikganj study area, which is arsenic-free, is believed to have undergone through the same process of active flushing during the low-stand of Holocene sea level.

Between 15,000 and 10,000 years BP de-glaciation started in the high mountains with a temperature rise that led to reinvigoration of monsoon climatic conditions in this region, and initiated a sea level rise (Goodbred and Kuehl, 2000). Meltwater from the

mountains increased runoff when the major rivers deposited sediments mostly in the submarine delta, and alluvial aggradation was limited within the incised river valleys of the Bengal Basin (Ravenscroft et al., 2005). Temperature and precipitation increased during the Early to Middle Holocene time leading to a humid climatic condition due to strong monsoon circulations in the Bengal Basin. The upper part of the middle stratigraphic unit in the study area was deposited under fluvial conditions during a transgressive to highstand sea level.

Sea level began to rise slowly between 7,000 and 5,500 years BP to reach about 2-3 m higher than present-day sea level (Islam and Tooley, 1999). Southern part of the Ganges delta was invaded by the sea and numerous marine and fresh-water peat, mangrove forests and swamps were formed infront of the coastline. Extensive peat basins were developed on flooded coastal platform with the elevated temperature and high surface water discharge throughout the middle Holocene time (Ravenscroft et al., 2001). Subdued topography resulted in sluggish groundwater flow with little flushing of sediments of the upper Holocene stratigraphic unit in Bengal Basin, which is relatively high in groundwater arsenic content (Acharyya et al., 2000; Ravenscroft et al., 2005).

4.2. Hydrogeological conditions

4.2.1. Aquifer distributions in Manikganj

Aquifers in the Manikganj study area are composed of alluvial deposits ranging from gravel-rich coarse sand to fine sand. Three major aquifer systems are formed by three fining-upward sedimentary sequences in Manikganj that is comparable with the three-aquifer classification scheme originally proposed by UNDP (1982), but later on

modified by BGS and DPHE (2001). In this study, these aquifers are rather called as aquifer systems since there are multiple aquifers in each alluvial aquifer system. The aquifers are described below:

i. Upper shallow aquifer system: There is surficial clay/silty clay layer at the top of the upper aquifer system in Manikganj area as noticed in both drill cores. The uppermost aquifer starts at approximately 10 m below the surface and extend vertically up to a depth of 33 m, which is composed mainly of very fine sand mixed with silt (Fig. 4.2, 4.3). The average thickness of this upper shallow aquifer system is approximately 15-20 m, consisting of several inter-connected aquifers of various sediment types. The sand is rich in mica and other heavy minerals. The bottom part of this upper shallow aquifer system is composed of coarser sediments, mostly medium-grained sand. The sediments are mainly light-gray to dark-gray suggesting reducing chemical conditions of this upper shallow aquifer system. Most of the high arsenic-contaminated tubewells are screened in this aquifer system.

ii. Lower shallow aquifer system: This aquifer system consists of several potential groundwater aquifers ranging in total thickness of 55-60 m. Sediment sizes in this aquifer system vary from fine sand to medium sand to even coarse sand with gravels toward the bottom of this middle stratigraphic unit (Fig. 4.2, 4.3). Aquifer sediments are mostly moderate to well sorted, composed mostly of quartz, feldspar and micas. Sediment colors change from gray to light yellowish-brown towards the bottom, indicating a change in chemical environment from reducing to slightly oxidizing to the bottom. High porosity

and permeability make this aquifers system one of the best aquifers in the study area. Few wells toward the top part of this aquifer system are arsenic-affected, but most tubewells at deeper depths are arsenic-free. More detail description of arsenic and other groundwater properties of these aquifers will be discussed in the following chapter.

iii. Deep aquifer system: The aquifer system in the Manikganj study area extends below ~ 100 m with a major change in sediment composition and color. Most aquifers in this system are composed of fine to medium grained yellowish-brown to bright orange-brown sands, indicating highly oxidized subsurface condition in aquifers. This system is the same as the "deeper aquifer" as proposed by BGS and DPHE (2001) and is believed to yield excellent quality groundwater in most parts of Bangladesh. Only a few tubewells are installed in this aquifer system, which is arsenic-free.

4.2.2. Hydraulic properties of aquifers

Groundwater flow within the aquifer systems in Manikganj area is largely controlled by the topography, elevation and the two major rivers, the Ganges to the south and the Brahmaputra to the west. The digital elevation model of Manikganj district shows that the elevation decreases toward the south/south-east direction where the relief is approximately 8 m across the district (Fig. 4.4). Groundwater flow within the upper shallow aquifer system has been modeled based on water table information in 2003 from the dugwells and shallow piezometers during driest (March-April) and peak monsoon (July-August) periods. The depth ranges from approximately 5 m to 22 m that supply groundwater from the upper shallow aquifer in Manikganj district. In both periods,

groundwater flow direction is towards the south of the map area (Fig. 4.4). In dry period, the upper shallow aquifers are fed by the Ganges and Brahmaputra rivers from the west. However, due to high elevation in the northeast of the map area, some groundwater flows into the aquifers from the recharge areas in the higher catchment. Groundwater flow direction does not change significantly from the dry period to the wet period. However, water table elevation becomes higher (maximum ~ 10 m) in the west, close to the major rivers to lower toward the south. Groundwater flow within the lower shallow aquifer system (> 30-100 m) as modeled using water table data from piezometers ranging in depth from 32 m to 55 m has revealed similar flow pattern as the upper shallow aquifers in Manikganj district area (Fig. 4.5). Groundwater flow within this shallow aquifer system is controlled mainly by topography, elevation, and enormous water flow along the Ganges and Brahmaputra rivers. The groundwater flow in both upper and lower shallow aquifers within the study area are more or less same toward to the south. Due to lack of enough deep tubewells within the deep aquifer system (> 100 m), the groundwater flow pattern has not been modeled.

Hydraulic parameters in the study area were measured using sediment grain-size and pumping test data by GRG and HG (2002). The pumping tests indicate that the shallow aquifers are hydraulically leaky with a transmissivity of approximately 3500 m^2/day. The average hydraulic conductivity is approximately 1.5 m/day for the fine to medium sands in shallow alluvial aquifers to approximately 25 m/day for the coarse sand to gravel-sand toward the bottom of lower shallow aquifers. Hydraulic conductivity is expected to be high in coarser sediments with substantial permeability.

Groundwater fluctuations within the shallow and deep aquifers in the study area are similar to other areas in the country (GRG and HG, 2002). Groundwater occurs at very shallow depth within a meter from the land surface in wet season, whereas the water level goes down to about 8-10 m during the dry periods. Similar groundwater fluctuation patterns have been observed both in upper shallow and lower shallow aquifer systems in the study area (Fig. 4.4, 4.5). Water level elevation models suggest that groundwater in Manikganj area is mostly recharged from the Ganges and Brahmaputra rivers throughout the year. Groundwater elevation seems to decrease in the northwestern corner of the elevation models where surface elevations are high (Fig. 4.4, 4.5), which could be the artifacts of gridding process from fewer data points. However, the local groundwater flow, particularly during the dry period is controlled by the large-scale irrigation pumping in the study area.

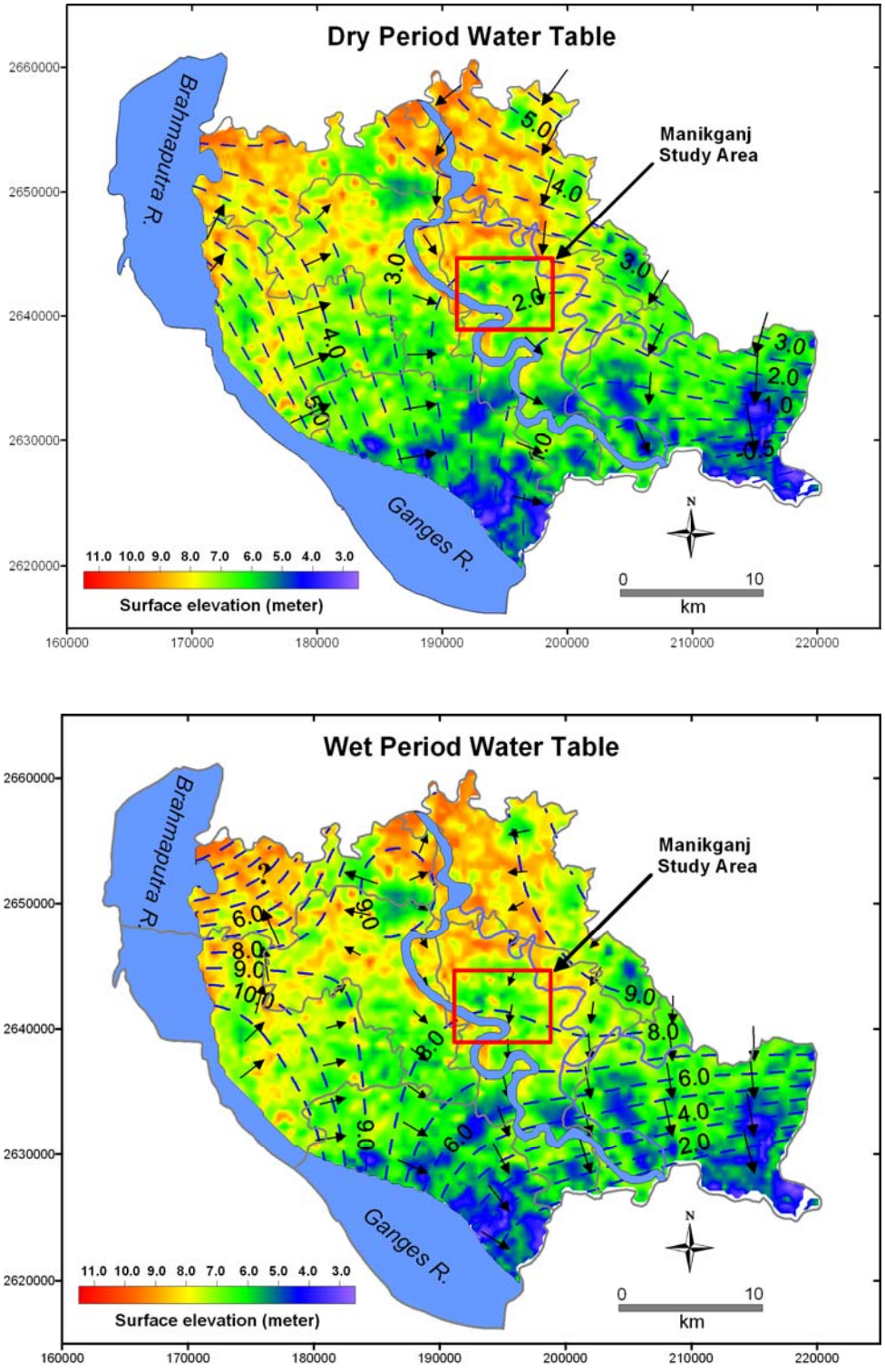

Fig. 4.4 Maps of groundwater flow in the upper shallow aquifers in Manikganj area. (**a**) Water table in upper shallow aquifer during the summer (dry) and (**b**) in monsoon (wet) season.

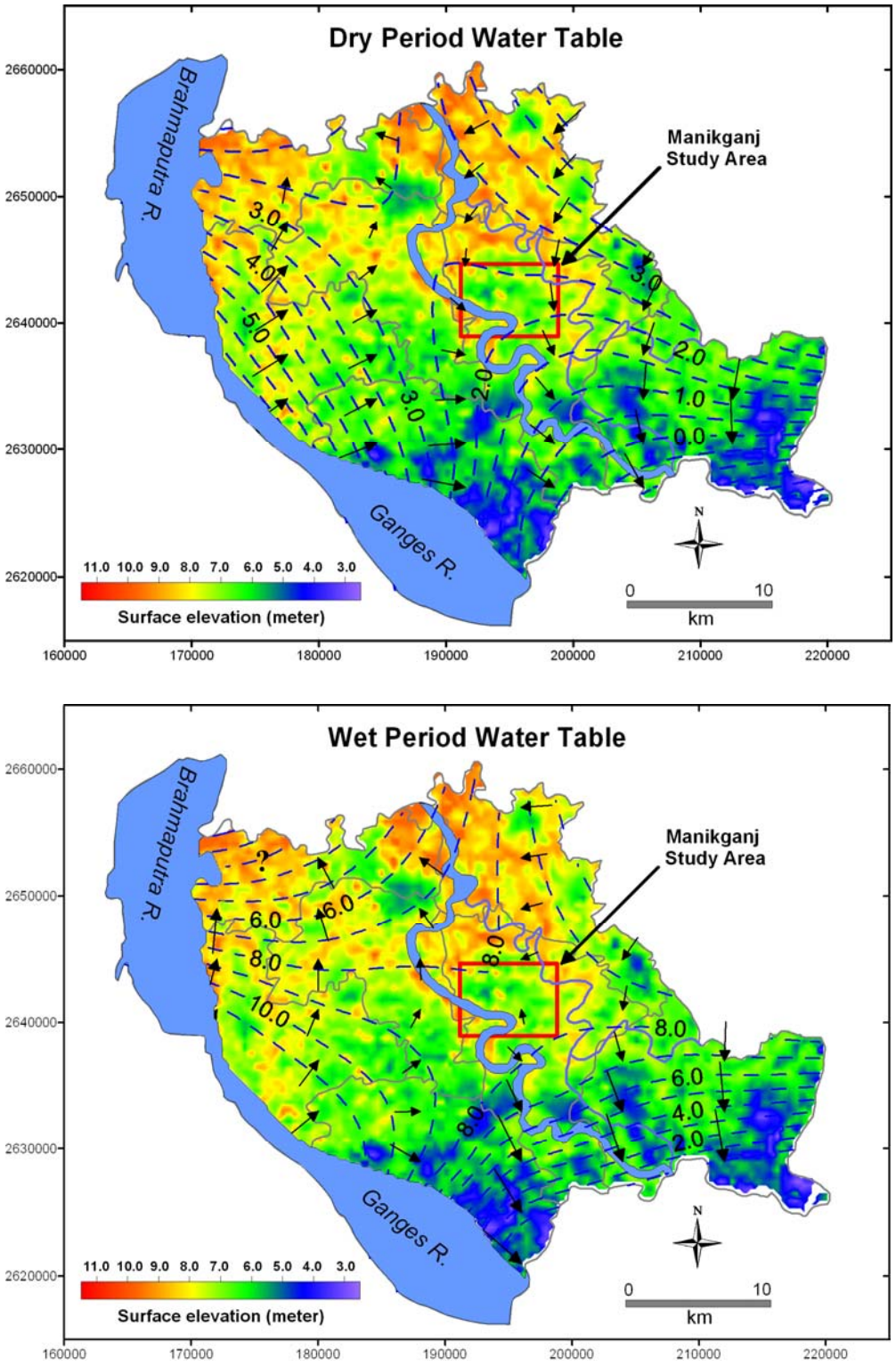

Fig. 4.5 Maps of groundwater flow in the lower shallow aquifer in Manikganj area. (**a**) Water table in lower shallow aquifer during the summer (dry) and (**b**) in monsoon (wet) season.

CHAPTER 5

GROUNDWATER GEOCHEMISTRY

5. Groundwater Geochemistry

5.1. Groundwater analyses and results

A total of 88 groundwater samples were analyzed using several standard methods described in the chapter three. A geochemical database was created with all results, including tubewell location, owner's name, well depth, physical properties of water, major and minor ions and trace element concentrations. The geochemistry of Manikganj groundwater is presented and interpreted in this chapter.

5.1.1. Field parameters

Physical parameters were measured at each sampling location prior to water sampling. Physical parameters of each tubewell are presented in Table 5.1. Depths of tubewells range from ~ 8 m to 228 m below the surface (Fig. 5.1). Most of the shallow tubewells (< 50 m) are located in the northern part of the study area, whereas the deeper wells are mainly in the central and southern parts. Readings of pH vary from 6.11 to 7.28 in sampled groundwaters with a mean value of 6.75. Groundwaters with high pH values (> 7.0) are mainly located in the northern part of Manikganj area at shallow depths (Fig. 5.2). ORP (redox potential) values vary from -152 mV to the maximum of 177 mV with

an average value of -88 mV in Manikganj area (Table 5.2). Electrical conductivity in 85 tubewells shows a wide range with a minimum of 338 µS/cm and the maximum of 2500 µS/cm (Fig. 5.3). Higher conductivities are commonly found within shallow aquifers (< 50 m depth). Dissolved oxygen in Manikganj study area ranges from 0.25 to 5.94 mg/L with a mean value of 0.86 mg/L. Temperatures in 85 tubewells were found within a narrow range of 23 to 29 °C with a mean temperature of about 26 °C. The concentrations of dissolved H_2S were found always < 0.1 mg/L.

5.1.2. Major ion composition of groundwater

Major ion composition of groundwater samples from the study area are presented in Table 5.3. In the study area, spatial variations in the major ion concentrations in groundwater are considerable. The major cations in the sampled groundwater are Ca (32-43 mg/L) and Na (8-99 mg/L). Spatial variations in major cation concentrations are shown in Fig. 5.4. Significant spatial variations are observed in the concentrations of Ca, Na, K, and Mg in groundwater. Descriptive statistical parameters of all these cations in Manikganj groundwater are given in Table 5.4. Concentrations of Ca decrease with depth, which is opposite to the depth-wise distributions of Na in groundwater (Fig. 5.5). Concentrations of Mg (13.3-46.1 mg/L) and K (0.67-40.0 mg/L) also decrease with increasing tubewell depths in Manikganj. Considerable spatial variations are observed in the concentrations of groundwater anions in Manikganj area (Fig. 5.6). HCO_3 is the major anion of the groundwater in the study area, whereas Cl is the second dominant anion.

Table 5.1 Physical parameters in groundwater samples in the study area.

Sample No.	Latitude (degree)	Longitude (degree)	Well depth (m)	Elevation (m)	Aquifer Type	pH	ORP (mV)	Conductivity (μS/cm)	Dissolved Oxygen (mg/L)	Temperature (℃)	H_2S (mg/L)
MK-01	23.865	90.001	178.3	7.0	Deep	6.62	n.m.	710	0.42	26.6	n.m.
MK-02	23.865	90.001	45.0	8.0	Shallow	6.95	n.m.	690	0.34	26.6	n.m.
MK-03	23.848	90.003	79.5	14.0	Shallow	6.84	n.m.	560	0.56	26.6	n.m.
MK-04	23.851	90.004	0.0	13.0	Shallow	6.93	n.m.	520	5.94	28.8	n.m.
MK-05	23.852	90.004	105.9	10.0	Deep	6.93	n.m.	510	0.48	26.6	n.m.
MK-06	23.853	90.004	100.0	8.0	Deep	6.92	n.m.	500	0.32	26.4	n.m.
MK-07	23.869	90.002	137.2	11.0	Deep	6.94	n.m.	560	0.64	26.4	n.m.
MK-08	23.873	90.009	228.6	12.0	Deep	6.95	n.m.	480	0.31	26.3	n.m.
MK-09	23.846	90.017	73.2	9.0	Shallow	6.48	n.m.	510	0.48	26.2	n.m.
MK-10	23.848	90.015	36.6	8.0	Shallow	6.28	n.m.	580	0.58	26.2	n.m.
MK-11	23.847	90.016	18.3	10.0	Shallow	6.18	n.m.	750	0.48	26.0	n.m.
MK-12	23.850	90.015	73.2	11.0	Shallow	6.48	n.m.	580	0.58	26.1	n.m.
MK-13	23.846	90.022	36.6	8.0	Shallow	6.54	n.m.	620	0.47	26.1	n.m.
MK-14	23.845	90.023	27.4	9.0	Shallow	6.22	n.m.	670	0.40	26.2	n.m.
MK-15	23.846	90.023	73.2	7.0	Shallow	6.35	n.m.	490	0.63	26.2	n.m.
MK-16	23.866	89.998	22.9	13.0	Shallow	6.11	n.m.	760	0.49	26.6	n.m.
MK-17	23.867	89.998	15.2	11.0	Shallow	6.30	n.m.	520	0.39	26.1	n.m.
MK-18	23.872	89.996	73.2	12.0	Shallow	6.86	54	550	0.47	27.1	<0.1
MK-19	23.873	89.996	36.6	12.0	Shallow	7.02	-101	650	0.41	26.6	<0.1
MK-20	23.873	89.996	18.3	11.0	Shallow	6.90	n.m.	510	0.37	26.5	n.m.
MK-21	23.853	90.030	73.2	8.0	Shallow	6.96	n.m.	490	0.41	26.0	n.m.
MK-22	23.852	90.026	22.9	9.0	Shallow	6.94	n.m.	470	0.53	26.3	n.m.
MK-23	23.852	90.027	36.6	13.0	Shallow	6.95	n.m.	530	0.70	26.0	n.m.
MK-24	23.856	89.983	73.2	13.0	Shallow	6.96	n.m.	460	0.40	26.0	n.m.
MK-25	23.854	89.982	36.6	14.0	Shallow	6.81	n.m.	600	0.40	25.8	n.m.
MK-26	23.858	90.032	22.9	11.0	Shallow	6.30	n.m.	800	0.40	26.0	n.m.
MK-27	23.857	90.033	36.6	11.0	Shallow	6.23	n.m.	560	0.37	26.2	n.m.
MK-28	23.861	90.033	73.2	9.0	Shallow	6.35	n.m.	610	0.44	25.4	n.m.
MK-29	23.858	90.034	15.2	9.0	Shallow	6.60	n.m.	520	0.57	25.7	n.m.
MK-30	23.863	90.015	21.4	8.0	Shallow	6.42	n.m.	640	2.85	25.5	n.m.
MK-31	23.864	90.015	18.3	9.0	Shallow	6.50	n.m.	440	0.39	24.9	n.m.
MK-32	23.860	90.017	37.2	12.0	Shallow	6.22	n.m.	590	0.57	25.7	n.m.
MK-33	23.867	90.025	73.2	10.0	Shallow	6.57	n.m.	530	0.45	26.3	n.m.
MK-34	23.867	90.025	22.9	11.0	Shallow	6.37	n.m.	870	0.57	26.2	n.m.
MK-35	23.869	90.025	45.7	12.0	Shallow	6.46	n.m.	550	0.47	26.1	n.m.
MK-36	23.857	89.996	73.2	14.0	Shallow	6.45	n.m.	520	0.44	25.9	n.m.
MK-37	23.858	89.996	36.6	14.0	Shallow	6.48	-99	610	0.42	26.1	<0.1
MK-38	23.855	90.000	21.3	10.0	Shallow	6.50	n.m.	870	0.42	26.6	n.m.
MK-39	23.863	89.998	45.7	15.0	Shallow	6.49	-101	740	0.30	26.1	<0.1
MK-40	23.872	90.017	73.2	12.0	Shallow	6.39	n.m.	510	0.48	26.1	n.m.

Table 5.1 (cont'd.)

Sample No.	Latitude (degree)	Longitude (degree)	Well depth (m)	Elevation (m)	Aquifer Type	pH	ORP (mV)	Conductivity (μS/cm)	Dissolved Oxygen (mg/L)	Temperature (°C)	H_2S (mg/L)
MK-41	23.872	90.017	18.3	8.0	Shallow	6.56	n.m.	560	0.79	26.2	n.m.
MK-42	23.869	90.019	37.2	9.0	Shallow	6.52	n.m.	520	0.36	26.4	n.m.
MK-43	23.844	90.027	73.2	13.0	Shallow	6.63	n.m.	710	0.46	26.2	n.m.
MK-44	23.844	90.027	45.7	11.0	Shallow	6.38	n.m.	500	0.54	26.2	n.m.
MK-45	23.844	90.022	18.3	11.0	Shallow	6.39	n.m.	920	0.39	26.0	n.m.
MK-46	23.841	89.987	202.7	7.0	Deep	6.78	n.m.	1810	0.54	26.6	n.m.
MK-47	23.872	89.974	192.0	10.0	Deep	6.53	n.m.	420	0.31	25.8	n.m.
MK-48	23.877	89.986	185.9	9.0	Deep	6.22	n.m.	490	0.35	28.2	n.m.
MK-49	23.879	89.996	185.9	10.0	Deep	6.40	n.m.	540	0.25	26.3	n.m.
MK-50	23.878	90.021	195.1	12.0	Deep	6.45	n.m.	550	0.34	26.2	n.m.
MK-51	23.861	90.001	137.2	12.0	Deep	6.45	n.m.	630	0.38	26.1	n.m.
MK-60	23.880	89.992	25.0	16.0	Shallow	7.13	-103	1431	n.m.	25.0	< 0.1
MK-61	23.881	89.992	15.0	11.0	Shallow	6.91	-96	2110	n.m.	24.8	< 0.1
MK-62	23.857	89.975	39.6	11.0	Shallow	6.93	-106	1850	n.m.	25.1	< 0.1
MK-63	23.857	89.975	22.9	10.0	Shallow	6.87	-105	2290	n.m.	25.6	< 0.1
MK-64	23.857	89.976	24.4	12.0	Shallow	6.80	-108	1812	n.m.	24.8	< 0.1
MK-65	23.881	89.992	21.3	10.0	Shallow	7.00	-125	1906	n.m.	24.6	< 0.1
MK-66	23.881	89.992	18.3	11.0	Shallow	6.88	-71	2500	n.m.	24.3	< 0.1
MK-67	23.881	89.993	9.2	11.0	Shallow	7.14	103	2280	n.m.	23.2	< 0.1
MK-68	23.874	89.993	29.0	10.0	Shallow	7.05	-114	2300	n.m.	23.0	< 0.1
MK-69	23.873	89.993	73.2	11.0	Shallow	7.03	-103	1836	n.m.	23.3	< 0.1
MK-52	23.880	89.992	22.9	11.0	Shallow	7.05	-105	1265	n.m.	24.2	< 0.1
MK-70	23.879	89.993	15.9	11.0	Shallow	7.05	-136	450	1.19	25.4	< 0.1
MK-71	23.883	89.992	15.2	11.0	Shallow	7.02	-143	755	1.02	25.4	< 0.1
MK-72	23.886	89.989	29.6	13.0	Shallow	7.09	-145	840	1.92	25.1	< 0.1
MK-73	23.886	89.989	48.8	14.0	Shallow	7.12	-152	850	1.12	24.6	< 0.1
MK-74	23.860	89.997	16.8	14.0	Shallow	7.20	-93	868	1.20	25.4	< 0.1
MK-75	23.856	89.984	15.9	14.0	Shallow	6.95	-130	2500	2.08	24.8	< 0.1
MK-76	23.886	89.981	15.9	10.0	Shallow	7.16	-120	766	1.00	24.4	< 0.1
MK-77	23.884	89.976	27.4	13.0	Shallow	7.00	-125	679	0.82	24.9	< 0.1
MK-78	23.902	89.988	61.0	15.0	Shallow	6.94	-117	858	0.94	24.7	< 0.1
MK-79	23.902	89.988	15.9	15.0	Shallow	6.93	-124	594	1.00	25.0	< 0.1
MK-80	23.888	89.990	7.6	13.0	Shallow	7.12	177	828	2.69	23.9	< 0.1
MK-81	23.880	89.992	12.2	11.0	Shallow	6.84	-97	776	1.54	24.8	< 0.1
MK-82	23.888	89.989	15.9	14.0	Shallow	7.01	-134	778	1.73	24.4	< 0.1
MK-83	23.894	89.995	19.8	14.0	Shallow	7.01	-1	658	2.31	24.9	< 0.1
MK-84	23.890	89.995	15.2	9.0	Shallow	7.28	-97	486	1.02	25.1	< 0.1
MK-85	23.888	89.994	22.9	11.0	Shallow	7.11	-122	684	1.12	25.3	< 0.1
MK-86	23.882	89.994	21.3	14.0	Shallow	6.96	-136	653	1.15	25.0	< 0.1
MK-87	23.876	89.996	35.1	12.0	Shallow	7.07	-100	641	1.38	25.3	< 0.1
MK-88	23.874	89.994	13.7	11.0	Shallow	7.04	-99	1584	1.34	26.2	< 0.1
MK-89	23.873	89.979	16.8	13.0	Shallow	7.16	60	563	1.54	25.2	< 0.1
MK-90	23.873	89.970	24.4	17.0	Shallow	7.20	-81	338	1.18	24.2	< 0.1
MKIW-01	23.880	89.992	24.4	11.0	Shallow	7.21	-124	1157	2.34	24.6	< 0.1
MKIW-02	23.874	89.993	36.6	11.0	Shallow	6.78	-124	1697	1.28	25.3	< 0.1

Table 5.2 Statistical parameters of physical properties of groundwater in the study area.

Statistical Parameters	pH	ORP (mV)	Conductivity (µS/cm)	Dissolved Oxygen (mg/L)	Temperature (°C)
Number of values	85	38	85	74	85
Minimum	6.11	-152	338	0.25	23
Maximum	7.28	177	2500	5.94	29
Mean	6.75	-87.96	857.21	0.86	25.7
Median	6.87	-104.8	640	0.535	26.0
Standard error	0.034	11.58	59.17	0.10	0.10
Variance	0.098	5097	297580	0.708	0.931
Standard deviation	0.314	71.39	545.51	0.841	0.965

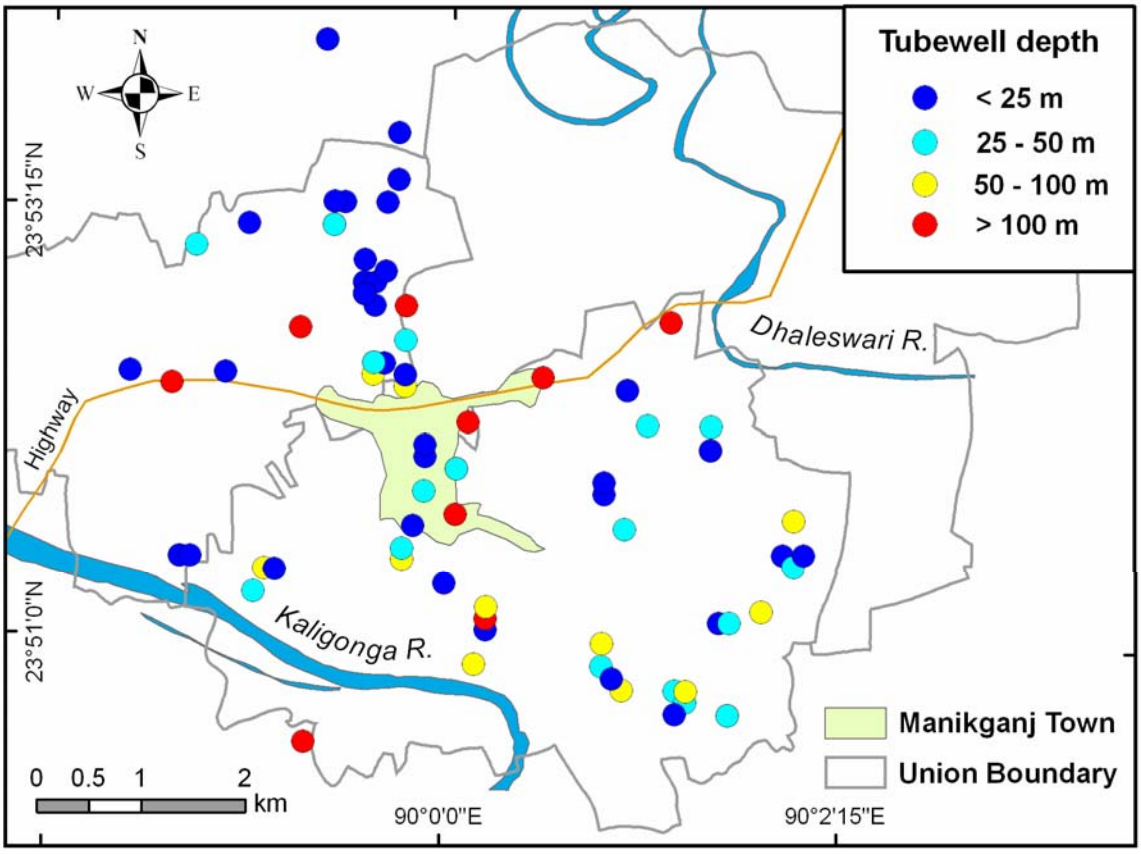

Fig. 5.1 Map showing depths of tubewells sampled for groundwater chemistry in Manikganj area.

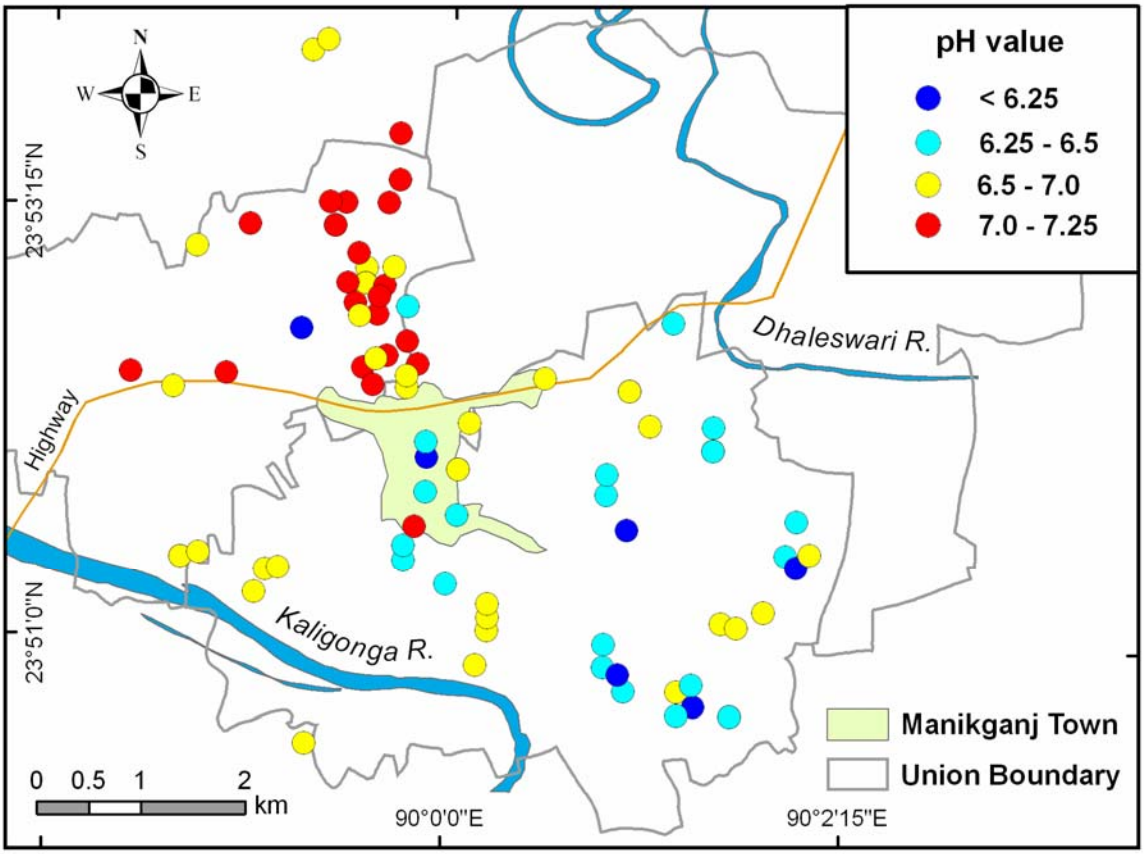

Fig. 5.2 Map showing the distribution of groundwater pH in Manikganj study area.

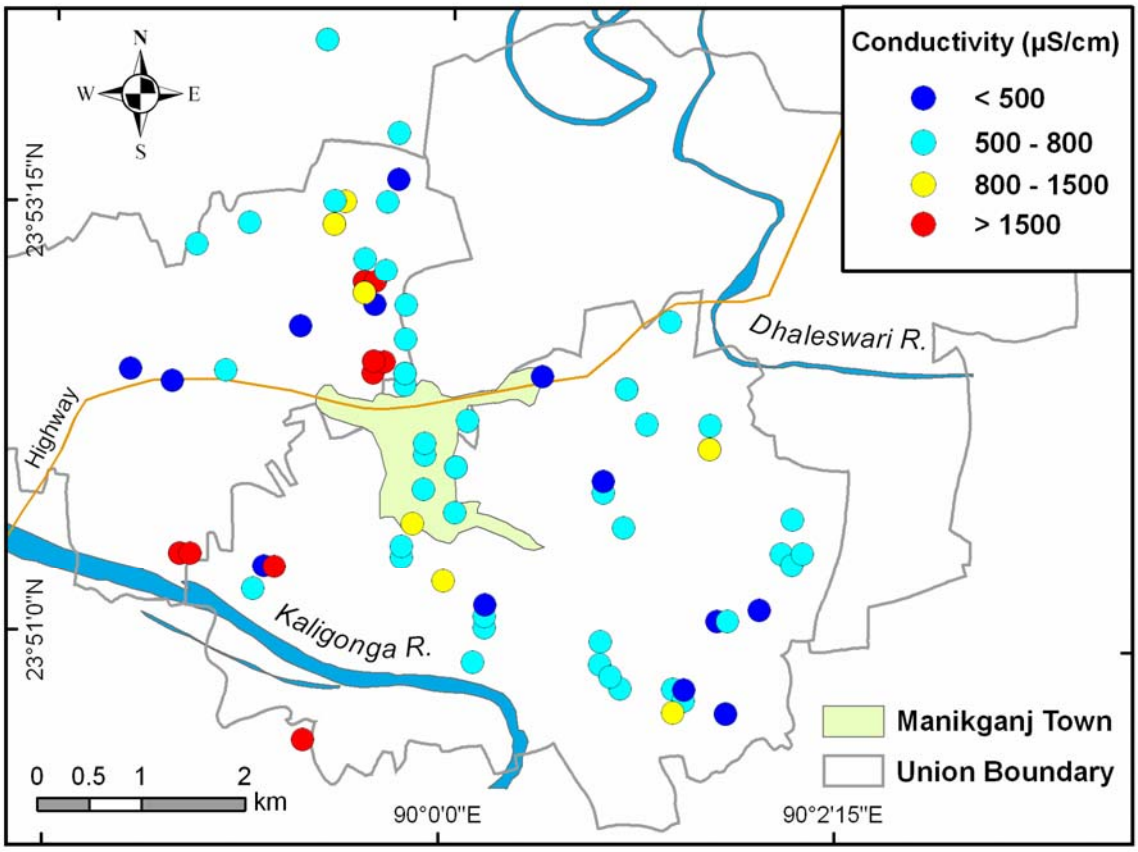

Fig. 5.3 Map showing spatial distribution of groundwater specific electrical conductivity in Manikganj study area.

Table 5.3 Major groundwater chemistry in Manikganj study area.

Sample No.	Latitude (degree)	Longitude (degree)	Well depth (m)	Ca	Na	Mg	K	NO_3	Cl	PO_4	SO_4	HCO_3
MK-01	23.865	90.001	178.3	68.2	58.8	25.9	4.50	0.01	25.4	0.01	3.42	412.4
MK-02	23.865	90.001	45.0	88.1	16.2	32.5	3.81	0.01	7.1	0.01	6.35	439.2
MK-03	23.848	90.003	79.5	71.3	27.2	25.8	4.25	1.06	11.4	0.01	2.40	370.9
MK-04	23.851	90.004	0.0	64.7	22.7	24.0	4.19	4.43	10.9	0.01	1.86	334.3
MK-05	23.852	90.004	105.9	61.4	22.7	25.2	4.54	6.02	10.4	0.01	0.01	341.6
MK-06	23.853	90.004	100.0	65.1	19.9	21.6	3.87	5.26	10.6	0.01	0.01	336.7
MK-07	23.869	90.002	137.2	62.4	45.1	24.7	3.25	0.01	15.4	0.01	0.01	383.1
MK-08	23.873	90.009	228.6	54.4	35.0	20.8	3.08	0.01	15.5	0.01	1.89	297.7
MK-09	23.846	90.017	73.2	62.2	18.6	23.4	3.86	1.25	4.5	0.01	4.26	327.0
MK-10	23.848	90.015	36.6	71.7	13.2	32.2	2.76	0.01	17.9	0.01	26.22	339.2
MK-11	23.847	90.016	18.3	102.4	26.4	28.5	2.43	1.83	35.9	0.01	2.47	417.2
MK-12	23.850	90.015	73.2	67.6	15.3	28.5	3.27	0.01	14.2	0.01	0.01	339.2
MK-13	23.846	90.022	36.6	82.1	17.6	30.2	7.23	4.45	7.3	0.01	8.52	388.0
MK-14	23.845	90.023	27.4	75.2	18.1	34.5	13.97	0.01	10.5	0.01	40.00	363.5
MK-15	23.846	90.023	73.2	61.3	13.7	21.0	4.21	4.05	4.3	0.01	3.35	307.4
MK-16	23.866	89.998	22.9	78.8	46.3	26.4	39.97	28.88	58.5	5.32	49.92	312.2
MK-17	23.867	89.998	15.2	71.6	14.8	20.9	8.67	0.01	23.3	6.74	12.62	263.5
MK-18	23.872	89.996	73.2	67.6	25.2	24.4	3.36	0.01	15.0	0.01	0.01	317.2
MK-19	23.873	89.996	36.6	85.5	16.7	25.9	3.72	0.01	19.3	0.01	0.01	351.4
MK-20	23.873	89.996	18.3	68.6	12.8	21.8	3.09	0.01	12.2	0.01	1.84	314.8
MK-21	23.853	90.030	73.2	58.8	14.3	24.7	3.65	0.01	21.3	0.01	43.00	322.1
MK-22	23.852	90.026	22.9	58.0	8.2	21.6	2.98	0.01	4.0	0.01	0.01	295.2
MK-23	23.852	90.027	36.6	68.4	10.8	21.2	3.62	0.01	4.0	0.01	0.01	317.2
MK-24	23.856	89.983	73.2	56.9	11.7	19.9	4.27	0.01	4.9	0.01	0.01	270.9
MK-25	23.854	89.982	36.6	71.4	10.7	21.3	3.03	0.01	5.5	0.01	0.01	348.9
MK-26	23.858	90.032	22.9	116.1	12.5	30.3	3.23	0.01	61.5	0.01	17.65	370.9
MK-27	23.857	90.033	36.6	57.6	12.8	25.7	4.23	0.01	5.3	0.01	1.96	329.4
MK-28	23.861	90.033	73.2	71.4	16.4	25.0	3.64	0.01	6.2	0.01	0.01	368.4
MK-29	23.858	90.034	15.2	71.9	11.2	20.0	3.67	0.69	11.7	0.01	0.01	290.4
MK-30	23.863	90.015	21.4	95.1	13.1	19.8	3.75	5.56	34.0	0.01	41.70	273.3
MK-31	23.864	90.015	18.3	51.0	12.8	19.6	12.21	1.04	4.0	3.26	14.32	244.0
MK-32	23.860	90.017	37.2	55.7	7.5	23.5	2.41	0.01	4.2	0.01	22.34	263.5
MK-33	23.867	90.025	73.2	56.3	11.9	22.6	28.63	1.14	7.4	0.01	0.01	305.0
MK-34	23.867	90.025	22.9	91.1	21.6	43.7	4.38	4.61	71.0	0.01	73.42	341.6
MK-35	23.869	90.025	45.7	58.1	13.8	23.9	18.36	0.01	6.9	0.01	12.41	307.4
MK-36	23.857	89.996	73.2	70.4	11.7	22.6	6.08	0.01	20.7	0.01	12.33	290.4
MK-37	23.858	89.996	36.6	73.6	10.9	27.8	10.20	0.01	7.2	0.01	13.91	348.9
MK-38	23.855	90.000	21.3	135.2	18.2	34.5	0.67	0.01	21.5	0.01	41.68	483.1
MK-39	23.863	89.998	45.7	93.5	10.5	40.1	5.62	0.01	36.3	0.01	18.87	397.7
MK-40	23.872	90.017	73.2	62.0	12.7	18.6	3.73	0.01	5.0	0.01	1.81	297.7
MK-41	23.872	90.017	18.3	72.9	11.5	29.0	3.91	0.01	2.6	0.01	19.12	322.1
MK-42	23.869	90.019	37.2	47.8	19.0	28.1	20.83	0.01	6.2	0.01	1.87	312.3
MK-43	23.844	90.027	73.2	86.2	22.0	43.9	4.26	0.01	34.2	0.01	47.17	375.8
MK-44	23.844	90.027	45.7	51.5	18.9	28.6	21.40	0.01	52.2	0.01	75.73	305.0
MK-45	23.844	90.022	18.3	125.4	22.0	38.5	1.81	0.01	6.9	0.01	4.20	422.1
MK-46	23.841	89.987	202.7	143.0	18.9	33.8	0.82	0.01	1.4	0.01	1.85	336.7
MK-47	23.872	89.974	192.0	41.7	36.1	20.1	3.66	0.01	4.1	0.01	2.90	256.2
MK-48	23.877	89.986	185.9	58.7	31.4	21.6	3.32	3.34	5.4	0.01	0.01	305.0
MK-49	23.879	89.996	185.9	64.3	36.2	28.8	3.01	0.01	9.8	0.01	1.76	341.6
MK-50	23.878	90.021	195.1	54.3	56.1	21.0	3.09	0.01	13.3	0.01	2.25	341.6

Table 5.3 (cont'd.)

Sample No.	Latitude (degree)	Longitude (degree)	Well depth (m)	Ca	Na	Mg	K	NO_3	Cl	PO_4	SO_4	HCO_3
MK-51	23.861	90.001	137.2	39.3	98.8	16.0	3.32	0.01	32.6	0.01	1.73	353.8
MK-60	23.880	89.992	25.0	63.4	13.3	27.7	2.96	0.02	5.7	0.04	0.06	151.3
MK-61	23.881	89.992	15.0	108.0	12.5	30.7	1.70	0.02	22.6	0.04	1.86	198.3
MK-62	23.857	89.975	39.6	83.5	19.2	29.4	7.98	0.02	4.8	0.04	4.19	194.0
MK-63	23.857	89.975	22.9	111.0	18.2	40.5	5.83	0.02	12.0	0.04	9.27	241.0
MK-64	23.857	89.976	24.4	84.0	14.0	24.5	2.99	0.02	9.4	0.04	0.06	183.0
MK-65	23.881	89.992	21.3	82.6	19.2	30.9	4.10	0.02	33.7	0.04	0.06	178.7
MK-66	23.881	89.992	18.3	133.0	27.6	45.5	2.48	0.19	42.9	0.04	18.30	231.8
MK-67	23.881	89.993	9.2	118.0	16.4	29.0	6.92	0.06	16.9	0.04	9.90	205.0
MK-68	23.874	89.993	29.0	120.0	31.6	35.9	5.39	0.02	58.8	0.04	26.20	214.7
MK-69	23.873	89.993	73.2	78.2	36.7	27.1	4.14	0.02	11.5	0.02	0.06	197.0
MK-52	23.880	89.992	22.9	49.2	15.2	20.4	3.69	0.02	5.5	0.05	0.06	134.2
MK-70	23.879	89.993	15.9	87.9	14.9	27.6	2.78	0.01	18.4	0.02	0.03	198.3
MK-71	23.883	89.992	15.2	73.5	11.2	21.7	3.36	0.01	10.7	0.02	0.03	171.4
MK-72	23.886	89.989	29.6	54.5	15.4	34.0	28.00	0.01	16.8	0.02	26.40	175.7
MK-73	23.886	89.989	48.8	50.0	18.4	22.6	8.10	0.02	14.5	0.02	1.10	145.8
MK-74	23.860	89.997	16.8	107.0	15.1	27.2	0.67	0.02	22.2	0.03	2.30	222.0
MK-75	23.856	89.984	15.9	96.1	15.5	46.1	38.00	0.02	39.4	0.03	12.20	276.9
MK-76	23.886	89.981	15.9	105.0	19.9	21.7	4.38	0.01	27.2	0.02	17.00	203.7
MK-77	23.884	89.976	27.4	82.6	16.1	22.3	4.00	0.02	10.0	0.02	0.03	190.9
MK-78	23.902	89.988	61.0	126.0	17.9	29.1	1.87	0.02	9.0	0.03	25.20	250.1
MK-79	23.902	89.988	15.9	63.2	17.8	19.7	4.50	0.01	4.4	0.02	0.03	168.4
MK-80	23.888	89.990	7.6	118.0	24.4	26.8	4.10	0.02	30.8	0.03	8.35	242.8
MK-81	23.880	89.992	12.2	85.2	24.7	31.9	3.55	0.02	17.1	0.03	0.91	219.0
MK-82	23.888	89.989	15.9	74.1	20.1	40.0	7.22	0.02	30.0	0.03	8.15	210.5
MK-83	23.894	89.995	19.8	67.6	12.2	31.3	4.03	0.01	12.9	0.02	22.80	170.8
MK-84	23.890	89.995	15.2	41.1	16.1	13.3	2.72	0.01	5.9	0.02	10.90	133.0
MK-85	23.888	89.994	22.9	98.3	14.2	21.4	4.00	0.01	4.9	0.02	11.70	208.6
MK-86	23.882	89.994	21.3	71.4	17.4	25.5	3.03	0.01	15.3	0.02	19.10	167.8
MK-87	23.876	89.996	35.1	69.8	20.3	25.9	2.76	0.01	9.0	0.02	5.80	181.8
MK-88	23.874	89.994	13.7	76.2	25.0	22.4	5.83	0.01	12.3	0.02	0.03	189.1
MK-89	23.873	89.979	16.8	60.8	17.5	21.8	10.70	0.12	12.5	0.23	16.20	153.7
MK-90	23.873	89.970	24.4	32.1	7.8	19.7	2.38	0.02	5.1	0.01	6.65	90.9
MKIW-01	23.880	89.992	24.4	52.9	13.9	21.8	2.51	0.01	5.4	0.01	0.03	147.6
MKIW-02	23.874	89.993	36.6	74.6	28.3	21.6	15.80	-	-	-	-	-

Table 5.4 Descriptive statistical parameters of major groundwater chemistry in Manikganj study area.

Statistical Parametrs	Ca	Na	Mg	K	NO_3	Cl	PO_4	SO_4	HCO_3
Number of values	85	85	85	85	84	84	84	84	84
Minimum	32.10	7.52	13.30	0.67	0.01	1.44	0.01	0.01	90.89
Maximum	143.0	98.8	46.1	40.0	28.9	71.0	6.7	75.7	483.1
Mean	76.31	20.45	26.71	6.33	0.89	16.65	0.20	10.76	277.88
Median	71.37	17.40	25.50	3.86	0.01	11.58	0.01	3.12	296.46
Standard error	2.56	1.41	0.74	0.80	0.37	1.62	0.11	1.73	9.20
Variance	558.69	169.10	45.92	53.94	11.56	219.80	0.98	252.59	7115.60
Standard deviation	23.6	13.0	6.8	7.3	3.4	14.8	1.0	15.9	84.4

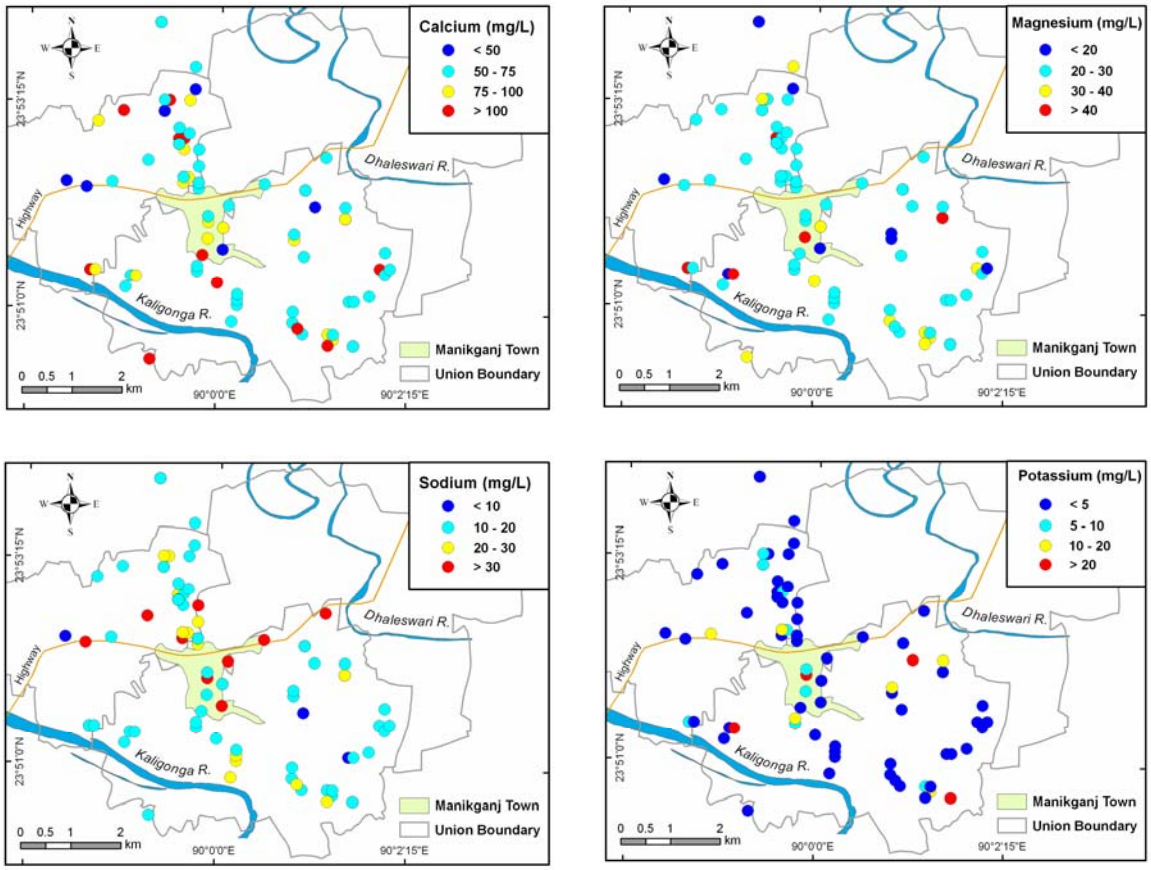

Fig. 5.4 Maps of spatial distributions of major cations (Ca, Mg, Na, and K) in groundwater in Manikganj.

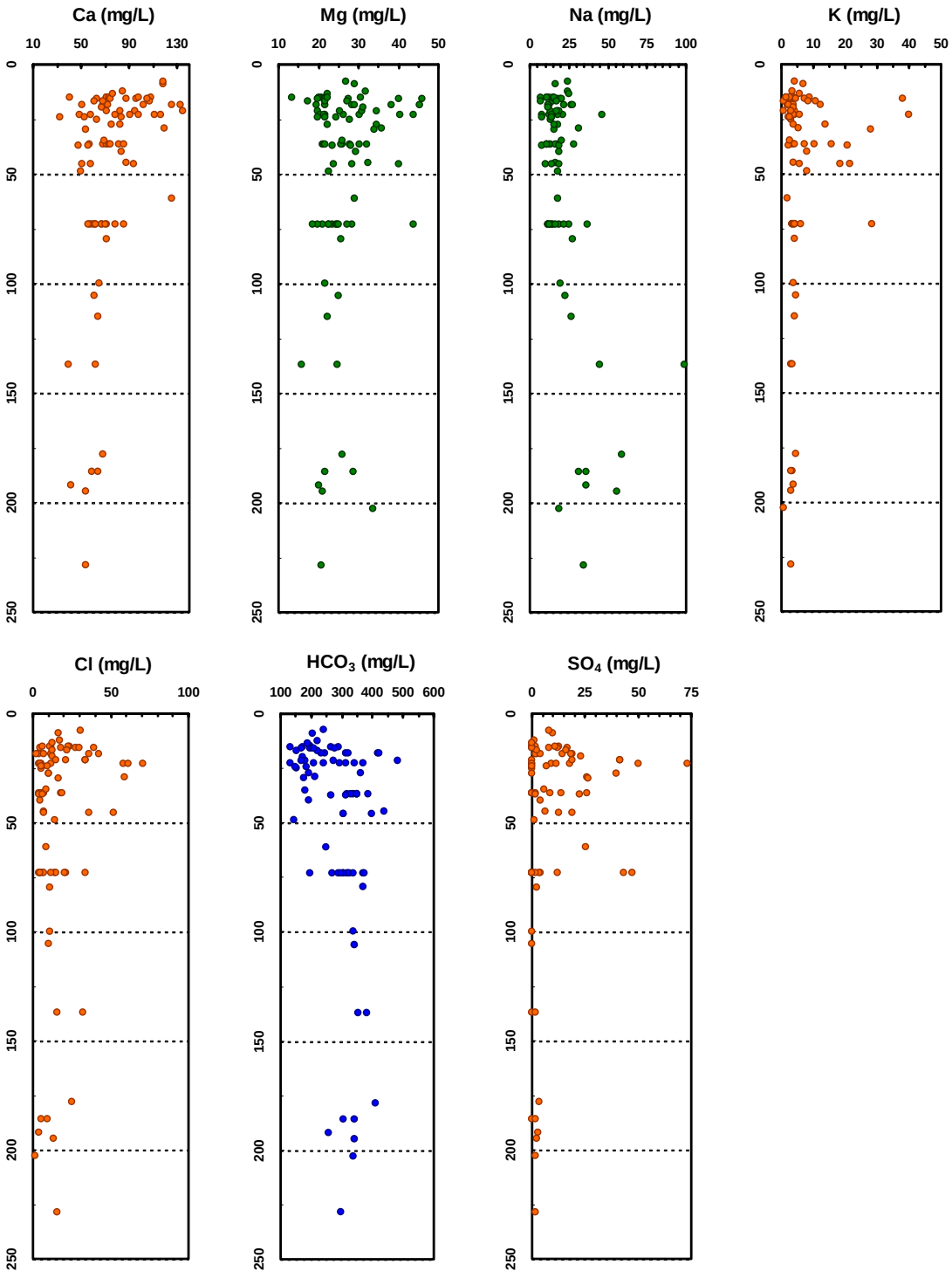

Fig. 5.5 Plots of vertical distribution of major cations and anions in groundwater in Manikganj.

Concentrations of HCO_3 (90.9-483.1 mg/L) are higher towards the southern part of Manikganj where groundwater SO_4 concentrations (0.01-75.7 mg/L) are also high (Fig. 5.6). At shallow depths (< 50 m) the concentrations of HCO_3 vary greatly (130-483 mg/L), but remains approximately 300-350 mg/L below a depth of 100 m (Fig. 5.5).

Major ion compositions in Manikganj groundwaters plotted on a Piper diagram, indicate that the groundwater is mostly Ca-HCO_3 type (Fig. 5.7). Occurrence of high dissolved HCO_3 in groundwater in Manikganj is probably due to active biodegradation of organic matter mostly at shallow depths in aquifers (GRG and HG, 2002). Figure 5.7 also shows a clear difference between shallow (< 80 m) and deep groundwater (> 80 m) in Manikganj aquifers. Shallow groundwaters are high in Ca concentrations, but contain wide range of HCO_3 and SO_4 concentrations. Deeper groundwaters contain higher concentrations of HCO_3 and Ca, but low concentration of SO_4. Concentration of Ca varies slightly in deeper aquifers, but concentrations of HCO_3 ranges from 300-350 mg/L.

5.1.3. Arsenic and other trace elements

Concentrations of dissolved As, Fe, Mn, Si, Mo and other important trace metals in groundwater of Manikganj area are shown in Table 5.5. Considerable spatial and depth variations are observed in trace metals in groundwater of Manikganj study area. Several important trace metals including As, Fe, Mn, and Si are shown in Fig. 5.8. Descriptive statistical parameters of different trace metals including dissolved arsenic are given in Table 5.6. Mean concentration of arsenic in sampled 85 tubewells in Manikganj is ~33 μg/L, even though the range is between 0.25 and 191 μg/L (Table 5.6). The maximum arsenic level is 191 μg/L, which is almost 20 times higher than the WHO standard.

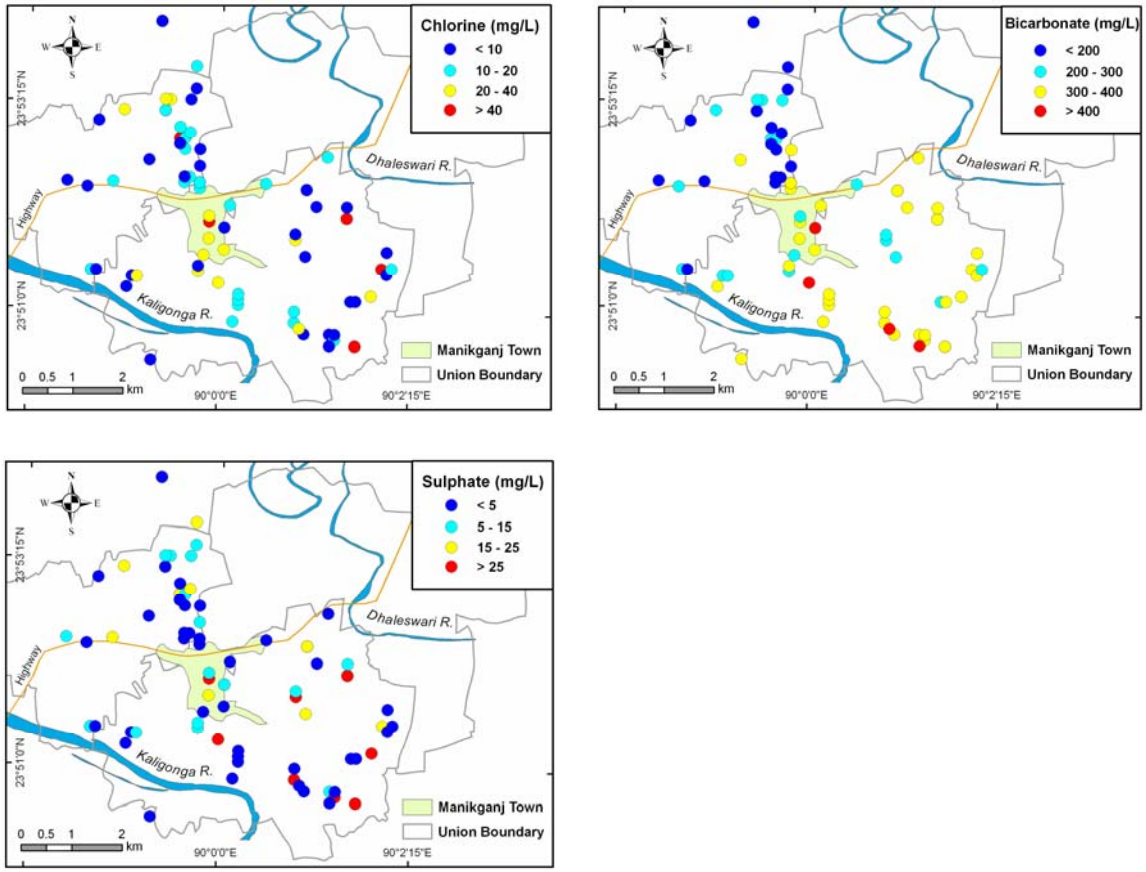

Fig. 5.6 Maps of spatial distributions of groundwater anions in Manikganj study area.

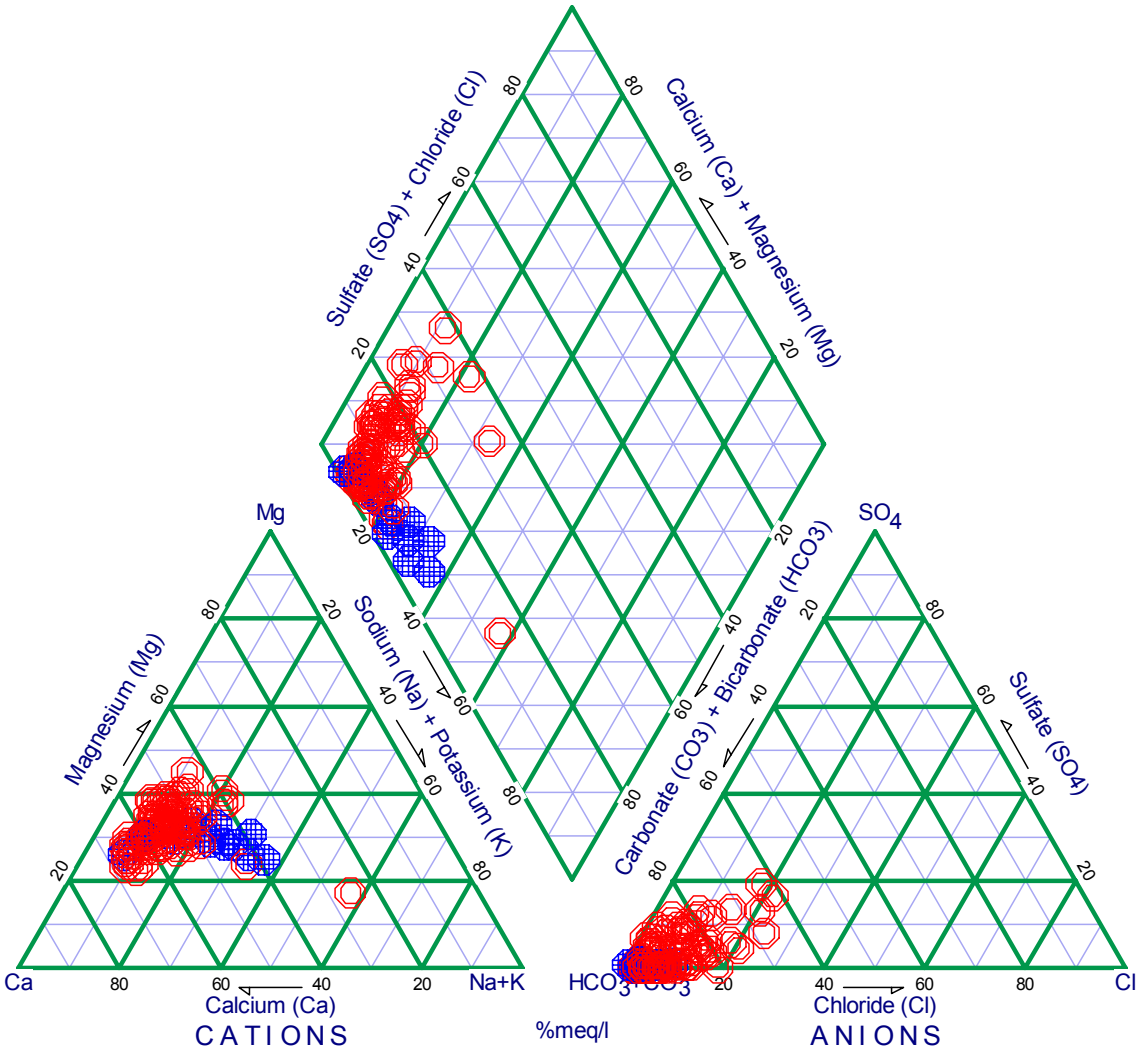

Fig. 5.7 Piper diagram illustrating the main hydrochemical features of Manikganj groundwater. Shallow (< 100 m; red circles) and deep (> 100 m; blue mesh) groundwater chemistry are slightly different in the study area.

Table 5.5 Concentrations of important trace metals in Manikganj groundwater.

Sample No.	Depth (m)	Fe (mg/L)	As (µg/L)	Mn (mg/L)	Sr (mg/L)	Zn (µg/L)	Al (mg/L)	Ba (mg/L)
MK-01	178.3	4.59	8.4	0.87	0.68	0.22	0.01	0.13
MK-02	45.0	17.74	31.2	0.26	0.39	0.14	0.03	0.16
MK-03	79.5	9.11	43.9	0.29	0.33	0.02	0.01	0.13
MK-04	-	0.07	17.6	0.12	0.30	0.18	0.01	0.08
MK-05	105.9	7.32	46.9	0.22	0.30	0.02	0.02	0.11
MK-06	100.0	7.72	64.8	0.28	0.29	0.01	0.02	0.16
MK-07	137.2	0.77	33.1	0.75	0.40	0.02	0.02	0.16
MK-08	228.6	0.90	4.1	0.69	0.38	0.03	0.01	0.10
MK-09	73.2	11.60	18.1	0.61	0.24	0.03	0.02	0.17
MK-10	36.6	14.82	3.6	0.20	0.24	0.02	0.01	0.19
MK-11	18.3	14.35	28.4	1.60	0.32	0.02	0.03	0.09
MK-12	73.2	15.95	22.3	0.59	0.28	0.11	0.01	0.16
MK-13	36.6	7.54	17.1	0.53	0.35	0.02	0.02	0.24
MK-14	27.4	13.15	14.1	1.23	0.20	0.03	0.01	0.26
MK-15	73.2	10.37	59.5	0.33	0.27	0.05	0.00	0.16
MK-16	22.9	0.16	4.0	0.04	0.12	0.02	0.01	0.06
MK-17	15.2	0.25	4.8	0.54	0.13	0.01	0.02	0.04
MK-18	73.2	6.55	43.5	0.21	0.34	0.01	0.02	0.17
MK-19	36.6	10.16	105.9	0.36	0.42	0.03	0.01	0.19
MK-20	18.3	8.67	102.0	0.35	0.33	0.01	0.02	0.14
MK-21	73.2	9.27	55.3	0.51	0.26	0.02	0.01	0.15
MK-22	22.9	16.54	35.3	1.43	0.24	0.02	0.02	0.11
MK-23	36.6	13.25	69.4	0.30	0.29	0.01	0.01	0.15
MK-24	73.2	7.95	78.6	0.41	0.24	0.02	0.01	0.13
MK-25	36.6	26.98	60.2	0.52	0.21	0.04	0.02	0.20
MK-26	22.9	2.23	12.2	4.16	0.37	0.02	0.03	0.11
MK-27	36.6	18.92	51.2	0.66	0.26	0.01	0.03	0.15
MK-28	73.2	15.13	27.6	0.71	0.29	0.01	0.02	0.20
MK-29	15.2	0.71	5.8	1.12	0.23	0.01	0.13	0.09
MK-30	21.4	0.21	1.2	0.60	0.22	0.02	0.02	0.09
MK-31	18.3	0.19	3.9	0.44	0.06	0.01	0.02	0.06
MK-32	37.2	10.55	9.8	0.87	0.20	0.02	0.01	0.09
MK-33	73.2	2.46	0.8	0.66	0.23	0.01	0.02	0.25
MK-34	22.9	8.06	16.4	0.94	0.29	0.02	0.02	0.20
MK-35	45.7	0.00	9.4	0.88	0.22	0.01	0.01	0.18
MK-36	73.2	6.67	63.7	0.28	0.27	0.01	0.03	0.15
MK-37	36.6	5.69	38.9	1.04	0.25	0.02	0.01	0.20
MK-38	21.3	0.00	2.3	0.94	0.31	0.02	0.02	0.09
MK-39	45.7	0.60	58.8	0.76	0.42	0.01	0.00	0.14
MK-40	73.2	0.01	n.m.	0.88	0.25	0.31	0.00	0.16
MK-41	18.3	0.16	24.0	2.05	0.28	0.01	0.02	0.09
MK-42	37.2	0.00	11.1	0.75	0.14	0.02	0.02	0.17
MK-43	73.2	0.03	4.1	0.90	0.29	0.01	0.03	0.14
MK-44	45.7	7.79	21.2	0.79	0.15	0.02	0.01	0.20
MK-45	18.3	0.19	14.9	3.36	0.38	0.03	0.03	0.20
MK-46	202.7	3.51	0.3	1.23	0.31	0.03	0.00	0.12
MK-47	192.0	0.40	9.2	0.38	0.28	0.03	0.01	0.12
MK-48	185.9	0.32	0.4	0.73	0.37	0.03	0.04	0.14
MK-49	185.9	0.00	0.3	0.89	0.44	0.02	0.03	0.16
MK-50	195.1	0.00	0.5	0.63	0.37	0.07	0.02	0.16

Table 5.5 (Cont'd.)

Sample No.	Depth (m)	Fe (mg/L)	As (µg/L)	Mn (mg/L)	Sr (mg/L)	Zn (µg/L)	Al (mg/L)	Ba (mg/L)
MK-51	137.2	0.00	8.9	0.31	0.26	0.42	0.01	0.12
MK-60	25.0	0.13	12.3	0.37	0.32	0.00	0.00	0.06
MK-61	15.0	0.13	8.8	0.00	0.34	0.01	0.00	0.07
MK-62	39.6	0.32	5.2	0.95	0.33	0.02	0.00	0.13
MK-63	22.9	0.15	6.5	0.00	0.29	0.00	0.00	0.10
MK-64	24.4	1.15	6.1	0.44	0.20	0.06	0.00	0.11
MK-65	21.3	0.15	11.1	0.00	0.39	0.00	0.00	0.07
MK-66	18.3	0.19	4.4	0.00	0.51	0.00	0.00	0.11
MK-67	9.2	0.15	4.8	0.00	0.36	0.02	0.00	0.10
MK-68	29.0	0.49	58.1	0.36	0.50	0.00	0.00	0.18
MK-69	73.2	0.26	20.8	0.23	0.32	0.02	0.00	0.14
MK-52	22.9	0.25	12.5	0.49	0.26	0.00	0.00	0.06
MK-70	15.9	8.86	118.0	0.55	0.41	0.04	0.00	0.14
MK-71	15.2	6.65	163.0	1.73	0.41	0.00	0.00	0.14
MK-72	29.6	5.74	15.9	0.68	0.20	0.02	0.00	0.31
MK-73	48.8	7.06	47.7	0.75	0.23	0.10	0.00	0.22
MK-74	16.8	2.27	2.9	0.92	0.29	0.00	0.00	0.05
MK-75	15.9	9.71	14.4	0.30	0.34	0.00	0.00	0.04
MK-76	15.9	4.85	20.2	1.30	0.23	0.03	0.00	0.05
MK-77	27.4	0.13	16.2	0.61	0.23	0.00	0.00	0.12
MK-78	61.0	12.40	20.0	0.49	0.32	0.02	0.00	0.16
MK-79	15.9	9.47	54.8	0.85	0.30	0.00	0.00	0.19
MK-80	7.6	0.20	1.7	2.24	0.32	0.34	0.01	0.08
MK-81	12.2	13.40	78.4	0.70	0.45	0.01	0.00	0.18
MK-82	15.9	3.51	8.6	0.28	0.22	0.00	0.00	0.02
MK-83	19.8	0.59	41.5	0.85	0.17	0.00	0.00	0.08
MK-84	15.2	0.10	9.6	0.58	0.15	0.00	0.00	0.69
MK-85	22.9	1.83	5.6	0.28	0.18	0.01	0.00	0.15
MK-86	21.3	12.70	63.9	1.18	0.27	0.01	0.00	0.16
MK-87	35.1	4.32	11.9	0.56	0.21	0.00	0.00	0.13
MK-88	13.7	6.92	184.0	0.36	0.33	0.00	0.00	0.16
MK-89	16.8	0.47	39.0	1.05	0.32	0.05	0.00	0.80
MK-90	24.4	1.61	40.3	0.65	0.08	0.01	0.00	0.05
MKIW-01	24.4	5.62	91.4	0.38	0.27	0.00	0.00	0.01
MKIW-02	36.6	7.88	191.0	0.27	0.24	12.60	0.01	0.04

Table 5.6 Descriptive statistics of major trace metals in Manikganj groundwater.

Statistical Parameters	Fe	As	Mn	Sr	Zn	Al	Ba
Number of samples	85	84	85	85	85	85	85
Minimum	0.001	0.25	0.001	0.06	0.001	0.00	0.013
Maximum	26.98	191.0	4.16	0.68	12.6	0.13	0.80
Range	26.98	190.7	4.16	0.62	12.6	0.13	0.79
Mean	5.29	32.85	0.71	0.29	0.18	0.01	0.15
Median	3.51	16.75	0.60	0.29	0.02	0.01	0.14
Variance	34.3	1552	0.42	0.01	1.86	0.00	0.01
Standard deviation	5.85	39.4	0.65	0.10	1.36	0.02	0.11
Coefficient of variation	1.11	1.20	0.91	0.33	7.38	1.31	0.74

Statistical Parameters	Cd	Co	Ni	Mo	V	Si	Pb
Number of samples	15	13	26	34	16	34	24
Minimum	0.01	0.02	0.03	0.30	0.01	7.73	0.01
Maximum	1.22	1.17	2.40	4.50	2.70	25.80	21.6
Range	1.21	1.15	2.37	4.20	2.69	18.07	21.6
Mean	0.10	0.26	0.74	1.40	0.46	19.39	0.96
Median	0.02	0.09	0.60	1.10	0.11	20.95	0.02
Variance	0.10	0.14	0.25	1.28	0.58	23.2	19.3
Standard deviation	0.31	0.37	0.50	1.13	0.76	4.82	4.40
Coefficient of variation	3.09	1.42	0.67	0.81	1.66	0.25	4.57

The median arsenic concentration is 16.8 µg/L, which is two times higher than the average arsenic level (Table 5.6). Only 6 samples in 87 tubewells contain arsenic concentration of >100 µg/L. The spatial distributions of groundwater arsenic are observed within Manikganj study area, which will be described in the following section in detail.

Fe is another important trace element commonly found at higher concentrations in Bangladesh groundwater. In Manikganj, the average groundwater Fe concentration is 5.29 mg/L. The maximum Fe concentration is approximately 27 mg/L and the minimum is 0.001 mg/L (Table 5.6). High Fe concentrations are found in tubewells where As concentrations are also higher than the average value. Considerable spatial distribution of Fe is seen in the study area (Fig. 5.8). Mn concentrations in the study area range from 0.001 mg/L to the maximum level of 4.16 mg/L with a mean value of 0.71 mg/L. In Manikganj, the spatial distribution of Mn in groundwater is also variable (Fig. 5.8). The groundwater has high concentrations of Si with an average value of approximately 19.4 mg/L. The maximum concentration of dissolved Si in Manikganj groundwater is 25 mg/L. The spatial distribution of Si in groundwater follows the distribution of arsenic in the northern part of the study area (Fig. 5.8).

The concentration of dissolved Al in Manikganj groundwaters is very low. The average Al concentration is approximately 0.01 mg/L. Concentration of Sr in groundwater varies from 0.06 mg/L to 0.68 mg/L with a mean value of 0.29 mg/L. High concentrations of Sr are found in tubewells that contain higher arsenic concentrations. Concentrations of dissolved Ba (0.013 – 0.80 mg/L), Zn (0.001 – 12.60 mg/L), Ni (0.03 –

2.4 µg/L), Mo (0.03 – 4.5 µg/L) and Pb (0.01 – 26.6 µg/L) are found medium to low in groundwater of Manikganj area (Table 5.6).

Groundwaters with high As concentrations contain relatively high amount of Fe and Mn concentrations in most cases, but low in dissolved SO_4 concentrations. This relationship is consistent with groundwaters of other parts of Bangladesh where groundwater contains high concentration of dissolved As (BGS and DPHE, 2001).

5.1.4. Isotope geochemistry

The δ^2H and $\delta^{18}O$ values of groundwater from 11 tubewells screened within the alluvial aquifers in Manikganj range from -19 to -40.2‰ and -1.6 to -6.1‰ respectively. The normal reference standard is V-SMOW (Vienna Standard Mean Ocean Water). Most groundwater falls within or slightly below the Global Meteoric Water Line (Fig. 5.9). This indicates that the origin of groundwater in alluvial aquifers in Manikganj or even throughout the whole country is from local rainfall and rivers with some evaporation before infiltration (Aggarwal et al., 2000). The isotopically lightest precipitation occurs at the poles as opposed to equatorial region because of temperature effects and lack of water vapor due to precipitation that originally present in the air before it actually reaches the polar region (Drever, 1997).

In Manikganj groundwater, the δ^2H and $\delta^{18}O$ values at shallow depths (< 70 m) are lower (less negative) compared to the groundwater from deeper depths (Fig. 5.9). Those values in the shallow groundwaters are similar to that expected for recharge from the present-day rain and floodwaters in Bangladesh (Aggarwal et al., 2000).

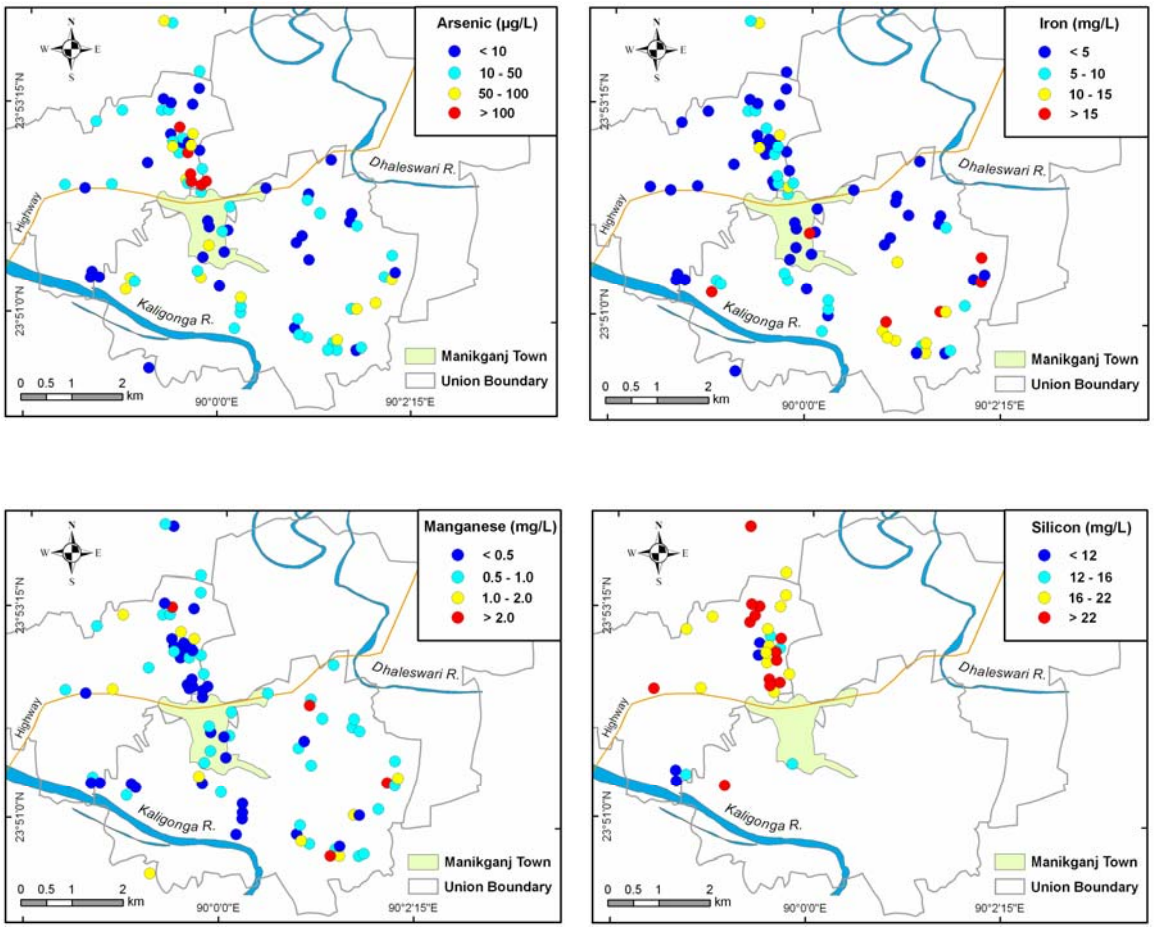

Fig. 5.8 Maps of spatial distributions of groundwater As, Fe, Mn and Si in Manikganj aquifers.

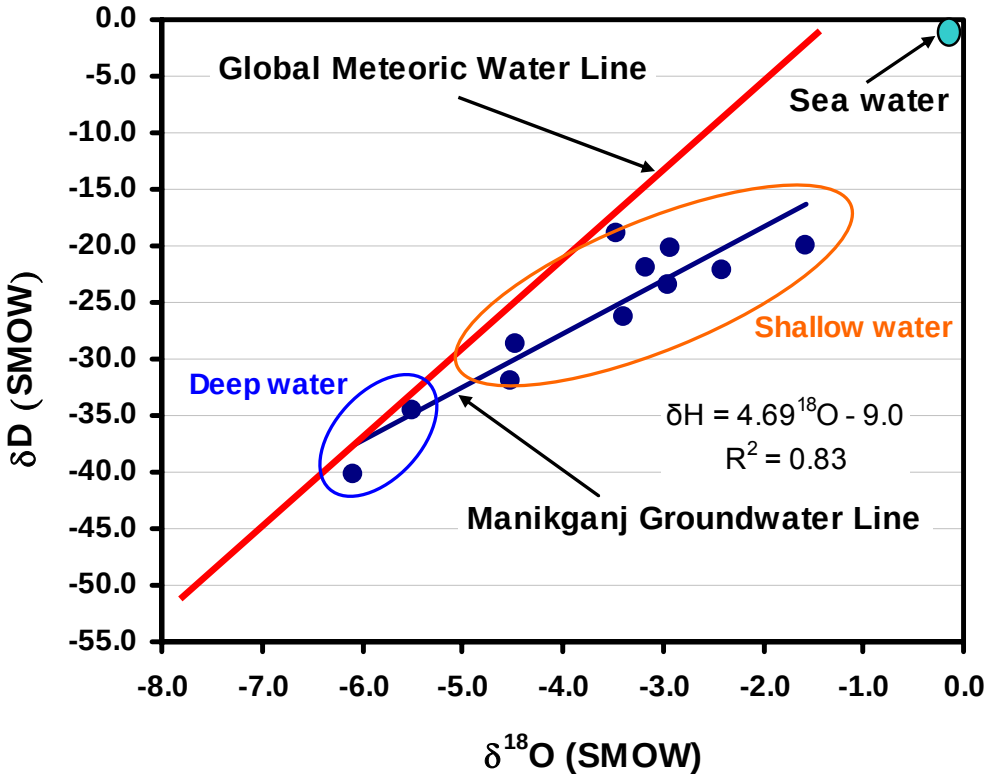

Fig. 5.9 Plot of stable isotope compositions in Manikganj groundwaters. Shallow groundwater samples are just below the Global Meteoric Water Line and aligned with Bangladesh groundwater composition as shown in Aggarwal et al. (2000) study. Groundwater in deeper aquifers might be compositionally different, but requires more data to evaluate this.

Similar stable isotope analyses of groundwaters from different location in Bangladesh shows that the composition of δ^2H and $\delta^{18}O$ is lighter (Aggarwal et al., 2000). Lighter isotopes in shallow groundwater mostly fall below the Global Meteoric Water Line indicating evaporation before or during infiltration. Not much information on stable isotopic composition has been derived due to small number of data from Manikganj area. However, groundwater from deep aquifers (> 70 m) in Manikganj contain low specific conductivity (< 600 µS/cm) and lower δ^2H and $\delta^{18}O$ values, which is consistent with the findings of Aggarwal et al. (2000) study, which falls within the meteoric water line.

The $\delta^{13}C$ is used to identify sources of carbon and to distinguish the isotopically lighter carbon derived from organic matter from the heavier carbon derived from carbonate minerals (Drever, 1997). The ^{12}C /^{13}C ratios are reported as ^{13}C with the PDB (Pee Dee Belemnite) calcite as the reference standard. The $\delta^{13}C$ values for dissolved inorganic carbon (DIC) varies from -3.32‰ to 4.07‰ indicating a relatively heavier isotopic signature for DIC in Manikganj groundwater (Turner, 2006). The DIC values (Table 5.7) fall within the range reported in the special study areas (Lakshmipur, Faridpur and Nawabganj, Fig. 1.1) of the National Hydrochemical Survey (BGS and DPHE, 2001), although most of the Manikganj values are heavier than the results reported from throughout Bangladesh (Turner, 2006). The $\delta^{13}C$ values for dissolved organic carbon (DOC) range from -22.63‰ to -28.79‰ (V-PDB) in Manikganj groundwater (Table 5.7). Only one groundwater sample (MKIW-1) from the well, which is being used as the injection well of arsenic-bioremediation in the study area, has the highest $\delta^{13}C$ of –28.79‰. As the natural groundwater chemistry has been modified greatly because of

injection of molasses into this well, the $\delta^{13}C$ value went high, whereas the mean $\delta^{13}C$ value is -24.15‰. The relationships between arsenic, iron, $\delta^{13}C$ and well depths are shown in Fig. 5.10, which suggest higher arsenic and iron concentrations are commonly associated with the lower $\delta^{13}C$ values.

Depletion of DIC in groundwater by oxidation of organic matter should produce the lighter $\delta^{13}C$ as opposed to dissolution of carbonate minerals and mixing of marine water (BGS and DPHE, 2001). Most of the $\delta^{13}C$ values in Manikganj area are high negative (isotopically lighter) indicating oxidation of organic matter in aquifers. The large $\delta^{13}C$ variations observed in Bangladesh groundwater reflect derivation of the DIC from the multiple sources including soil-zone CO_2, oxidation of organic matter, potential oxidation of CH_4, and dissolution of carbonate minerals (BGS and DPHE, 2001).

5.2. Groundwater arsenic in Manikganj

5.2.1. Arsenic distribution in groundwater

Groundwater arsenic concentrations in Manikganj show a considerable spatial variability, especially at shallow depths. High groundwater (> 50 µg/L) arsenic wells are located mostly within the northern parts and a few toward the south of the study area (Fig. 5.11). High As tubewells are generally located within abandoned channel or natural levees whereas the low As wells are found within floodplain areas. Spatial variability in groundwater arsenic concentrations is extremely high within a small lateral distance in Manikganj and this is consistent with many As-contaminated areas in Bangladesh (BGS and DPHE, 2001; GRG and HG, 2002; van Geen et al., 2003).

Table 5.7 Stable carbon isotope ($\delta^{13}C$, DOC) concentrations in Manikganj groundwater.

Sample ID	$\delta^{13}C$ (PDB)	Depth (m)	Arsenic (µg/L)	Iron (mg/L)
MKIW-1	-28.8	24.4	91.4	5.620
MKIW-2	-23.1	36.6	191.0	7.880
MK-70	-23.4	15.9	118.0	8.860
MK-71	-22.9	15.2	163.0	6.650
MK-72	-24.4	29.6	15.9	5.740
MK-73	-22.8	48.8	47.7	7.060
MK-74	-25.5	16.8	2.9	2.270
MK-75	-24.0	15.9	14.4	9.710
MK-76	-24.1	15.9	20.2	4.850
MK-77	-22.6	27.4	16.2	0.130
MK-78	-25.4	61.0	20.0	12.400
MK-79	-25.0	15.9	54.8	9.470
MK-80	-25.7	7.6	1.7	0.200
MK-81	-23.7	12.2	78.4	13.400
MK-82	-23.4	15.9	8.6	3.510
MK-83	-23.4	19.8	41.5	0.590
MK-84	-24.6	15.2	9.6	0.100
MK-85	-25.1	22.9	5.6	1.830
MK-86	-23.3	21.3	63.9	12.700
MK-87	-23.8	35.1	11.9	4.320
MK-88	-24.4	13.7	184.0	6.920
MK-89	-24.1	16.8	39.0	0.470
MK-19	-22.8	36.6	105.9	10.160
MK-37	-24.5	36.6	38.9	5.690
MK-39	-24.3	45.7	58.8	0.600
MK-60	-24.6	25.0	12.3	0.129
MK-61	-23.8	15.0	8.8	0.131
MK-62	-24.2	39.6	5.2	0.322
MK-63	-24.2	22.9	6.5	0.154
MK-64	-23.0	24.4	6.1	1.150
MK-65	-23.3	21.3	11.1	0.153
MK-66	-23.9	18.3	4.4	0.188
MK-67	-24.9	9.2	4.8	0.149
MK-68	-25.0	29.0	58.1	0.495
MK-69	-23.6	73.2	20.8	0.261
MK-52	-24.0	22.9	12.5	0.245

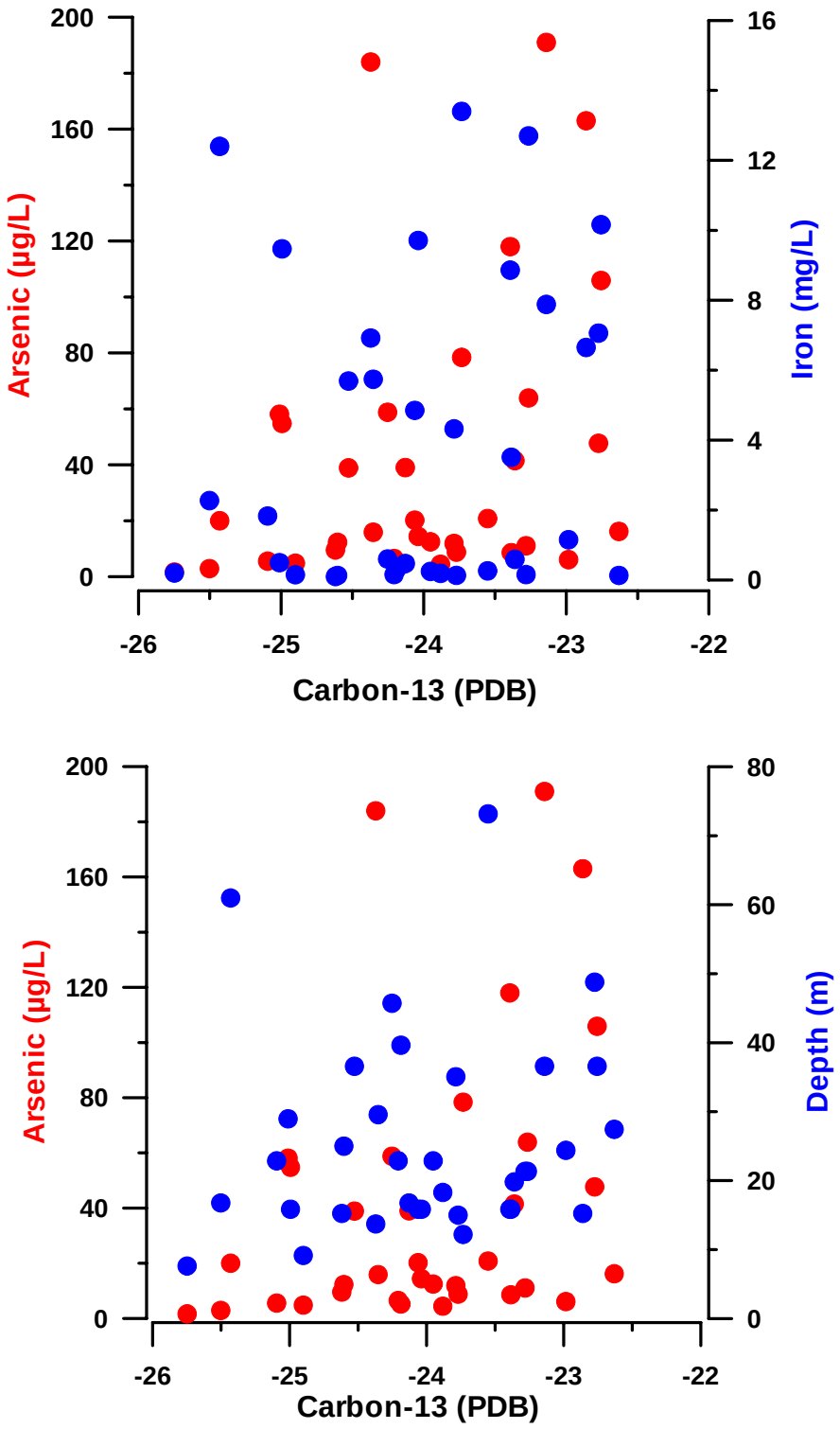

Fig. 5.10 (a) Plot of groundwater As and Fe concentrations with $\delta^{13}C$ (DOC). **(b)** Plot of groundwater As and tubewell depths with $\delta^{13}C$ (DOC) in Manikganj.

A contour map of arsenic concentration in groundwater of Manikganj area has been created with ordinary kriging geostatistical interpolation method (Fig. 5.12; Deutsch and Journel, 1998). All 88 data points were used to create this predicted arsenic model in the study area. A solid model of groundwater arsenic illustrates the spatial as well as vertical arsenic distributions in groundwater of Manikganj (Fig. 5.13). Since only 12 samples represent the arsenic concentration in deeper aquifers (> 80 m) in Manikganj, no separate attempt was made to map the spatial distribution of arsenic in deeper aquifers. Only 1 sample of a total of 12 deep wells (> 80 m) contains arsenic concentration more than 50 μg/L. There is no distinct trend of arsenic distribution visible in the study area. High arsenic concentrations (> 50 μg/L) that are located within some isolated clusters between the Kaligonga and Dhaleswari rivers might be related to the local geomorphology and geologic units as shown in Fig. 5.12.

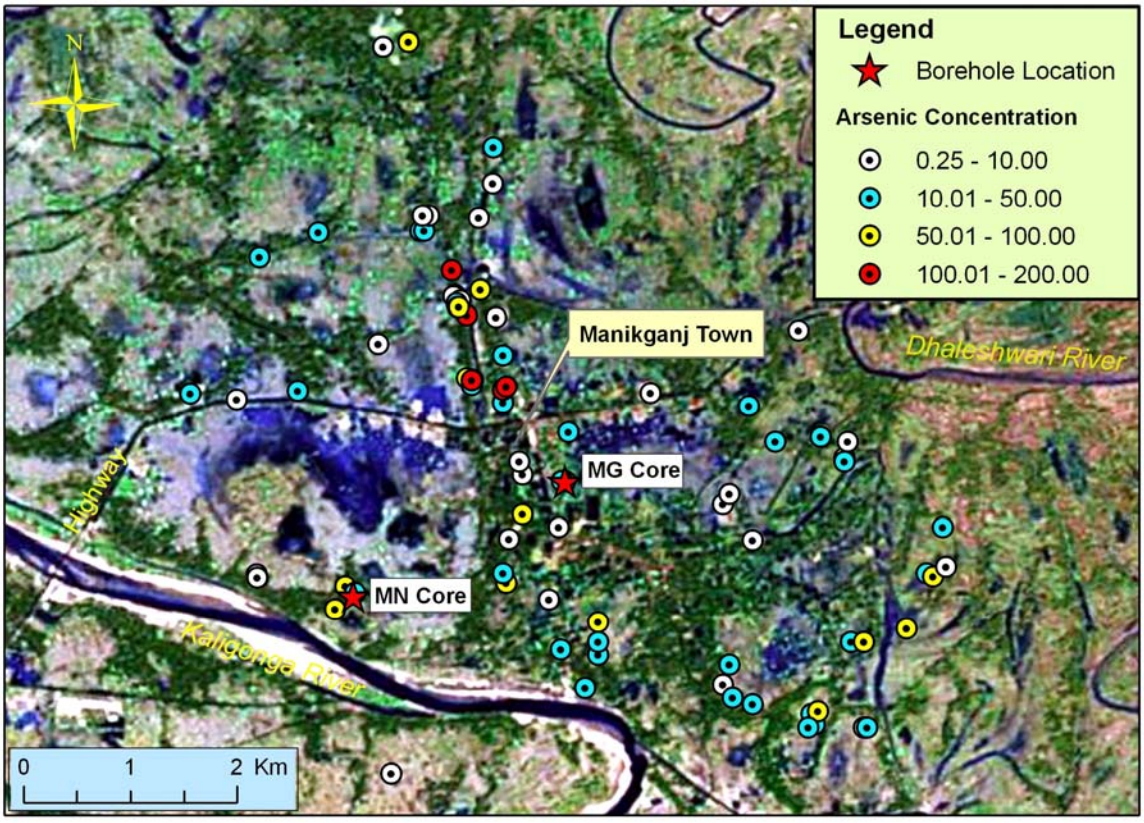

Fig. 5.11 Map of groundwater arsenic distributions in Manikganj area. Samples are plotted on a false-colored satellite image (Image source: Google Earth).

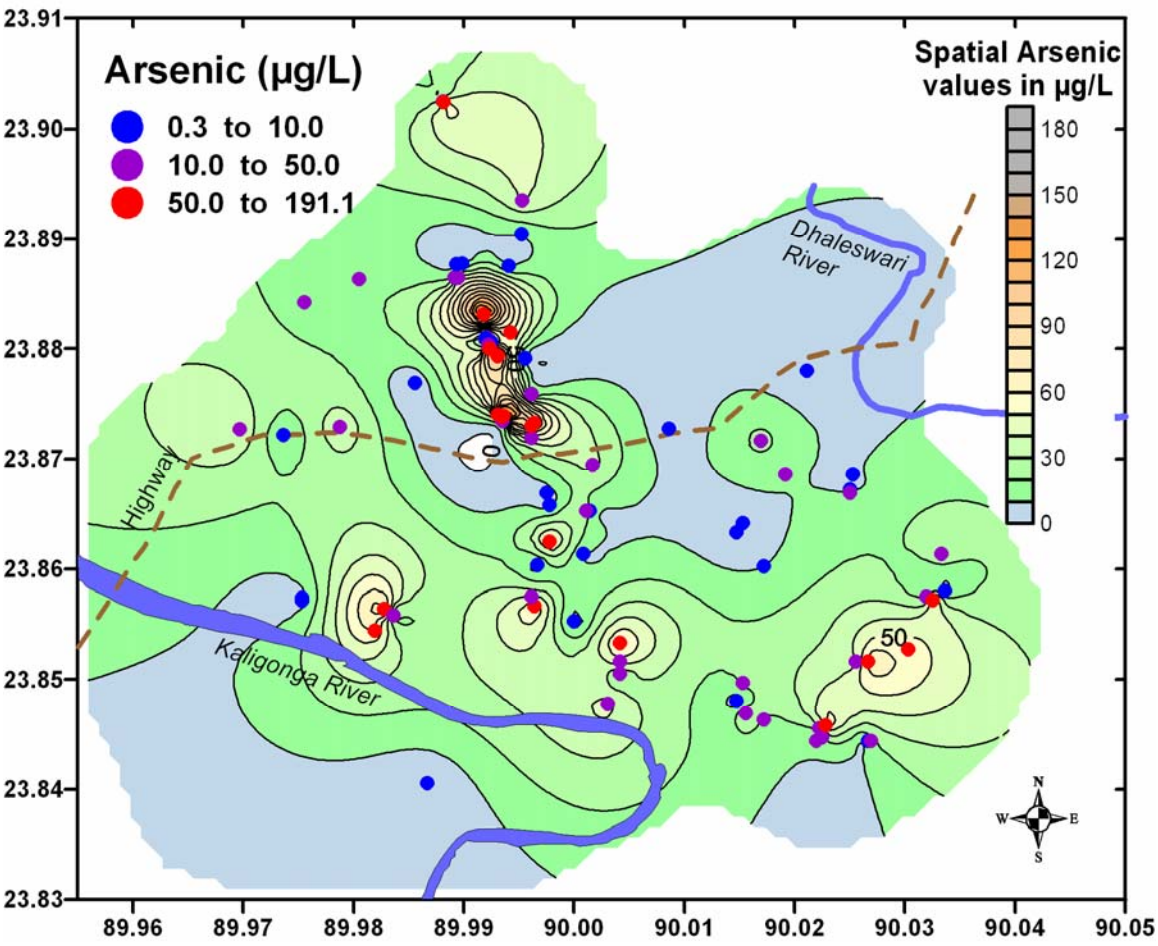

Fig. 5.12 Map shows the spatial arsenic distribution in Manikganj groundwater. Ordinary Kriging method was applied to create this interpolated arsenic concentration map. The map illustrates high degree of spatial variability in arsenic concentrations in Manikganj.

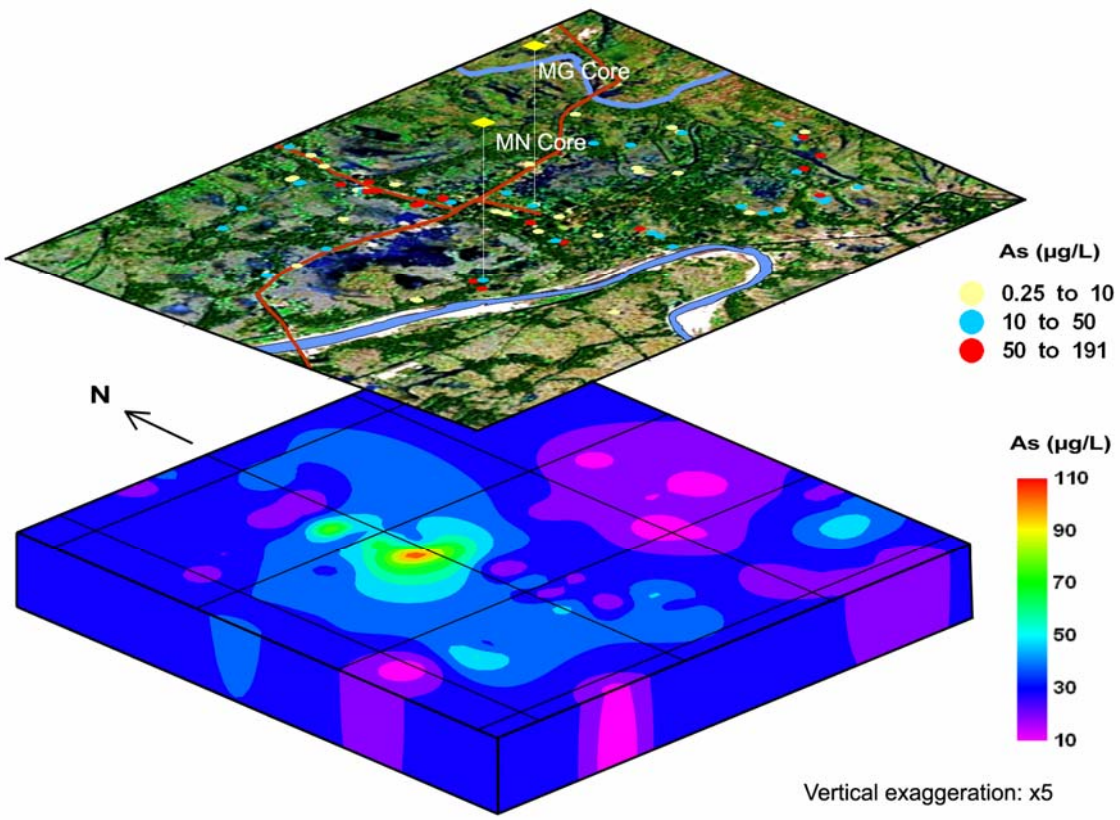

Fig. 5.13 Solid model of groundwater arsenic distribution in Manikganj aquifers. High arsenic concentrations are mostly limited within the shallow depths. The maximum depth shows in the solid model is approximately 200 m below surface. The top satellite image shows tubewells and drill core sampling locations. Arsenic concentrations in each tubewell are also shows in color.

5.2.2. Arsenic, well depth and surface elevation

Consistent with the rest of Bangladesh, high arsenic concentrations in groundwater in Manikganj area are found at shallow depths (< 100 m). Low arsenic concentrations (< 50 µg/L) are found both at deeper and shallower depths (Fig. 5.14). In Manikganj, two major aquifer systems were identified within the fining-upward sedimentary sequences. The upper fining upward unit forms the shallow aquifer system, which is highly contaminated with arsenic. Shallow aquifers formed by medium- to fine-grained sands and silts are highly reducing as opposed to the deeper sediments that are mostly oxidized and contain less arsenic in groundwater.

Variations of groundwater arsenic with depth are shown in 3D diagrams (Fig. 5.15), which shows that the high arsenic (> 50 µg/L) tubewells are located to the northern part of the study area at shallower depths. Only a few tubewells with higher arsenic concentrations are found at intermediate depths (50-100 m) in the south. Interestingly enough, the clustering of tubewells in the hot-spots with a wide range of arsenic concentrations (5-150 µg/L) illustrates high spatial variability of arsenic in aquifers.

Groundwater arsenic distributions seem to be related with surface elevation and geomorphology. In Manikganj area, low arsenic wells are found within higher surface elevation (Fig. 5.14). High arsenic concentrations (> 50 µg/L) are located in topographically low-lying areas. On regional scale across the whole country, an inverse relationship between arsenic and surface elevation exists (Shamsudduha et al., 2006). A similar relationship has been reported in the Pannonian Basin of Hungary, where most of the high-arsenic wells are located within topographically low areas of the basin (Varsanyi and Kovacs 2006).

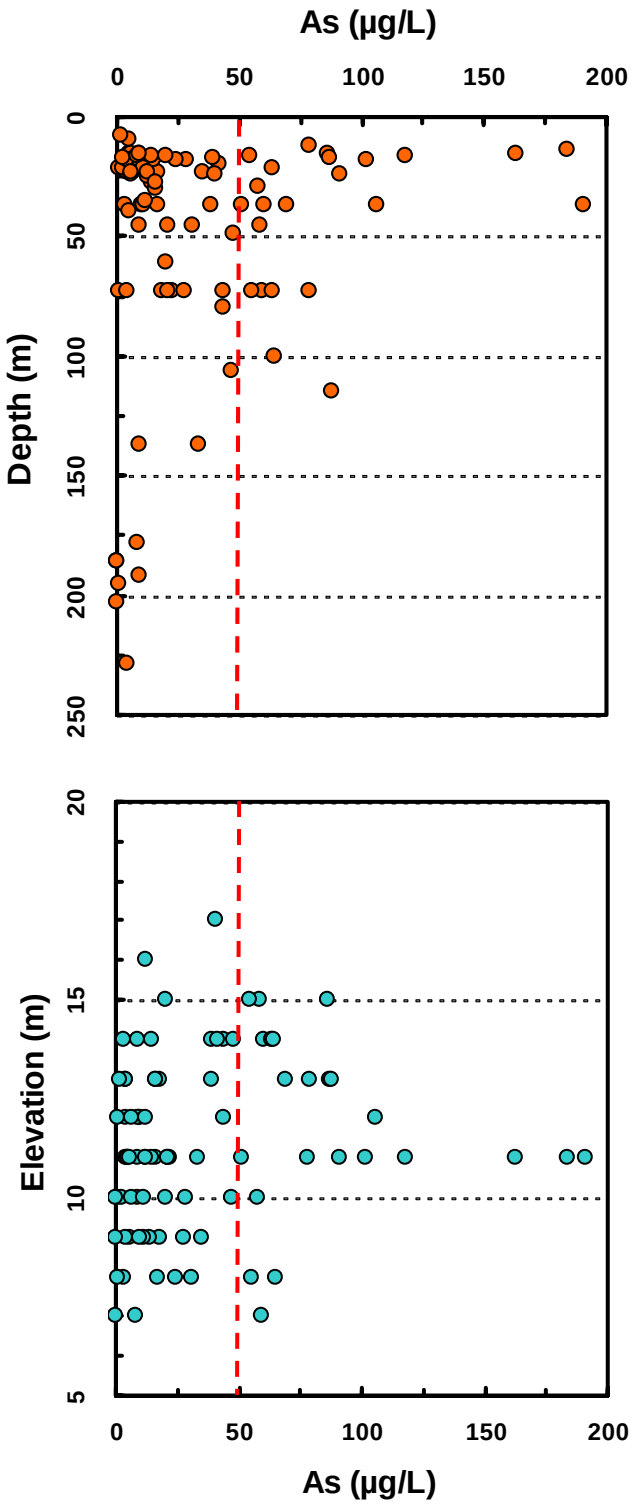

Fig. 5.14 (a) Variation in the groundwater arsenic concentrations with depth. High arsenic values are located within a depth of 50 m below surface. **(b)** Scatterplot between surface elevation and groundwater arsenic in Manikganj study area.

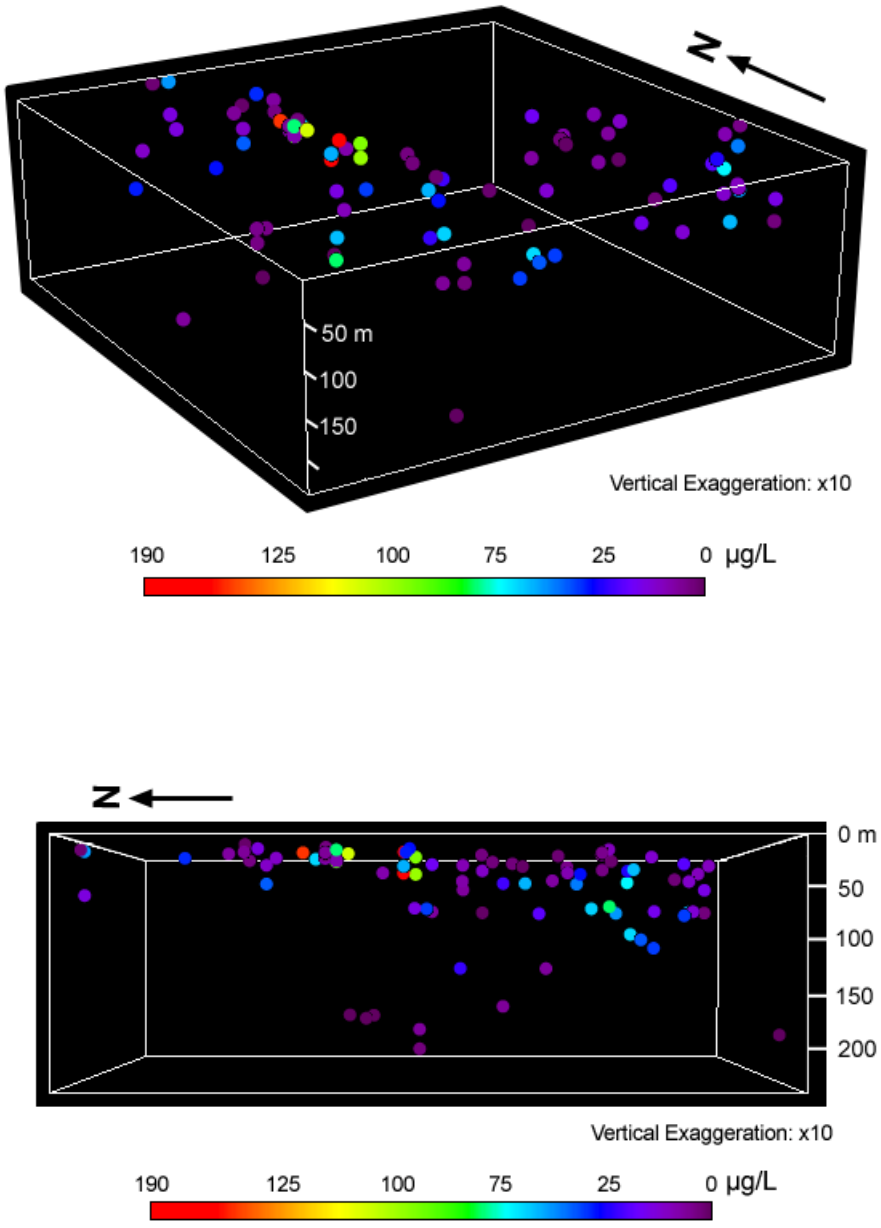

Fig. 5.15 3D diagrams show groundwater arsenic distributions in Manikganj aquifers. **(a)** High arsenic wells are located mainly in the northern parts of the study area. **(b)** High arsenic wells are found at shallow depths (< 50 m).

5.3. Multivariate statistical analyses

5.3.1. Correlation analysis

Several multivariate statistical analyses are undertaken in this chapter to examine the relationship between arsenic and other groundwater properties and ions. Pearson's correlation analysis was performed on multivariate properties of Manikganj groundwater on their log-transformed values. The correlation matrices of groundwater variables in the Manikganj study area is given in Table 5.8. Results show that As is moderate to strongly correlated with Fe (r=0.57) and Si (r=0.52) in groundwaters. Mn seems to be positively correlated (r=0.36) with groundwater As in Manikganj. Weak correlations also exists between pH and As (r=0.30) and Ba and As (r=0.16). As is negatively correlated with SO_4 (r=-0.36), EC (r=-0.32), HCO_3 (r=-0.34) and other ions in groundwater. Statistical correlation between groundwater parameters and other ions are also shown in Table 5.8.

5.3.2. Factor analysis

Factor analysis examines the underlying patterns or relationships for a large number of variables and determines whether or not the information can be condensed or summarized in a smaller set of factors or components (Hair et al., 1992). Factor analysis is used to interpret the structure within the variance-covariance matrix of a multivariate data set. The technique, which it uses, is the extraction of the eigenvalues and eigenvectors from matrix of correlations or covariances (Brown, 1998).

Factor analysis on log-transformed geochemical data revealed the elemental association in groundwater. A model was limited to five factors that explain a very high portion of variance expressed by the data matrix (0.70% of communality). A varimax

rotation algorithm was applied on the factors for easier interpretation of factor associations. Factor loadings are presented in Fig. 5.16.

Factor one explaining 24% of the variance has high loadings for groundwater Ca, Na, Mg, Cl, HCO_3 and EC and trace element Sr, and Ni (Fig. 5.16). This factor represents the main dissolved load of groundwaters as a result of the interaction with minerals in aquifers and chemical weathering of catchment rocks. Factor two (18% of the total variance) includes As, Fe, Mn, K and Si in groundwater mainly suggesting a reducing condition in aquifers. Strong to moderate statistical correlations among these variables were also observed in correlation analysis earlier in this section. Factor three (12% of the variance) includes Cl, Mo, Ni, Zn and pH in groundwater. Factor four explaining approximately 10% of the total variance represents high factor loadings for Na, K, Ba, NO_3, and PO_4 in groundwater of the study area. Factor five represents less than 10% of the variance and has high factor loading among As, Sr, and Mo. Even though this factor in groundwater does not represents a bigger portion of factor loading, these high-loading elements are often found together in groundwater contaminated with elevated arsenic concentration.

The factor score cross-plot between the first two factors is shown in Fig. 5.17. Groundwater As in Manikganj is closely associated with Fe, Mn, Si, Ba and pH, which is also observed in many other arsenic-contaminated groundwater aquifers in Bangladesh and West Bengal, India (BGS and DHPE, 2001; Stüben et al., 2003; Dowling et al., 2002).

Table 5.8 Pearson's correlation matrices of groundwater arsenic, physical parameters and different cations and anions in Manikganj study area. EC means electrical conductivity.

	pH	EC	As	Ca	Na	Mg	K	NO_3
EC	-0.427							
As	0.298	-0.321						
Ca	-0.442	**0.529**	-0.376					
Na	-0.222	0.389	-0.072	0.452				
Mg	**-0.539**	**0.586**	-0.249	**0.590**	0.316			
K	-0.066	0.207	0.073	-0.094	0.150	0.311		
NO_3	-0.128	0.407	-0.353	0.291	0.264	0.317	0.078	
Cl	-0.179	0.370	-0.130	0.580	0.447	**0.658**	0.189	0.294
PO_4	-0.211	0.349	-0.307	0.305	0.218	0.262	0.192	**0.692**
SO_4	0.106	-0.045	-0.364	0.230	0.077	0.331	0.220	0.202
HCO_3	-0.478	0.477	-0.337	**0.906**	**0.520**	**0.670**	0.144	0.132
Fe	-0.073	-0.392	**0.571**	-0.112	-0.075	-0.023	0.115	-0.510
Mn	0.300	-0.634	0.355	-0.404	-0.098	-0.456	0.047	-0.495
Sr	-0.404	**0.558**	0.087	**0.645**	**0.559**	0.473	0.039	0.369
Zn	-0.016	-0.057	-0.137	0.185	0.098	0.003	0.177	0.189
Ba	0.005	-0.245	0.160	-0.110	0.216	-0.300	0.185	0.166
Ni	-0.083	0.255	-0.229	0.359	0.213	0.245	0.263	0.298
Mo	0.202	0.174	-0.115	0.211	0.131	-0.015	-0.182	0.255
Si	0.205	-0.518	**0.520**	-0.260	0.211	-0.165	0.259	-0.279

	Cl	PO_4	SO_4	HCO_3	Fe	Mn	Sr	Zn
PO_4	0.246							
SO_4	0.336	0.187						
HCO_3	**0.579**	0.235	0.243					
Fe	-0.013	-0.414	-0.023	0.068				
Mn	-0.314	-0.263	-0.070	-0.253	**0.504**			
Sr	0.491	0.437	-0.193	**0.608**	-0.035	-0.315		
Zn	0.166	0.184	0.113	0.126	0.067	0.151	0.018	
Ba	-0.123	0.307	0.183	-0.094	-0.052	0.157	0.046	0.127
Ni	**0.505**	0.270	0.157	0.380	0.027	0.084	0.284	**0.524**
Mo	0.329	0.146	0.112	0.099	-0.302	-0.256	0.293	0.050
Si	0.116	-0.391	0.049	-0.085	**0.576**	**0.521**	-0.168	0.040

	Ba	Ni	Mo
Ni	-0.086		
Mo	-0.098	0.355	
Si	0.151	0.086	-0.192

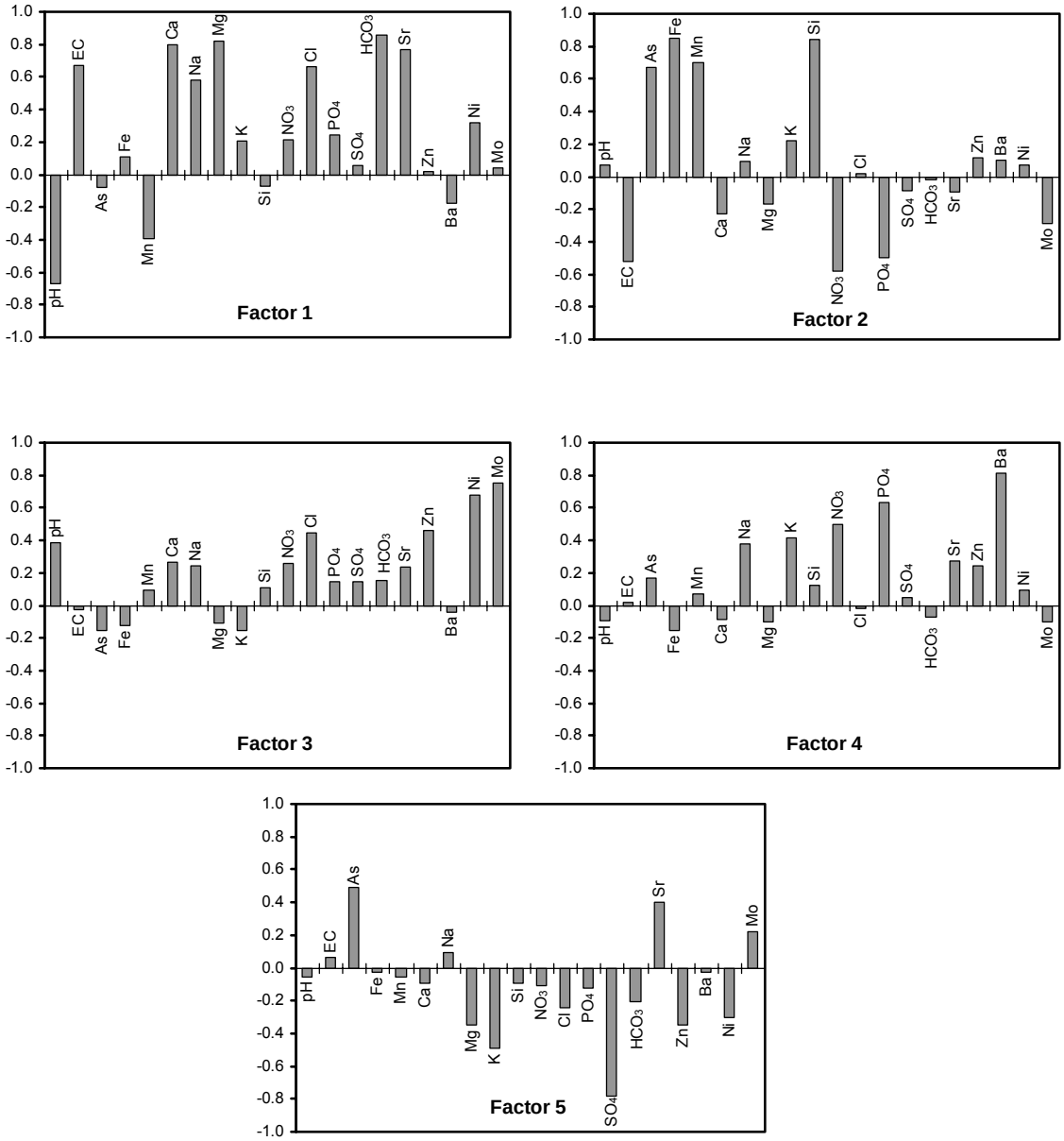

Fig. 5.16 Graphs showing factor loading of groundwater variables on five factors. High loadings are on left-hand axis indicate a close relationship among groundwater chemical and physical parameters.

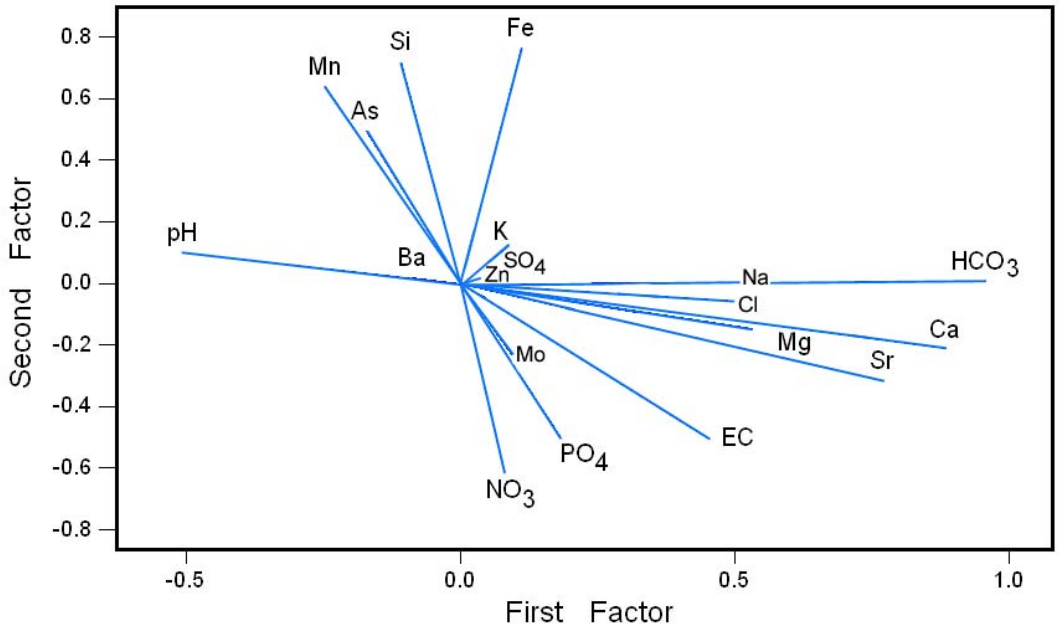

Fig. 5.17 Factor score cross-plot between Factor 1 and 2 shows that As, Fe, Mn, Si, and pH in groundwater of Manikganj are closely associated.

5.3.3. Cluster analysis

Cluster analysis is used for grouping individuals or objects into clusters so that objects in the same cluster are more like each other than they are like objects in the other clusters (Hair et al., 1992). It examines the internally related variables of a population and makes smaller clusters so that the entire homogeneity or heterogeneity of the variables can be easily interpreted. Several techniques exist in the cluster analysis of which the hierarchical technique is the most commonly used in the groundwater geochemistry. In this study, all the clusters are constructed with the agglomerative hierarchical cluster technique with complete linkage method. The log-transformed groundwater variables are used for cluster analysis with correlation coefficient distance.

Four clusters were formed after the final partitioning of variables during the amalgamation process (i.e., linkage of clusters that are sufficiently similar) following the highest similarity levels among the variables. Clusters with their internal statistical similarity levels are represented by inverted tree structures or dendrograms (Fig. 5.18). Ca, Na, HCO_3, Sr and EC form the first cluster in Manikganj groundwater. Ca, Na and HCO_3 represent the major ions in groundwater. Sr is strongly correlated with Ca, Na and EC in groundwater. Mg, Cl, K, SO_4, Ni, NO_3, PO_4 and Zn form the largest cluster in groundwater of Manikganj (Fig. 5.18). These elements that are predominantly influenced by chemical weathering of rocks and minerals represent the major groundwater chemistry. Cluster three is formed by pH and Mo in groundwaters. Molybdenum adsorption in sediments is the maximum at low pH that extended to about pH 4 to 5 (Goldberg et al., 1996). Adsorption decreased rapidly as pH was increased from pH 5 to 8, which leads to high Mo concentration in groundwater.

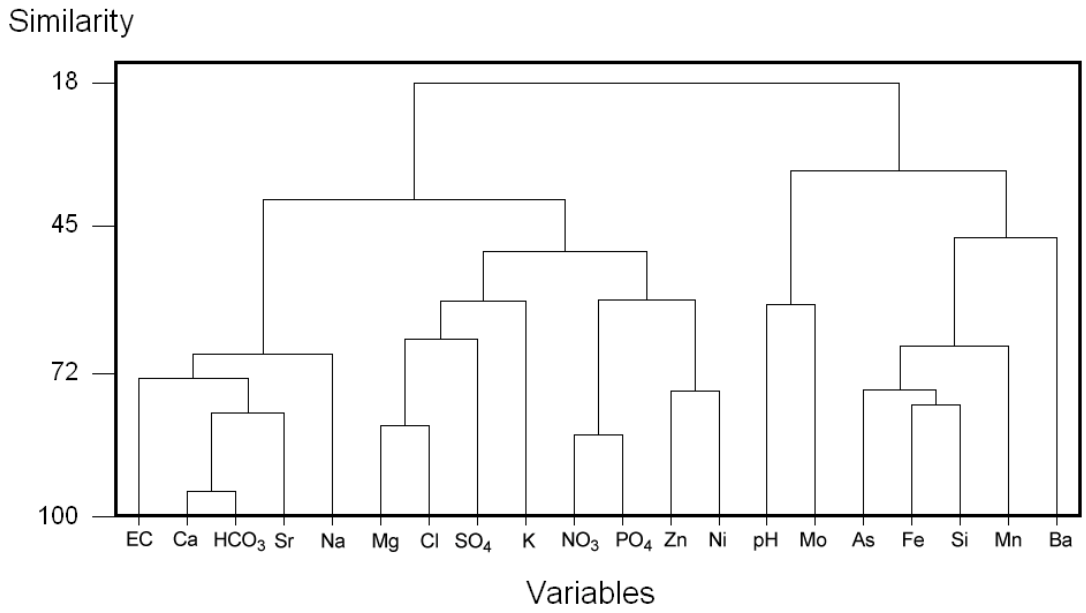

Fig. 5.18 Dendrogram illustrating major clusters in groundwater of the study area. Dissolved As, Fe, Si, Mn, and Ba form one of the major clusters in groundwater and suggest close geochemical association in aquifers.

CHAPTER 6

SEDIMENT GEOCHEMISTRY AND MINERALOGY

6. Sediment geochemistry and mineralogy

6.1. Lithological descriptions

A total of 83 sediment samples from two drill-cores are used for describing the general lithological characters of the Quaternary sedimentary facies in the study area (Fig. 6.1). The summaries on different lithofacies are given in this section. A detailed description of individual core samples can be found in the Appendix. Based on sediment characters and depositional settings of the Quaternary sediments in the study area, three distinct stratigraphic sequences were described in the earlier chapter. Based on color, texture, grain-size, sorting and composition the sediments are classified into five sedimentary facies ("A" through "E"). There are substantial variations in sediment grain-size, shape and colors within these sedimentary facies.

1. **Facies A – Gray silt and silty-clay:** Most of the shallow sediments are composed of facies A. In the upper fining-upward sequence, gray silts and silty clay form thin-lamination within fine sands (Fig. 6.1). At deeper depths (> 100 m), clay becomes sticky with very little silt. Facies A contributes less than 10% sediments in the study area. This facies is associated with floodplain or channel-fill deposits.

2. **Facies B – Gray fine-grained sand:** This facies dominates the sedimentary deposits in Manikganj area (Fig. 6.1). The intensity of gray varies from light to dark, and sometimes slight yellowish-gray. In many places at the vertical core profile this facies consists of muscovite and dark-colored heavy minerals. High amount of silt modifies this fine-grained sand facies at several depths. Some plant debris is found in this sedimentary facies but no other visible fossils were encountered in the study area. This facies was formed in the channel-bar and natural levee deposits.

3. **Facies C – Gray to yellow medium sand:** This facies type forms the most common aquifer in the study area. Sediments at shallow depths are mainly grayish indicating reducing subsurface condition. This facies varies from gray to yellowish-gray towards the deeper cores indicating gradual change in geochemical environment in sequences (Fig. 6.1). Minerals of this facies are mostly quartz and feldspars with other dark-colored minerals. In most places this facies is moderate to well-sorted with no obvious sedimentary structures. Silts, fine sand to even coarse sands are also found within this sedimentary facies in several layers. High porosity and permeability make this facies one of the better aquifers in the study area.

4. **Facies D – Gravel-rich clean sand:** The bottom part of the middle fining-upward sedimentary sequence consists of gravel-rich medium to coarse sands (Fig. 6.1). In both core sites, gravels of various compositions are found. At the MN site, the gravels are mixed with medium to coarse sands, which are moderate- to well-sorted. Sands are composed of clean quartz grains with feldspar and other heavy minerals. Groundwater in

this facies is also clean (less turbid) as noticed during pore-water collection. In MG core site, gravels are found within clay/silty-clay layer, indicating channel lag to overbank deposits. Gravels contents increases toward the bottom of the middle fining-upward sequence in the study area. The gravel-rich sandy deposits were probably formed in braided river-bed where sedimentary load was high with higher velocity.

5. **Facies E – Oxidized yellow to brown sand:** Typical yellowish-brown to bright orange-brown sands are found in the lower fining-upward sequence in Manikganj indicating a highly oxidizing condition in sediments (Fig. 6.1). Some yellowish-brown sands are also found in the middle fining-upward sequence, which are substantially different in texture and composition from the Dupi Tila sands. Gravels are found in these medium- to fine-grained sands (facies E) in some places. These facies form the best aquifers in the study area and as well as in most parts of Bangladesh (BGS and DPHE, 2001). These facies were deposited in migrating river channels in a fluvial system.

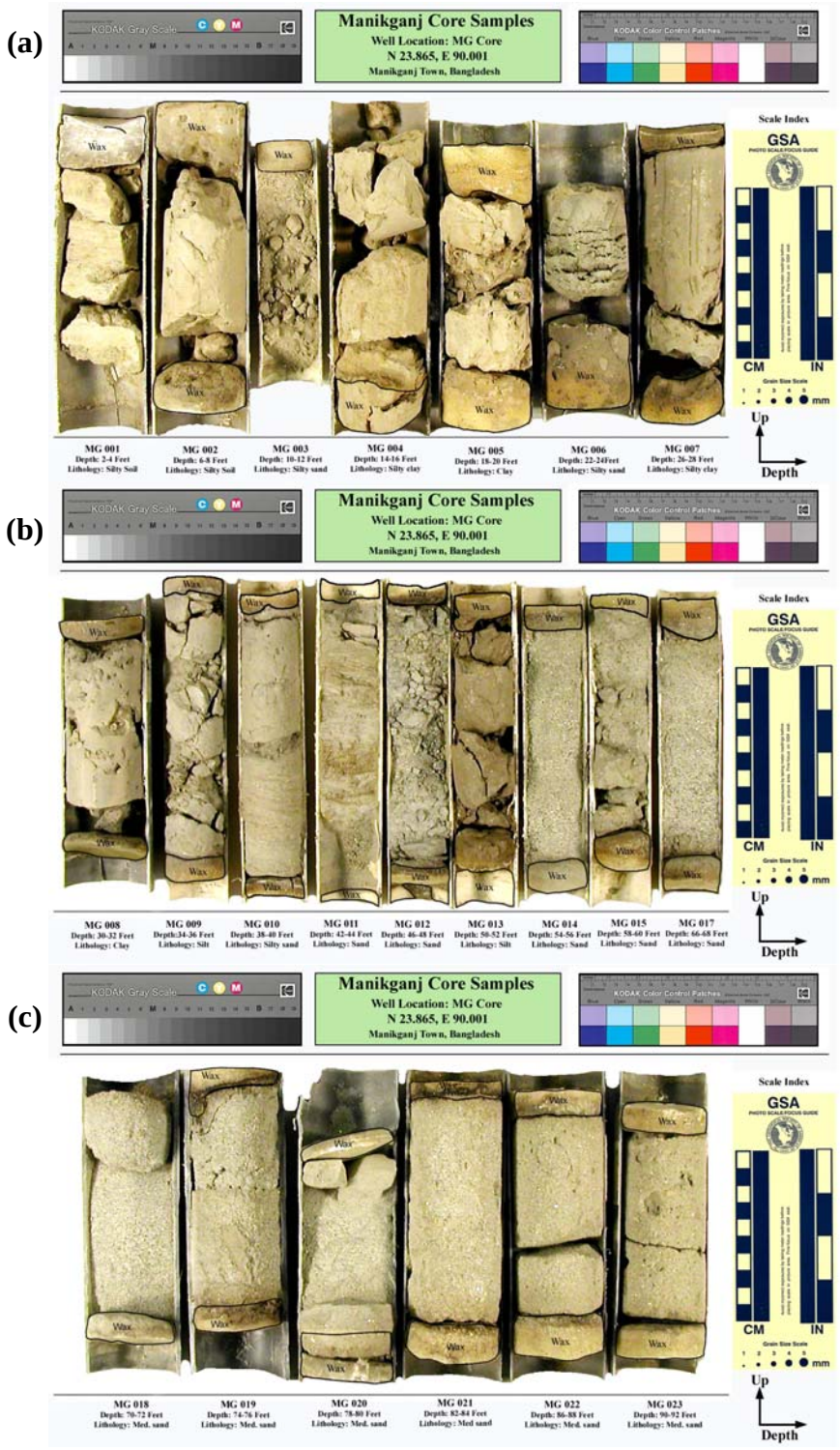

Fig. 6.1 Lithologies of sediment core samples from Manikganj study area. Samples from MG and MN cores are shown from the shallowest (top) to the deepest (bottom) depths. Several sediment samples are shown in each panel with increasing depth. Panels (**a**-**g**) are samples from core MG and panels (**h**-**l**) are showing sediment samples from core MN.

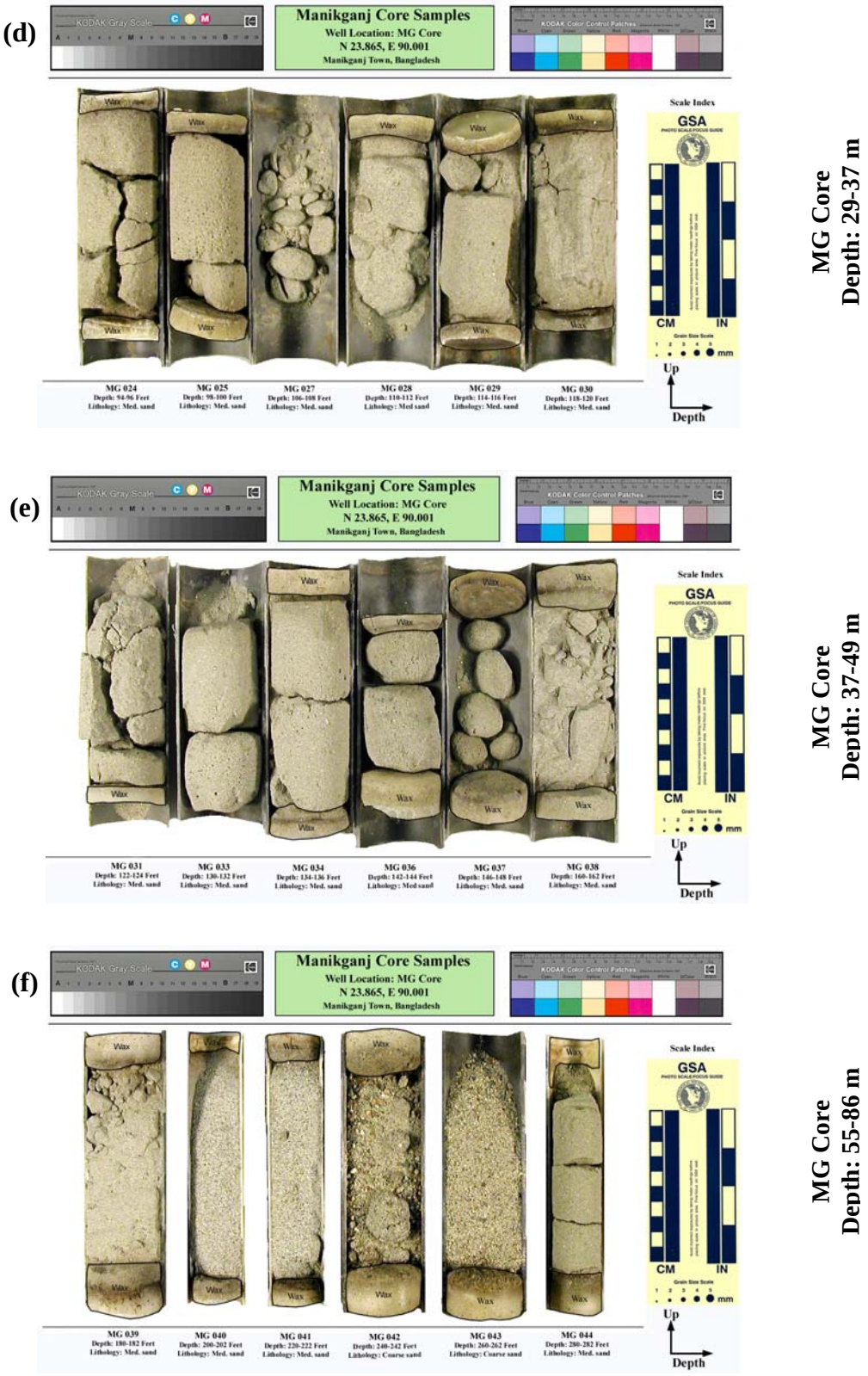
(d)
Manikganj Core Samples
Well Location: MG Core
N 23.865, E 90.001
Manikganj Town, Bangladesh
Scale Index
GSA
CM
IN
mm
Up
Depth
MG 024
Depth: 94-96 Feet
Lithology: Med. sand
MG 025
Depth: 98-100 Feet
Lithology: Med. sand
MG 027
Depth: 106-108 Feet
Lithology: Med. sand
MG 028
Depth: 110-112 Feet
Lithology: Med sand
MG 029
Depth: 114-116 Feet
Lithology: Med. sand
MG 030
Depth: 118-120 Feet
Lithology: Med. sand
MG Core
Depth: 29-37 m
(e)
Manikganj Core Samples
Well Location: MG Core
N 23.865, E 90.001
Manikganj Town, Bangladesh
Scale Index
GSA
CM
IN
mm
Up
Depth
MG 031
Depth: 122-124 Feet
Lithology: Med. sand
MG 033
Depth: 130-132 Feet
Lithology: Med. sand
MG 034
Depth: 134-136 Feet
Lithology: Med. sand
MG 036
Depth: 142-144 Feet
Lithology: Med sand
MG 037
Depth: 146-148 Feet
Lithology: Med. sand
MG 038
Depth: 160-162 Feet
Lithology: Med. sand
MG Core
Depth: 37-49 m
(f)
Manikganj Core Samples
Well Location: MG Core
N 23.865, E 90.001
Manikganj Town, Bangladesh
Scale Index
GSA
CM
IN
mm
Up
Depth
MG 039
Depth: 180-182 Feet
Lithology: Med. sand
MG 040
Depth: 200-202 Feet
Lithology: Med. sand
MG 041
Depth: 220-222 Feet
Lithology: Med. sand
MG 042
Depth: 240-242 Feet
Lithology: Coarse sand
MG 043
Depth: 260-262 Feet
Lithology: Coarse sand
MG 044
Depth: 280-282 Feet
Lithology: Med. sand
MG Core
Depth: 55-86 m

Fig. 6.1 Cont'd.

(g)

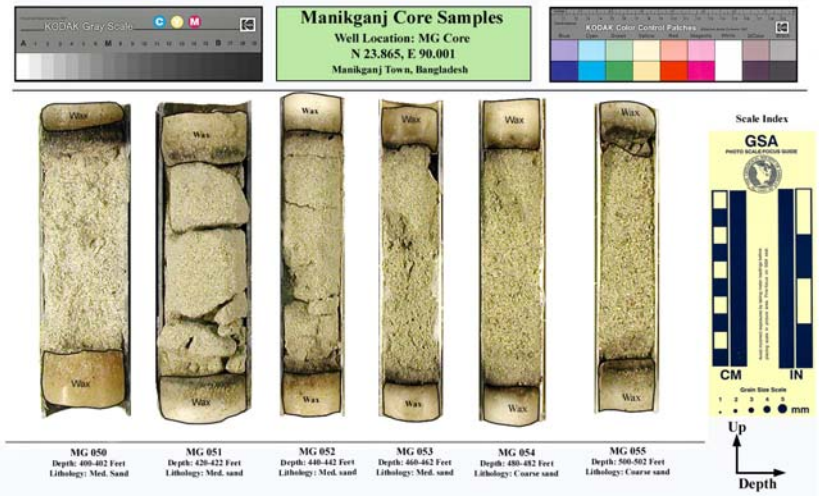

MG Core
Depth: 122-153 m

(h)

MN Core
Depth: 0-8 m

(i)

MN Core
Depth: 9-19 m

Fig. 6.1 Cont'd.

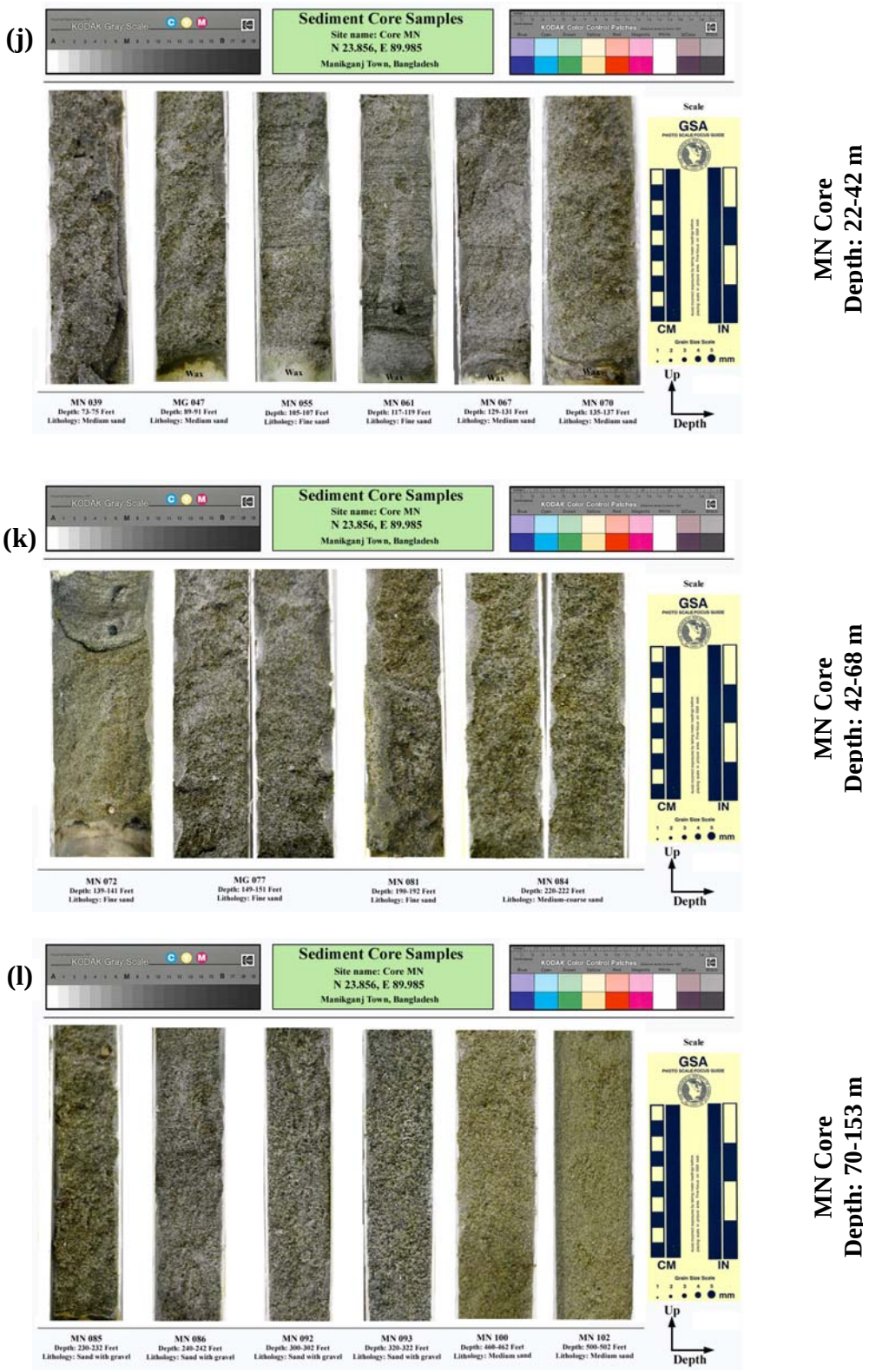
(j)
Sediment Core Samples
Site name: Core MN
N 23.856, E 89.985
Manikganj Town, Bangladesh
MN 039
MG 047
MN 055
MN 061
MN 067
MN 070
MN Core
Depth: 22-42 m
(k)
Sediment Core Samples
Site name: Core MN
N 23.856, E 89.985
Manikganj Town, Bangladesh
MN 072
MG 077
MN 081
MN 084
MN Core
Depth: 42-68 m
(l)
Sediment Core Samples
Site name: Core MN
N 23.856, E 89.985
Manikganj Town, Bangladesh
MN 085
MN 086
MN 092
MN 093
MN 100
MN 102
MN Core
Depth: 70-153 m
Scale
GSA
CM
IN
mm
Up
Depth

Fig. 6.1 Cont'd.

6.2. Sediment geochemical profiling

6.2.1. Whole rock geochemistry and arsenic

Sediment core samples digested with "Aqua Regia" were analyzed by the ICP-MS method, which shows variations in concentrations for 36 different elements from the shallow to deep aquifers in Manikganj (Table 6.1). The highest arsenic concentration in sediments is about 8.8 ppm, but the minimum concentration is about 0.3 ppm, whereas the typical average concentration of arsenic in rocks is 1.0-5.0 ppm. Average arsenic concentrations are about 2.2 ppm and 1.7 ppm in MG-core and MN-core respectively (Table 6.2). Ranges of arsenic concentrations are about 3.7 ppm and 7.7 ppm within 15 m (~50 ft) and 9 m (~30 ft) depth at MG and MN core samples respectively. Mean concentrations of Fe in sediments are 1.78% and 1.54% in wells MG and MN respectively. Maximum concentrations of Fe are 4.26% in core MG and 3.78% in core MN in Manikganj. The mean concentrations of Mn are approximately 220 mg/kg and 257 mg/kg in core MG and MN respectively. Arsenic concentration in sediments is found to be very low (< 1.5 ppm) at any depth below 50 ft from the surface. Concentrations of other trace elements in sediments (e.g., Ni, Cu, Pb, Zn, Sr, Co, La, Bi, V etc.) are also higher in the high-arsenic zones. Multivariate statistical correlation analysis was performed on elemental concentrations in sediments to examine the relationships between arsenic and other elements. Results suggests that As in Manikganj sediments is strongly correlated with Fe, Mn, Ca, P and other trace metals (e.g., Zn, Ni, Co, Cr, V, Cu, La and Cd) (Table 6.3).

Table 6.1 Concentrations of elements in sediment samples from MG and MN cores.

Sample	Depth	As	Fe	Mo	Mn	Ni	Cu	Pb	Zn	Co	Sr	Ca
Unit	m	ppm	%	ppm	ppm	ppm	ppm	ppm	ppm	ppm	ppm	%
MG-002	2	7	4.29	0.5	659	65.0	60.0	32.2	97	20.4	34	0.72
MG-006	7	3.3	3.24	0.2	315	42.5	38.3	20.9	72	14.9	17	0.29
MG-008	9	5.5	3.55	0.3	434	48.8	44.0	21.6	77	16.7	26	0.69
MG-013	16	5.6	3.06	0.3	438	39.4	37.7	14.5	64	14.4	22	0.44
MG-017	20	0.6	0.82	0.1	103	10.2	2.4	5.7	19	3.7	6	0.12
MG-022	27	1.4	0.63	0.1	90	6.7	3.6	3.1	15	2.5	9	0.12
MG-030	36	0.8	0.61	0.1	82	6.4	2.3	3.0	18	2.4	8	0.14
MG-038	49	0.7	0.73	0.1	99	8.7	2.6	3.5	25	2.8	9	0.2
MG-041	67	0.5	0.94	0.1	122	11.3	3.9	4.2	20	4.0	7	0.12
MG-046	98	0.25	0.56	0.3	99	5.8	7.0	3.8	17	4.8	5	0.08
MG-049	116	0.6	2.13	0.5	127	23.2	12.0	12.9	52	10.7	15	0.26
MG-054	147	0.25	0.84	0.1	77	11.2	1.7	6.9	22	4.1	8	0.1

Sample	P	La	Cr	Mg	Ba	Al	Na	K	V	Bi	Cd	U
Unit	%	ppm	ppm	%	ppm	%	%	%	ppm	ppm	ppm	ppm
MG-002	0.05	18	64	1.18	146	2.74	0.04	0.33	66	1.1	0.10	4.1
MG-006	0.04	11	45	0.73	110	1.96	0.01	0.15	49	0.5	0.10	1.6
MG-008	0.04	15	46	0.97	122	2.34	0.02	0.29	54	0.8	0.10	3.0
MG-013	0.07	8	39	1.00	85	1.54	0.03	0.45	44	0.3	0.20	2.6
MG-017	0.02	5	10	0.23	20	0.47	0.01	0.12	12	0.1	0.05	0.5
MG-022	0.02	4	7	0.17	16	0.32	0.02	0.08	10	0.1	0.05	0.4
MG-030	0.03	4	7	0.16	13	0.3	0.02	0.09	11	0.05	0.05	0.4
MG-038	0.04	5	9	0.20	16	0.38	0.02	0.10	14	0.1	0.05	0.6
MG-041	0.02	4	11	0.27	22	0.49	0.02	0.14	16	0.1	0.05	0.3
MG-046	0.02	4	8	0.13	8	0.27	0.01	0.06	10	0.1	0.05	0.4
MG-049	0.02	22	31	0.45	47	1.41	0.01	0.28	24	0.3	0.05	1.0
MG-054	0.02	4	14	0.17	10	0.39	0.02	0.08	15	0.1	0.05	0.3

Table 6.1 Cont'd.

Sample	Depth	As	Fe	Mo	Mn	Ni	Cu	Pb	Zn	Co	Sr	Ca
Unit	m	ppm	%	ppm	ppm	ppm	ppm	ppm	ppm	ppm	ppm	%
MN-004	2	6.9	2.79	4.3	538	29.9	31.2	12.9	56	12.5	52	2.73
MN-007	4	8.8	3.20	0.5	749	35.9	38.9	20	85	13.2	40	0.66
MN-010	5	6.1	3.78	0.7	871	53.6	48.6	27.2	82	18.7	21	0.36
MN-014	7	2.6	3.13	0.3	560	44.0	29.4	11.3	75	16.1	10	0.31
MN-017	9	1.1	1.57	0.2	223	20.7	7.2	6.2	36	8.0	7	0.17
MN-023	13	0.9	1.10	0.1	128	12.9	4.0	3.6	22	4.5	5	0.13
MN-027	15	0.5	1.01	0.1	119	12.2	3.6	4.9	23	4.8	5	0.1
MN-032	18	0.6	1.17	0.4	202	11.5	7.9	2.7	21	5.3	9	0.13
MN-039	23	0.8	1.28	0.6	203	12.3	9.2	5.5	26	5.6	9	0.13
MN-047	27	0.5	0.81	0.5	111	9.7	2.2	4.3	16	3.8	4	0.08
MN-055	32	0.7	1.19	0.1	193	12.9	3.3	4.2	21	4.8	5	0.12
MN-061	36	0.5	1.00	0.1	129	11.8	3.3	3.5	19	3.7	8	0.23
MN-072	43	0.8	1.52	0.5	219	18.7	6.8	4.7	33	7.2	7	0.16
MN-077	46	0.6	1.11	0.1	162	14.0	3.6	5.3	24	5.0	5	0.13
MN-081	58	0.5	0.74	0.1	99	10.0	3.2	6.5	17	3.6	5	0.1
MN-084	67	0.6	0.87	0.1	128	10.9	5.8	8.3	17	4.2	7	0.12
MN-086	73	0.25	1.35	0.1	146	10.1	3.6	4.7	16	3.8	7	0.18
MN-092	92	0.25	0.75	0.5	105	9.4	3.3	4.4	17	3.5	5	0.11
MN-100	141	0.6	0.96	0.5	126	11.6	7.7	5.5	18	4.1	7	0.13
MN-102	152	0.25	1.46	0.1	130	19.6	6.0	4.4	32	7.5	10	0.17

Sample	P	La	Cr	Mg	Ba	Al	Na	K	V	Bi	Cd	U
Unit	%	ppm	ppm	%	ppm	%	%	%	ppm	ppm	ppm	ppm
MN-004	0.048	10	51	1.02	83	1.56	0.011	0.3	39	0.4	0.10	0.8
MN-007	0.349	10	40	0.74	173	1.74	0.012	0.38	44	0.5	0.10	3.8
MN-010	0.079	16	54	1.07	143	2.32	0.015	0.45	57	0.8	0.05	1.2
MN-014	0.049	6	39	1.02	86	1.66	0.017	0.64	47	0.3	0.10	2.1
MN-017	0.036	5	18	0.45	35	0.84	0.014	0.31	24	0.1	0.05	0.5
MN-023	0.039	4	13	0.29	23	0.54	0.009	0.15	17	0.1	0.05	0.6
MN-027	0.021	4	11	0.27	25	0.56	0.012	0.16	14	0.1	0.05	0.4
MN-032	0.028	4	11	0.22	24	0.41	0.011	0.13	15	0.05	0.05	0.4
MN-039	0.037	4	12	0.19	23	0.39	0.013	0.11	15	0.1	0.05	0.4
MN-047	0.017	4	10	0.21	20	0.43	0.007	0.12	11	0.1	0.05	0.3
MN-055	0.025	5	13	0.27	23	0.53	0.014	0.15	17	0.1	0.05	1.0
MN-061	0.062	5	12	0.28	20	0.49	0.012	0.12	16	0.1	0.05	0.5
MN-072	0.033	4	17	0.42	38	0.77	0.022	0.23	21	0.1	0.05	0.4
MN-077	0.024	4	12	0.3	27	0.58	0.009	0.17	16	0.1	0.05	0.5
MN-081	0.015	4	10	0.21	18	0.42	0.015	0.11	10	0.1	0.05	1.1
MN-084	0.022	4	11	0.21	17	0.41	0.015	0.1	12	0.1	0.05	0.7
MN-086	0.038	8	16	0.22	17	0.42	0.012	0.09	26	0.1	0.05	0.5
MN-092	0.022	4	9	0.22	16	0.42	0.007	0.1	11	0.1	0.05	0.5
MN-100	0.032	4	11	0.19	17	0.4	0.011	0.1	14	0.1	0.10	0.6
MN-102	0.031	5	18	0.34	16	0.69	0.007	0.16	22	0.1	0.05	0.3

Table 6.2 Statistical parameters of trace elements in sediment core samples.

MG core samples										
Parameters	As	Cu	Pb	Zn	Ni	Co	Mn	Fe	Mo	Sr
Unit	ppm	ppm	ppm	ppm	ppm	ppm	ppm	%	ppm	ppm
Minimum	0.25	1.7	3	15	5.8	2.4	77	0.56	0.1	5
Maximum	7.00	60	32.2	97	65	20.4	659	4.29	0.5	34
Range	6.75	58.3	29.2	82	59.2	18	582	3.73	0.4	29
Mean	2.21	17.96	11.03	41.5	23.27	8.45	220.4	1.78	0.23	13.8
Median	0.75	5.45	6.3	23.5	11.25	4.45	112.5	0.89	0.15	9
Variance	6.11	436	91.03	851	414.5	42.86	37520	1.92	0.024	84.9
Standard deviation	2.47	20.88	9.54	29.2	20.36	6.55	193.7	1.39	0.15	9.21
Skew	1.09	1.02	1.17	0.78	1.00	0.71	1.36	0.74	0.92	1.18

Parameters	Sr	Ca	P	La	Cr	Mg	Ba	Al	Na	K
Unit	ppm	%	%	ppm	ppm	%	ppm	%	%	%
Minimum	5	0.08	0.02	4	7	0.13	8	0.27	0.01	0.06
Maximum	34	0.72	0.07	22	64	1.18	146	2.74	0.04	0.45
Range	29	0.64	0.05	18	57	1.05	138	2.47	0.03	0.39
Mean	13.8	0.27	0.03	8.67	24.3	0.47	51.25	1.05	0.02	0.18
Median	9	0.17	0.024	5	12.5	0.25	21	0.48	0.02	0.13
Variance	84.9	0.05	0.00	40.6	393	0.15	2540	0.81	0.00	0.02
Standard deviation	9.21	0.23	0.02	6.37	19.8	0.39	50.4	0.90	0.01	0.13
Skew	1.18	1.32	1.30	1.20	0.86	0.88	0.93	0.84	1.53	1.09

MN core samples										
Parameters	As	Cu	Pb	Zn	Ni	Co	Mn	Fe	Mo	Sr
Unit	ppm	ppm	ppm	ppm	ppm	ppm	ppm	%	ppm	ppm
Minimum	0.25	2.2	2.7	16	9.4	3.5	99	0.74	0.1	4
Maximum	8.8	48.6	27.2	85	53.6	18.7	871	3.78	4.3	52
Range	8.55	46.4	24.5	69	44.2	15.2	772	3.04	4.2	48
Mean	1.69	11.44	7.51	32.8	18.59	7.00	257.1	1.54	0.50	11.4
Median	0.6	5.9	5.1	22.5	12.6	4.9	154	1.18	0.25	7
Variance	6.22	188	37.96	516	157.1	20.31	52380	0.83	0.85	157
Standard deviation	2.49	13.71	6.16	22.70	12.53	4.51	228.9	0.91	0.92	12.50
Skew	2.12	1.82	2.34	1.57	1.81	1.59	1.82	1.50	4.10	2.64

Parameters	Sr	Ca	P	La	Cr	Mg	Ba	Al	Na	K
Unit	ppm	%	%	ppm	ppm	%	ppm	%	%	%
Minimum	4	0.08	0.02	4	9	0.19	16	0.39	0.01	0.09
Maximum	52	2.73	0.35	16	54	1.07	173	2.32	0.02	0.64
Range	48	2.65	0.33	12	45	0.88	157	1.93	0.02	0.55
Mean	11.4	0.31	0.05	5.7	19.4	0.41	42.2	0.78	0.01	0.20
Median	7	0.13	0.03	4	12.5	0.28	23	0.54	0.01	0.15
Variance	157	0.34	0.01	9.59	202	0.09	1986	0.32	0.00	0.02
Standard deviation	12.5	0.58	0.07	3.1	14.2	0.30	44.57	0.56	0.00	0.14
Skew	2.64	4.13	4.14	2.38	1.68	1.56	2.15	1.70	0.71	1.88

Table 6.3 Pearson's correlation matrices of trace element concentrations in sediment samples in MG and MN cores in Manikganj.

MG Core								
	As	Fe	P	Mn	Mo	Cu	Pb	Zn
Fe	0.827							
P	0.891	0.743						
Mn	0.909	0.932	0.831					
Mo	0.481	0.730	0.394	0.687				
Cu	0.841	0.926	0.709	0.950	0.821			
Pb	0.742	0.972	0.633	0.892	0.748	0.888		
Zn	0.807	0.985	0.759	0.918	0.761	0.921	0.963	
Ni	0.824	0.996	0.751	0.937	0.693	0.906	0.978	0.980
Co	0.735	0.966	0.633	0.914	0.841	0.953	0.970	0.959
Sr	0.897	0.940	0.832	0.909	0.684	0.878	0.892	0.946
Ca	0.900	0.920	0.863	0.919	0.666	0.867	0.860	0.937
La	0.628	0.881	0.520	0.732	0.834	0.806	0.878	0.900
Cr	0.764	0.991	0.689	0.907	0.759	0.909	0.989	0.984
Mg	0.882	0.986	0.818	0.961	0.688	0.924	0.933	0.963
Ba	0.898	0.976	0.787	0.939	0.655	0.918	0.920	0.953
Al	0.814	0.995	0.712	0.916	0.738	0.917	0.971	0.981
Na	0.613	0.438	0.719	0.603	0.249	0.408	0.375	0.419
K	0.759	0.892	0.776	0.833	0.685	0.792	0.811	0.863

	Ni	Co	Sr	Ca	La	Cr	Mg	Ba
Co	0.957							
Sr	0.935	0.870						
Ca	0.918	0.849	0.971					
La	0.855	0.869	0.844	0.837				
Cr	0.990	0.977	0.920	0.888	0.885			
Mg	0.983	0.936	0.941	0.942	0.832	0.959		
Ba	0.969	0.911	0.934	0.936	0.852	0.940	0.985	
Al	0.989	0.960	0.932	0.921	0.912	0.984	0.978	0.979
Na	0.471	0.364	0.602	0.587	0.204	0.412	0.528	0.438
K	0.879	0.832	0.865	0.881	0.808	0.858	0.925	0.882

	Al	Na
Na	0.392	
K	0.887	0.573

Table 6.3 Cont'd.

MN Core								
	As	Fe	P	Mn	Mo	Cu	Pb	Zn
Fe	0.853							
P	0.727	0.753						
Mn	0.924	0.964	0.753					
Mo	0.451	0.369	0.322	0.486				
Cu	0.889	0.919	0.726	0.941	0.545			
Pb	0.842	0.781	0.620	0.826	0.361	0.843		
Zn	0.878	0.959	0.736	0.942	0.402	0.918	0.810	
Ni	0.848	0.959	0.681	0.928	0.353	0.903	0.815	0.982
Co	0.850	0.965	0.648	0.941	0.414	0.925	0.795	0.983
Sr	0.825	0.817	0.765	0.827	0.425	0.874	0.738	0.786
Ca	0.785	0.881	0.941	0.857	0.271	0.832	0.723	0.848
La	0.733	0.838	0.701	0.820	0.250	0.757	0.800	0.737
Cr	0.870	0.974	0.709	0.937	0.327	0.905	0.833	0.937
Mg	0.856	0.930	0.634	0.903	0.282	0.846	0.780	0.946
Ba	0.950	0.921	0.767	0.964	0.458	0.894	0.849	0.947
Al	0.874	0.942	0.686	0.920	0.320	0.866	0.833	0.968
Na	0.358	0.353	0.184	0.395	0.072	0.359	0.341	0.328
K	0.813	0.888	0.584	0.870	0.299	0.795	0.709	0.943

	Ni	Co	Sr	Ca	La	Cr	Mg	Ba
Co	0.986							
Sr	0.744	0.770						
Ca	0.829	0.792	0.913					
La	0.764	0.741	0.795	0.809				
Cr	0.950	0.944	0.854	0.888	0.881			
Mg	0.963	0.945	0.754	0.817	0.773	0.958		
Ba	0.919	0.915	0.790	0.843	0.783	0.911	0.917	
Al	0.979	0.958	0.763	0.833	0.804	0.960	0.987	0.946
Na	0.347	0.346	0.159	0.310	0.187	0.307	0.318	0.368
K	0.950	0.938	0.598	0.725	0.618	0.867	0.947	0.899

	Al	Na
Na	0.304	
K	0.947	0.383

6.2.2. Sequential extractions and arsenic

Results for sequential leaching experiment on sediments show concentrations of arsenic and other trace elements in sediments that are found associated with high arsenic (Table 6.4). Extraction by 1M $MgCl_2$ released the highest concentration of arsenic in all sediment samples in Manikganj area. However, $MgCl_2$ was selected considering the fact that it would only extract the portion of arsenic associated with the very soluble or ionically bound arsenic in sediments (Keon et al., 2001). The highest As concentration is approximately 15.28 mg/kg in the sample MG038 at a depth about 48.5 m below surface (Table 6.4). It is really unexpected that so much of arsenic in sediments is very loosely sorbed onto minerals surface that is highly soluble in $MgCl_2$. No other studies in Bangladesh has reported high amount of arsenic concentrations in sediments that are soluble or ionically bound/exchangeable. This extractant also leached high amount of iron, iodine, selenium and bromine from the sediments. The second extractant was 0.1M $NH_2OH.HCl$ that was used to target arsenic associated with amorphous and/or crystalline Fe-oxyhydroxides fraction of sediments. Interestingly enough, only a small amount of arsenic, which was left out after leaching with $MgCl_2$ solution, was extracted from the sediments. The third sequential extractant, 0.25M $NH_2OH.HCl$ was used to extract the rest of the arsenic associated with more crystalline Fe-oxyhydroxides, other As-oxides and silicates from the sediments. But very low amounts of arsenic and iron were extracted by this leaching agent.

Table 6.4 Results of sequential extraction of sediments from MN and MG core samples from Manikganj area. Concentrations are in mg/kg for all the elements. 'MC' means 1M of $MgCl_2$; 'HH1' means 0.1M of $NH_2OH.HCl$; and 'HH2' means 0.25M of $NH_2OH.HCl$ that were used for sequential leaching of sediment samples.

MN sediment samples									
Element	Well	As	Fe	Zn	Mn	K	Se	I	Br
Detection Limit	depth (m)	0.03	10	0.5	0.1	30	0.2	1	3
MN-04 (MC)	2.0	0.24	640	16.0	74.4	120	3.2	48	88
MN-07 (MC)	3.5	2.48	1200	20.0	150.4	120	2.4	40	88
MN-14 (MC)	7.5	5.92	1600	28.8	86.4	960	3.2	48	96
MN-39 (MC)	22.5	9.04	1520	18.4	18.4	120	3.2	32	88
MN-72 (MC)	42.5	11.68	1760	18.4	13.6	120	3.2	24	88
MN-04 (HH1)	2.0	1.49	184	19.8	117.6	88	0.2	2.4	8
MN-07 (HH1)	3.5	1.31	248	23.0	289.6	144	0.3	1.6	8.8
MN-14 (HH1)	7.5	0.65	928	23.0	64.6	120	0.2	1.6	16.8
MN-39 (HH1)	22.5	0.47	400	23.9	27.4	80	0.2	1.6	8
MN-72 (HH1)	42.5	0.41	704	21.2	8.7	80	0.2	0.8	8
MN-04 (HH2)	2.0	0.26	248	19.0	17.5	64	0.1	0.8	16.8
MN-07 (HH2)	3.5	0.76	1040	20.2	60.2	72	0.2	0.8	17.6
MN-14 (HH2)	7.5	0.20	1744	20.1	48.2	104	0.3	0.8	18.4
MN-39 (HH2)	22.5	0.18	256	19.8	7.7	56	0.5	0.8	16
MN-72 (HH2)	42.5	0.23	576	20.2	7.3	64	0.3	0.8	17.6
MG sediment samples									
Element	Well	As	Fe	Zn	Mn	K	Se	I	Br
Detection Limit	Depth (m)	0.03	10	0.5	0.1	30	0.2	1	3
MG-02 (MC)	2.0	11.44	1840	16.8	107.2	120	3.2	24	88
MG-08 (MC)	9.5	11.68	1680	16.8	64.8	120	2.4	16	88
MG-22 (MC)	26.5	13.20	1840	17.6	19.2	120	2.4	24	88
MG-30 (MC)	36.0	13.36	1680	17.6	12.0	120	3.2	24	88
MG-38 (MC)	48.5	15.28	1840	18.4	12.0	120	2.4	4	88
MG-02 (HH1)	2.0	0.40	216	23.0	94.4	128	0.1	1.6	9.6
MG-08 (HH1)	9.5	0.36	912	20.1	17.9	120	0.3	0.8	8.8
MG-22 (HH1)	26.5	0.32	176	21.8	7.4	80	0.2	0.8	8
MG-30 (HH1)	36.0	0.10	160	20.4	2.6	56	0.2	0.4	8.8
MG-38 (HH1)	48.5	0.30	208	24.0	3.9	80	0.1	0.8	8.8
MG-02 (HH2)	2.0	0.14	488	20.7	16.4	72	0.1	0.8	17.6
MG-08 (HH2)	9.5	0.23	1640	17.0	6.8	56	0.1	0.4	17.6
MG-22 (HH2)	26.5	0.02	104	20.7	1.6	48	0.3	0.4	16
MG-30 (HH2)	36.0	0.35	104	20.2	1.4	48	0.1	0.4	16.8
MG-38 (HH2)	48.5	0.22	160	17.9	2.6	56	0.1	0.4	18.4

6.3. Petrography and mineralogical profiling

6.3.1. Thin-section petrography

A total of 16 thinsections were studied for petrographic analysis. Sands from the core samples in this study are dominated by quartz, feldspar, mica (muscovite), lithic fragments, and heavy minerals, such as amphibole, pyroxene, garnet, biotite, chlorite, kyanite, sillimanite and epidote. The stable heavy minerals (e.g., zircon, rutile) are not abundant in the Quaternary sands analyzed so far in this study. A detail description of heavy minerals and their variation along complete core sequence will be discussed in the following section.

The mean percentage of quartz in sands is approximately 60%, which are mostly dominated by monocrystalline type. The mean percentage of polycrystalline quartz is about 7% in the bulk sediment composition, which increases with depth (Table 6.5). The mean percentages of feldspar and lithic fragments are about 25% and 15% respectively. Potassium feldspar is the predominant species in feldspar group with a mean percentage of approximately 19% of the bulk composition. The ratio between plagioclase to potassium feldspar ranges from 0.2 to 0.86 with an average ratio of 0.47. Sedimentary lithic fragments are the predominant lithic framework of the Quaternary sands in Manikganj. The percentage of sedimentary lithic fragments is approximately 5% of the total sand composition. The percentage of metamorphic lithic is 3% of the bulk composition, whereas the volcanic lithic fragments are the least dominant (Table 6.5).

Sands from the shallow depths (< 100 m) are dominated mainly by monocrystalline quartz with very little polycrystalline quartz but the percentage increases in the sands from deeper depths (Fig. 6.2). Quartz grain mostly shows both straight and undulose

extinctions in all samples. However, undulosity in quartz grains increases from slight to highly undulose as the depth increases. Framework grains in the shallow depths are relatively smaller in size than the deeper sediments. Minerals are angular to subangular in the shallow sediments, but the overall grain shape broadly varies from subangular to subrounded in the deeper sediments (Fig. 6.2). Some overgrowth texture in quartz is also observed in several thin-sections. Inclusions are also common in quartz grains that are mostly zircon, tourmaline, and pyroxene minerals. Both potassium and plagioclase feldspar grains are stained. K-spars are mainly fresh and unaltered throughout the vertical core profile, which indicates that weathering of the sequence was minimal. Plagioclase feldspars predominantly show polysynthetic twinning. K-spars are mostly orthoclase, and microclines are rarely found in these Quaternary sediments. Intergrowth structures between potassium and plagioclase feldspars (perthitic) and between quartz and feldspar (myrmekitic) are observed. Lithic fragments are mainly sedimentary (e.g., shale, mudstone, argillite and siltstone) in the shallow aquifers, but the medium- to high-grade metamorphic lithic grains dominate the deeper sands. Average sorting of minerals in sands is moderate to fair suggesting variations in the depositional energy during the Quaternary time in this part of the Bengal Basin.

Compositional data from 11 thin-sections were plotted on a triangular sandstone (sand) classification diagram (Quartz-Feldspar-Lithic) to classify the sand in Manikganj. The plot suggests that the sand (sandstone) in the Quaternary alluvium in Manikganj is mainly arkose to subarkose type (Fig. 6.3). A sand from the shallowest depth (14 m) falls within the common boundary between sublitharenite and subarkose. One of the samples falls in the lithic subarkose field and another falls within the field of lithic arkose.

Table 6.5 (**a**) Shows the raw counts for major framework grains in 11 thin-sections in Manikganj study area; (**b**) Shows the percentages of each framework grains. Keys: Qm-Monocrystalline Quartz; Qp-Polycrystalline Quartz; Qt-Total Quartz; K-spar-Potassium feldspar; Plag.-Plagioclase feldspar; Ls-Sedimentary lithic; Lv-Volcanic (plutonic) lithic; Lm-Metamorphic lithic.

(a)

Sample	Count	Qm	Qp	Qt	Plag	K-spar	F	Ls	Lv	Lm	L	Lt	P/F ratio	P/K ratio
MG-12	255	205	5	210	5	16	21	19	0	5	24	29	0.24	0.31
MG-14	285	193	13	206	14	45	59	19	0	1	20	33	0.24	0.31
MG-17	357	214	28	242	33	69	102	10	2	1	13	41	0.32	0.48
MG-21	242	141	12	153	25	43	68	11	3	7	21	33	0.37	0.58
MG-23	309	195	14	209	18	56	74	20	0	6	26	40	0.24	0.32
MG-27	297	166	25	191	32	59	91	3	0	12	15	40	0.35	0.54
MG-31	237	130	30	160	30	35	65	5	3	4	12	42	0.46	0.86
MG-40	251	162	12	174	18	38	56	14	0	7	21	33	0.32	0.47
MG-44	296	168	28	196	25	48	73	8	3	16	27	55	0.34	0.52
MG-45	270	148	23	171	20	44	64	14	0	21	35	58	0.31	0.45
MG-50	271	131	18	149	32	50	82	22	0	18	40	58	0.39	0.64
MG-53	295	175	18	193	12	64	76	23	0	3	26	44	0.16	0.19
MG-55	231	118	26	144	23	47	70	6	0	11	17	43	0.33	0.49

(b)

Sample	Count	Qm%	Qp%	Qt%	Plag%	K-spar%	F%	Ls%	Lv%	Lm%	L%	Lt%	P/F ratio
MG-12	250	80.4	2.0	82.4	2.0	6.3	8.2	7.5	0.0	2.0	9.4	11.4	0.24
MG-14	285	67.7	4.6	72.3	4.9	17.6	20.7	6.7	0.0	0.4	7.0	11.6	0.24
MG-17	357	59.9	7.8	67.8	9.2	27.1	28.6	2.8	0.6	0.3	3.6	11.5	0.32
MG-21	242	58.3	5.0	63.2	10.3	16.9	28.1	4.5	1.2	2.9	8.7	13.6	0.37
MG-23	309	63.1	4.5	67.6	5.8	22.0	23.9	6.5	0.0	1.9	8.4	12.9	0.24
MG-27	297	55.9	8.4	64.3	10.8	23.1	30.6	1.0	0.0	4.0	5.1	13.5	0.35
MG-31	237	54.9	12.7	67.5	12.7	13.7	27.4	2.1	1.3	1.7	5.1	17.7	0.46
MG-40	251	64.5	4.8	69.3	7.2	14.9	22.3	5.6	0.0	2.8	8.4	13.1	0.32
MG-44	296	56.8	9.5	66.2	8.4	18.8	24.7	2.7	1.0	5.4	9.1	18.6	0.34
MG-45	270	54.8	8.5	63.3	7.4	17.3	23.7	5.2	0.0	7.8	13.0	21.5	0.31
MG-50	271	48.3	6.6	55.0	11.8	19.6	30.3	8.1	0.0	6.6	14.8	21.4	0.39
MG-53	295	59.3	6.1	65.4	4.1	25.1	25.8	7.8	0.0	1.0	8.8	14.9	0.16
MG-55	231	51.1	11.3	62.3	10.0	18.4	30.3	2.6	0.0	4.8	7.4	18.6	0.33
Mean	280	60.3	6.7	67.0	7.9	18.5	24.5	5.0	0.3	3.1	8.4	15.1	0.3

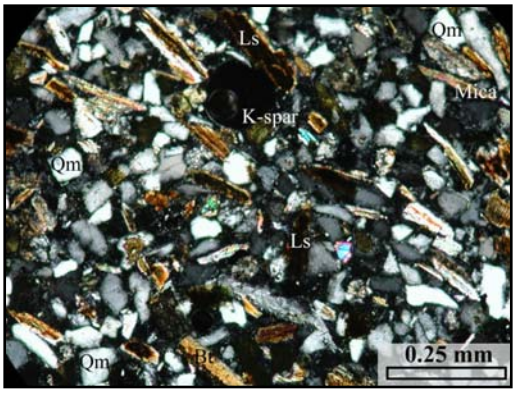

MG-012 (14 m)

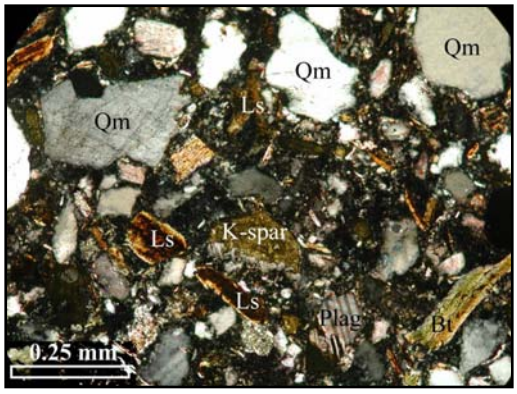

MG-014 (17 m)

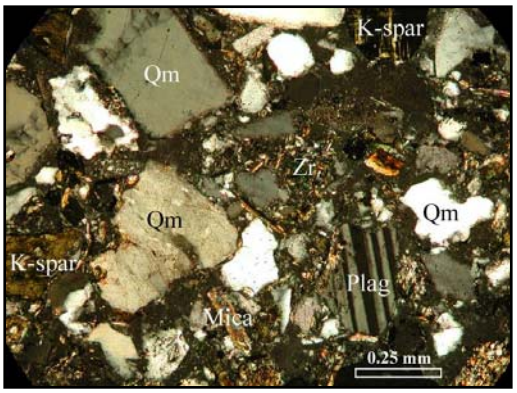

MG-017 (20 m)

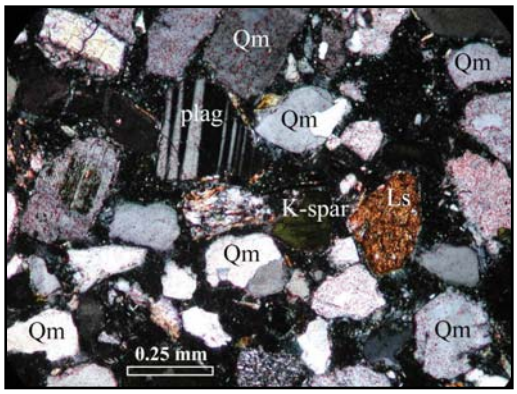

MG-021 (25 m)

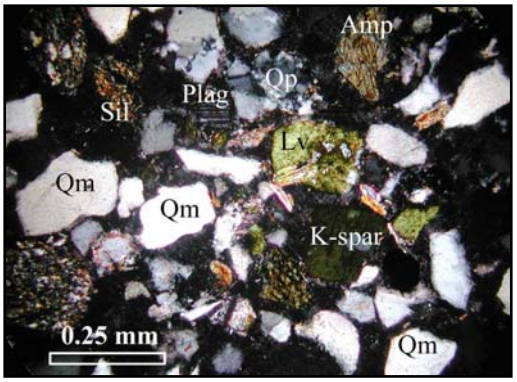

MG-027 (33 m)

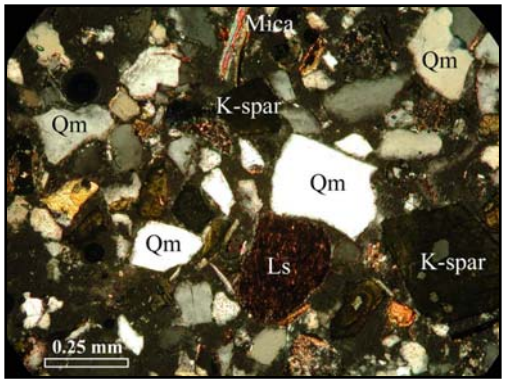

MG-031 (37 m)

Fig. 6.2 Representative photomicrographs of sands from Manikganj study area. The sample number and corresponding depths are given with the plates. Keys: Qm-Monocrystalline Quartz; Qp-Polycrystalline Quartz; K-spar-Potassium feldspar; Plag.-Plagioclase feldspar; Ls-Sedimentary lithic; Lv-Volcanic (plutonic) lithic; Lm-Metamorphic lithic; Gt-Garnet; Sil-Sillimanite; Bt-Biotite; Amp-Amphibole; Zr-Zircon.

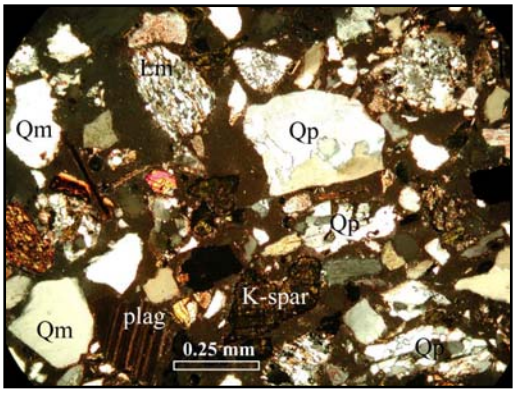

MG-043 (80 m)

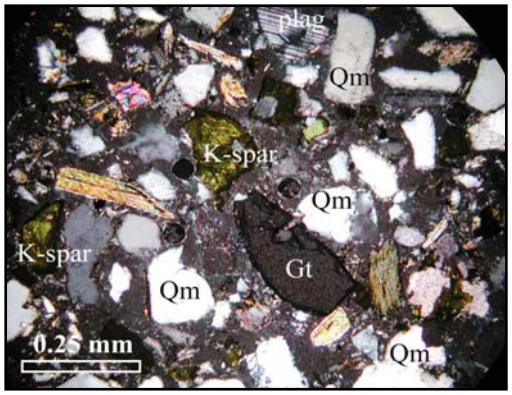

MG-045 (92 m)

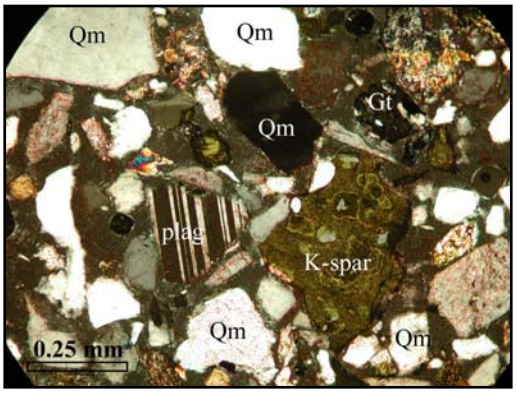

MG-046 (98 m)

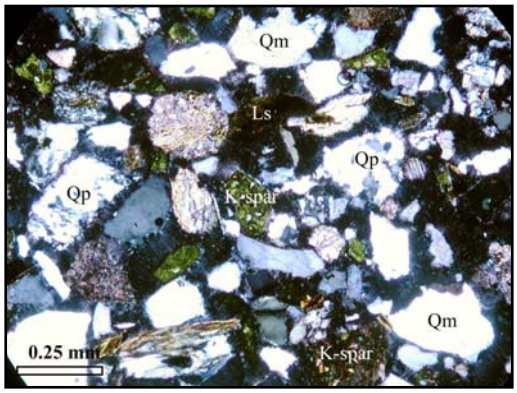

MG-050 (122 m)

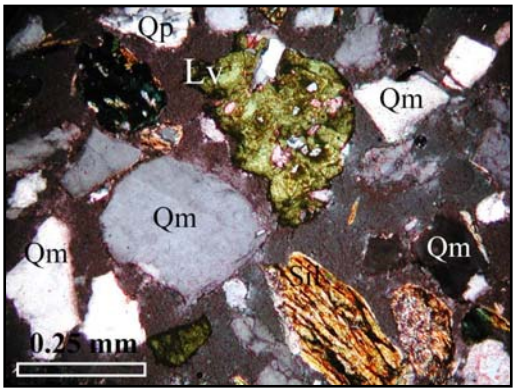

MG-052 (134 m)

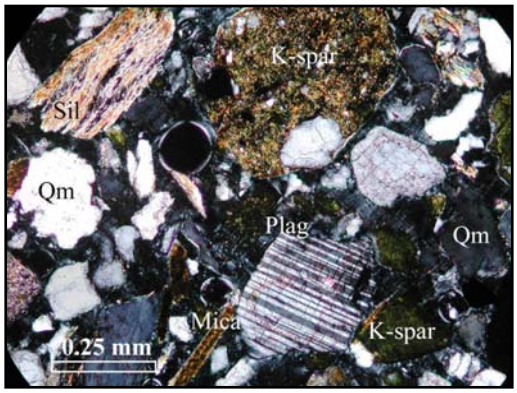

MG-055 (152 m)

Fig. 6.2 Cont'd.

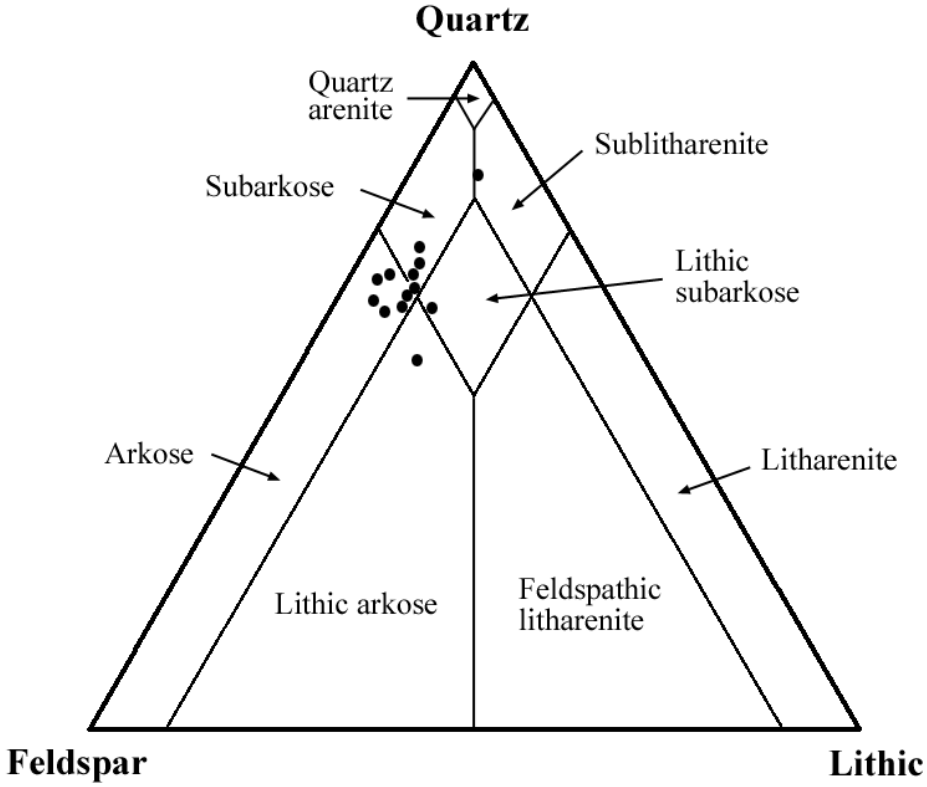

Fig. 6.3 Quartz-Feldspar-Lithic (QFL) triangular sandstone (sand) classification diagram shows the average sands in Manikganj area is subarkose to arkose.

6.3.2. Heavy mineral assemblages

Heavy minerals in the Quaternary sediments from Manikganj area were studied with petrographic microscope, Energy Dispersive Spectroscopy (EDS), Wavelength Dispersive Spectroscopy (WDS), and Electron Microprobe (EM) facilities. A total of 16 polished thinsections with four domains of different magnetic susceptibilities were used for this study. Four magnetic fractions are named as: Group-A Strongly magnetic; Group-B, Moderately magnetic; Group-C, Weakly magnetic; and Group-D, Poorly magnetic. Each group has its own magnetic susceptibility and characteristic minerals. However, due to intergrowth of minerals of variable magnetic properties, and the degree of efficiency in separation, there has been some interference of minerals assemblages within these designated groups. Minerals were first identified with EDS and/or WDS, and also under petrographic microscope and were photographed.

Concentration of heavy minerals in the Quaternary sediments in Manikganj area is significant. The average concentration of heavy minerals is approximately 4.36 (wt%) whereas the maximum concentration is 10.28 (wt%) and the minimum is 2.44 (wt%) as measured from core MG sediments. The shallow sediments tend to have more heavy minerals than the older sediments (Fig. 6.4). Similar variations in the heavy mineral concentrations are observed from core MN sediments with a maximum concentration of approximately 8.64 (wt%), whereas the average concentration (7.34 wt%) is higher than the heavy minerals (wt%) from MG core samples. Results from this study shows that the concentrations of heavy minerals in the Quaternary sediments are higher than the older Cenozoic sediments in the Bengal Basin (Uddin and Lundberg, 1998a).

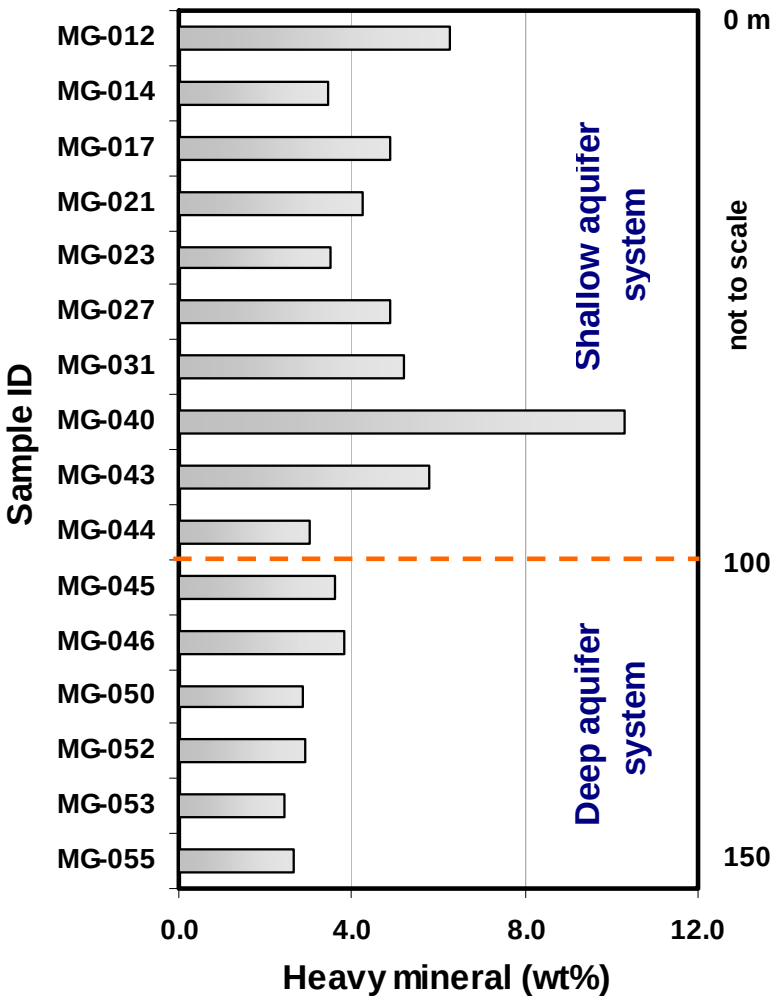

Fig. 6.4 Variation in the heavy mineral concentrations in Manikganj aquifer sediments. Shallow aquifer sediments tend to have more heavy minerals than the deeper aquifer sediments.

As many as 30 different heavy mineral species were identified in the Quaternary sediments of Manikganj. The common heavy minerals include biotite, garnet, amphiboles (mostly hornblende), pyroxenes (augite and enstatite), kyanite, sillimanite, epidote, magnetite, ilmenite, sphene, allanite, apatite, goethite and siderite in most sands. Sediments from shallow depths are represented by abundant biotite, hornblende, kyanite, epidote, sillimanite, epidote and garnet (Fig. 6.5). Stable minerals (e.g., zircon, rutile, and tourmaline) are not abundant in shallow sediments. However, some less commonly found minerals like apatite, monazite, olivine, rutile and pyrite are found in shallow sediments. The deeper sediments are abundant in garnet, amphiboles, pyroxene, kyanite, sillimanite and sphene with some tourmaline, rutile, zircon, corundum, and zoisite.

Group-A (strongly magnetic) minerals consist of opaque minerals and other non-opaque varieties attached with magnetic minerals. EDS analysis shows that most of the opaque minerals are magnetite, ilmenite, hematite and goethite. The average concentration of opaque minerals in the Quaternary sediments is approximately 5 wt%, whereas the older sediments (Oligocene to Pliocene) contains higher amount of opaque minerals in the Bengal Basin (Uddin et al., 2007). Moderately magnetic minerals (Group-B) contribute the highest amount (~50 wt%) of heavy minerals in these sediments. This group mainly consists of biotite, chlorite, garnet and amphibole, but the percentage of garnet (mainly almandine) increases with depth. Group-C (weakly magnetic) is the second largest category, consisting of amphibole, pyroxene, sphene, epidote, staurolite, zoisite, allanite, garnet and some biotite. Group-D (poorly magnetic) mainly consists of aluminosilicates (kyanite and sillimanite), sphene, chlorite, zircon, apatite, and some rutile.

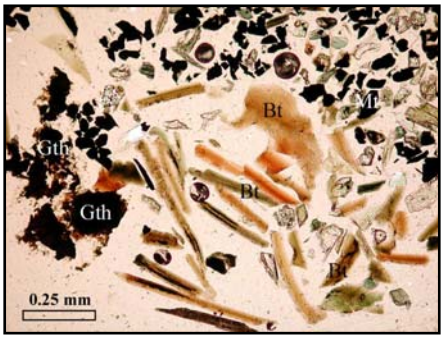

MG-012 (14 m): Strongly Magnetic

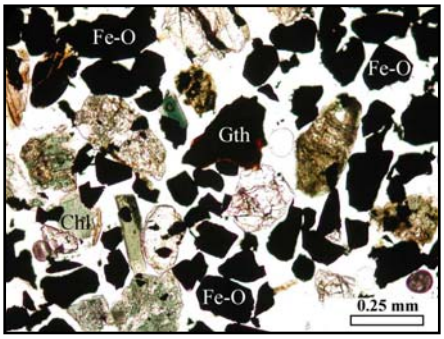

MG-017 (20 m): Strongly Magnetic

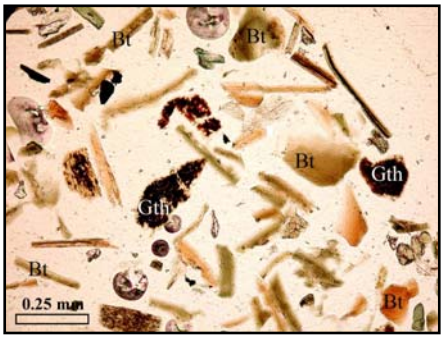

MG-012 (14 m): Moderately Magnetic

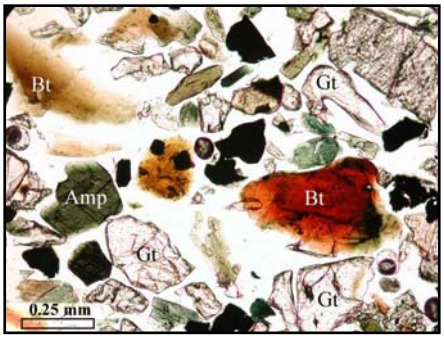

MG-017 (20 m): Moderately Magnetic

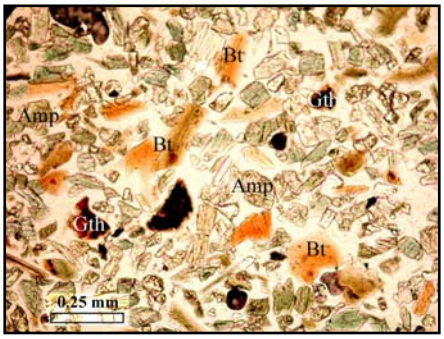

MG-012 (14 m): Weakly Magnetic

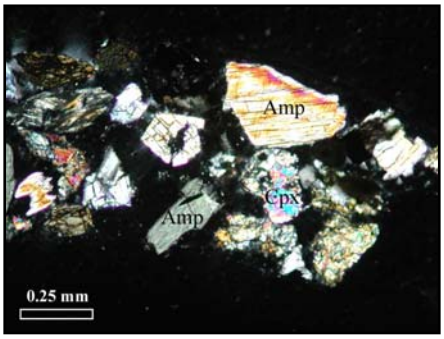

MG-017 (20 m): Weakly Magnetic

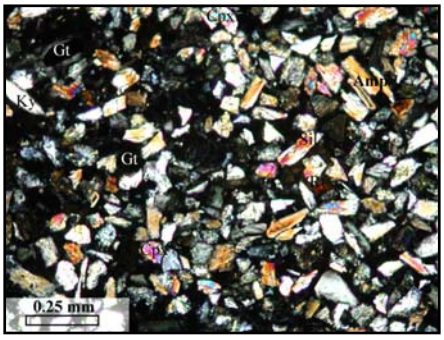

MG-012 (14 m): Poorly Magnetic

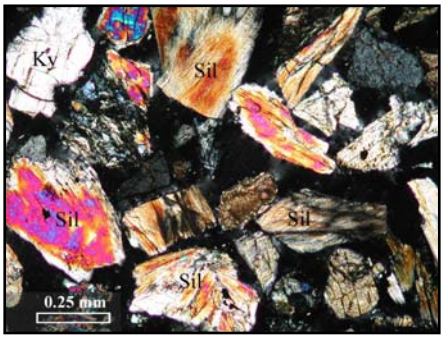

MG-017 (20 m): Poorly Magnetic

Fig. 6.5 Representative photomicrographs of heavy minerals from Manikganj. Keys: Gt-Garnet; Ky-Kyanite; Sil-Sillimanite; Bt-Biotite; Amp-Amphibole; Zr-Zircon; FeO-Iron oxide; Gth-Goethite; Cpx-Clinopyroxene; Ep-Epidote; St-Staurolite; Ap-Apatite; Zs-Zoisite; Sid-Siderite; Sph-Sphene; Chld-Chloritoid.

MG-023 (28 m): Strongly Magnetic

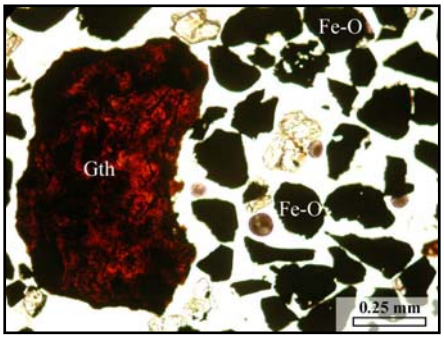

MG-031 (37 m): Strongly Magnetic

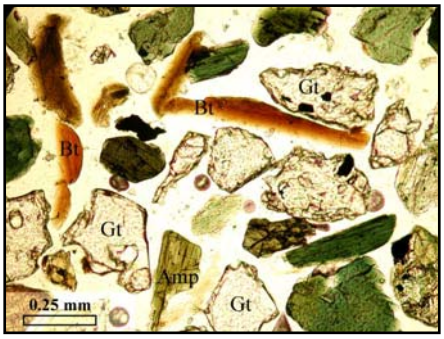

MG-023 (28 m): Moderately Magnetic

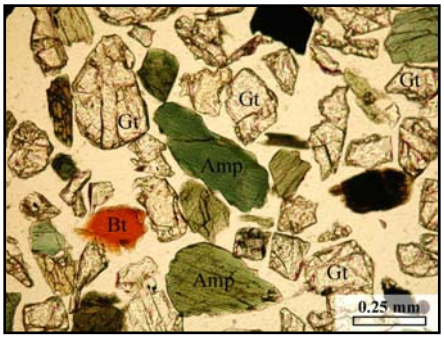

MG-031 (37 m): Moderately Magnetic

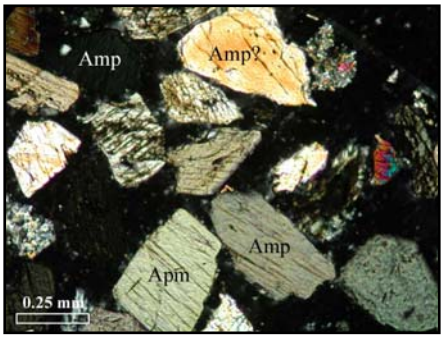

MG-023 (28 m): Weakly Magnetic

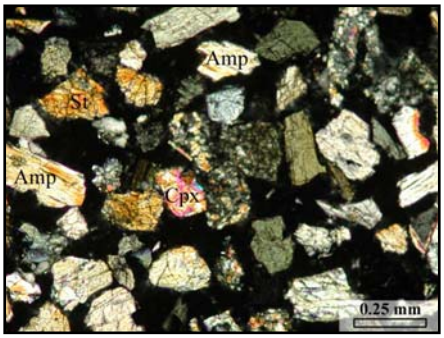

MG-031 (37 m): Weakly Magnetic

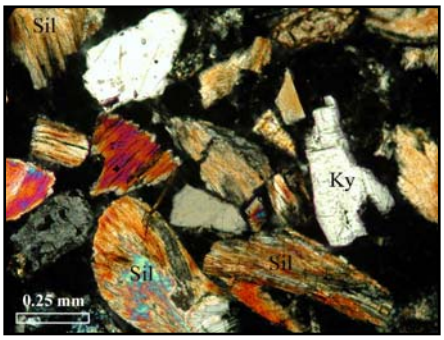

MG-023 (28 m): Poorly Magnetic

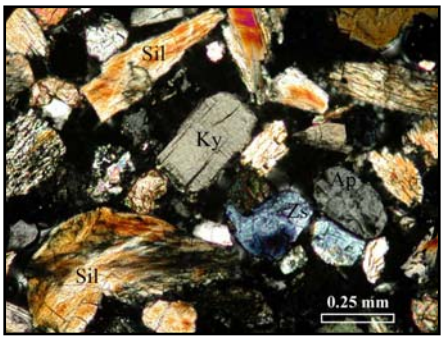

MG-031 (37 m): Poorly Magnetic

Fig. 6.5 Cont'd.

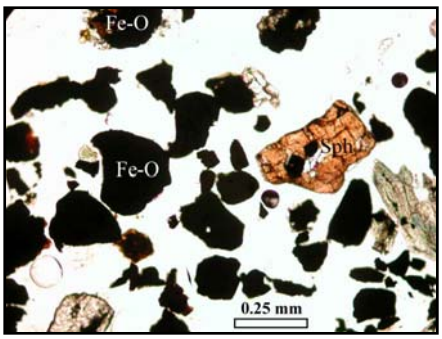

MG-044 (86 m): Strongly Magnetic

MG-046 (98 m): Strongly Magnetic

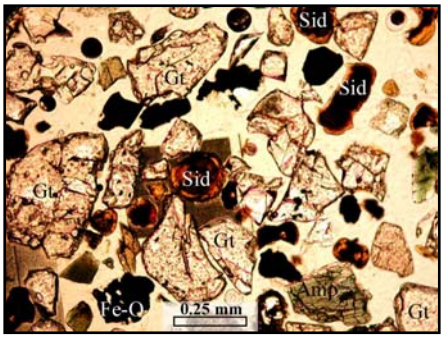

MG-044 (86 m): Moderately Magnetic

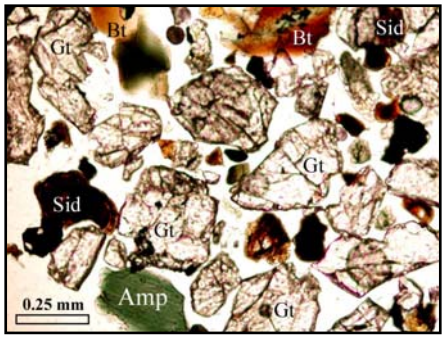

MG-046 (98 m): Moderately Magnetic

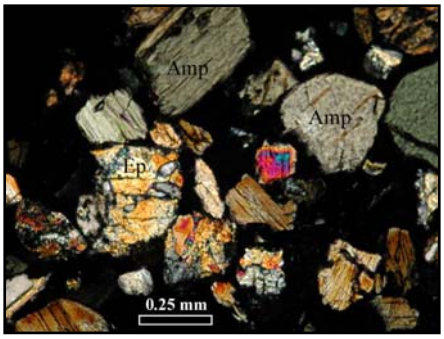

MG-044 (86 m): Weakly Magnetic

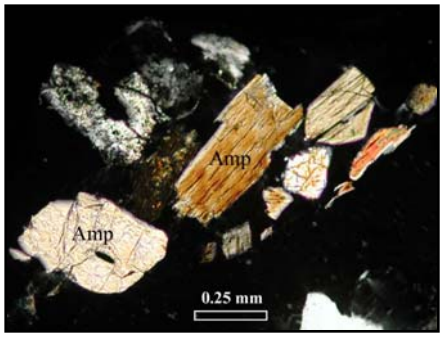

MG-046 (98 m): Weakly Magnetic

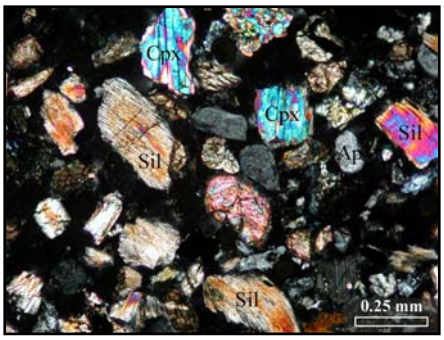

MG-044 (86 m): Poorly Magnetic

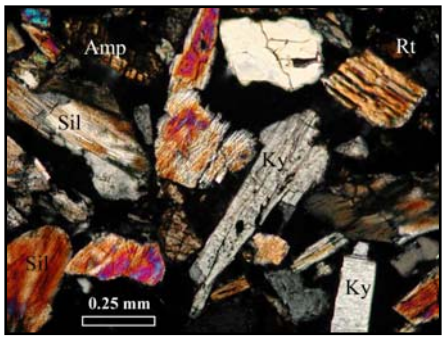

MG-046 (98 m): Poorly Magnetic

Fig. 6.5 Cont'd.

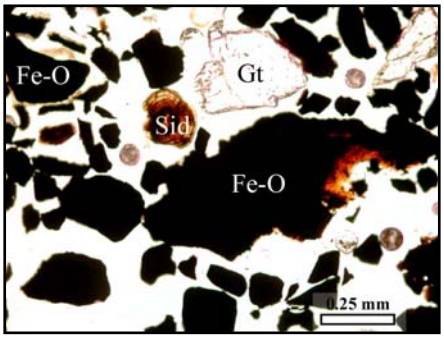

MG-050 (122 m): Strongly Magnetic

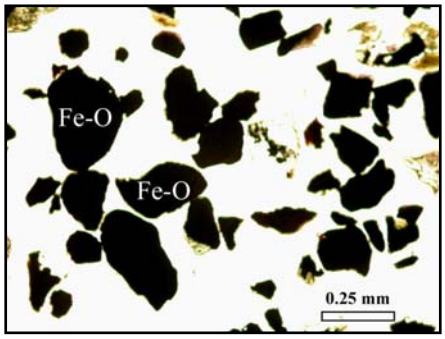

MG-055 (152 m): Strongly Magnetic

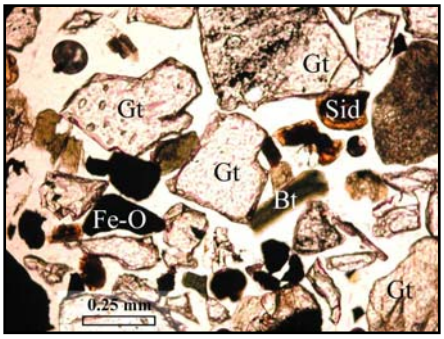

MG-050 (122 m): Moderately Magnetic

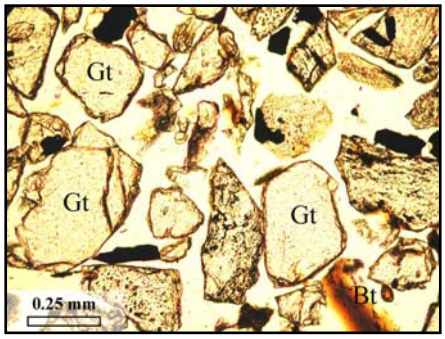

MG-055 (152 m): Moderately Magnetic

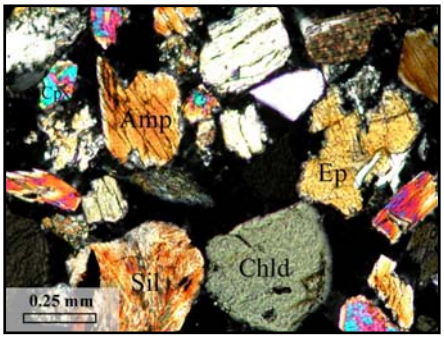

MG-050 (122 m): Weakly Magnetic

MG-055 (152 m): Weakly Magnetic

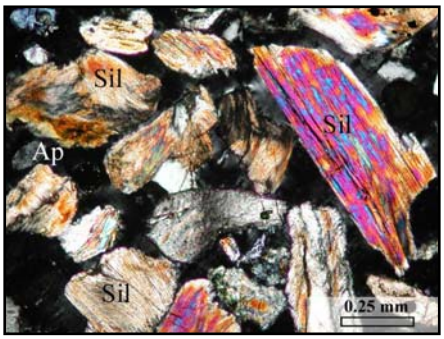

MG-050 (122 m): Poorly Magnetic

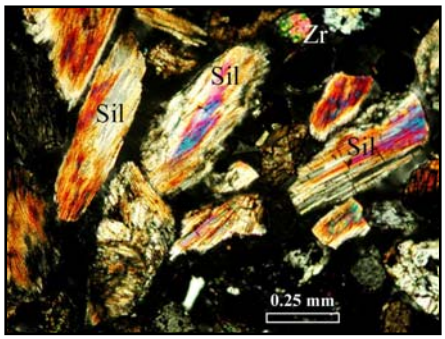

MG-055 (152 m): Poorly Magnetic

Fig. 6.5 Cont'd.

6.3.3. Authigenic minerals

Authigenic minerals are found within the sediment core samples from Manikganj. EDS with backscattered imaging on polished thin-sections suggests the presence of some authigenic Fe-oxides and Fe-carbonates in the sediment core samples from Manikganj area. In the MN-core samples, at a depth about 4 m, some brown, hard concretions are found within a dark-gray clay layer. This layer has the highest arsenic concentration of 8.8 ppm as measured by ICP-MS analysis. Grains were gold-coated and observed immediately under the electron microscope. EDS analysis on the concretion revealed that the grain was goethite (FeOOH) (Fig. 6.6). Results show that the Fe-oxide (goethite) concretion contain several elements other than iron and oxygen, such as Ca, P, Mn and small percentage of As. Numerous Fe-oxides (mostly goethite) are found in the MN core samples with the EDS and electron microprobe analysis. Backscatter images help to study the structure of these authigenic Fe-oxides present in the sediments (Fig. 6.7). Sediments at shallow depths under reducing conditions mostly host these goethite minerals, but at deeper depths these Fe-oxides are found mainly as hematites under highly oxidizing conditions. Electron microprobe analysis was performed on some of these goethite grains at various spots to find out chemical variations and possible arsenic content (Table 6.6). The general detection limit for arsenic in the electron microprobe was approximately 900 ppm, which is high for detecting arsenic content in these Fe-oxides. However, the detection limit was brought down to approximately 366 ppm with increasing the number of counts for some analyses. In a goethite grain at shallow depth (MG-21) several spots were found where arsenic content was measured approximately 341 ppm, which is just below to the detection limit of that particular electron microprobe

used in this study. Further analysis is necessary to quantify the arsenic content in these Fe-oxide minerals. Ion microprobe analysis would be one of the best options to detect low level of arsenic and to map the distributions within these minerals.

Numerous siderite grains were found in many samples ranging in depth from 80 to 120 m in Manikganj area (Fig. 6.8). The composition and structures suggest that these siderites were formed authigenically (possibly biogenic) within the alluvial aquifers. Electron microprobe analysis on these siderite grains revealed that the nuclei of most of these minerals are dolomitic in composition (Table 6.7). CO_2 was calculated stoichiometricly in microprobe analysis. Numbers of ions were calculated on the basis of 6 Oxygen for all four analyses (Table 6.7). Chemical compositions of these siderite grains vary from pure $FeCO_3$ to $(Fe,Mn)CO_3$ and sometimes consist of some $CaCO_3$ and SiO_2. Electron microprobe analysis could not confirm the presence of arsenic in these siderites. Several siderite concentrations were found from MG-core samples at different depths ranging from 100 ft to 400 ft below the surface (Turner, 2006). EDS analysis shows that these siderite concretions contain variable amount of Fe (24-38%), O (32-40%), C (10-13%), and minor amounts of Ca (2-3%) and Mn (1-2%) (Turner, 2006). The presence of significant amount of siderite ($FeCO_3$) and some possible rhodochrosite ($MnCO_3$) in the Manikganj aquifers relatively in deeper depths at arsenic level of 50 µg/L indicates a highly reducing groundwater with relatively high pH conditions that help to precipitate Fe and Mn and may remove some arsenic as it sorbed with these minerals.

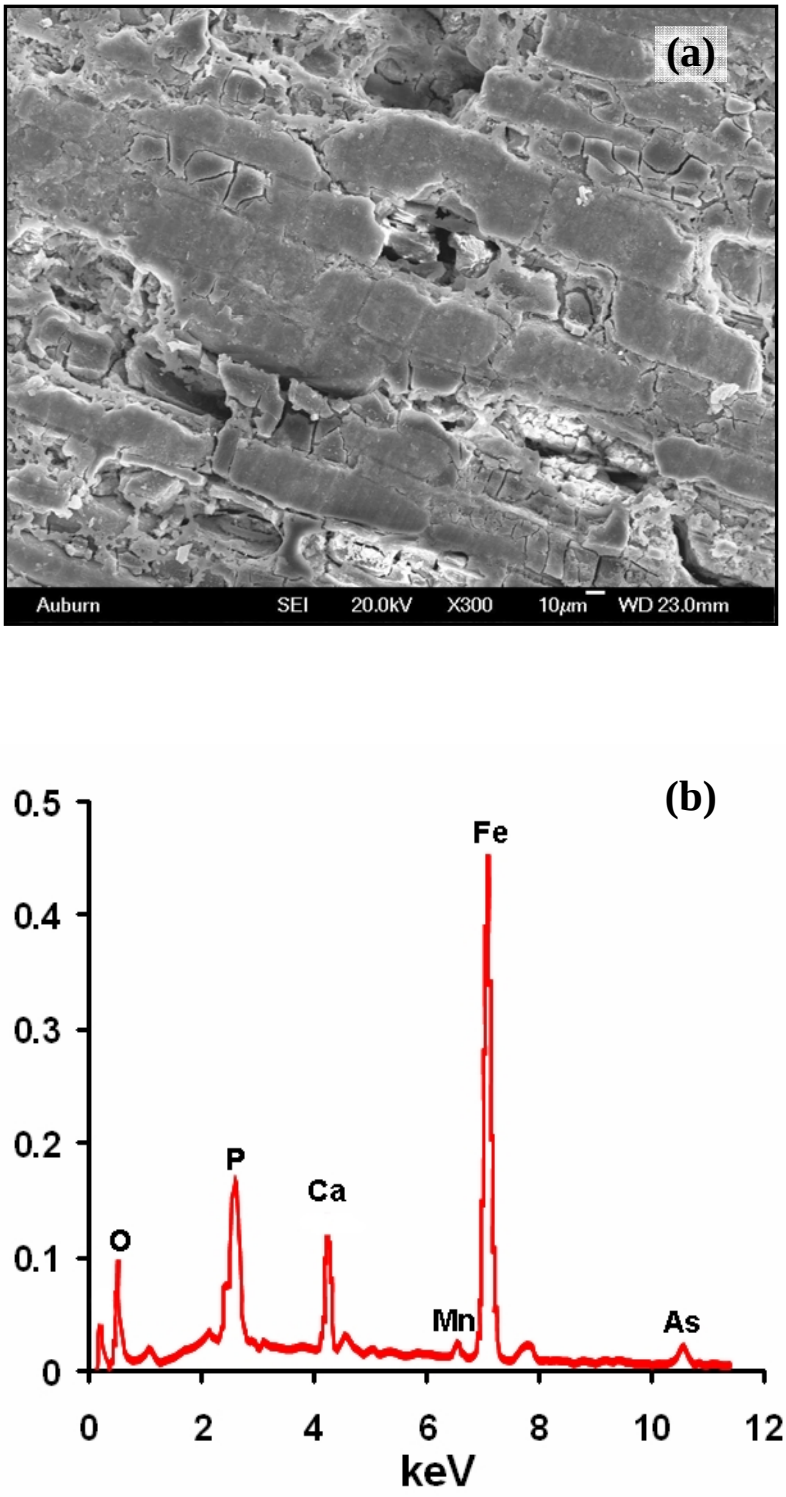

Fig. 6.6 (**a**) SEM picture shows a box-work structure of a Fe-oxyhydroxide concretion within a clay layer that contain 8.8 ppm of arsenic; (**b**) EDS spectrum shows the chemical composition of the concretion where the peaks for Fe, P, Ca and O are seen.

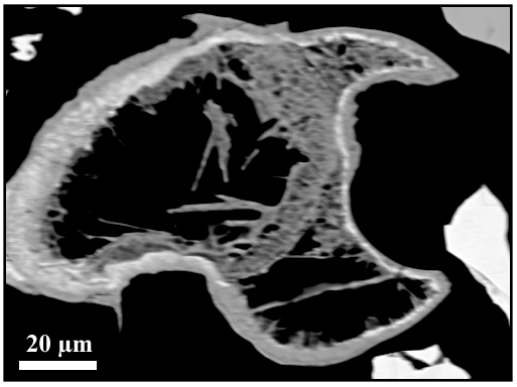

MG-012 (14 m) Goethite

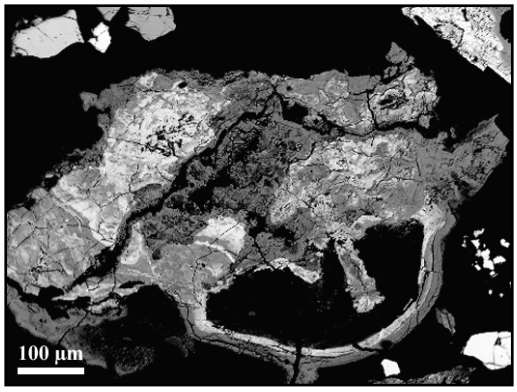

MG-021 (25 m) Goethite

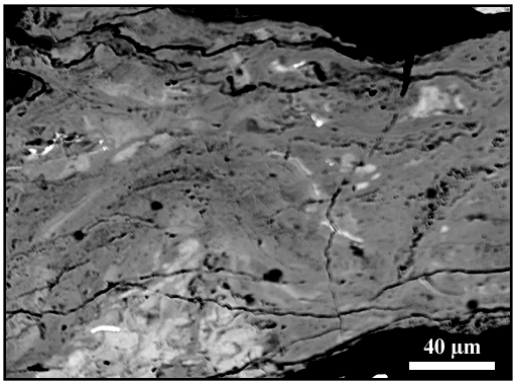

MG-050 (122 m) Goethite/Hematite

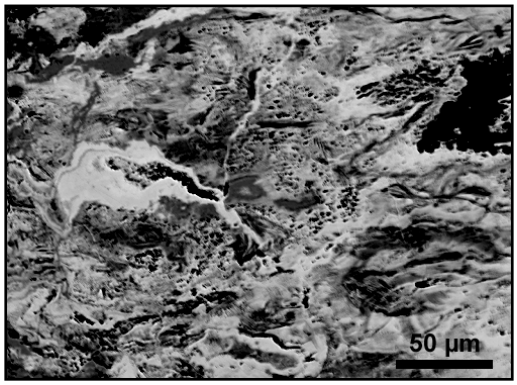

MG-050 (122 m) Goethite/Hematite

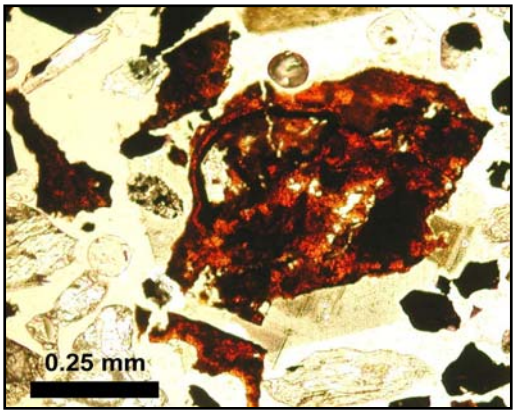

MG-021 (25 m) Goethite

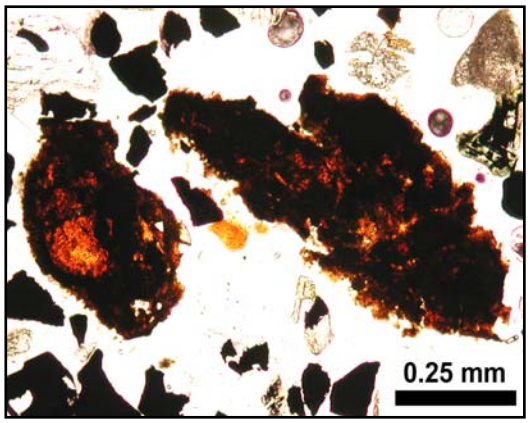

MG-021 (25 m) Goethite

Fig. 6.7 Backscattered images (upper four pictures) and petrographic microscope pictures (lower two pictures) of authigenic Fe-oxyhydroxides/oxides found in different depths in Manikganj aquifer sediments.

Table 6.6 Results from electron microprobe analysis on some selected Fe-oxides in two samples (MG-21 and MG-50) at several spots.

Oxides (wt%)	MG-21(1)	MG-21(2)	MG-21(3)	MG-21(4)	MG-50(1)	MG-50(2)	MG-50(3)	MG-50(4)
SiO_2	3.82	0.64	1.05	0.88	0.08	1.84	3.42	1.84
TiO_2	0.04	0.03	0.00	0.01	0.07	0.03	0.07	0.05
Al_2O_3	0.46	0.04	0.09	0.09	0.22	0.09	0.07	0.03
MgO	0.12	0.10	0.24	0.24	0.03	0.15	0.13	0.16
FeO	69.15	82.29	72.51	79.34	92.93	72.94	55.30	59.67
CaO	0.79	0.42	0.35	0.36	0.01	0.34	0.72	1.40
MnO	0.44	0.61	1.07	0.79	0.12	0.88	13.70	2.76
Cr_2O_3	0.23	0.14	0.00	0.12	0.03	0.00	0.00	0.02
NiO	0.15	0.02	0.00	0.20	0.00	0.00	0.00	0.10
P_2O_5	0.06	0.03	0.04	0.08	0.08	0.08	0.08	0.08

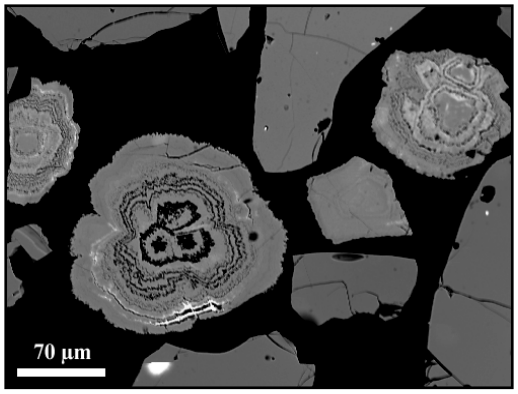

MG-044 (86 m) Siderite

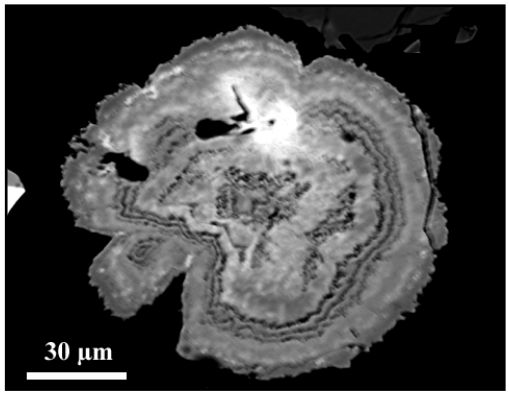

MG-050 (122 m) Siderite

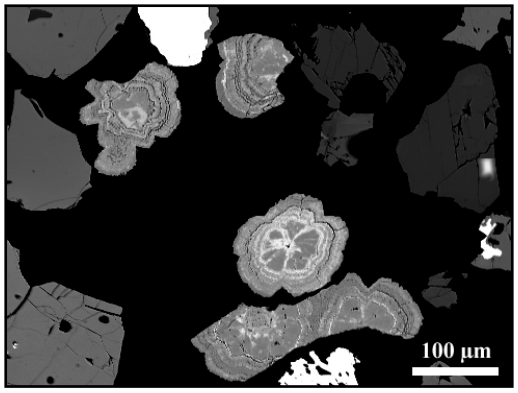

MG-044 (86 m) Siderite

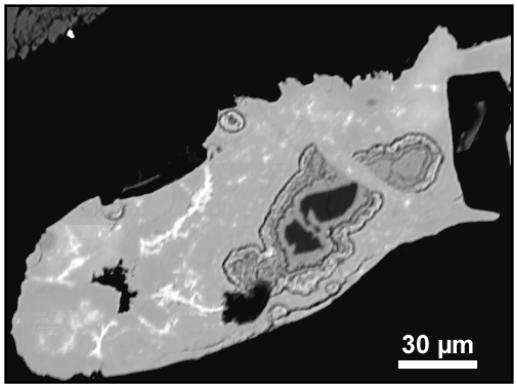

MG-044 (86 m) Siderite in Fe-oxide

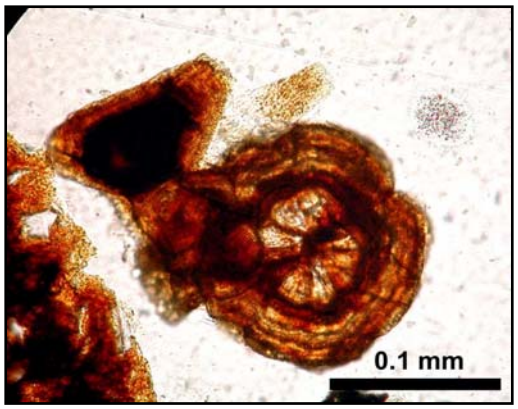

MG-044 (86 m) Siderite

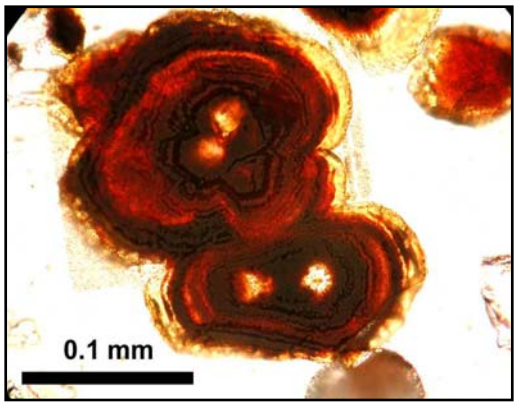

MG-044 (86 m) Siderite

Fig. 6.8 Backscattered images (upper four pictures) and petrographic microscope pictures (lower two pictures) of authigenic siderite found in different depths in Manikganj aquifer sediments.

Table 6.7 Results from electron microprobe analysis on some selected siderite concretions in one sample (MG-44) at several spots. CO_2 was calculated stoichiometricly for all the elements. Numbers of ions on the basis of 6 O are shown.

Oxides (wt%)	MG-44(1)	MG-44(2)	MG-44(3)	MG-44(4)
CaO	4.13	29.08	29.07	3.82
MgO	0.16	16.28	16.27	0.20
FeO	52.59	7.41	7.41	57.82
MnO	4.17	1.54	1.54	2.17
SrO	0.00	0.03	0.03	0.03
BaO	0.03	0.00	0.00	0.04
CO_2	38.23	46.10	46.09	40.00
Total	99.32	100.44	100.41	104.07
Major mineral	Siderite	Dolomite	Dolomite	Siderite
Numbers of ions on the basis of 6 O				
Element	MG-44(1)	MG-44(2)	MG-44(3)	MG-44(4)
Ca	0.17	0.99	0.99	0.15
Mg	0.01	0.77	0.77	0.01
Fe	1.69	0.20	0.20	1.77
Mn	0.14	0.04	0.04	0.07
Sr	0.00	0.00	0.00	0.00
Ba	0.00	0.00	0.00	0.00
C	4.00	4.00	4.00	4.00
Total	6.00	6.00	6.00	6.00

6.4. Provenance of Manikganj sands

Petrographic analyses were conducted following the Gazzi-Dickinson method, counting sand-sized minerals included in lithic fragments as the mineral phase rather than the host lithic fragment (Dickinson, 1970; Ingersoll et al., 1984). Approximately a total of 250 framework points were counted for each sample. Point-counting parameters and recalculated parameters are defined in Table 6.8.

Modal analyses of the sands from the Quaternary sediments are presented in Table 6.9. Compositional field characteristics of different provenances can be shown on one or more triangular diagrams (Dickinson and Suczek, 1979). In these compositional fields the QtFL emphasizes on the maturity of mineral grains, QmFLt emphasizes on source rocks, and QmPK emphasizes on mineral grains and the dominance of types of feldspar grain in sediments. The major provenance types in terms of overall tectonic setting within or adjacent to continental blocks, and key aspects of derivative and compositions are described in Dickinson (1985).

Sands in Manikganj aquifers are composed of quartz, feldspar (mostly potassium), mica, and lithic fragments (mainly sedimentary and metamorphic). Volcanic lithic (igneous rock fragments) are also seen in sand samples. Sediments are medium- to poorly-sorted with angular to subangular texture. Feldspars are mostly fresh and unaltered. Biotite micas are abundant at shallow depths. Quartz grains are mostly subangular and contain inclusions of tourmaline and zircon crystals. Other quartz grains show weathering marks and pressure solutions, suggesting metamorphic origin. Sediment texture, sorting and composition suggest that the detritus were transported within a short distance from the neighboring source areas before they were deposited in the basin.

Composition suggests that most of these sediments were mainly derived from large igneous provinces; however, contributions from medium to high grade metamorphic and recycled sedimentary sources are also evident in the sand samples.

To visualize the variations in sand composition and to interpret the major tectonic provenance of these Quaternary sands from Manikganj aquifers, some ternary diagrams of major components, the monocrystalline grains and phaneritic lithic fragments are drawn (Fig. 6.9). The samples from the Quaternary sediments (Holocene alluvium and Pliocene-Pleistocene Dupi Tila sand) fall within the border between "recycled orogen" and "transitional continental", which is slightly different from the provenance (completely "recycled orogen") for the Dupi Tila Sandstone in one of the comprehensive studies on provenance, tectonic and unroofing history of the Bengal Basin by Uddin and Lundberg (1998b).

The study area is located very close to the confluence between the Brahmaputra and Ganges rivers. These two major rivers controlled the sedimentation and geomorphology in the Bengal Basin, especially throughout the Quaternary period (Goodbred and Kuehl, 2000). The Ganges and Brahmaputra rivers have distinctive mineralogical assemblages resulting from geologically distinct source areas. The ratios of epidote (E) to garnet (G) help distinguish the contribution between the Ganges and Brahmaputra river-carried sediments in the Bengal Basin (Heroy et al., 2003). This study has also applied this technique to determine the sedimentary history of Manikganj study area based on E/G ratios.

Table 6.8 Sandstone (Sand) modal parameters used in this study.

1. Primary parameters (after Graham et al., 1976; Dickinson and Suczek, 1979)
Qt = Qm + Qp, where Qt = total quartzose grains Qm = monocrystalline quartzose grains Qp = polycrystalline quartz grains, including chert grains
F = P + K, where F = total feldspar grains P = plagioclase feldspar grains K = potassium feldspar grains
L = Ls + Lv + Lm = Lsm + Lvm = Lt - Qp, where Ls = sedimentary lithic fragments, mostly argillites Lv = volcanic lithic fragments Lm = metamorphic lithic fragments Lsm = sedimentary and metasedimentary lithic fragments Lvm = volcanic, hypabyssal, metavolcanic lithic fragments Lt = total aphanitic lithic fragments
2. Secondary parameters (after Dickinson, 1970)
P/F = plagioclase/ total feldspar grains

Table 6.9 Normalized modal analyses of sand from the Quaternary alluvial sediments in Manikganj core samples.

Sample	Point	QtFL(%)			QmFLt(%)			QmPK(%)			LsLvLm(%)		
Number	Count	Qt	F	L	Qm	F	Lt	Qm	P	K	Ls	Lv	Lm
MG-12	250	82	8	9	80	8	11	91	2	7	79	0	21
MG-14	285	72	21	7	68	21	12	77	6	18	95	0	5
MG-17	357	68	29	4	60	29	11	68	10	22	77	15	8
MG-21	242	63	28	9	58	28	14	67	12	21	52	14	33
MG-23	309	68	24	8	63	24	13	72	7	21	77	0	23
MG-27	297	64	31	5	56	31	13	65	12	23	20	0	80
MG-31	237	68	27	5	55	27	18	67	15	18	42	25	33
MG-40	251	69	22	8	65	22	13	74	8	17	67	0	33
MG-44	296	66	25	9	57	25	19	70	10	20	30	11	59
MG-45	270	63	24	13	55	24	21	70	9	21	40	0	60
MG-50	271	55	30	15	48	30	21	62	15	23	55	0	45
MG-53	295	65	26	9	59	26	15	70	5	25	88	0	12
MG-55	231	62	30	7	51	30	19	63	12	25	35	0	65
Mean	276.2	66.7	25.0	8.4	59.6	25.0	15.4	70.3	9.6	20.1	58.2	5.1	36.7
Std. Dev.	35.4	6.3	6.0	3.0	8.2	6.0	3.7	7.5	4.0	4.7	24.0	8.4	23.7

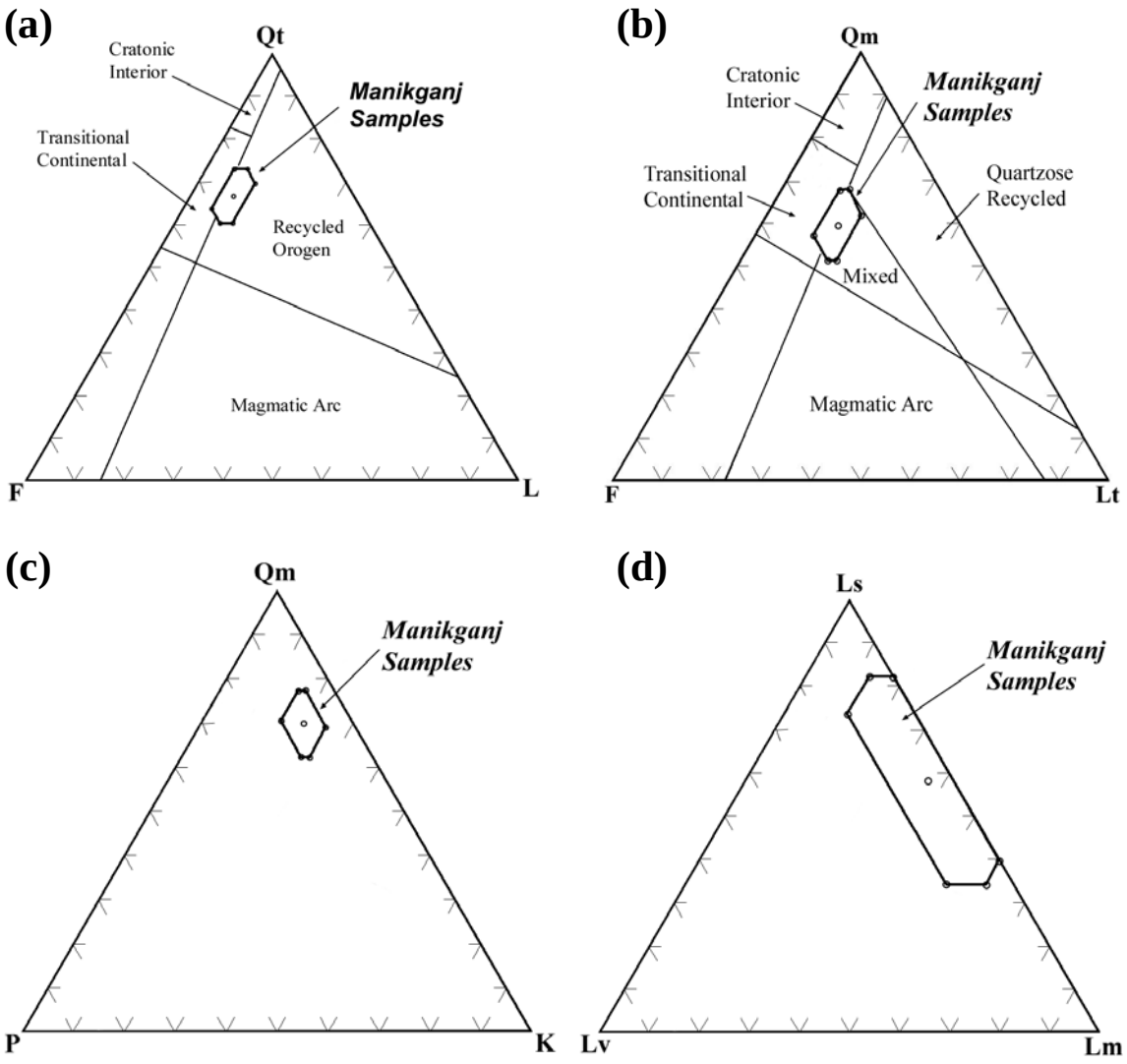

Fig. 6.9 Ternary diagrams showing overall provenance modes in (QtFL and QmFLt plots), light microcrystalline component (QmPK), and lithic-grain component (LsLvLm) of sand composition. (a) QtFL plot shows quartz- and feldspar-rich compositions lie within the border between "recycled orogen" and "transitional continental" provenances; (b) QmFLt plot shows that sands are derived from mixed tectonic provenance; however, contributions from "transitional continental" are also descendible; (c) Quaternary sands from Manikganj area are dominated by potassium feldspars; (d) Lithic fragments are mainly sedimentary (e.g., mud, shale, silty sand) and low-grade metamorphic rocks (slate, phyllite, schist and gneiss). Provenance fields in (a) and (b) are taken from Dickinson (1985).

A pilot study on 5 sand samples shows that there are some variations in E/G ratios from the deeper sediments to the shallowest in Manikganj area. There are other minerals like zoisite and allanite belong to epidote group that are not considered in this preliminary analysis. The E/G ratio increases from 0.28 to 0.86 from deeper sands (MG-55 at 152 m) to shallow sands (MG-12 at 14 m) respectively. The E/G ratios in other three samples are: 0.29 in MG-50 (122 m), 0.69 in MG-40 (61 m), and 0.85 in MG-27 (33 m). These results suggest that the deeper sediments (> 100 m) were mainly deposited by the Ganges apparently during the Late Pleistocene to early Holocene time in the basin. During the low stand of Holocene sea level when the Brahmaputra was flowing directly to the south (Goodbred and Kuehl, 2000) and sediments were deposited mainly by the Brahmaputra as indicated by increases in the E/G ratio towards the top of the Quaternary sequences in Manikganj.

CHAPTER 7

DISCUSSION

7.1. Hydrogeochemistry and groundwater arsenic

The chemistry of groundwater in Manikganj area is similar to other arsenic-affected areas in Bangladesh. The pH values in groundwater range from 6.1 to 7.3 with a mean value of 6.8 in the study area. The redox potential (Eh) varies from -152 to 177 mV and wells with higher arsenic concentrations typically have negative values of Eh. The groundwater type is mainly Ca-HCO_3, which is similar to groundwater of GBM delta and major floodplain areas in Bangladesh (BGS and DPHE, 2001; Ahmed et al., 2004).

As is associated with Fe, Mn, Si and Ba in groundwater and sediments of Manikganj study area (Fig. 7.1). These elements in groundwater typically shows a correlation in other parts of Bangladesh where groundwater arsenic concentration is high (BGS and DPHE, 2001; Ahmed et al., 2004; Zheng et al., 2004). The breakdown of organic matter by bacteria influences the groundwater As concentration by serving as an electron donor for the reductive dissolution of Fe- and Mn-oxyhydroxides in aquifer sediments. The relationship between groundwater As and SO_4 is generally negative, which is the common relationship in other high-As areas in Bangladesh and West Bengal (Stüben et al., 2003; Ahmed et al., 2004; Zheng et al., 2005).

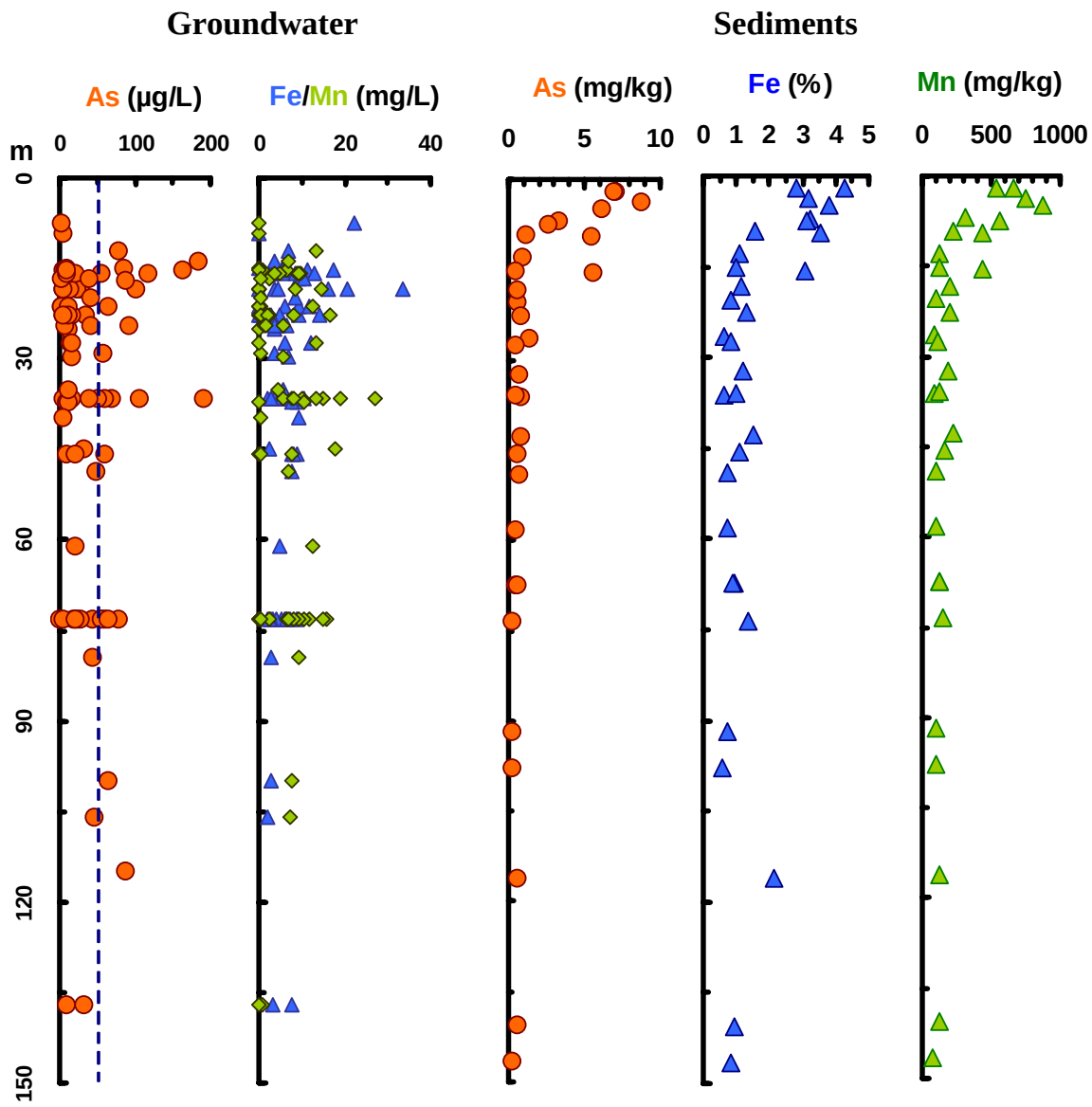

Fig. 7.1 Plots show the variation with depth in concentrations of As, Fe and Mn in groundwater and sediments in Manikganj area. The concentration of Mn in groundwater is expressed 10 times higher than the actual concentrations.

Cluster analysis results show that As, Fe and Mn in groundwater and sediments are closely associated in As-affected shallow aquifers in Manikganj. Multivariate statistical results suggest that As in sediments is strongly correlated with Fe, Mn, Ca, P and other trace metals (e.g., Zn, Ni, Co, Cr, V, Cu, La and Cd) in sediments. However, sequential extraction results of sediments in core samples show that most of the extractable As and Fe concentrations are easily soluble or ionically-bound/exchangeable that are loosely attached with Fe-oxyhydroxides, clay minerals or colloids in the sediments. Other extractable fraction of arsenic in sediments is associated with amorphous or crystalline Fe-oxyhydroxides. Several previous studies of sequential extraction on the Holocene sediments in Bangladesh revealed that significant amount of As, Fe and Mn are associated closely with the amorphous or crystalline Fe-oxyhydroxides (BGS and DPHE, 2001; Ahmed et al., 2004; Zheng et al., 2005). Single-solution extraction for arsenic and other trace elements would be necessary to verify the presence of soluble or ionically-bound/exchangeable arsenic in sediments.

Groundwater As and Fe concentrations and well depths correlate with isotopically heavier $\delta^{13}C$ DIC levels in Manikganj groundwater. High As and Fe concentrations are correlated with $\delta^{13}C$ (PDB) in groundwater though the $\delta^{13}C$ values are very negative throughout the study area. Depleted $\delta^{13}C$ (PDB) are thought to be associated with greater degree of organic-matter oxidation leading to the generation of highly reducing condition in groundwater (BGS and DHPE, 2001). Isotopic fractionation may be caused by bacterial respiration of lighter ^{12}C from organic matter in aquifer sediments. During the bacterial Fe(III)-reduction, groundwater becomes enriched in heavier $\delta^{13}C$, Fe, and As. More depleted $\delta^{13}C$ (PDB) (< -20‰) are found in Chandpur area where groundwater

arsenic concentrations are the highest in Bangladesh (BGS and DPHE, 2001). Moreover, de-watering and fluid expulsion of deep-crustal rocks associated with tectonic collision in the Himalayas could have contributed CO_2 (and perhaps other metals) that is isotopically heavier than atmospheric CO_2 (Turner, 2006).

It has been widely accepted that Fe and Mn are dissolved into groundwater through the reductive dissolution process from Fe- and Mn-oxyhydroxides and helps release of dissolved As into groundwater (BGS and DPHE, 2001; Nickson et al., 2000, Zheng et al., 2004; Saunders et al., 2005). High silicon in groundwater may be derived from chemical weathering of silicate minerals (e.g., biotite) in aquifers that might introduce As in groundwater (Sengupta et al., 2004).

7.2. Quaternary sedimentation and climatic effects on arsenic distributions

Sedimentation patterns and deposits during the Quaternary period are different from the Tertiary and older geologic time in the Bengal Basin (Uddin and Lundberg, 1999; Goodbred and Kuehl, 2000). High groundwater arsenic is well-linked with the Quaternary deposits and no arsenic has been reported from the older sediments in the Bengal Basin (Uddin and Abdullah, 2003). Saunders et al. (2005) tried to link the elevated arsenic occurrences in groundwater with the retreat of continental glaciation at the end of Pleistocene, which led to the rise of sea level during the Early to Middle Holocene, and deposition of alluvium, extensive marsh and peat, and finer sediments in Bengal lowlands (Ravenscroft et al., 2001). During the Pleistocene time, the mechanical weathering of rocks in source areas (e.g., Himalayas, Indian craton, and Indo-Burman mountains) was enhanced due to mountain building activities and glaciation. The aquifer

sands in the Bengal Basin were largely derived from physical weathering and erosion at a time of extended glaciation in the Himalayas, but the intensity of chemical weathering was limited by the low temperatures during erosion (McArthur et al., 2004). Close connection between groundwater arsenic and presence of glacial deposits was observed in many places in North America and Europe (Saunders et al., 2005).

In Manikganj, the As-free deeper aquifers (> 100 m) are composed of highly oxidized and weathered Dupi Tila sands, which was probably deposited during the very Late Pliocene to Early Pleistocene time (Reimann, 1993). Yellowish-brown to orange-brown sediments are mostly composed of quartz, feldspar, mica and some heavy minerals. The Dupi Tila sands contain less organic matter than the overlying As-rich Holocene sediments that are mainly fine-grained, gray to dark-gray in color. Percentage of heavy minerals in the Holocene sediments that form the shallow aquifers (< 100 m) in Manikganj is higher than the older deposits. The clay layer separating the Dupi Tila sands and overlying Holocene deposits is also highly oxidized and sticky and thus can be correlated with the Pleistocene Madhupur Clay. However, this clay layer was greatly eroded during the last glacial maximum and sea-level lowstand in the early Holocene time (Goodbred and Kuehl, 2000). In Manikganj area, the Holocene sedimentation started with gravel-rich medium to coarse sands recorded at approximately 100 m below surface. Sedimentation rate was very high and rapid as indicated by the presence of unbroken prismatic quartz crystals and very unstable minerals like olivine in the core samples from Manikganj. Significant sedimentation started in the early Holocene time with increased precipitation in warm and humid climatic conditions in the Himalayan region (Goodbred and Kuehl, 2000). Two distinct fining-upward sedimentary sequences are recorded in the

Quaternary stratigraphic column probably indicating episodic major channel shifting in the study area. The bottom fining-up sequence, which is relatively coarser and contain low arsenic, was probably deposited by a braided river during the Pliocene-Pleistocene time. Sedimentation during the Middle to Late Holocene time in the study area was probably contributed by a meander river system relatively smaller than the Brahmaputra river, which was apparently flowing through its easterly course into the Sylhet trough (Goodbred and Kuehl, 2000). Sediments in the upper fining-up sequence are predominantly fine-grained with clay and peat in several depths indicating the limit of the Holocene sea-level highstand when extensive mangrove forests and swamplands were developed in the Bengal Basin (Umitsu, 1987; Goodbred and Kuehl, 2000). This upper fining-up sequence forms most of the high-arsenic contaminated aquifers in the study area as well as in other parts of Bangladesh.

7.3. Lithology, mineralogy and provenance of As-rich aquifer sediments

General lithological and mineralogical compositions of the sediments both in arsenic-affected and arsenic-free aquifers in the study area are very similar. However, fine to coarse sediment ratio is smaller in the arsenic-free deeper (> 100 m) aquifers which is similar to other areas in the country (Ahmed et al., 2004). These aquifers sediments varies from gray at the shallow depths to yellowish-brown at deeper depths indicating a reducing to oxidizing geochemical environments. Studies have shown that high-As concentrations are associated with gray to dark-gray sediments, whereas yellowish-brown aquifer sediments host low groundwater arsenic (BGS and DPHE, 2001; Horneman et al., 2004).

The mineralogy of sediments both in shallow and deep aquifers are mainly quartz, feldspar, both potassium and plagioclase, and micas. Quartz is both monocrystalline and polycrystalline with variable undulosity ranges from straight to highly undulose. Feldspars are mostly potassium at shallow depths with some plagioclase mainly albite and Ca-rich varieties. Lithic fragments are mainly sedimentary, but metamorphic lithic grains are also abundant in the sediments. Volcanic lithic fragments (only plutonic igneous rocks) are also abundant throughout the Quaternary sediments in Manikganj. Feldspars are fresh and larger in sizes. Perthitic and myrmekite intergrowth structures are observed in the thin-sections of aquifer sediments. These Quaternary sediments contain high amount (3-10%) of heavy minerals of various types. Highly magnetic minerals are mainly magnetite, ilmenite, and hematite that contribute approximately 5% of the heavy minerals (Fig. 7.2). The magnetic minerals are fairly homogenous with minor Ti content indicating low Ti-magnetite that appears to be plutonic in origin. Ilmenite is the second largest phase of magnetic minerals, which contains very high amount of Ti and Fe. Moderate magnetic minerals are garnet, biotite, chlorite, ilmenite, and some amphiboles containing magnetite inclusions. This is the second largest (~ 50%) group of heavy minerals observed in Manikganj core samples. The third (37%) dominant heavy minerals assemblages are amphibole, epidote, allanite, biotite, chlorite, staurolite, zoisite, pyroxene, and authigenic siderite. Sillimanite, kyanite, zircon, sphene, apatite, and some rutile are found in the poorly magnetic fraction, which contributes approximately 8% heavy minerals in the core samples. Some detrital pyrite grains are found in shallow sediments. Tourmaline, monazite, corundum and olivine are found in some samples.

Provenance analysis revealed that these Quaternary sediments were derived mostly from igneous and metamorphic terranes located in the Indian Craton, Himalayan Mountains, Shillong Plateau and Indo-Burman ranges. Provenance field analysis shows that the sands from Quaternary deposits fall within the border between "recycled orogen" and "transitional continental", which is slightly different from the provenance determined by Ahmed et al. (2004). The Ganges, Brahmaputra and Meghna rivers have distinctive sedimentary characteristics which result from geologically distinct source areas and catchment geomorphology (Fig. 7.3). The Brahmaputra drains the Tibetan Plateau of China and Shillong Plateau of Assam and is dominated by upland tributaries originating from the Himalayan mountain ranges (Heroy et al., 2003). This river flows through rock types including Precambrian metamorphic (high-grade schists, gneisses, quartzite, and metamorphosed limestones), felsic igneous intrusive, and Paleozoic-Mesozoic sandstones and limestones (Heroy et al., 2003; Huizing, 1971). The Ganges travels through similar rock types, but unlike the Brahmaputra, it flows through a vast Precambrian Indian craton. The Ganges is also fed by many tributaries draining the Mesozoic and Tertiary mafic effusives, Rajmahal traps, and Gondwana basins in the eastern India that contain bituminous coals. The Meghna drains most of the western side of the Indo-Burman ranges through Tertiary sandstones, shale and limestones and igneous intrusions (Fig. 7.3). Heavy mineral assemblages in these Quaternary sediments suggest a mixed source of origin where contributions from high- to medium-grade metamorphic rocks, plutonic igneous rocks, and preexisting sedimentary rocks are significant.

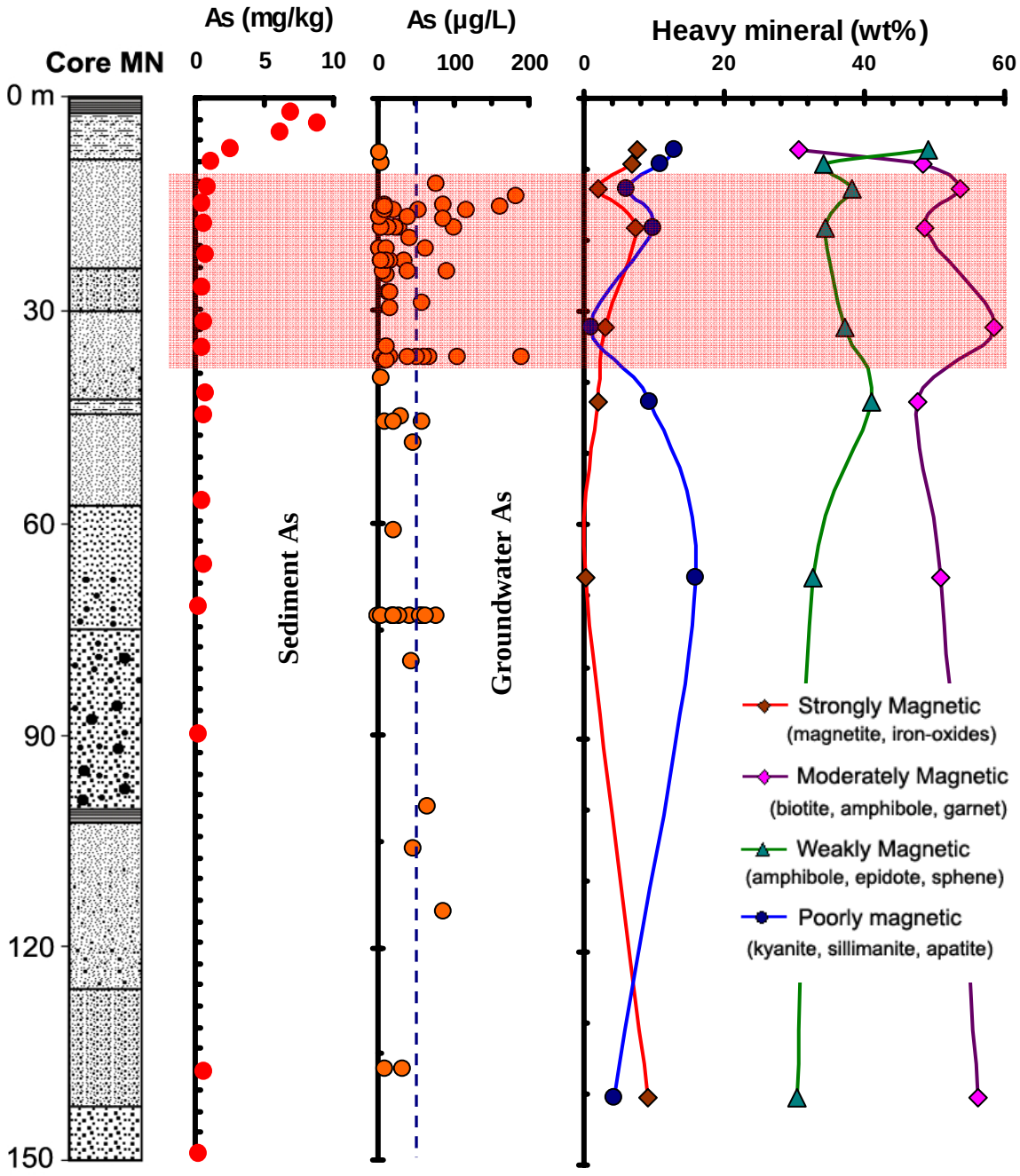

Fig. 7.2 Plots of arsenic concentrations in sediments of MN core samples and groundwater in Manikganj area. Dashed blue line at arsenic concentration in groundwater corresponds to Bangladesh country standard. Depth-wise variation in weight percent of different magnetic fractions in MN core samples are shown in right column. High arsenic concentrations in groundwater are found where the abundance of magnetite, iron-oxides, biotite, amphibole and apatite in sediments, which is highlighted with pink color.

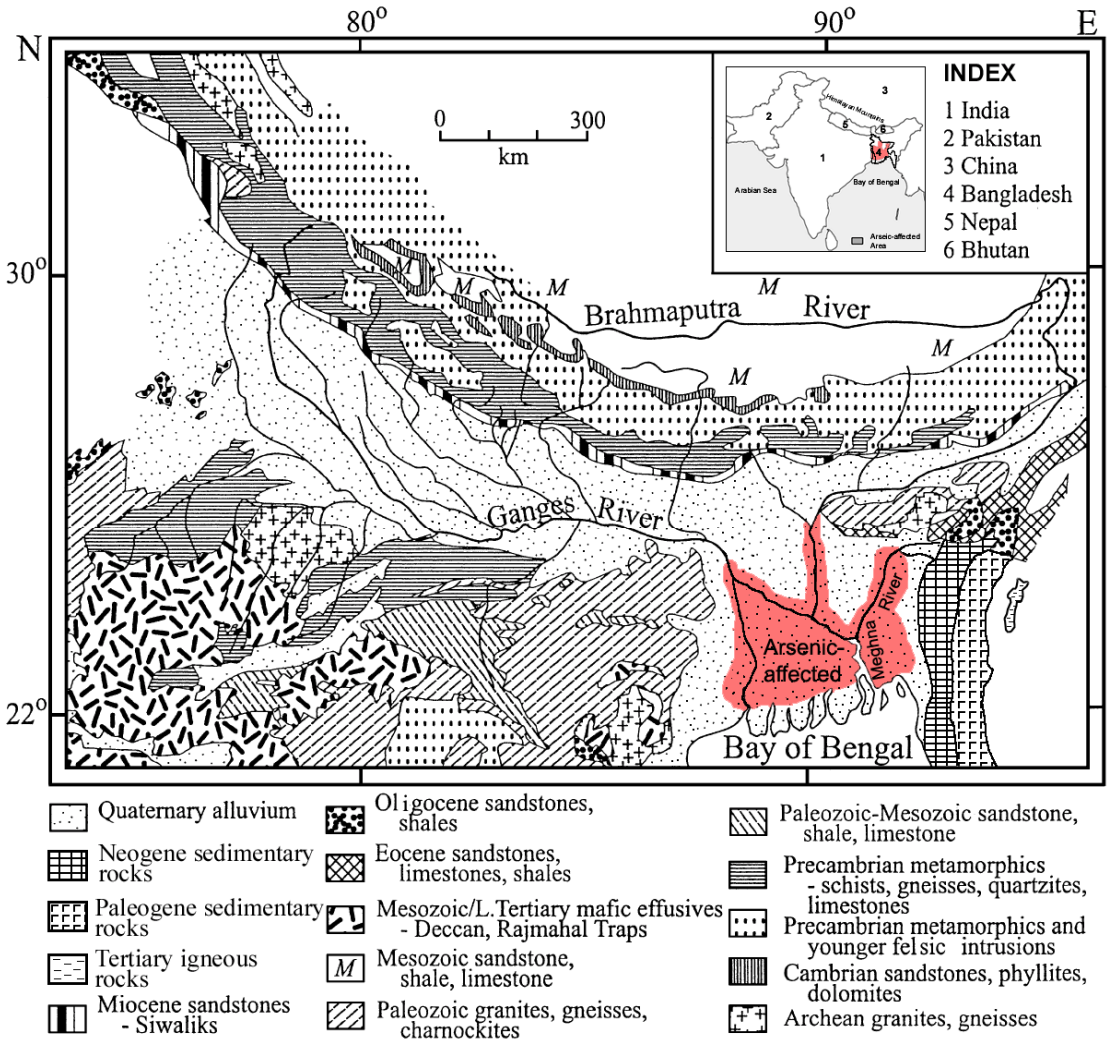

Fig. 7.3 Geological map of the Ganges, Brahmaputra and Meghna drainage basins and surrounding area. The Ganges drains the Indian Craton and southern slope of the Himalayas, The Brahmaputra flows through northern slope of the Himalayas and the Meghna drains the western slope of the Indo-Burman Ranges. The map also shows the geographic extent of arsenic-affected aquifers in the Bengal Basin. This map is modified after Heroy et al. (2003).

In the basin, it reflects continued unroofing of the Himalayas and alluvial samples represent the latest stages in this ongoing process (Uddin and Lundberg, 1998b). Arsenic concentration in the Ganges sediments is 1.2-2.6 mg/kg, in the Brahmaputra sediments is 1.4-5.9 mg/kg, and in the Meghna sediments is 1.3-5.6 mg/kg (Datta and Subramanian, 1997). The maximum concentration of arsenic in the Manikganj core samples is approximately 8.8 mg/kg.

7.4. Effects of authigenic minerals on groundwater arsenic

Several authigenic minerals were identified in the Quaternary sediments from Manikganj core samples. The most abundant authigenic mineral is goethite (FeOOH), which is found mostly within the upper part (< 100 m) of the stratigraphic column. Backscattered imaging and energy dispersive spectroscopy methods were used along with electron microprobe analysis to determine the texture and chemical composition of these goethite grains. The texture and heterogeneity in chemical composition of some of these goethite minerals suggest that they were formed authigenically by oxidation of ferrous iron (Fe^{2+}) present in the primary minerals (sulphide and silicate) in felsic or mafic igneous rocks in the source areas. Electron microprobe analysis indicated that these Fe-oxyhydroxides contains some arsenic (~ 341 mg/kg) and also Mn and Si. Studies show that Fe-Mn-oxyhydroxides are widespread in the environment and can adsorb arsenic onto their larger surfaces in acidic and near-neutral pH conditions (Korte et al., 1991; Nickson et al., 2000; Saunders et al., 2005). High amount of arsenic, adsorbed on Fe-Mn-oxyhydroxides, would have been transported by the GBM rivers and their numerous tributaries into the low-lying deltaic and floodplain areas in the Bengal Basin. Arsenic

adsorbed on the Fe-Mn-oxyhydroxides in the suspended and bed-loads of streams and rivers are concentrated and eventually deposited with organic matter in the floodplains and delta plains due to flooding or changes in river channels (Saunders et al., 2005). Subsequently, under anaerobic and reducing conditions iron-reducing bacteria cause the reductive dissolution of arsenic-bearing Fe(Mn)-oxyhydroxides and release arsenic into the groundwater of the Holocene aquifers (Nickson et al., 1998; McArthur et al., 2001; Bhattacharya et al., 2002; Smedley and Kinniburgh, 2002; Stüben et al., 2003; Islam et al., 2004; Zheng et al., 2004; Saunders et al., 2005).

Siderite ($FeCO_3$) and some mangano-siderite [$Fe(Mn)CO_3$] are found approximately 85 m below the surface in the core samples from Manikganj area. Petrographic study along with backscatter imaging and electron microprobe analyses confirmed the presence of these authigenic siderites within the lower shallow aquifers and the upper part of deeper aquifers that are mainly arsenic-free. Present study and a previous investigation by GRG and HG (2002) found several deep wells (85-120 m) in Manikganj contain high-As (> 50 µg/L). The mean arsenic value in groundwater within this depth range is 38 µg/L, which is much higher than the WHO/USEPA standard. The pH of groundwater in this depth range has a mean value of approximately 6.8. The average groundwater Fe and Mn concentrations are 4.0 mg/L and 0.40 mg/L respectively. Studies show that As-rich groundwaters with high concentration of dissolved Fe^{2+} and high pH (7-9) could precipitate authigenic siderite ($FeCO_3$) and/or rhodochrosite ($MnCO_3$) or mangano-siderite [$Fe(Mn)CO_3$] (Saunders and Swann, 1992; Pal et al., 2002). Electron microprobe analysis revealed that most of these siderites formed with a dolomitic nucleus at initial stage when groundwater became oversaturated for the

precipitation of calcite/dolomite. Recent studies (e.g., Lee et al., 2007) show that the siderite concretions formed in Fe-rich groundwater could be biogenic due to its low $\delta^{13}C$ values. The concentration of arsenic in these siderite grains could not be determined as the electron microprobe that was used in this study has the minimum detection limit of approximately 350-400 mg/kg. Further analysis with ion microprobe is being conducted to find out the chemical composition of these siderite grains in the Manikganj core samples. Biogenic siderite concretions were found in Holocene sediments in West Bengal, India that contain arsenic of a concentration of 7-9 mg/kg (Pal et al., 2002). Siderite grains remain stable under a narrow pH limit of approximately 7-9, which can be seen on the Eh-pH diagram that is constructed from the Manikganj groundwater (Fig. 7.4; Saunders et al., 2005). Under reducing condition, the early formed Fe-oxyhydroxides would dissolve and contribute its adsorbed arsenic to groundwater. On the other hand, with lower pH (< 7), the siderite concretions would dissolve and can release arsenic associated with them (Pal et al., 2002). Groundwater pH values in Manikganj aquifers are generally less than 7.0 in the lower shallow and deeper aquifers and thus it might be expected that these authigenic siderite grains are possibly releasing arsenic into the groundwater in the lower shallow aquifers. Further isotope and chemical analysis can be performed to confirm the concentration of arsenic and to learn more about the origin of these authigenic minerals in the Holocene aquifers in Manikganj.

7.5. Geomorphic evolution through Quaternary period and arsenic

Occurrences of high groundwater arsenic are significantly linked with the geology-geomorphology of development of deltas and alluvial deposits in the Bengal Basin

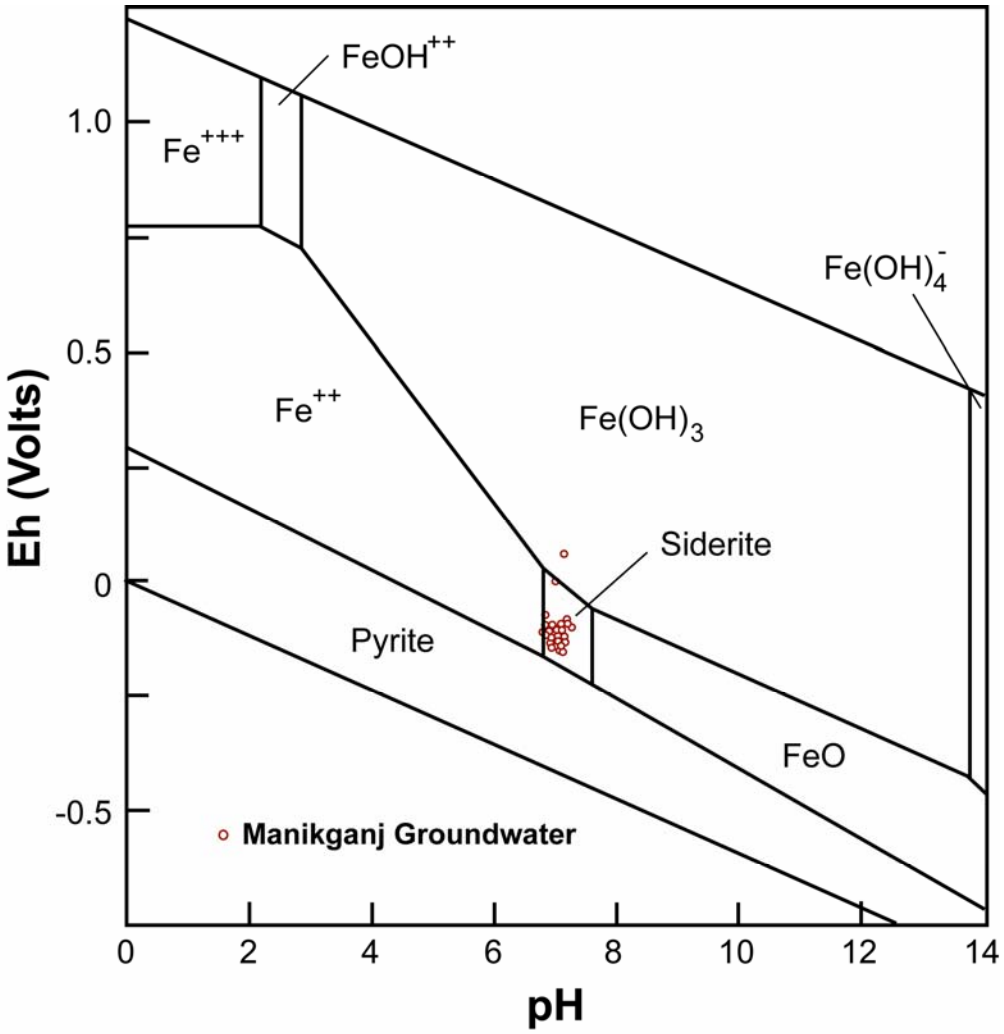

Fig. 7.4 Eh-pH diagram for average chemical conditions in Fe-Mn-S-HCO_3-H_2O system and the positions for the Manikganj groundwaters, which mainly fall within the narrow zone of authigenic siderite ($FeCO_3$) and $Fe(OH)_3$. Siderite concretions and goethite are found in Manikganj core sediments. Activity of species for this stability diagrams: Fe^{2+} = 10^{-3}, Mn^{2+} = 10^{-4}, SO_4^{2-} = 10^{-6}, and HCO_3^- = 10^{-4}. A total number of 30 groundwater samples was used for this stability diagram.

throughout the Quaternary period (Ahmed et al., 2004; Ravenscroft et al., 2005). The Quaternary sedimentation and river dynamics were controlled by the global climatic changes, uplift of the Himalayans, and tectonic subsidence in the Bengal Basin (Umitsu, 1993; Goodbred and Kuehl, 2000). During the sea-level lowstand at 18,000 yr BP, much of the GBM system was occupied with deeply incised channels within a series of terraces that are covered by thick Holocene deposits (Ravenscroft et al., 2005). Much of the Bengal Basin comprised incised alluvial valleys and exposed lateritic uplands during the last sea-level lowstand (Fig. 7.5). The pre-existing sediments (Pliocene-Pleistocene Dupi Tila sands) were exposed and deeply oxidized. Steeper hydraulic gradients allowed sufficient flushing of the Dupi Tila aquifers and recrystallization of iron-oxyhydroxides in dry climatic conditions (Ravenscroft et al., 2005). Sedimentation started with the climatic warming during the Late Pleistocene to Early Holocene time when voluminous sediment poured into the basin and filled the deep river valleys with coarser deposits (Fig. 7.5; Goodbred and Kuehl, 2000). During the rising sea-level conditions (11,000-6,000 yr BP) relatively fine-grained sediments started depositing over the coarser sediments that deposited earlier and the sediment depocenter migrated toward onshore (Goodbred and Kuehl, 2000). In Manikganj area, the Brahmaputra was probably depositing medium to fine-grained sediments forming fining-upward sedimentary sequence as recorded in both core samples (Fig. 7.5). Increased rainfall and humid climatic conditions favored the formation of mangrove swamps and peat basins behind the advancing delta fronts where degradation of abundant organic matter started (Ravenscroft et al., 2005). These sediments form the lower shallow aquifers in Manikganj

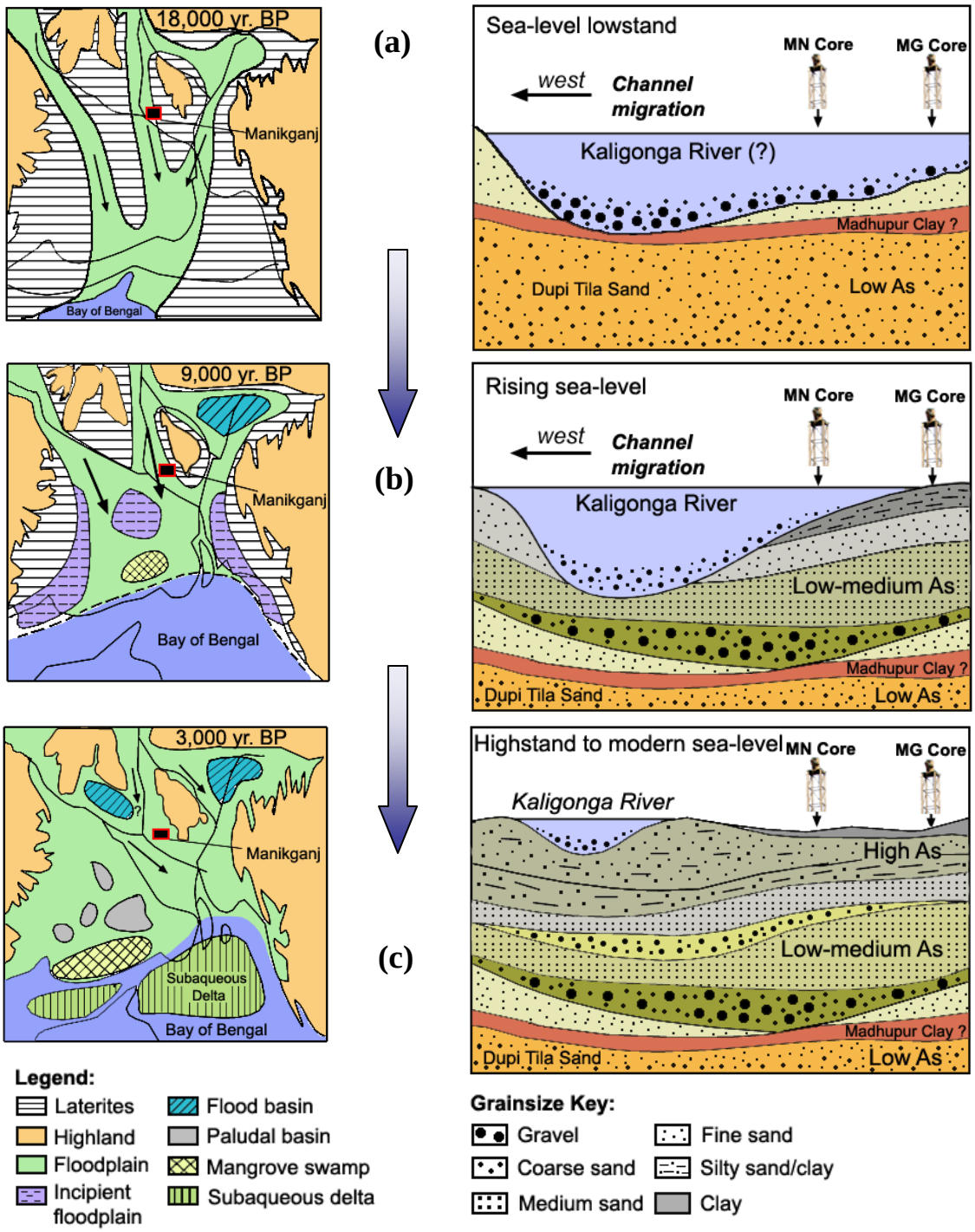

Fig. 7.4 Paleogeographic reconstruction of the Bengal Basin through the Quaternary period (after Goodbred and Kuehl, 2000) and postulated sedimentation patterns in Manikganj. (a) Low sea-level condition and sedimentation only within the incised river valleys; (b) Rapid sea-level rise and infilling of channel beds and adjoining floodplains; (c) Sea-level fall and appearance of the modern delta, and fine-grained deposits within numerous extensive peat basins and mangrove swamps that are highly As-contaminated.

area that contain low to medium arsenic (0-50 μg/L) in groundwater. The delta progradation started when the rate of sea-level rise slowed and the maximum transgression was reached in the western Bengal Basin (Umitsu, 1993; Goodbred and Kuehl, 2000). The Brahmaputra river switched to its eastern course and drained into the Sylhet trough from ~7,500 to 6,000 yr BP. In the western side of the Madhupur Tract, sedimentation was slower and mostly fine-grained sediments were deposited in the wide floodplains as noticed in core samples from Manikganj. Subdued topography resulted in sluggish groundwater movement with little flushing that favored accumulation of organic matter, finer sediments and Fe-oxyhydroxides in the floodplains and natural levees, while sediments within the riverbeds were mostly coarse-grained (Ravenscroft et al., 2005). Between 5,000 and 6,000 yr BP, the Brahmaputra probably switched back to its western course (Goodbred and Kuehl, 2000). Extensive paludal basin and mangrove swamps in the Bengal Basin were developed on the previously flooded coastal platform as the sea-level started dropping slowly and eventually stood at its modern stand. Mostly fine-grained sands and silts with clay were deposited in Manikganj area that formed the upper shallow alluvial aquifers, which contain high arsenic concentration. These sedimentary facies, which were formed by meandering rivers are characterized by medium to fine channel sands, overbank mud, and some peats that are noticed in Manikganj core sediments. Accumulation and degradation of organic matter and reducing conditions triggered arsenic release from Fe-oxyhydroxides due to microbially mediated reductive dissolution process at shallow depths. In Manikganj cores, the relative abundance of arsenic in sediments is higher in the MG core than the MN core. At shallow depths, the MG core samples are dominated by fine sands, silts and clay than the MN core samples.

This study has integrated information through a multidisciplinary research on groundwater, sediment and minerals of an arsenic-affected area in the central Bangladesh. Several issues are yet to be resolved in order to adequately explain the sources and mechanisms of elevated groundwater arsenic concentrations in the Quaternary aquifers. The future research in Manikganj area should include several important components that were not accomplished in the present study due to time and resource limitations. Stable oxygen and hydrogen isotope analysis for more groundwater samples especially from deeper aquifers (> 100 m) will be helpful to understand the groundwater recharge. Borehole lithologs would be necessary to create a solid subsurface geological model of Manikganj area. Sequential extraction of arsenic and other elements from sediments with $MgCl_2$ (weak solvent) has leached the maximum arsenic content, which was not expected and needs further analysis in future. Chemical analysis (ICP-MS) of different magnetic fractions of heavy minerals will help to determine the concentrations of arsenic, and also to find out the depth-wise variations of arsenic contents in sedimentary sequences. Ion microprobe analysis on individual authigenic goethite and siderite will help to map the elemental composition and arsenic concentrations. Finally, radiometric (^{14}C) age-dating of the aquifer sediments is important to link the occurrences of groundwater arsenic with the depositional age in the study area. Modeling of hydrologic transport, adsorption and biotransformation of arsenic in the aquifers in needed to assess the minimum flow rate required to "flush out" arsenic. Reaction kinetics of arsenic on the surface of Fe-oxides needs to be measured to better understand various mechanisms responsible for arsenic mobilization in groundwater.

CHAPTER 8

SUMMARY AND CONCLUSIONS

The present thesis combined the studies of groundwater, sediments and minerals of the Quaternary alluvial aquifers in Manikganj town, located in one of the As-hotspots in the central Bangladesh. Initial questions of this research were: (i) to determine any significant differences in groundwater and sediment geochemistry, and mineralogy between the high-As shallow (< 100 m) aquifers and low-As deeper (> 100 m) aquifers in Manikganj study area; (ii) to characterize the detrital and authigenic mineral assemblages typical of sediments in vertical core profiles; and (ii) to evaluate possible relationships between occurrences of high-As in groundwater with the mineralogy and depositional environments of aquifer sediments. The following conclusions can be drawn based on detailed research on groundwater chemistry, sediments characteristics and mineralogical profiling in As-affected sedimentary aquifers in Manikganj town.

- Groundwater in the study area is moderately to highly reducing with a mean redox potential (Eh) of approximately -88.0 mV and a median of -104.8 mV. Groundwater pH ranges from 6.11 to 7.28 in Manikganj area. Groundwater both in shallow and deep aquifers is mainly Ca-HCO_3 type. Arsenic concentrations in the study area are as high as 191 µg/L with a mean value of 32.85 µg/L. The spatial variability of arsenic concentration is also considerable with high small-scale variability. Stable

isotopes, δ^2H and $\delta^{18}O$ values indicate the groundwater in Manikganj area falls within or slightly below the Global Meteoric Water Line indicating the origin of groundwater from local rainfall and rivers with some evaporation before infiltration. Most of the $\delta^{13}C$ values of DIC in Manikganj groundwaters are isotopically lighter in composition, which indicates oxidation of organic matter. High arsenic tubewells are located at shallow depths within the low-lying areas. Multivariate statistical analyses of the groundwater chemical parameters suggest close association of As, Fe, Mn, Si and high pH in groundwaters. As is negatively correlated with SO_4, which is common in groundwater in many other areas in Bangladesh.

- Sediments consist of clay, silt, sand and gravels with several fining-upward sequences in the Quaternary stratigraphy. Sediments are gray to dark-gray in shallow aquifers, but relatively yellowish-gray to brown in the deeper aquifers, which are free of arsenic contamination. High arsenic concentrations both in groundwater and sediments are associated with finer sediments rich in organic matter. High arsenic levels are associated with fine-grained meandering river overbank floodplain and natural levees deposits. Lithostratigraphic correlation suggests that the sediments, which were deposited during the Early Holocene time at lowstand of the sea-level, formed the base of the lower shallow aquifer system. Geochemical analysis of sediment samples shows that the highest arsenic level (8.8 mg/kg) is associated with clay/silty-clay deposits. Very low arsenic concentrations in sediments are found at deeper depths where groundwater also contains low level of arsenic. Sequential extraction analysis revealed that a significant amount of arsenic in sediments is present as easily soluble or exchangeable/ionically-bound phases.

However, some amount of arsenic is also associated with amorphous/crystalline Fe-oxyhydroxides in sediments. Multivariate analyses show that elevated As concentrations in sediment are closely associated with elevated Fe, Mn, P and other trace elements such as Co, Ni, Cd, Zn and V.

- Sands in aquifers are mostly composed of quartz (mono- and polycrystalline), feldspar (mostly potassium and plagioclase), mica (biotite and muscovite), and lithic grains (mostly sedimentary and metamorphic) and a significant amount (average ~4.4 wt%) of heavy minerals. Sands at shallow depths are dominated by monocrystalline quartz, but with increasing depth the percentage of polycrystalline quartz takes over the monocrystalline type. Potassium feldspars dominate over plagioclase at all depths. Presence of perthitic and myrmekite intergrowth are commonly seen in the sands, suggesting an igneous origin (plutonic) of sediments, probably derived from granite pegmatite or other felsic to intermediate rocks. Presence of some volcanic lithics fragments (large crystals and felsic in nature) also supports an inference of sediment contribution from the igneous-type source rocks. In addition to an igneous source, a significant portion of sediment was derived from recycled sedimentary and medium- to high-grade metamorphic rocks. Provenance study shows that these Quaternary sediments were mainly derived from a "mixed" provenance with significant contributions from the "recycled orogen" and "transitional continental" provenance fields. Heavy minerals are abundant in the Quaternary sediments throughout the stratigraphic sequence. Percentages of heavy minerals are slightly higher in shallow sediments, and are dominated by magnetite, ilmenite, biotite, amphibole, epidote, apatite, kyanite, sillimanite, goethite and

siderite. In deep sedimentary deposits, medium- to high-grade metamorphic suites, including kyanite, sillimanite, garnet, amphibole, sphene, biotite, and some stable minerals, rutile, zircon, and corundum occur. Authigenic Fe-oxide(oxyhydroxide) minerals and siderite are not very common at deeper depths (>100 m). At shallow depth (<100 m), the authigenic goethite contains a significant amount of arsenic (~340 mg/kg) in sediments. Siderite concretions are found at shallow to intermediate depths (80-100 m), which may also contain some arsenic. Amorphous Fe-oxyhydroxides and colloids are probably one of the major sources of arsenic into groundwater. In addition, to Fe-oxyhydroxides and the authigenic minerals, some detrital minerals, such as magnetite, apatite, biotite and amphibole are the other potential carriers of arsenic in groundwater.

- This study has integrated the results of groundwater geochemistry with sediment characteristics and chemistry, petrography and mineralogy of aquifer sediments from Manikganj town in central Bangladesh. Results show that the elevated arsenic concentrations in the shallow (< 100 m) alluvial aquifers are associated with gray, fine-grained overbank and floodplain deposits enriched with organic matter and peat. Microbially-mediated reductive dissolution of amorphous/colloids and crystalline Fe-oxyhydroxides (goethite), desorption in neutral to moderately alkaline condition, combined with the dissolution of authigenic siderite concretions, and detrital magnetite, apatite, biotite, and amphibole are the controlling mechanisms for the occurrence of high arsenic in alluvial aquifers in Manikganj as well as other similar fluvial environments in Bangladesh. Small-scale spatial variations in arsenic distribution might be controlled by

the local variation in redox conditions (Mn/Fe reduction vs. SO_4 reduction) and distribution of sedimentary facies and minerals in the alluvial aquifers.

- Future research in Manikganj area should include stable oxygen and hydrogen isotope analysis for more groundwater samples especially from deeper aquifers (> 100 m). Borehole lithologs and additional drilled information can be used to create a solid subsurface geological model of Manikganj area. Chemical analysis (ICP-MS) of different magnetic fractions of heavy minerals will help to determine the concentration of arsenic in different phases. Ion microprobe analysis on individual authigenic goethite and siderite that are found in sediments will help to determine arsenic concentrations. Radiocarbon dating or optically stimulated luminescence (OSL) dating of the aquifer sediments in the study area is necessary to link between the occurrences of groundwater arsenic and depositional ages.

REFERENCES

Acharyya, S.K., Lahiri, S., Raymahashay, B.C., Bhowmik, A., 2000. Arsenic toxicity of groundwater of the Bengal Basin in India and Bangladesh: the role of Quaternary stratigraphy and Holocene sea level fluctuation. Environmental Geology. 39, 1127–1137.

Aggarwal, P.K., Basu, A.R., Poreda, R.J., 2000. Isotope hydrology of groundwater in Bangladesh: implications for characterization and mitigation of arsenic in groundwater. International Atomic Energy Agency, Viena, TC Project BGD/8/016, 23p.

Ahmed, K.M., Bhattacharya, P., Hasan, M.A., Akhter, S.H., Alam, S.M.M., Bhuyian, M.A.H., Imam, M.B., Khan, A.A., and Sracek, O., 2004. Arsenic enrichment in groundwater of the alluvial aquifers in Bangladesh: An overview. Applied Geochemistry. 19, 181–200.

Amacher, M.C., and Kotuby-Amacher, J., 1994. Selective extraction of arsenic from minespoils, soils, and sediments. Agronomy abstracts 86, 256.

Arafin, K.S., 2003. Occurrence and distribution of arsenic in groundwater of Manikganj Pauroshava, (M.Sc. thesis), Department of Geology, University of Dhaka, 68p.

Armstrong, J.T., 1988. Quantitative analysis of silicate and oxide materials: comparison of Monte Carlo, ZAF, and phi-rho-z procedures, Microbeam Analysis. 239-246.

Banerjee, M., and Sen, P.K., 1987. Palaeobiology in understanding the change of sea level and coast line in Bengal Basin during Holocene period. Indian J Earth Sci. 14(3-4), 307-320.

Banglapedia, 2003. National Encyclopedia of Bangladesh, Multimedia English Version, 1st edition. Asiatic Society of Bangladesh, Dhaka (Compact Disk version).

BGS and DPHE, 2001. Arsenic Contamination of Groundwater in Bangladesh, Vol. 2. Final Report, BGS Technical Report WC/00/19.

Bhatacharya, A, and Banerjee, S.N., 1979. Quaternary geology and geomorphology of the Ajoy-Bhagirathi valley, Birbhum and Murshidabad districts, West Bengal. Indian J Earth Sci. 2, 51-61.

Bhattacharya, P., Chatterjee, D., Jacks, G., 1997. Occurrence of arsenic-contaminated groundwater in alluvial aquifers from delta plains, eastern India: options for safe drinking water supply. Journal Water Resources Dev. 13, 79–92.

Bhattacharya, P., Frisbie, S.H., Smith, E., Naidu, R., Jacks, G., Sarkar, B., 2002. Arsenic in the environment: a global perspective. In: Sarkar, B. (Ed.), Handbook of Heavy Metals in the Environment. Marcell Dekker Inc., New York, pp. 147–215.

Brannon J.M., Patrick W.H., Jr., 1987. Fixation, transformation, and mobilization of arsenic in sediments. Environ. Sci. Technology, 21, 450-459.

Brown, C.E., 1998. Applied multivariate statistics in geohydrology and related sciences. Springer-Verlag, Berlin, Heidelberg, Germany, 350p.

Chao, T.T., and Zhou, L., 1983. Extraction techniques for selective dissolution of amorphous iron oxides from soils and sediments. Soil Sci. Soc. Am. J. 47, 225-232.

Datta D.K. and Subramanian, V., 1997. Texture and mineralogy of sediments from the Ganges–Brahmaputra–Meghna river system in the Bengal Basin, Bangladesh and their environmental implications, Environ. Geol.30(3-4), 181–188.

Davies, J., 1989. The geology of the alluvial aquifers of central Bangladesh. Vol. 2 BGS Technical Report WD/89/9.

Deutsch, C.V., Journel, A.G., 1998. GSLIB: Geostatistical Software Library and User's Guide. 2nd ed., Oxford University Press, New York, 376p.

Dhar, R.K., Biswas, B.K., Samanta, G., Mandal, B.K., Chakraborti, D., Roy, S., Jafar, A., Islam, A., Ara, G., Kabir, S., Khan, A.W., Ahmed, S.A., Hadi, S.A., 1997. Groundwater arsenic calamity in Bangladesh. Current Science. 73, 48-59.

Dickinson, W.R., 1970. Interpreting detrital modes of graywacke and arkose: Journal of Sedimentary Petrology. 40, 695–707.

Dickinson, W.R., and Suczek, C., 1979. Plate tectonics and sandstone compositions, American Association of Petroleum Geologists Bulletin. 63, 2164-2182.

Dowling, C.B., Poreda, R.J., Basu, A.R., Peters, S.L., and Aggarwal, P.K., 2002. Geochemical study of arsenic release mechanisms in the Bengal Basin groundwater. Water Res. Research. 38, (doi:10.1029/2001WR000968).

Drever, J.I., 1997. The geochemistry of natural waters: surface and groundwater environments, third ed., Prentice Hall, New Jersey, 436p.

Gani, M.R., and Alam, M.M., 2004. Fluvial facies architecture in small-scale river systems in the Upper Dupi Tila Formation, northeast Bengal Basin, Bangladesh, Journal of Asian Earth Sciences. 24(2), 225-236.

Ghosh, S., and De, S., 1995. Source of the arsenious sediments at Kachua and Itina, Habra Block, North 24 Parganas, West Bengal – a case study: Indian J. of Earth Sci. 22(4), 183-189.

Goldberg, S., Forster, H. S., and Godfrey, C. L., 1996. Molybdenum adsorption on oxides, clay minerals, and soils, Soil Science Society of America Journal. 60(2), 425-432.

Goodbred, S.L., Kuehl, S.A., 2000. The significance of large sediment supply, active tectonism, and eustasy on margin sequence development: late Quaternary stratigraphy and evolution of the Ganges-Brahmaputra delta. Sedimentary Geology. 133, 227–248.

Graham, S.A., Ingersoll, R.V., Dickinson, W.R., 1976. Common provenance for lithic grains in Carboniferous sandstones from Ouachita Mountains and Black Warrior Basin, Journal of Sed. Petrology. 46, 620-632.

GRG and HG, 2002. The status of arsenic transport in the deep wells at Manikganj district town, Final Report for Research and Development, DPHE, Water and Environmental Sanitation Section, UCICEF, Bangladesh, 67p.

Hair, J.F.Jr., Anderson, R.E., Tatham, R.L., Black, W.C., 1992. Multivariate data analysis with reading. Macmillan Publishing Company, New York.

Harvey, C.F., Swartz, C.H., Badruzzaman, A.B.M., Keon-Blute, N., Yu, W, Ali, M.A., Jay, J., Beckie, R., Niedan, V., Brabander, D., Oates, P.M., Ashfaque, K.N., Islam, S., Hemond, H.F., Ahmed, M.F, 2002. Arsenic mobility and groundwater extraction in Bangladesh. Science. 298, 1602 –1606.

Heroy, D.C., Kuehl, S.A., Goodbred, S.L., 2003. Mineralogy of the Ganges and Brahmaputra rivers: implications for river switching and Late Quaternary climate change, Sedimentary Geology. 155, 343-359.

Hess, H.H., 1966. Notes on operation of Frantz isodynamic magnetic separator, Princeton University: User manual guide, 6p.

Horneman, A., van Geen A., Kent D., Mathe P. E., Zheng Y., Dhar, R. K., O'Connell S., Hoque M., Aziz Z., Shamsudduha, M., Seddique, A., Ahmed K. M., 2004. Decoupling of As and Fe release to Bangladesh groundwater under reducing conditions. Part I: Evidence from sediment profiles: Geochim. Cosmochim. Acta. 68, 3459–3473.

Huizing, H.G.J., 1971. A reconnaissance study of the mineralogy of sand fractions from East Pakistan sediments and soils, Geoderma. 6, 106-133.

Ingersoll, R.V., Bullard, T.F., Ford, R.L., Grimm, J.P., Pickle, J.D., Sares, S.W., 1984. The effect of grain size on detrital modes: A test of the Gazzi-Dickinson point-counting method: Journal of Sedimentary Petrology. 54, 103–116.

Islam, F, Gault, A, Boothman, C, Polya, D, Charnock, J, Chatterjee, D, Lloyd, J, 2004. Role of metal-reducing bacteria in arsenic release from Bengal delta sediments: Nature. 430, 68-71.

Islam, M.S., Tooley, M.J., 1999. Coastal and sea level changes during the Holocene in Bangladesh. Quaternary International. 55, 61-75.

Johnson, M.R.W., 1994. Volume balance of erosional loss and sediment deposition related to Himalayan uplifts. Journal of the Geological Society of London. 151, 217-220.

Johnson, S.Y., and Nur Alam, A.M., 1991. Sedimentation and tectonics of the Sylhet trough, Bangladesh, Geological Society of America Bulletin. 103, 1513-1527.

Keon, N.E., Swartz, C.H., Brarander, D.J., Harvey, C., and Hemond, H.F., 2001. Validation of an arsenic sequential extraction method for evaluating mobility in sediments, Environ. Sci. Technol. 35, 2778-2784.

Khan, F.H., 1991. Geology of Bangladesh. The University Press, Bangladesh, 207p.

Korte, N., 1991. Naturally-occurring arsenic in groundwaters of the midwestern United States, Environmental Geol. Water Sci.18, 137-141.

Lee, M.-K., Griffin, J., Saunders, J.A., Wang, Y., and Jean, J., 2007 (in press). Reactive transport of trace elements and isotopes in Alabama coastal plain aquifers. J. Geophysical Research.

Liu, C.-W., Wang, S.-W., Jang, C.-S., and Lin, K.-H., 2006. Occurrence of arsenic in ground water in the Choushui river alluvial fan, Taiwan. Journal of Environ. Quality. 35, 68-75.

McArthur, J.M., Banerjeeb, D.M., Hudson-Edwardsc, K.A., Mishrab, R., Purohitb, R., Ravenscroftd, P., Cronine, A., Howartha, R.J., Chatterjeef, A., Talukderf, T., Lowryg, D., Houghtona, S., Chadhah, D.K., 2004. Natural organic matter in sedimentary basins and its relation to arsenic in anoxic ground water: the example of West Bengal and its worldwide implications. Applied Geochemistry. 19, 1255–1293.

McArthur, J.M., Ravenscroft, P., Safiullah, S. and Thirlwall, M.F. 2001. Arsenic in groundwater: testing pollution mechanisms for sedimentary aquifers in Bangladesh: Water Resources Res. 37, 109-117.

McCarthy, E.M.T., 2001. Spatial and depth distribution of arsenic in groundwater of the Bengal Basin, M.Sc. thesis (unpublished), University College London.

Morgan, J.P., McIntire, W.G., 1959. Quaternary geology of the Bengal Basin, East Pakistan and India. Geological Society of America Bulletin. 70, 319–342.

Nickson, R., McArthur, J., Burgess, W., Ahmed, K.M., Ravenscroft, P., Rahman, M., 1998. Arsenic poisoning of Bangladesh groundwater. Nature 395, 338.

Nickson, R.T., McArthur, J.M., Ravenscroft, P., Burgess, W.G., Ahmed, K.M., 2000. Mechanism of arsenic release to groundwater, Bangladesh and West Bengal. Applied Geochemistry. 15, 403–413.

Nickson, R.T., McArthur, J.M., Shrestha, B., Kyaw-Myint, T.O., Lowry, D., 2005. Arsenic and other drinking water quality issues, Muzaffargarh District, Pakistan. Applied Geochemistry. 20, 55–68.

Pal, T., Mukherjee, P.K., and Sengupta, S., 2002. Nature of arsenic pollutants in groundwater of Bengal Basin – a case study from Baruipur area, West Bengal, India. Current Science. 82, 554-561.

Pickering, W.F., 1981. Selective chemical extraction of soil components and bound metal species, CRC Crit. Rev. Anal. Chem.12, 233-266.

Ravenscroft, P., Burgess, W.G., Ahmed, K.M., Burren, M., Perrin, Jerome, 2005. Arsenic in groundwater of the Bengal Basin, Bangladesh: distribution, field relations, and hydrogeological setting. Hydrogeology Journal. 13, 727-751.

Ravenscroft, P., McArthur, J.M. and Hoque, B.A., 2001. Geochemical and palaeohydrological controls on pollution of groundwater by arsenic. In: Chappell, W.R., Abernathy, C.O., Calderon, R.L. (Eds.) Arsenic Exposure and Health Effects IV, Elsevier, Oxford, pp. 53-77.

Reimann, K-U., 1993. The Geology of Bangladesh. Gebruder Borntraeger, Berlin, Germany. 160p.

Saunders, J.A., Lee, M.-K., Uddin, A., Mohammad, S., Wilkin, R.T., Fayek, M., Korte, N.E., 2005. Natural arsenic contamination of Holocene alluvial aquifers by linked tectonic, weathering, and microbial processes. Geochemistry, Geophysics and Geosystems 6, (doi:10.1029/2004GC000803).

Saunders, J.A., Swann, C.T., 1992. Nature and origin of authigenic rhodochrosite and siderite from the Paleozoic aquifer, northeast Mississippi, U.S.A., Applied Geochemistry. 7, 375-387.

Sengupta, S., Mukherjee, P.K., Pal, T., Shone, S., 2004. Nature and origin of arsenic carriers in shallow aquifer sediments of Bengal delta, India, Environmental Geology. 45, 1071-1081.

Shamsudduha, M., Uddin, A., Lee, M.-K., Saunders, J.A., 2006. Geomorphological control on spatial correlation between groundwater arsenic and other ions in alluvial aquifers of Bangladesh. Abstract with Programs, Geological Society of America. 38(3), 14.

Sikder, A.M., Khan, M.H., Hasan, M.A., Ahmed, K.M., 2005. Mineralogical characteristics of the Meghna floodplain sediments and arsenic enrichment in groundwater, in Bundschuh, J., Bhattacharya, P., and Chandrasekharam, D. (Eds.), Natural arsenic in groundwater, Taylor & Francis Group, London., pp. 31-48.

Smedley, P.L. Kinniburgh, D.G., 2002. A review of the source, behaviour and distribution of arsenic in natural waters. Applied Geochemistry. 17, 517–568.

Smith, A., Lingas, E. Rahman, M., 2000. Contamination of drinking-water by As in Bangladesh. Bulletin of the World Health Organization. 78, 1093-1103.

Stüben, D., Bernera, Z., Chandrasekharam, D., Karmakarb, J., 2003. Arsenic enrichment in groundwater of West Bengal, India: geochemical evidence for mobilization of As under reducing conditions. Applied Geochemistry. 18, 1417–1434.

Tareq, S.M., Safiullah, S., Anawar, H.M., Rahman, M.M., Ishazuka, T., 2003. Arsenic pollution in groundwater: a self-organizing complex geochemical process in the deltaic sedimentary environment, Bangladesh: Sci. Total Environ. 313, 213–226.

Tessier, A., Campbell, P.G.C., Bisson, M., 1979. Sequential extraction procedure for the speciation of particulate trace metals, Anal. Chem. 51(7), 844-851.

Turner, J., 2006. Groundwater Geochemistry, Geology, and Microbiology of Arsenic-contaminated Holocene Alluvial Aquifers, Manikganj, Bangladesh, (MS thesis), Auburn University, Alabama, 76p.

Uddin, A., Kumar, P., Sarma, J.N., Akhter, S.H. (2007). Heavy-mineral constraints on provenance of Cenozoic sediments from the foreland basins of Assam, India and

Bangladesh: Erosional history of the eastern Himalayas and the Indo-Burman ranges, in Mange, M.A., and Wright, D.T., (Eds.), Heavy minerals in use, Developments in Sedimentology, Volume 58, Elsevier, Amsterdam, pp. 823-847.

Uddin, A., Lundberg, N., 1998a. Unroofing history of the Eastern Himalaya and the Indo-Burman ranges: Heavy-mineral study of Cenozoic sediments from the Bengal Basin, Bangladesh: Journal of Sedimentary Research. 68, 465-472.

Uddin, A., Lundberg, N., 1998b. Cenozoic history of the Himalayan-Bengal system: Sand composition in the Bengal Basin, Bangladesh. Geological Society of America Bulletin. 110, 497–511.

Uddin, A., Lundberg, N., 1999. A paleo-Brahmaputra? Subsurface lithofacies analysis of Miocene deltaic sediments in the Himalayan-Bengal system, Bangladesh. Sedimentary Geology. 123, 227-242.

Uddin, M.N., Abdullah, S.K.M., 2003. Quaternary geology and aquifer systems in the Ganges-Brahmaputra-Meghna delta complex, Bangladesh. Proc. GEOSAS-IV, Geological Survey of India, pp. 400-416.

Umitsu, M., 1987. Late Quaternary sedimentary environment and landform evolution in the Bengal lowland, Geography Rev. Japan. Ser. B 60, 164-178.

Umitsu, M., 1993. Late Quaternary sedimentary environments and landforms in the Ganges Delta. Sedimentary Geology. 83, 177–186.

UNDP, 1982. Groundwater Survey: The Hydrogeological Conditions of Bangladesh. UNDP Technical Report DP/UN/BGD-74-009/1, 113p.

van Geen, A., Zheng Y., Versteeg R., Stute M., Horneman A., Dhar R., Steckler M., Gelman A., Small C., Ahsan H., Graziano J.H., Hussain I., Ahmed K.M, 2003. Spatial variability of arsenic in 6000 tubewells in a 25 km^2 area of Bangladesh, Water Res. Research. 39(5), 1140 (doi:10.1029/2002WR001617).

Varsanyi, I, Kovacs, L.O., 2006. Arsenic, iron and organic matter in sediments and groundwater in the Pannonian Basin, Hungary. Applied Geochemistry. 21, 949-963.

WARPO, 2000. National Water Management Plan Project, Draft Development Strategy, Main final, vol. 2, Water Resources Planning Organization, Bangladesh.

Zheng, Y., Stute, M., van Geen, A., Gavrieli, I., Dhar, R., Simpson, J., Ahmed, K. M., 2004. Redox control of arsenic mobilization in Bangladesh groundwater. Applied Geochemistry. 19, 201–214.

Zheng, Y., van Geen, A., Stute, M., Dhar, R., Mo, Z., Cheng, Z., Horneman, A., Gavrieli, I., Simpson, H.J., Versteeg, R., Steckler, M., Grazioli-Venier, A., Goodbred, S., Shahnewaz, M., Shamsudduha, M., Hoque, M.A., Ahmed, K.M., 2005. Geochemical and hydrogeological contrasts between shallow and deeper aquifers in two villages of Araihazar, Bangladesh: Implications for deeper aquifers as drinking water sources. Geochim. Cosmochim. Acta. 69(22), 5203-5218.

APPENDIX

A1. Description of core MG samples

MG-01 (2-4 ft): Light yellowish-gray (5Y 7/2) silty-clay with some fine sands formed hard and compact weathered soil. Some coarse-grained sands and oxidized pockets/lens are observed. Plant roots and organic-structures (e.g., holes) are found within this soil layer.

MG-02 (6-8 ft): Light yellowish-gray (5Y 7/2) silty-clay with fine to medium sands. Mica grains are present in this layer. This layer is also part of the weathered soil zone. A few plat roots are seen. Some oxidized pockets/lens are also observed.

MG-03 (10-12 ft): Yellowish-gray to medium gray (5Y 7/2) fine silty sand with some medium sands. Micas (mostly muscovite) are observed in this layer. Grains are subrounded to subangular and are medium to well-sorted. Very thin laminations of mica-rich fine to medium silty-sands are noticed in the upper part of this core sample. No fossil or plant roots are found in this layer. This layer is possibly located within the groundwater table and becomes saturated during the wet seasons.

MG-04 (14-16 ft): Yellowish-brown with spotted dark-brown (5Y 7/2) fine silty sand with some silts. Numerous oxidized pockets/lens of silty-clay materials are observed in

this layer. No plant or organic materials are seen in this sample. Bottom part of this core sample (~ 8 inches long) is mostly silty with fine sands.

MG-05 (18-20 ft): Medium to dark-gray (5Y 7/2) silty clay with light gray (5Y 5/2) fine sands at the bottom of this core sample (~ 5 inches long). Some oxidized pockets/lens are seen in this layer. Some unidentified organic structures are seen, but no visible plant debris. This layer is an aquiclude.

MG-06 (22-24 ft): Medium to dark-gray (5Y7/2 and 5Y 5/2) silt with fine sands and clay. Some mica grains are seen. This sample is hard and compact with no visible plant materials. This layer can be called as aquiclude.

MG-07 (26-28 ft): Yellowish-gray (5Y 7/2) to light olive-gray (5Y 6/1) silty-clay with very fine sands, and some oxidized clay lens. This layer is hard and compact with no visible plant materials. This is also an aquiclude.

MG-08 (30-32 ft): Yellowish-gray (5Y 7/2) to light olive-gray (5Y 6/1) silty-clay with very fine sands. This layer is hard and compact with no visible plant materials. This is also an aquiclude.

MG-09 (34-36 ft): Yellowish-gray (5Y 7/2) to light olive-gray (5Y 6/1) silts with fine sands and micas. This layer is an aquitard.

MG-10 (38-40 ft): Light olive-gray (5Y 6/1) to yellowish-gray (5Y 7/2) silts with very fine sands and clay. Thin laminations of very fine sands rich in mica are observed in this layer. Grains are moderately sorted. This layer is an aquitard.

MG-11 (42-44 ft): Light gray (N7) to very light-gray (N8) with moderate yellowish-brown (10YR 5/4) laminated sands with some silts and clay. Micas are observed in this layer within the thin laminations. Numerous dark-colored (mostly opaque) minerals are seen. This layer is an aquitard to a poor aquifer.

MG-12 (46-48 ft): Very light-gray (N8) to light gray (N7), very fine to fine sands with silts and some clay. Laminations of mica-rich fine sands with lots of dark-colored minerals are seen in this layer. This layer is an aquitard to a poor aquifer.

MG-13 (50-52 ft): Dark yellowish-brown (10YR 4/2) to brown gray (5YR 4/1) silty clay with very fine sands. Thin laminations of mica-rich fine sand/silt are observed. This is an aquitard to aquiclude.

MG-14 (54-56 ft): Very light gray (N8) to light gray (N7), fine to medium sands with silt and clay, and abundant mica and dark-colored minerals. This is probably the first aquifer in Manikganj study area with potential for groundwater supplies.

MG-15 (58-60 ft): Light gray (N7) to yellowish-gray (5Y 8/1), fine sand with silts and little clay. Some clay galls and thin lamination of mica-rich sands and opaque minerals are observed in this layer. This layer is probably a poor aquifer.

MG-17 (66-68 ft) through MG-21 (82-84 ft): Very light gray (N8), fine to medium sands with silts. This layer is also rich in mica and opaque heavy minerals. Sediments are moderately sorted. This layer is probably a good aquifer in Manikganj.

MG-22 (86-88 ft) through MG-25 (98-100 ft): Medium light-gray (N6-N8), medium to fine sand with occasional coarse sands. Some coarse grained brown/red colored mineral/rock fragments are found. This layer is highly porous and permeable. Presence of abundant mica and dark-colored opaque minerals are also noticed. This layer is considered as a good aquifer.

MG-27 (114-116 ft) through MG-30 (118-120 ft): Medium light-gray (N6-N8), medium to fine sand. This layer is highly porous and permeable. Presence of abundant mica and dark-colored opaque minerals are also noticed. Sediments are moderate to well sorted. This layer is considered as a good aquifer.

MG-31 (122-124 ft) through MG-37 (146-148 ft): Medium light gray (N6) to light gray (N7), medium to fine sand with occasional coarse sands. Sediments are moderate to well-sorted with high porosity and permeability. The layer is rich in mica (muscovite and biotite) and dark-colored opaque minerals. This is a good aquifer.

MG-38 (160-162 ft) through MG-39 (180-182 ft): Medium light gray (N6) to light gray (N7), medium- to fine-grained sand with occasional coarse sands. Sediments are moderately sorted with high porosity and permeability. The layer is rich in mica and dark-colored opaque minerals. This layer is a good aquifer.

MG-40 (200-202 ft) through MG-41 (220-222 ft): Light gray (N7) to very light-gray (N8), medium-grained medium to well sorted sands. Abundant mica and dark-colored opaque minerals are present in this layer. Sediments are highly porous and permeable. This layer represents a very good aquifer.

MG-42 (240-242 ft) through MG-43 (260-262 ft): Yellowish gray (5Y 8/1) to dark yellowish-gray (5Y 7/2), coarse-grained sand with lots of granules. Medium sand are also found within the coarse sands. Lithic fragments like chert and quartzite of various colors are found in this layer. Presence of dark-colored opaque minerals is also noticed in this layer. This sedimentary layer is highly porous and can be called an excellent aquifer.

MG-44 (280-282 ft): Light gray (N7) to very light-gray (N8), fine to medium sands with some silts. Dark colored opaque minerals are significantly present in this layer. This layer is highly porous and can be considered as a good aquifer.

MG-45 (300-302 ft): Medium gray (N5) to light gray (N7), medium to fine grained sand with clay at the bottom. Upper part of this core sample is graven-rich clay. The gravels are subangular to subrounded, mostly fragments of quartzite and chert. The bottom part is

clayey with less gravel. This layer documents a major facies change in the Quaternary sediments in the study area.

MG-46 (320-322 ft): Light gray (N7) to very light-gray (N8), medium to coarse grained sand with fine sands. This layer is rich in dark-colored opaque minerals and micas. These sediments are moderate to well-sorted. This layer is a good aquifer.

MG-47 (340-342 ft): Pale greenish-yellow (10Y 8/2) to yellowish-gray (5Y 8/1) silty-clay. This layer is fairly hard and compact. This layer works as an aquitard.

MG-48 (360-362 ft) through MG-49 (380-382 ft): Moderate greenish-yellow (10Y 7/4) to yellowish gray (5Y 7/2) silty-clay to very fine sand. Presence of oxidized pockets and some pink/red minerals are found in this layer. This layer is an aquiclude to aquitard.

MG-50 (400-402 ft): Light-gray (N7) to very light-gray (N8), medium to coarse sand with fine sand. Sediments are moderately sorted with high porosity. Dark-colored opaque minerals and micas are present in this layer. This layer is a good aquifer.

MG-51 (420-422 ft): Yellowish-gray (5Y 8/1) to light greenish-gray (5 GY 8/1), medium to fine sand with occasional coarse sands. Sediments are moderate to well-sorted with high porosity. Numerous dark-colored opaque minerals and micas are present. This layer serves as an excellent aquifer.

MG-52 (440-442 ft) through MG-53 (460-462 ft): Grayish yellowish-green (5GY 7/2) to pale greenish yellow (10Y 8/2) medium sand with some fine sands. Occasional gravels are also found in this layer. Sediments are moderate to well-sorted. Some dark-colored opaque minerals are found in this layer.

MG-54 (480-482 ft) through MG-55 (500-502 ft): Yellowish gray (5Y 7/2) to pale greenish-yellow (10Y 8/2) medium to coarse sands with little fine sands and occasional gravels. Abundant dark-colored opaque minerals are present in this layer. This layer is highly porous with high permeability. This is one of the excellent aquifers in the Manikganj area.

A2. Description of core MG samples

MN-002 (3-5 ft): Yellowish-gray to yellowish-brown, very fine grained silty sand. Bottom part is predominantly composed of fine sand with some lamination. Some mica is present in this layer. This layer remains above the water table for most time.

MN-004 (6-7 ft): Yellowish-brown silt with some clay. Some areas are highly oxidized and brown. The silt is thinly laminated in most parts. This layer is right at the water table and connected with atmosphere.

MN-007 (11-13 ft): Dark-gray silty-clay (predominantly clay) with some hard nodules. No other sedimentary structure is seen in this layer but is highly reducing. This layer remains below the water table during the wet seasons. This is a good aquiclude.

MN-010 (15-17 ft): Light yellowish-gray, hard and sticky clay. Very little silt is present in this layer. This is an aquiclude and probably remains above the dry-season water table in Manikganj.

MN-012 (19-21 ft): Yellowish-gray to brownish-gray clay with some silt. Some places are highly oxidized. No other sedimentary structure is seen. This layer works as an aquiclude to aquitard.

MN-014 (23-25 ft): Dark-gray to gray, fine to very fine sands with laminated silt and little mica-rich sand. Thin laminations of fine mica-rich silt are observed in this layer. Some small-scale ripple marks are seen in this layer. This probably forms the first aquifer at this location in Manikganj.

MN-017 (29-31 ft): Light yellowish-gray to gray, fine sand with some silt. Laminations of mica-rich sand are observed in this layer. This is more porous than the upper-lying layer and can be considered as fair to good aquifer.

MN-021 (36-39 ft): Light gray, fine sand with some silt and mica. No definite sedimentary structure is seen. This layer is also good aquifers in the study area.

MN-023 (41-43 ft): Light gray, fine sand with some silt. Mica is present in this layer. This layer is also good aquifers in the study area.

MN-027 (49-51 ft): Light gray to gray, medium to fine grained sand. Some laminations are observed in this layer. These laminations are formed mostly by dark-colored opaque minerals and micas. This is also good aquifer.

MN-031 (57-59 ft): Medium gray to dark gray, medium to fine sand. Some plant debris is found in this layer. This layer can also be considered as good aquifer.

MN-032 (59-61 ft): Light gray, medium to fine sand with some silt. The sand layer is sort of massive without any apparent sedimentary structure. Some mica is present. This layer probably works as a good aquifer.

MN-039 (73-75 ft): Medium to light gray, medium to fine sand. Some organic matters (plant debris) are found. This layer is part of a good aquifer.

MN-047 (89-91 ft): Light yellowish-gray to gray, medium to fine grained sand. Some organic materials (plant debris) are present. This layer is also part of a good aquifer.

MN-055 (105-107 ft): Light gray, medium to fine sand. Thin laminations of dark colored opaque heavy minerals are observed. This layer is considered as good aquifer material.

MN-061 (117-119 ft): Medium to light gray, fine sand with sole silt. Dark colored heavy minerals and micas are seen that form thin laminations. This layer works as an aquifer.

MN-067 (129-131 ft): Light gray, fine to medium sand with some silt. Dark colored heavy minerals and micas are seen that form thin laminations. This layer works as a fair to good aquifer.

MN-070 (135-137 ft): Light yellowish-gray, medium to fine grained sand. Mica flakes are coarse-grained. This layer is sort of massive without any apparent structure. This forms good aquifer.

MN-072 (139-141 ft): Yellowish-brown to light yellowish-gray, medium to fine grained sand. Bottom part is fine grained with light gray sand. Thin mica-rich lamination separates these two layers. This is probably part of a good aquifer.

MN-077 (149-151 ft): Medium to light gray, fine sand with some silt. Lots of dark-colored heavy minerals are present. No sedimentary structure is seen. This forms fair to good aquifer.

MN-081 (190-192 ft): Yellowish-brown to yellowish-gray, coarse to medium sand with gravels. Gravels are subrounded to well-rounded lithic fragments of quartzite and chert. This forms excellent aquifer in Manikganj area.

MN-084 (220-222 ft): Yellowish-brown to yellowish-gray, coarse to medium sand with gravels. Gravels are subrounded to well-rounded lithic fragments of quartzite and chert, and even granites. This forms excellent aquifer in Manikganj area.

MN-085 (230-232 ft): Yellowish-brown to light yellowish-gray, coarse to medium sand with large gravels. Gravels are subrounded to well-rounded lithic fragments of quartzite, chert, and granite. This forms excellent aquifer in Manikganj area.

MN-086 (240-242 ft): Light yellowish-gray, medium sand with abundant dark-colored heavy minerals. Pink-colored garnets are easily identified in this layer. No gravel is found. This forms a very good aquifer.

MN-092 (300-302 ft): Light yellowish-gray, coarse to medium sand with gravels. Gravels are subangular to subrounded lithic fragments of chert, quartzite and granites. Size of gravels increases with increasing depth. This forms an excellent aquifer.

MN-093 (320-322 ft): Light yellowish-gray, coarse to medium grained sand with traces of gravels. Gravels are subangular to subrounded lithic fragments of chert, quartzite and granites. This layer forms a good aquifer.

MN-094 (340-342 ft): Orange-brown to bright yellowish-brown, medium to fine sand. The change in grayish to orange-brown indicates a change in facies type. This layer can be lithologically correlated with the Dupi Tila Formation. This layer serves as the excellent aquifer in Manikganj as well as other parts of Bangladesh.

MN-097 (400-402 ft): Brownish-yellow, medium to fine sand. Sands are highly oxidized with iron coating. The layer does not show any apparent sedimentary structure. This is part of the Dupi Tila aquifer.

MN-100 (460-462 ft) through MN-102 (500-502 ft): Yellowish-brown, medium to fine sand. Sediments are moderate to well-sorted. Sands are highly oxidized with iron coating. This layer forms the excellent aquifer in the study area.